

Distribution Agreement

In presenting this thesis or dissertation as a partial fulfillment of the requirements for an advanced degree from Emory University, I hereby grant to Emory University and its agents the non-exclusive license to archive, make accessible, and display my thesis or dissertation in whole or in part in all forms of media, now or hereafter known, including display on the world wide web. I understand that I may select some access restrictions as part of the online submission of this thesis or dissertation. I retain all ownership rights to the copyright of the thesis or dissertation. I also retain the right to use in future works (such as articles or books) all or part of this thesis or dissertation.

Signature:

David Laws III

Date

The Development of Planar Chiral Indenyl Catalysts and the Progress Towards
Synthesis of the Western Macrocyclic of Darobactin A

By

David Laws III

Doctor of Philosophy

Chemistry

Simon B. Blakey, Ph.D.
Advisor

Frank E. McDonald
Committee Member

Vincent P. Conticello
Committee Member

Accepted:

Kimberly J. Arriola, Ph.D. MPH
Dean of the James T. Laney School of Graduate Studies

Date

**The Development of Planar Chiral Indenyl Catalysts and the Progress Towards
Synthesis of the Western Macrocyclic of Darobactin A**

By

David Laws III
B.S. Coastal Carolina University, 2018

Advisor: Simon B. Blakey

An abstract of
A dissertation submitted to the Faculty of the
James T. Laney School of Graduate Studies of Emory University
in partial fulfillment of the requirements for the degree of
Doctor of Philosophy
in Chemistry
2023

Abstract

The Development of Planar Chiral Indenyl Catalysts and the Progress Towards Synthesis of the Western Macrocycle of Darobactin A

By David Laws III

Planar chiral catalysis has been growing in both popularity and relative usefulness over the last two decades. However, synthesizing and resolving these catalysts remains a challenge. The first half of this dissertation will address efforts to provide a streamlined enantioselective synthesis of indenyl planar chiral catalysts, as well as more targeted catalyst development in the context of planar chiral indenyl complexes to improve utility in a variety of reaction profiles. Secondly, we will pivot to the area of ribosomally synthesized and post-translationally modified peptides. These natural products contain unique and valuable bioactivity profiles, but the post translational modifications also render them difficult to provide via chemical synthesis. In the second half of this dissertation, we will explore a novel approach towards the synthesis of darobactin A and its western macrocycle.

**The Development of Planar Chiral Indenyl Catalysts and the Progress Towards
Synthesis of the Western Macrocyclic of Darobactin A**

By

David Laws III
B.S. Coastal Carolina University, 2018

Advisor: Simon B. Blakey

A dissertation submitted to the Faculty of the
James T. Laney School of Graduate Studies of Emory University
in partial fulfillment of the requirements for the degree of
Doctor of Philosophy
in Chemistry
2023

Acknowledgements

This journey has been an unforgettable chapter in my life, many different people have helped shape me as a chemist and person. I hope that each of those people in my life understand the impact they have had on me and my development. Firstly, I would like to thank my advisor Simon Blakey. Throughout my five years at Emory University, you have taught me a great deal about chemistry and about how to lead a research group. I hope when I have a lab of my own, that I can inspire students in the same way you inspired me when I thought I wasn't good enough or that I didn't belong. Whenever I left your office, you made me feel like I could do the hard things that come with this profession. I would also like to thank my Ph.D. committee, Dr. Frank McDonald and Dr. Vincent Conticello. Dr. McDonald, your attention to detail and extensive synthetic knowledge was always useful in my annual meetings and helped strengthen my reports and research where they were weak. Dr. Conticello, you often provided a unique insight during my annual meetings. I found it refreshing and especially helpful when developing my novel proposal for fourth year. Thank you to all three of you for the part you played in my Ph.D. career.

Next, I would like to thank the people from Coastal Carolina University that helped get me to this point. The first friendly face I met in the CCU chemistry department was Amber McWilliams. Amber is an exceptional teacher, and the first one that made me consider that teaching at the collegiate level was a goal of mine. Beyond being able to parse the dense info in a gen chem course to doe-eyed freshmen, Amber was instrumental in transforming the chemistry department into a community. So I would like to thank you for making CCU a home away from home. I would also like to thank my first boss, Carol Boyd. Carol, you were a joy to work for, and I'm sure having a boss that actually cares about you is a rarity, but I lucked out. You're an amazing person and without you I'm sure the teaching labs will fall apart shortly. Lastly, but certainly not least, I would like to thank Dr. Wakefield. Now that I'm a doctor myself we'll see if I ever use your first name, but it's not likely. There are many things I would like to thank you for Wakefield. You showed me the ropes in organic chemistry, your classes made me realize that while we do serious work we can enjoy it, and your lab is truly where I feel I came into my own, both as a chemist and a person. I hope that I can embody your enthusiasm for teaching and research in my independent career.

Now to thank some non-chemistry folks. I am eternally grateful for my mother, who brought me into this world. My mom was my first teacher, and most likely the reason why I'm food motivated. If not for my mom instilling my love of reading and learning, I have no idea where I would be, but it most likely wouldn't be completing a doctorate in chemistry. Next, I would like to thank my sister. Kristen, you've always had my back and without you looking out for me, I would've made it sure, but I would've certainly been less happy. Thanks for always being my friend. My father has always been a giant in my life. But no other person has had more of an influence on the man I am today than Dr. David Laws Jr. So, thanks big man, for teaching me many things and instilling in me a work ethic that

won't quit. I would also like to thank my cousin Dennis Oliver II, when I got to Emory, I was relatively alone. Having family here that checked up on me and made sure I wasn't starving meant more than I can say.

I've met many friends on this journey, but only a few have stuck. To the boys! Adrian and Quincy you guys have changed my life. Thanks for expanding my horizons and being a pair of ears that I can talk to. I expect to be friends with you guys til the end of my journey on this green rock, so here's to many more years together. Amaan while you began as my mentor you quickly became a good friend. Thanks for your constant help and friendship, you are the Obi Wan to my Luke, because I don't think I'm going to turn to the dark side.

To all those I haven't mentioned by name that have helped me in this journey, thank you I truly appreciate your support, help and friendship.

Table of Contents

Chapter 1. Synthesis, Chiral Resolution and Activity of Late-Transition Metal Planar Chiral Complexes	1
1.1 The Synthesis and Resolution of Late-Transition Metal Planar Chiral Complexes	1
1.2 The Catalytic Activity of Late-Transition Metal Planar Chiral Complexes in Enantioselective Transformations	11
1.3 Conclusions	16
1.4 References	18
Chapter 2. Progress towards the Enantioselective Synthesis of Planar Chiral Indenyl Complexes and Design of Planar Chiral Rh(III) Indenyl Catalysts	22
2.1 Recent Advances in Rh and Ir Catalyzed Allylic C–H Functionalization	22
2.2 The Development of the Blakey Indenyl Catalyst	27
2.2.1 Mechanistic Insight into Allylic C–H Functionalization Using External Oxidants	27
2.2.2 Development of the Blakey Indenyl Catalyst	30
2.3 Enantioselective Synthesis of Planar Chiral Rhodium Catalysts	33
2.3.1 Synthesis	34
2.3.2 Conclusions	36
2.4 Exploration of Electronic Effects in the Planar Chiral Indenyl Scaffold	37
2.4.1 Synthesis and Reactivity	39
2.4.2 Conclusions	42
2.5 Experimental Details	43
2.6 Spectral Data	55
2.7 References	85
Chapter 3. Ribosomally Synthesized and Post-translationally Modified Peptides containing C–O and C–C Crosslinks	93
3.1 The Generic Biosynthesis of Ribosomally Synthesized and Post-Translationally modified Peptides	93

3.2	Chemical Synthetic Approaches towards Ribosomally Synthesized and Post-translationally Modified Peptides containing C–O and C–C Crosslinks	95
3.2.1	Synthetic Approaches towards forging Alkyl-Aryl C–O Crosslinks in RiPPs	96
3.2.2	Synthetic Approaches towards RiPPs with C–C Crosslinks containing Tryptophan	99
3.2.2.1	Chemical Syntheses of Celogentin C	99
3.2.2.2	Chemical Synthesis of Streptide	105
3.2.2.3	Chemical Synthesis of Tryptorubin A	106
3.2.3	Chemical Syntheses of Darobactin A	109
3.3	Conclusions	113
3.4	References	115
Chapter 4. Progress Towards the Synthesis of the Western Macrocycle of Darobactin A		119
4.1	Synthetic Strategy towards the Total Synthesis of the Western Macrocycle of Darobactin A	119
4.2	Synthesis of Amino Acid Fragments	122
4.2.1	Synthesis of 7-substituted Tryptophan Derivatives	122
4.2.2	Synthesis of <i>erythro</i>-hydroxy-L-Tryptophan	124
4.2.3	Synthesis of <i>threo</i>-hydroxy-L-Tryptophan	127
4.3	Exploration of C–O Crosslinking Methods	128
4.4	Conclusions	133
4.5	Experimental Details	135
4.6	Spectral Data	152
4.7	References	175

List of Figures

Chapter 1

Figure 1.1 The two main strategies when approaching planar chiral catalyst synthesis **2**

Chapter 2

Figure 2.1 A selection of planar chiral Cp catalysts used over the last decade **30**

Figure 2.2 A suite of electronically biased indenyl complexes **39**

Chapter 3

Figure 3.1 Generic RiPP Biosynthesis **94**

Figure 3.2 The macrocyclic RiPP ustiloxin **96**

Figure 3.3 The structure of celogentin C **100**

Figure 3.4 The structure of streptide **105**

Figure 3.5 The structure of tryptorubin A a fused tri-macrocyclic RiPP **107**

Figure 3.6 The heptapeptide darobactin A **109**

List of Schemes

Chapter 1

- Scheme 1.1** Synthesis of the Takahashi catalyst library 3
- Scheme 1.2** Synthesis of the tethered η^6 benzene complex from Faller and coworkers. 5
- Scheme 1.3** The synthesis of the first facially selective ligand from the Perekalin Group 6
- Scheme 1.4** Synthesis of the second facial blocking ligand from the Perekalin Group 7
- Scheme 1.5** Perekalin and coworkers utilized *L*-proline in the resolution of racemic Cp complex 8
- Scheme 1.6** The Perekalin synthesis of planar chiral cyclohexadiene complexes using Na[S-Salox] to resolve the racemate 9
- Scheme 1.7** The modular ligand synthesis from Antonchick and Waldmann 10
- Scheme 1.8** Synthesis of the Blakey Indenyl Catalyst 11
- Scheme 1.9** Early Application of the Takahashi catalysts in allylic substitution 12
- Scheme 1.10** The full suite of intermolecular, monomeric allylic substitution reactions disclosed by Onitsuka and coworkers 13
- Scheme 1.11** Asymmetric hydrogen transfer reaction from the Perekalin Group 14
- Scheme 1.12** The suite of enantioselective C–H functionalization reactions disclosed by Antonchick and Waldmann 15

Chapter 2

- Scheme 2.1** The intramolecular allylic amination reported by Cossy in 2012, and the intermolecular allylic amination of internal olefins from Blakey 2017 23
- Scheme 2.2** The Blakey etherification procedure and the Glorius arylation methods 24
- Scheme 2.3** Regioselective Rh and Ir catalyzed allylic C–H amidation reactions disclosed in 2019 25
- Scheme 2.4** The regioselective sulfamidation of terminal olefins from the Blakey Group, and the highly regioselective functionalizations disclosed by the Rovis Group 26
- Scheme 2.5** Reactivity of several Rh π -allyl complexes to determine the initial reductive elimination product 28

Scheme 2.6 The catalytic cycle proposed by Blakey and coworkers	29
Scheme 2.7 A) Demonstration of indenyl ring slippage B) Baker Enantioinduction Study. C) Reactivity of the Blakey Planar Chiral Indenyl catalyst	31
Scheme 2.8 Our plan to adapt the You group's enantioselective arylation of transition metal complexes	33
Scheme 2.9 Retrosynthesis of the N,N-dimethylaminomethyl indene ligand	34
Scheme 2.10 Synthesis of the 2-(dimethylaminomethyl)indene via Mannich alkylation	35
Scheme 2.11 Direct synthesis of indenyl ligand and complexation onto Rh(I)	36
Scheme 2.12 Proposed catalytic cycle for allylic C–H amidation	38
Scheme 2.13 Synthesis of 4'-substituted-2-methyl-3-phenyl indenyl complexes	39
Scheme 2.14 Evaluation of electronically biased ligands and nitrene precursors in allylic C–H amidation	40
Scheme 2.15 Planar chiral indenyl catalysts and their performance in aziridination reactions	41
Chapter 3	
Scheme 3.1 The first total synthesis of ustiloxin D by Joullié and coworkers	97
Scheme 3.2 The Wandless synthesis of ustiloxin D	98
Scheme 3.3 the improved convergent synthesis of ustiloxin by Joullié and coworkers	99
Scheme 3.4 The first synthesis of the A ring of celogentin C by Moody and coworkers	101
Scheme 3.5 Synthesis of the central tryptophan residue by Campagne <i>et al.</i> using Suzuki-Miyaura coupling	102
Scheme 3.6 Castle's Total synthesis of celogentin C	103
Scheme 3.7 Synthesis of the celogentin C crosslink via Michael addition by Jia and coworkers	104
Scheme 3.8 The total synthesis of celogentin C using directed C–H activation	105
Scheme 3.9 Boger's synthesis of the streptide C–C crosslink via C–H arylation	106
Scheme 3.10 Baran's synthesis of tryptophan A. They utilized a Friedel-Crafts to build the C–C crosslink	108
Scheme 3.11 The Sarlah synthesis of darobactin A	110

Scheme 3.12 The Baran synthesis of darobactin A	112
Chapter 4	
Scheme 4.1 Our retrosynthetic analysis of darobactin A	120
Scheme 4.2 Retrosynthetic analysis of amino acid fragments	121
Scheme 4.3 The synthesis of 7-Bpin- <i>L</i> -Trp via directed borylation	122
Scheme 4.4 Generation of the 7-substituted <i>L</i> -tryptophan derivatives	123
Scheme 4.5 Our attempts at Sharpless amino-hydroxylation of indolyl acrylates	124
Scheme 4.6 Asymmetric aldol using Evan's auxiliary	126
Scheme 4.7 The synthesis of <i>erythro</i> - β -hydroxy- <i>L</i> -tryptophan utilizing Garner's aldehyde	127
Scheme 4.8 Synthesis of <i>threo</i> - β -hydroxy- <i>L</i> -tryptophan	127
Scheme 4.9 Chan-Lam couplings attempted with <i>erythro</i> - β -hydroxytryptophan	128
Scheme 4.10 Unproductive UV light mediated cross-coupling	130
Scheme 4.11 Initial Mitsunobu Studies	132
Scheme 4.12 Alternate pathway to enable Mitsunobu reactivity	133

List of Tables

Chapter 2

Table 2.1 Unsuccessful Mannich reactions with pre-prepared Eschenmoser's Salt	35
--	-----------

Chapter 4

Table 4.1 Explorationi of Ullman type cross-coupling utilizing DPEO ligand	129
Table 4.2 The effect of catalyst loading on blue light promoted arylation	131

Chapter 1. Synthesis, Chiral Resolution and Activity of Late-Transition Metal Planar Chiral Complexes

Planar chiral complexes offer an alternative to chiral catalysts that depend solely on axial or point chirality to induce stereoselectivity in reactions. Our work in catalyst development has centered around synthesizing planar chiral Rh(III) catalysts. While late-transition metal planar chiral catalysts are a growing subject of study, they are not as common in synthetic chemistry as other chiral catalysts. The underutilization of late-transition metal complexes is likely due to difficulties synthesizing or resolving these catalysts. In this chapter, we will discuss important developments in the synthesis and resolution of late-transition metal catalysts and highlight some examples of potent activity exhibited in this catalyst class. While the Blakey Indenyl catalyst represents a significant advancement in planar chiral catalysis, we will discuss its reactivity in a later chapter, when we focus on the development of the Blakey Indenyl catalyst family.

1.1 The Synthesis and Resolution of Late-Transition Metal Planar Chiral Complexes

Chiral late-transition metal complexes have been well explored in recent years in the context of stereoselective transformations.¹⁻⁶ However, planar chirality is relatively underrepresented in the current catalog of late-transition metal catalysts. Catalysis with Group VIII and IX metals often employs chiral C₂ symmetric cyclopentadienyl (Cp) ligands, as seen by the Cramer, You and Wang groups.⁷⁻⁹ These chiral ligands utilize steric blocking effects to guide stereoinduction but must contain all the necessary chiral information before complexation. Whereas planar chiral complexes offer a novel route to delivering chiral catalysts, given that planar chirality is introduced upon complexation. Our

lab has covered the synthesis, resolution, and catalytic activity of late-transition planar chiral complexes in a review.¹⁰ We will outline some important examples that have shaped the current state of the art when it comes to the synthesis, resolution, and activity of planar chiral complexes.

The synthesis of planar chiral complexes is an important factor that contributes to their use in the wider organic synthesis community. Catalysts that require lengthy syntheses and complicated resolution techniques are less likely to be used by labs that did not develop the technology. Currently there are two main synthetic strategies to delivering planar chiral complexes; the first is to synthesize a chiral ligand that will form planar chiral diastereomers upon complexation and thus simplifying purification, while the second method utilizes readily accessible achiral ligands that will form planar chiral enantiomers upon complexation (Figure 1.1). Diastereomeric syntheses often require lengthy ligand syntheses but are balanced by facile purification of the resultant

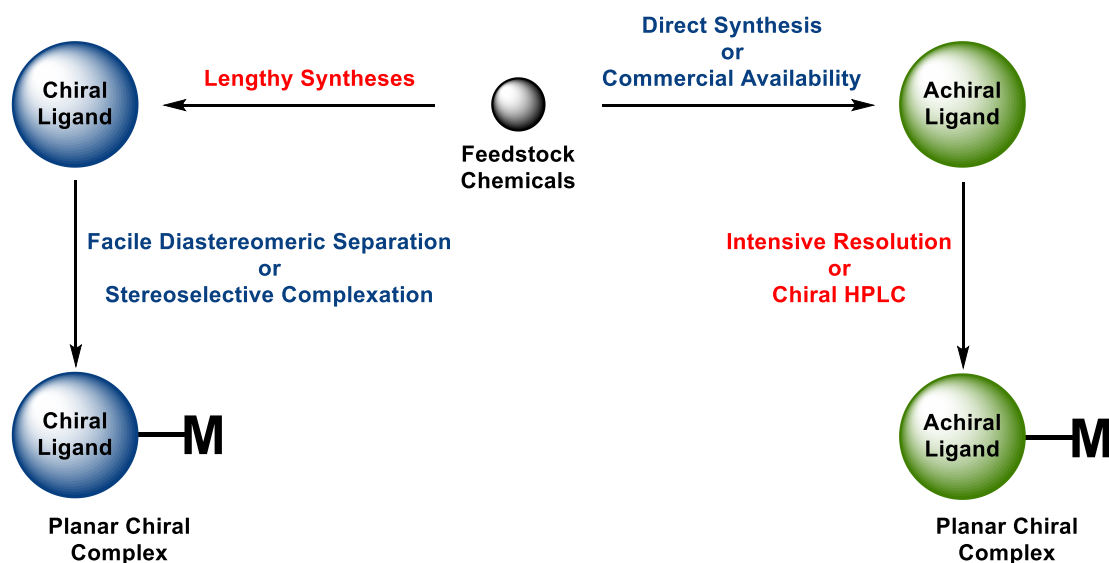
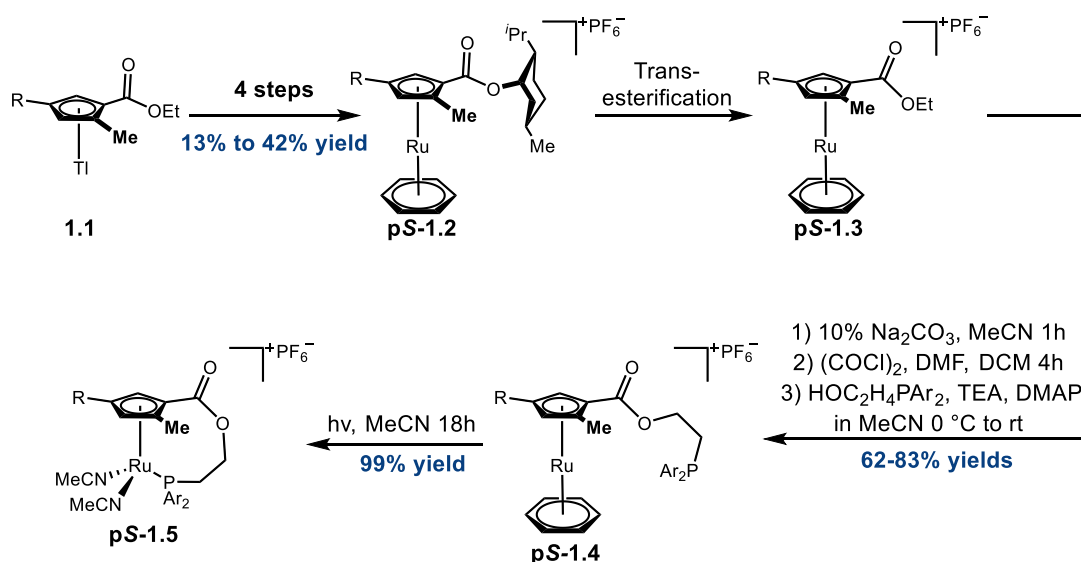


Figure 1.1: The two main synthetic strategies when approaching planar chiral catalyst synthesis.

diastereomers, while racemic syntheses usually employ simple ligands, but require more creative resolution techniques.

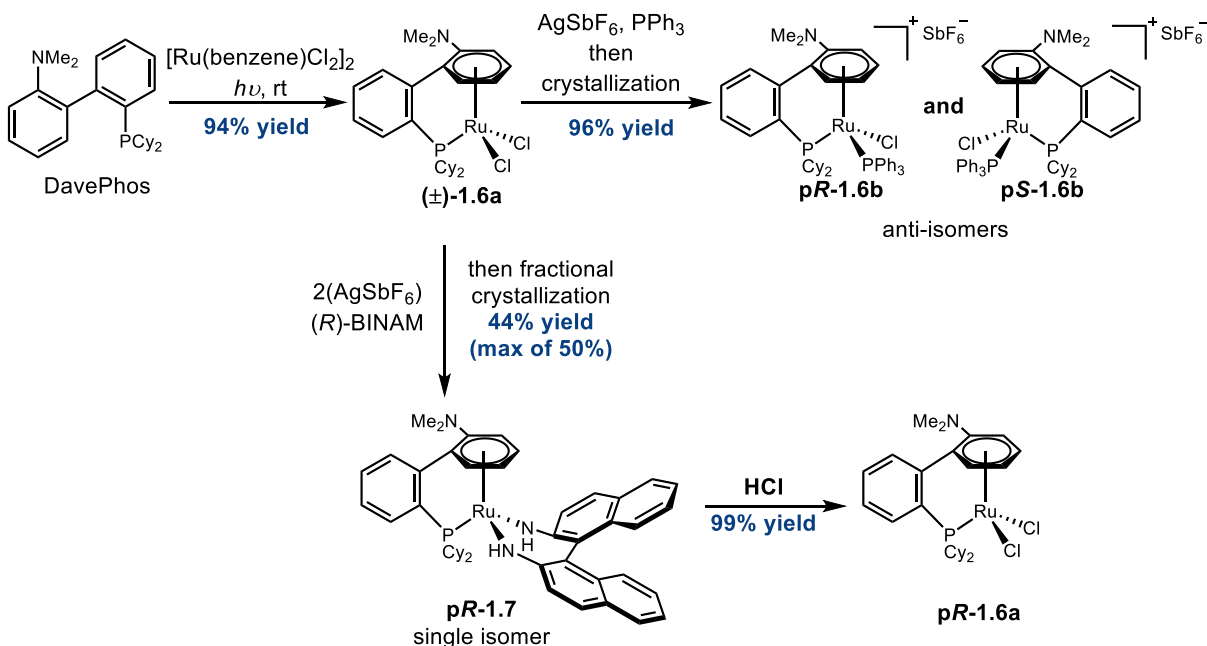
To our knowledge, Takahashi *et al.* disclosed the first late-transition metal complexes developed for an enantioselective transformation.¹¹ Takahashi's seminal library of tethered Ru catalysts set the standard for planar chiral catalysis, with good to excellent enantioinduction over a range of allylic substitution reactions. Preparation of the Takahashi catalyst family began with thallium Cp racemate **1.1** undergoing transmetalation with Ru(II). The ester was subsequently converted to *L*-menthol substituted Cp complex **pS-1.2** in four steps (Scheme 1.1).^{12,13} While fractional crystallization in EtOH:H₂O enabled separation of the diastereomers, it remained a major bottle-neck in catalyst synthesis, with yields of pure **pS-1.2** as low as 13%. Transesterification and conversion to the pendant phosphine complexes was efficient over four steps to deliver **1.4**.¹⁴ Irradiation of the pendant phosphines delivered the library of tethered Ru(II) catalysts (**1.5**, Scheme 1.1) that Takahashi and coworkers would use to develop a range



Scheme 1.1 Synthesis of the Takahashi catalyst library.

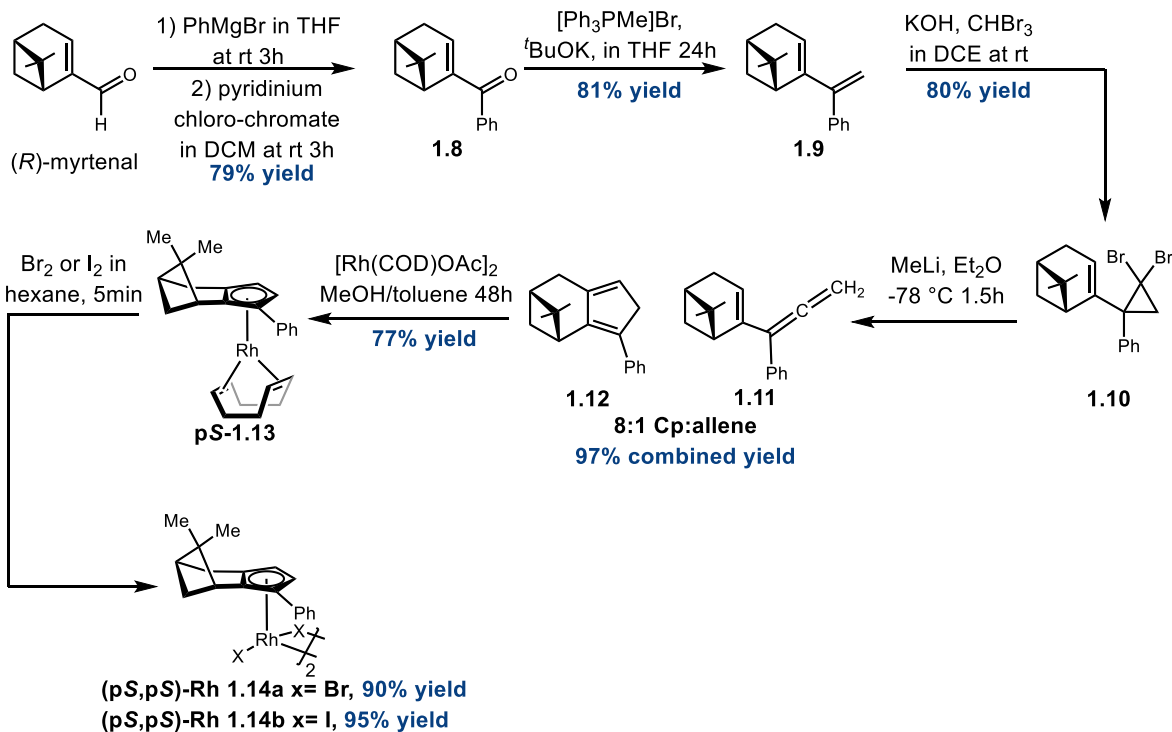
of allylic substitution reactions. While the syntheses of Takahashi's planar chiral catalysts were lengthy and low yielding at times, it provided a foundation for others to develop similar catalyst frameworks.

Later, the Faller group synthesized their η^6 -benzene Ru catalyst **1.6a** in one step from complexation with DavePhos.¹⁵ They were able to resolve the racemate via incorporation of triphenylphosphine, which complexed in an anti-fashion to deliver racemic **1.6b** and resolved spontaneously upon crystallization. Unfortunately, the pure enantiomer crystals needed to be manually separated and verified via optical rotation, but the Faller group managed to maintain a short synthetic route and ultimately obtain pure crystals of both enantiomers. Later, Faller and coworkers complexed (\pm)-**1.6a** with *R*-BINAM, and the resultant diastereomers were separated via fractional crystallization in which only **pR-1.7** precipitated and was quantitatively reconstituted with HCl to deliver **pR-1.6a**.¹⁶ Faller and coworkers demonstrated that concise syntheses paired with straightforward resolutions are possible in the context of planar chiral catalyst synthesis.



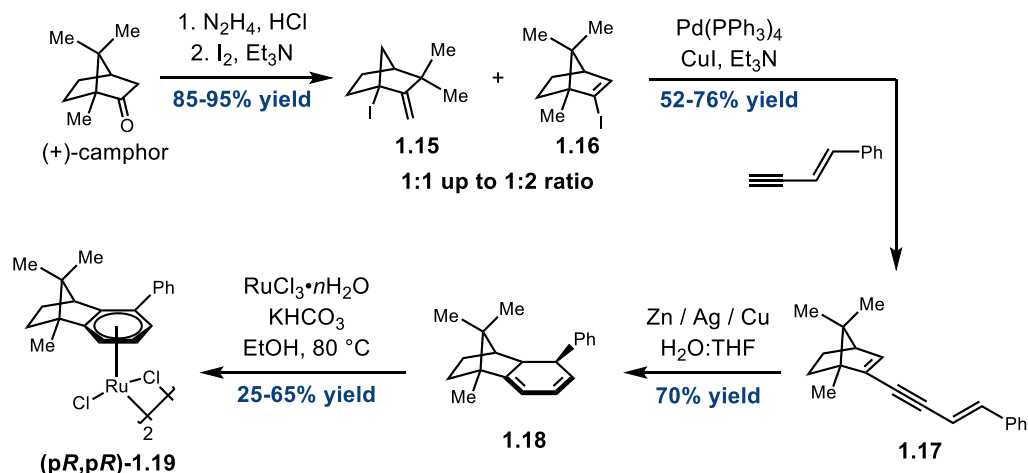
Scheme 1.2 Synthesis of the tethered η^6 -benzene complex from Faller and coworkers. Later iterations used (*R*)-BINAM complexation to improve resolution of the racemate.

The Perekalin group has made significant contributions in advancing the synthesis of planar chiral complexes and developing clever methods to deliver stereochemically pure catalysts. Perekalin and coworkers have utilized diastereomeric complexation in a truly unique fashion in which the chiral ligand blocks complexation from a single face delivering a single diastereomer of planar chiral complex. The first example of these facial blocking ligands was disclosed in 2020.¹⁷ The Perekalin group started with *R*-myrtenal as their commercially available chiral building block (Scheme 1.3). Conversion of *R*-myrtenal to acetophenone **1.8** proceeded in good yield and was followed by Wittig olefination to provide diene **1.9**. Cyclopropanation and Skattebøl rearrangement delivered the cyclopentadiene ligand **1.12** in good yields, although there was some allene byproduct recovered. Complexation of the ligand with $[Rh(COD)OAc]_2$ was straightforward and delivered a single diastereomer (**1.13**, Scheme 1.3). Subsequent oxidation provided the Rh(III) dimer **1.14**.



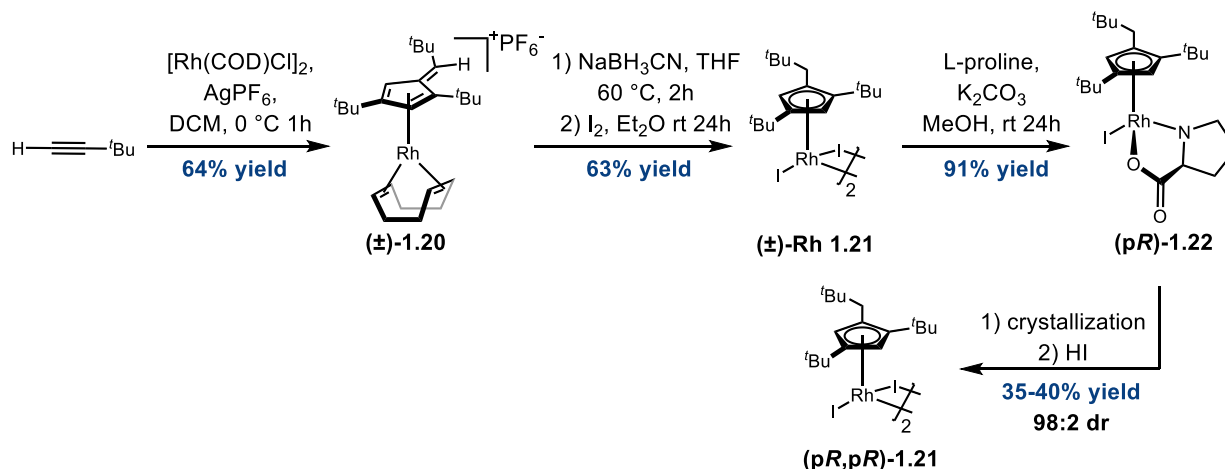
Scheme 1.3 The synthesis of the first facially selective chiral ligand from the Perekalin Group.

Perekalin and coworkers delivered another example of facial blocking in planar chiral catalyst synthesis in 2022.¹⁸ In this instance, the Perekalin group utilized 1-*R*-(+)-camphor as their chiral building block. Conversion to the hydrazone and subsequent iodination provided vinyl iodide **1.16** in good yield, although a mixture of the vinyl iodide and alkyl iodide (**1.15**, Scheme 1.4) were observed. The vinyl iodide was carried forward in a Sonogashira coupling to provide ene-yne fragment **1.17**. Reduction and electrocyclicization of **1.17** delivered diene **1.18**, which was readily complexed with RuCl₃•H₂O. Due to the dimethyl bridge and phenyl moieties, complexation occurred from the less hindered face to deliver the planar η⁶-benzene catalyst (**pR,pR**)-**1.19** as a single diastereomer. While facial blocking has been proven extremely effective in providing a single stereoisomer of planar chiral complex, it usually required lengthy ligand synthesis and only provided one stereoisomer of planar chiral complex.



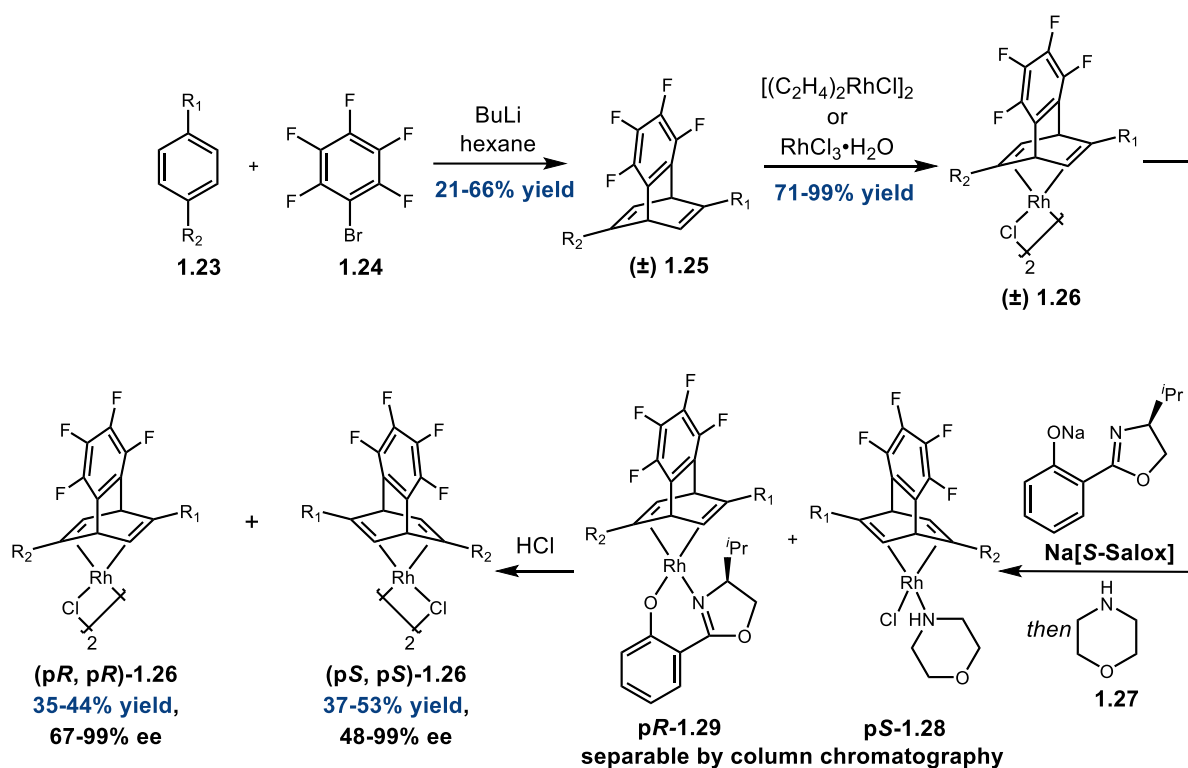
Scheme 1.4 Synthesis of the second facial blocking ligand developed by Perekalin.

Alongside developing facial blocking ligands, the Perekalin group has identified several labile chiral ligands to aid in the resolution of enantiomeric planar chiral complexes. In 2018, Perekalin and coworkers disclosed their planar chiral Cp catalyst **1.21** (Scheme 1.5). Direct cyclization of *tert*-butyl acetylene with $[\text{Rh}(\text{COD})\text{Cl}]_2$ delivered the racemic Rh(I) COD monomer **1.20**, then reduction of the exocyclic olefin and iodination provided the Rh(III) dimer **1.21**. Racemic **1.21** was complexed with L-proline to form a diastereomeric mixture. The resultant diastereomers were purified via fractional crystallization and dimer **1.21** was reconstituted with HCl.



Scheme 1.5 Perekalin and coworkers utilized L-proline in the resolution of racemic Cp complex.

Later in 2021, the Perekalin group utilized diastereomeric complexation to resolve another racemic catalyst (Scheme 1.6).¹⁹ Hexadiene ligand **1.25** was synthesized directly from pentafluorobromobenzene and 1,2-disubstituted benzene, and subsequent complexation delivered racemate **1.26**. Na[S-Salox] was complexed and the diastereomeric products (**1.27** and **1.28**, Scheme 1.6) were resolved via silica chromatography in the presence of morpholine. The enantiopure catalysts were then reconstituted with HCl. The use of labile ligands to resolve enantiomeric complexes was quite efficient. The Perekalin group showcased ligand-centric resolution of late-transition metal complexes while also maintaining concise syntheses.

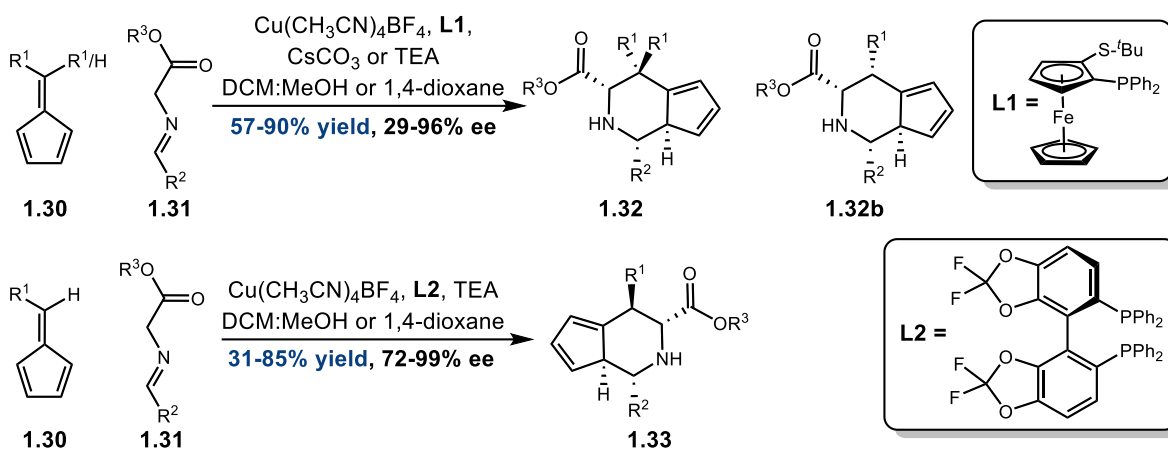


Scheme 1.6 The Perekalin synthesis of planar chiral cyclohexadiene complexes, using Na[S-Salox] to resolve the racemate.

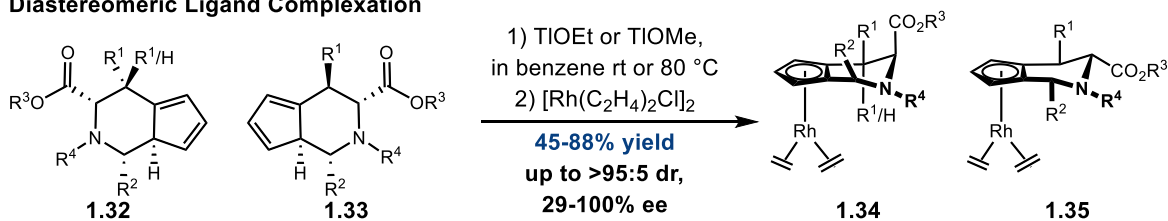
While we have examined cases where ligands with existing chirality are useful to access pure planar chiral catalysts, those chiral ligands usually require lengthy syntheses. Antonchick and Waldmann solved this problem in the context of their catalyst development program by employing chiral catalysis. Waldmann and coworkers utilized a Cu(I) catalyzed enantioselective [6+3] annulation as a critical tool for synthesizing a library of chiral JasCp ligands (Scheme 1.7).⁸ In one step, Cu(I) catalyzed annulation of feedstock fulvenes and imines delivered a variety of Cp compounds in enantioselective fashion. Waldmann and coworkers were able to deliver two stereochemical outcomes by choosing the correct ligand. The planar chiral ferrocenyl phosphine ligand (**L1**) produced *endo*-cyclized Cp rings, while the axially chiral phosphine ligand (**L2**) delivered the *exo*-products. This modular design allowed for rapid synthesis of Cp ligands with moderate to

great enantioselectivity, and subsequent complexation would proceed in diastereoselective fashion due to decoration around the Cp ligand. The JasCp library is a significant advance in planar chiral catalyst synthesis given that most of the JasCp ligands were made in one step and many of the resultant Rh(I) JasCp monomers are purified via flash chromatography.

Enantioselective Ligand Synthesis

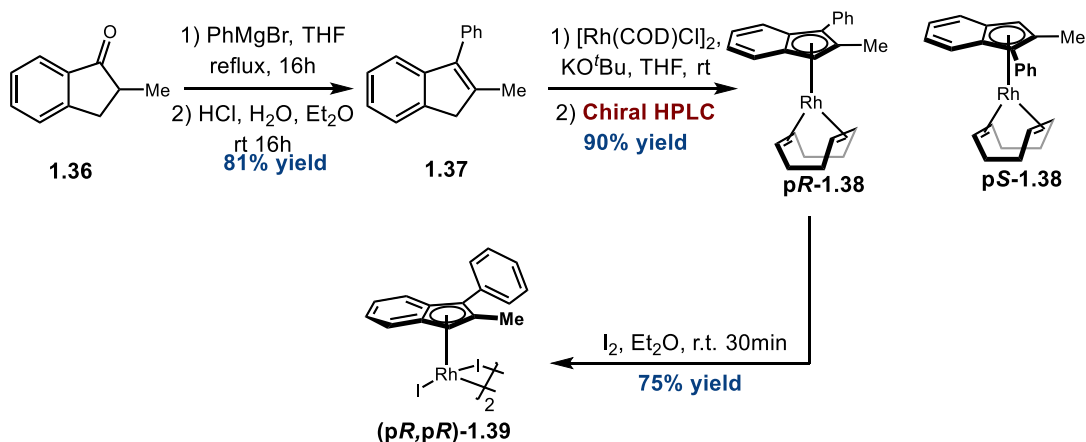


Diastereomeric Ligand Complexation



Scheme 1.7 The modular ligand synthesis from Antonchick and Waldmann.

In cases where there are no compatible chiral ligands to aid in resolving racemic complex or the ligand does not provide facial blocking, chiral preparatory HPLC is the last option for resolution. The Blakey group employed chiral preparatory HPLC in their synthesis of their planar chiral indenyl catalyst. The indenyl ligand **1.37** was synthesized in two steps from 2-methylindanone **1.36** and was easily complexed to form racemic Rh(I) COD monomer **1.38**. Unfortunately, complexation with *L*-proline was not amenable to



Scheme 1.8 Synthesis of the Blakey Indenyl Catalyst.

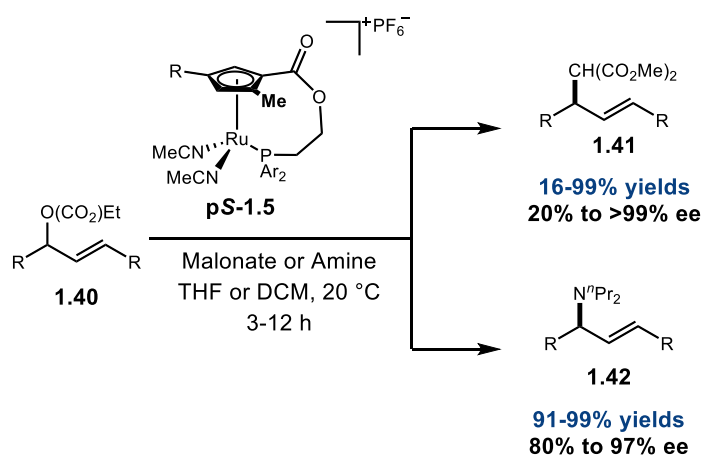
resolving the racemate and the monomer was purified via chiral preparatory HPLC, which severely limited catalyst production.

While chiral HPLC has been effective in the resolution of several planar chiral catalysts,^{20–22} it has been a limiting factor when it comes to producing catalyst libraries or even large quantities of enantiopure catalyst due to column loading limits and obtaining the requisite chiral column for resolution. In terms of producing a single isomer of planar chiral complex, diastereomeric complexation where the ligand contains other chiral information, is the most effective resolution strategy. Unfortunately incorporating additional chiral information into the ligand results in lengthy ligand synthesis. Even though there is not currently a ligand universally compatible with every racemic planar chiral complex, diastereomeric complexation of labile ligands remains the most promising method for a general method to resolve planar chiral complexes in the future. Employing chiral labile ligands unites concise ligand synthesis with diastereomer formation, which results in the facile separation of isomers via flash chromatography or recrystallization.

1.2 The Catalytic Activity of Late-Transition Metal Planar Chiral Complexes in Enantioselective Transformations

Late-transition metal planar chiral complexes are a tool in chiral catalysis that is growing in popularity. Planar chiral catalysts have been utilized in a variety of reactions from allylic substitution, polymerizations, and ene cascades. I will outline a few catalyst families that showcase the potency of planar chiral catalysis, although there are many more cases that have poor enantioinduction.

Takahashi was a pioneer in the field of planar chiral late transition metal catalysis and his group utilized a small library of tethered Cp Ru catalysts to great effect. Takahashi and coworkers report the substitution of allylic carbonates with amines and malonates catalyzed by **pS-1.5** in great yields and moderate to great enantioselectivity.^{11,23}

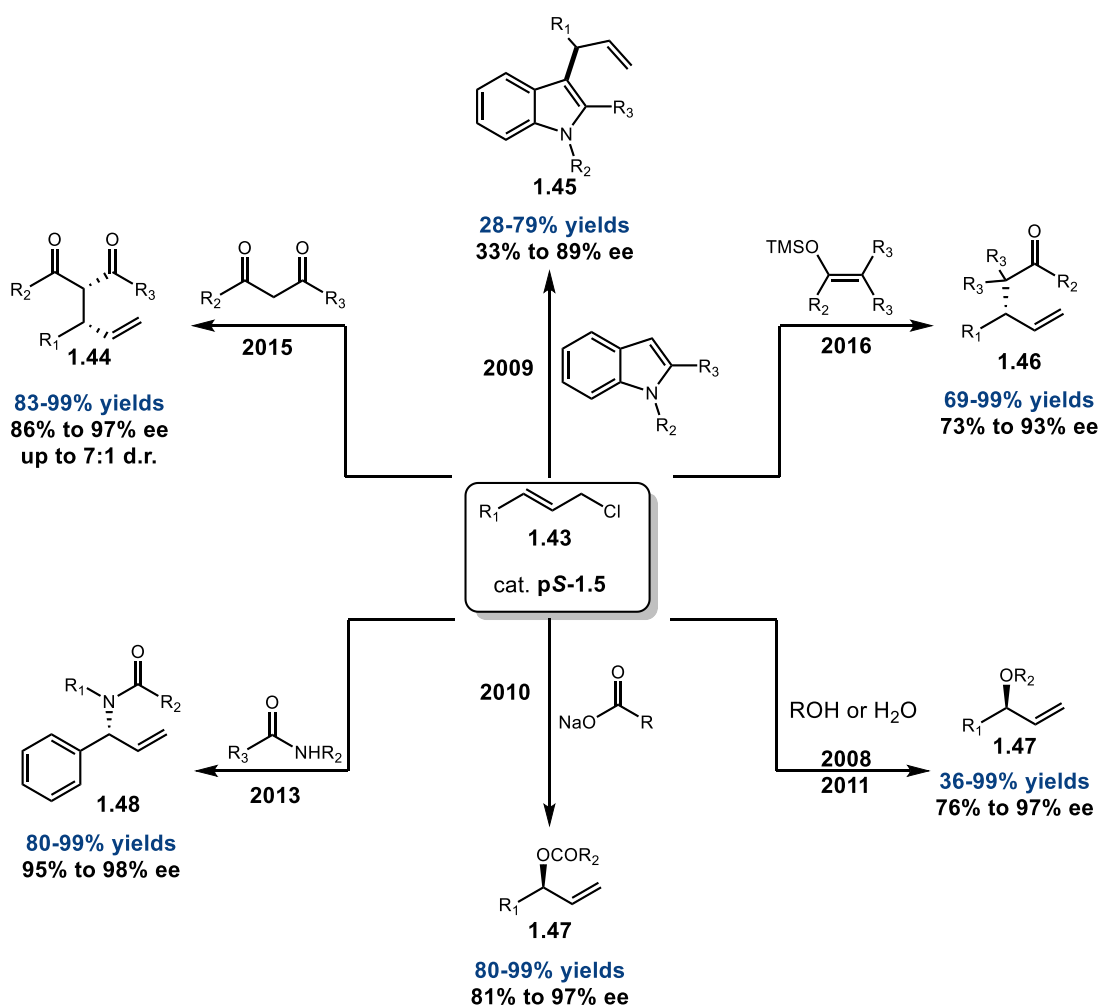


Scheme 1.9 Early Application of the Takahashi Catalysts in allylic substitution

Later, Onitsuka and coworkers carried the catalyst platform developed by Takahashi forward to substitution reactions with allylic chlorides. They were successful in substitution reactions with a variety of nucleophiles such as asymmetric malonates,²⁴ indoles,²⁵ alcohols,²⁶ water,²⁷ carboxylates,²⁸ and amides²⁹ (Scheme 1.10). In addition to broad nucleophile scopes, the tethered catalyst family also demonstrated good enantioselectivities (73% to 99% ee) and yields with a few exceptions. Onitsuka,

Kanbayashi and coworkers disclosed a series of allylic polymerization reactions using the previously developed substitution reactions, that also maintained excellent selectivities.^{30–32} The combined efforts of Takahashi, Onitsuka and Kanbayashi in allylic substitution showcased the ability of planar chiral complexes in imparting stereinduction across an array of reactions in the same class.

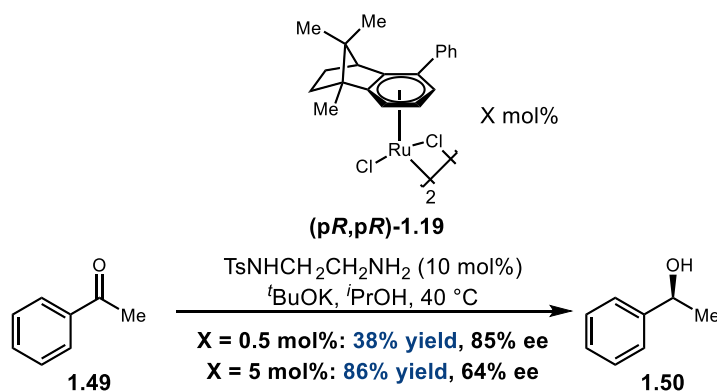
Asymmetric hydrogenation was another reaction class that many late-transition



Scheme 1.10 The full suite of intermolecular, monomeric allylic substitution reactions disclosed by Onitsuka and coworkers.

metal planar chiral complexes have been applied towards. While many of the catalysts were able to affect efficient conversion to the alcohol or amine products, stereinduction

remained low across an array of catalysts and examples (up to 64% ee).^{21,33–36} The best performing catalyst in this reaction class was the dimeric η^6 -benzene complex **1.19** from the Perekalin group (Scheme 1.11).¹⁸ With low catalyst loading they were able to achieve 85% ee, although the overall yield suffers, and higher catalyst loading improved yields but resulted in a decrease in enantioselectivity. Given that there are much more robust methods of asymmetric hydrogenation, such as enzymatic transformations,^{37,38} it is not likely that planar chiral catalysis will become a mainstay in this reaction class.

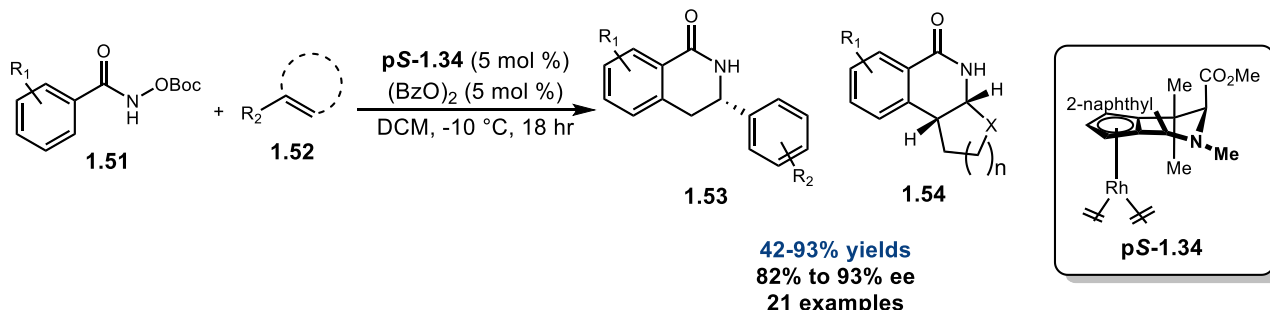


Scheme 1.11 Asymmetric hydrogen transfer reaction from the Perekalin Group.

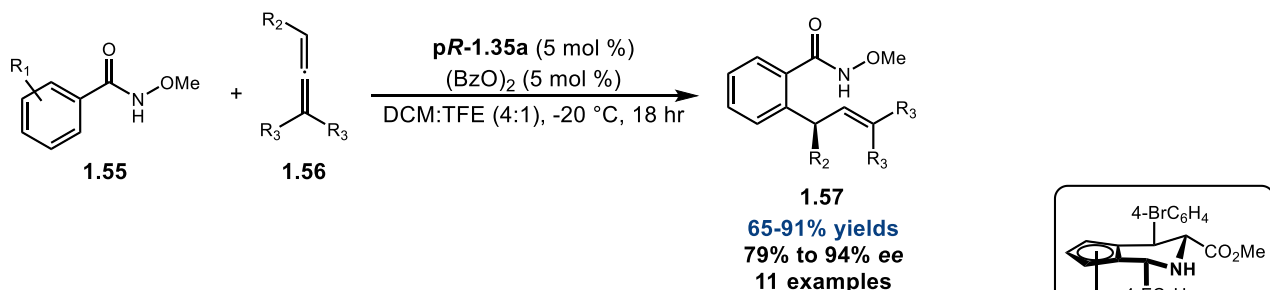
The JasCp Rh(I) catalysts developed by Antonchick and Waldmann were effective in several reactions. In the initial 2017 report, **1.34** catalyzed the cyclization of aryl hydroxamates with benzylic or internal olefins (Scheme 1.12, Generation of Isoquinolines).⁸ The catalyst maintained excellent stereoselectivity with moderate to great yields across 21 examples. Antonchick and Waldmann also utilized another catalyst to engage allenes in directed C–H functionalization to deliver chiral olefin products (Scheme 1.12, Allylation of Aryl Hydroxamate Esters).⁸ While **1.35a** was optimal for this set of reactions, the JasCp scaffold was once again efficacious in both yield and enantioinduction. The last method in the 2017 publication applied catalyst **1.35a** towards

C–H activation of benzamides to deliver axially chiral biaryl products.⁸ As with other JasCp reactions, **1.35a** maintained good yield and selectivities across a range of hydroxamate esters. Most recently Antonchick and Waldmann disclosed the JasCp Rh(I) catalyzed spirocyclization of α -arylidene pyrazolones and alkynes.³⁹ In this study, the

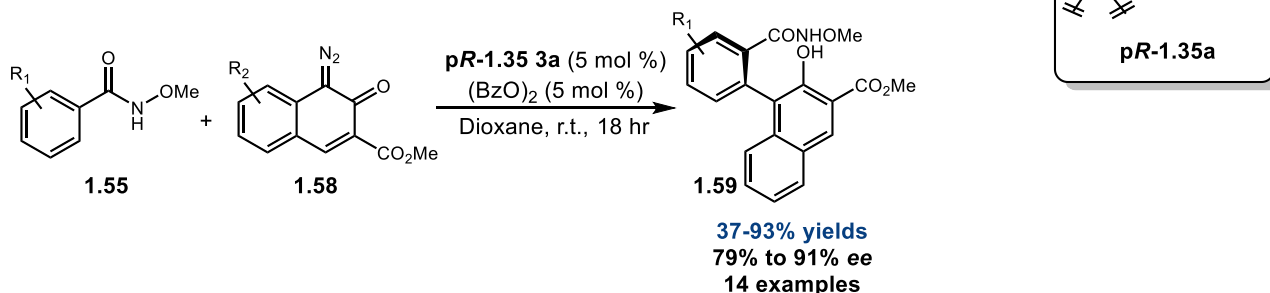
Generation of Isoquinolines



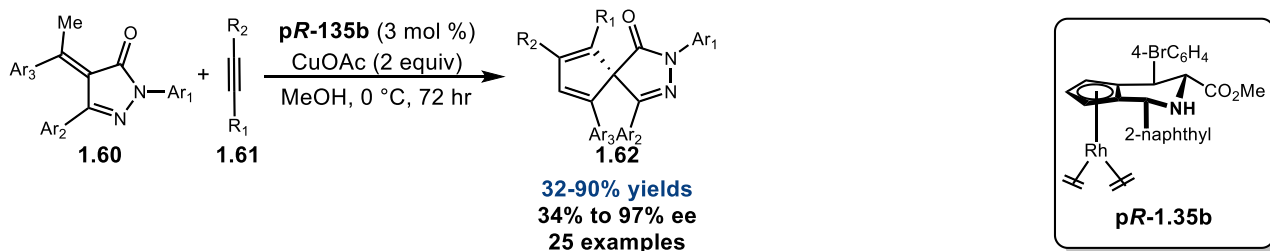
Allylation of Aryl Hydroxamate Esters



Generation of Axially Chiral Naphthols



Spirocyclization of Alkynes with α -Arylidene Pyrazolones



Scheme 1.12 The suite of enantioselective C–H functionalization reactions disclosed by Antonchick and Waldmann

modular library generated in previous investigations proved critical, as the enantioselectivity was boosted from 69% ee to 91% ee by utilizing catalyst **1.35b**. In addition to maintaining good yields and stereinduction with many examples, **1.35b** demonstrated tolerance for chiral alkyne substrates, which delivered several complex spirocyclic compounds. Antonchick, Waldmann, and coworkers have demonstrated the versatility of their catalyst platform, which was enabled by their modular synthesis of the planar chiral complex.

1.3 Conclusions

Late-transition metal planar chiral catalysts can be a powerful tool for stereinduction in organic synthesis. However, there are significant obstacles to the widespread use of planar chiral catalysts. One of the main barriers to utilizing planar chiral catalysts is the syntheses themselves. Shorter syntheses are typically indicative of simpler ligands and catalyst platforms, but usually require more extensive resolution techniques to provide pure catalyst. In contrast, lengthier syntheses usually provide more complex ligands and diastereomeric metal catalyst scaffolds, which are easily purified. At first glance, balancing synthetic ease and resolution/purification of the transition metal catalyst is a zero-sum game, but there have been several advances in the last decade to combat this trend. Antonchick and Waldmann demonstrated that effective stereoselective catalysis can be used to rapidly generate a family of ligands that can in turn generate diastereomeric planar chiral complexes which are easily purified. While this collaboration provided a conceptual advance in approaching planar chiral catalyst development, it is unlikely that it will be immediately exportable to existing planar chiral catalyst scaffolds. The Faller and Perekalin groups have shown diastereomeric complexation of labile

ligands is a potent method to resolve racemic complexes. Chiral labile ligands are more universal than single step generation of a chiral ligand library, but there are relatively few chiral ligands used to resolve late-transition metal complexes and they may not always be compatible with the planar chiral racemate that needs resolution. New methods of generating pure planar chiral complexes are needed to aid the field in advancing planar chiral catalysis.

1.4 References

- (1) Noyori, R. Asymmetric Catalysis: Science and Opportunities (Nobel Lecture 2001). *Adv. Synth. Catal.* **2003**, 345 (1–2), 15–32.
<https://doi.org/10.1002/ADSC.200390002>.
- (2) Steinlandt, P. S.; Zhang, L.; Meggers, E. Metal Stereogenicity in Asymmetric Transition Metal Catalysis. *Chem. Rev.* **2022**.
https://doi.org/10.1021/ACS.CHEMREV.2C00724/ASSET/IMAGES/LARGE/CR2C00724_0033.JPEG.
- (3) Hu, J.; Ferger, M.; Shi, Z.; Marder, T. B. Recent Advances in Asymmetric Borylation by Transition Metal Catalysis. *Chem. Soc. Rev.* **2021**, 50 (23), 13129–13188.
<https://doi.org/10.1039/D0CS00843E>.
- (4) Shu, T.; Cossy, J. Asymmetric Desymmetrization of Alkene-, Alkyne- and Allene-Tethered Cyclohexadienones Using Transition Metal Catalysis. *Chem. Soc. Rev.* **2021**, 50 (1), 658–666. <https://doi.org/10.1039/D0CS00666A>.
- (5) Cui, Y. M.; Lin, Y.; Xu, L. W. Catalytic Synthesis of Chiral Organoheteroatom Compounds of Silicon, Phosphorus, and Sulfur via Asymmetric Transition Metal-Catalyzed C–H Functionalization. *Coord. Chem. Rev.* **2017**, 330, 37–52.
<https://doi.org/10.1016/J.CCR.2016.09.011>.
- (6) Janssen-Müller, D.; Schleppehorst, C.; Glorius, F. Privileged Chiral N-Heterocyclic Carbene Ligands for Asymmetric Transition-Metal Catalysis. *Chem. Soc. Rev.* **2017**, 46 (16), 4845–4854. <https://doi.org/10.1039/C7CS00200A>.
- (7) Mas-Roselló, J.; Herraiz, A. G.; Audic, B.; Laverny, A.; Cramer, N. Chiral Cyclopentadienyl Ligands: Design, Syntheses, and Applications in Asymmetric Catalysis. *Angew. Chem. Int. Ed.* **2020**, 60 (24), 13198 – 13224.
<https://doi.org/10.1002/anie.202008166>.
- (8) Jia, Z.-J.; Merten, C.; Gontla, R.; Daniliuc, C. G.; Antonchick, A. P.; Waldmann, H. General Enantioselective C–H Activation with Efficiently Tunable Cyclopentadienyl Ligands. *Angew. Chem. Int. Ed.* **2017**, 56 (9), 2429–2434.
<https://doi.org/10.1002/anie.201611981>.
- (9) Cui, W. J.; Wu, Z. J.; Gu, Q.; You, S. L. Divergent Synthesis of Tunable Cyclopentadienyl Ligands and Their Application in Rh-Catalyzed Enantioselective Synthesis of Isoindolinone. *J. Am. Chem. Soc.* **2020**, 142 (16), 7379–7385.
<https://doi.org/10.1021/jacs.0c02813>.
- (10) Laws III, D.; Poff, C. D.; Heyboer, E. M.; Blakey, S. B. Synthesis, Stereochemical Assignment, and Enantioselective Catalytic Activity of Late Transition Metal Planar Chiral Complexes. *Chem. Soc. Rev.* **Manuscript accepted with revisions**.

- (11) Matsushima, Y.; Onitsuka, K.; Kondo, T.; Mitsudo, T. A.; Takahashi, S. Asymmetric Catalysis of Planar-Chiral Cyclopentadienylruthenium Complexes in Allylic Amination and Alkylation. *J. Am. Chem. Soc.* 123 (42) **2001**, 10405–10406. <https://doi.org/10.1021/ja016334l>.
- (12) Matsushima, Y.; Komatsuzaki, N.; Ajioka, Y.; Yamamoto, M.; Kikuchi, H.; Takata, Y.; Dodo, N.; Onitsuka, K.; Uno, M.; Takahashi, S. Synthesis and Properties of Planar-Chiral (η^6 -Benzene)(η^5 -Cyclopentadienyl)Ruthenium(II) Complexes in an Optically Pure Form. *Bull. Chem. Soc. Jap.* **2002**, 74 (3), 527–537. <https://doi.org/10.1246/BCSJ.74.527>.
- (13) Komatsuzaki, N.; Uno, M.; Kikuchi, H.; Takahashi, S. Synthesis and Property of Planar-Chiral Cyclopentadienyl-Ruthenium Complexes. *Chem. Lett.* **1996**, 8, 677–678. <https://doi.org/10.1246/cl.1996.677>.
- (14) Dodo, N.; Matsushima, Y.; Uno, M.; Onitsuka, K.; Takahashi, S. Synthesis of Ruthenium Complexes with Planar-Chiral Cyclopentadienyl-Pyridine or -Phosphine Bidentate Ligands. *J. Chem. Soc. Dalton Trans.* **2000**, 1, 35–41. <https://doi.org/10.1039/a907145h>.
- (15) Faller, J. W.; D'alliessi, D. G. Planar Chirality in Tethered η^6 : η^1 - (Phosphinophenylenearene-P)Ruthenium(II) Complexes and Their Potential Use as Asymmetric Catalysts. *Organometallics* **2003**, 22, 2749–2757. <https://doi.org/10.1021/om030080q>.
- (16) Faller, J. W.; Fontaine, P. P. Resolution and Diels - Alder Catalysis with Planar Chiral Arene-Tethered Ruthenium Complexes. *Organometallics* **2005**, 24 (17), 4132–4138. <https://doi.org/10.1021/om0501226>.
- (17) Pototskiy, R. A.; Kolos, A. V.; Nelyubina, Y. V.; Perekalin, D. S. Rhodium Catalysts with a Chiral Cyclopentadienyl Ligand Derived from Natural R-Myrtenal. *Eur. J. Org. Chem.* **2020**, 2020 (37), 6019–6025. <https://doi.org/10.1002/ejoc.202001029>.
- (18) Pototskiy, R. A.; Boym, M. A.; Nelyubina, Y. V.; Perekalin, D. S. Synthesis of Ruthenium Catalysts with a Chiral Arene Ligand Derived from Natural Camphor. *Synthesis* **2022**, 54 (21), 4721–4726. <https://doi.org/10.1055/A-1668-2075>.
- (19) Ankudinov, N. M.; Chusov, D. A.; Nelyubina, Y. V.; Perekalin, D. S. Synthesis of Rhodium Complexes with Chiral Diene Ligands via Diastereoselective Coordination and Their Application in the Asymmetric Insertion of Diazo Compounds into E–H Bonds. *Angew. Chem. Int. Ed.* **2021**, 60 (34), 18712–18720. <https://doi.org/10.1002/ANIE.202105179>.
- (20) Dou, X.; Hayashi, T. Synthesis of Planar Chiral Shvo Catalysts for Asymmetric Transfer Hydrogenation. *Adv. Synth. Catal.* **2016**, 358 (7), 1054–1058. <https://doi.org/10.1002/adsc.201501162>.

- (21) Bai, X.; Cettolin, M.; Mazzocanti, G.; Pierini, M.; Piarulli, U.; Colombo, V.; Dal Corso, A.; Pignataro, L.; Gennari, C. Chiral (Cyclopentadienone)Iron Complexes with a Stereogenic Plane as Pre-Catalysts for the Asymmetric Hydrogenation of Polar Double Bonds. *Tetrahedron* **2019**, 75 (10), 1415–1424. <https://doi.org/10.1016/j.tet.2019.01.057>.
- (22) Farr, C. M. B.; Kazerouni, A. M.; Park, B.; Poff, C. D.; Won, J.; Sharp, K. R.; Baik, M. H.; Blakey, S. B. Designing a Planar Chiral Rhodium Indenyl Catalyst for Regio- And Enantioselective Allylic C-H Amidation. *J. Am. Chem. Soc.* **2020**, 142 (32), 13996–14004. <https://doi.org/10.1021/jacs.0c07305>.
- (23) Onitsuka, K.; Matsushima, Y.; Takahashi, S. Kinetic Resolution of Allyl Carbonates in Asymmetric Allylic Alkylation Catalyzed by Planar-Chiral Cyclopentadienyl-Ruthenium Complexes. *Organometallics* **2005**, 24, 6472–6474. <https://doi.org/10.1021/om050739n>.
- (24) Kanbayashi, N.; Hosoda, K.; Kato, M.; Takii, K.; Okamura, T.-A.; Onitsuka, K. Enantio- and Diastereoselective Asymmetric Allylic Alkylation Catalyzed by a Planar-Chiral Cyclopentadienyl Ruthenium Complex. *Chem. Commun.* **2015**, 51, 10895. <https://doi.org/10.1039/c5cc02414e>.
- (25) Onitsuka, K.; Kameyama, A. C.; Sasai, H. Regio- and Enantioselective Allylation of Indole Catalyzed by a Planar-Chiral Cyclopentadienyl-Ruthenium Complex. *Chem. Lett.* **2009**, 38, 444–445. <https://doi.org/10.1246/cl.2009.444>.
- (26) Onitsuka, K.; Okuda, H.; Sasai, H. Regio- and Enantioselective O-Allylation of Phenol and Alcohol Catalyzed by a Planar-Chiral Cyclopentadienyl Ruthenium Complex. *Angew. Chem. Int. Ed.* **2008**, 47 (8), 1454–1457. <https://doi.org/10.1002/anie.200704457>.
- (27) Kanbayashi, N.; Onitsuka, K. Ruthenium-Catalyzed Regio- and Enantioselective Allylic Substitution with Water: Direct Synthesis of Chiral Allylic Alcohols. *Angew. Chem. Int. Ed.* **2011**, 50 (22), 5197–5199. <https://doi.org/10.1002/anie.201101078>.
- (28) Kanbayashi, N.; Onitsuka, K. Enantioselective Synthesis of Allylic Esters via Asymmetric Allylic Substitution with Metal Carboxylates Using Planar-Chiral Cyclopentadienyl Ruthenium Catalysts. *J. Am. Chem. Soc.* **2010**, 132, 1206–1207. <https://doi.org/10.1021/ja908456b>.
- (29) Kanbayashi, Naoya; Takenaka, Kazuhiro; Okamura, Taka-aki; Onitsuka, K. Asymmetric Auto-Tandem Catalysis with a Planar-Chiral Ruthenium Complex: Sequential Allylic Amidation and Atom-Transfer Radical Cyclization. *Angew. Chem. Int. Ed.* **2013**, 52, 4897–4901. <https://doi.org/10.1002/anie.201300485>.
- (30) Ishido, Y.; Kanbayashi, N.; Okamura, T.-A.; Onitsuka, K. Synthesis of Nonnatural Helical Polypeptide via Asymmetric Polymerization and Reductive Cleavage of N–O

Bond. *Macromolecules* **2017**, 50, 5301–5307.
<https://doi.org/10.1021/acs.macromol.7b01426>.

(31) Kanbayashi, N.; Okamura, T.-A.; Onitsuka, K. New Method for Asymmetric Polymerization: Asymmetric Allylic Substitution Catalyzed by a Planar-Chiral Ruthenium Complex. *Macromolecules* **2014**, 47, 4178–4185. <https://doi.org/10.1021/ma5008623>.

(32) Kanbayashi, N.; Okamura, T.-A.; Onitsuka, K. New Synthetic Approach for Optically Active Polymer Bearing Chiral Cyclic Architecture: Combination of Asymmetric Allylic Amidation and Ring-Closing Metathesis Reaction. *Macromolecules* **2015**, 48, 8437–8444. <https://doi.org/f>.

(33) Yamamoto, Y.; Yamashita, K.; Nakamura, M. Synthesis of Organometallic Analogues of Spirocyclic C-Arylribosides. *Organometallics* **2010**, 29, 1472–1478. <https://doi.org/10.1021/om100043f>.

(34) Hopewell, J. P.; Martins, J. E. D.; Johnson, T. C.; Godfrey, J.; Wills, M. Organic & Biomolecular Chemistry Developing Asymmetric Iron and Ruthenium-Based Cyclone Complexes; Complex Factors Influence the Asymmetric Induction in the Transfer Hydrogenation of Ketones. *Org. Biomol. Chem.* **2012**, 10, 145. <https://doi.org/10.1039/c1ob06010d>.

(35) Johnson, T. C.; Clarkson, G. J.; Wills, M. (Cyclopentadienone)Iron Shvo Complexes: Synthesis and Applications to Hydrogen Transfer Reactions. *Organometallics* **2011**, 30 (7), 1859–1868. <https://doi.org/10.1021/om101101r>.

(36) Grosso, A. Del; Chamberlain, A. E.; Clarkson, G. J.; Wills, M. Synthesis and Applications to Catalysis of Novel Cyclopentadienone Iron Tricarbonyl Complexes. *Dalton Trans.* **2018**, 47, 1470. <https://doi.org/10.1039/c7dt03250a>.

(37) Moore, J. C.; Pollard, D. J.; Kosjek, B.; Devine, P. N. Advances in the Enzymatic Reduction of Ketones. *Acc. Chem. Res.* **2007**, 40 (12), 1412–1419. https://doi.org/10.1021/AR700167A/ASSET/IMAGES/MEDIUM/AR-2007-00167A_0014.GIF.

(38) Rachwalski, M.; Vermue, N.; Rutjes, F. P. J. T. Recent Advances in Enzymatic and Chemical Deracemisation of Racemic Compounds. *Chem. Soc. Rev.* **2013**, 42 (24), 9268–9282. <https://doi.org/10.1039/C3CS60175G>.

(39) Li, H.; Gontla, R.; Flegel, J.; Merten, C.; Ziegler, S.; Antonchick, A. P.; Waldmann, H. Enantioselective Formal C(Sp³)-H Bond Activation in the Synthesis of Bioactive Spiropyrazolone Derivatives. *Angew. Chem. Int. Ed.* **2019**, 58 (1), 307–311. <https://doi.org/10.1002/anie.201811041>.

Chapter 2. Progress towards the Enantioselective Synthesis of Planar Chiral Indenyl Complexes and Design of Planar Chiral Rh(III) Indenyl Catalysts

The Blakey Group catalyst development program has largely been in the context of rhodium catalyzed allylic functionalization. We will discuss significant contributions to the field of rhodium and iridium catalyzed allylic functionalization before the disclosure of the Blakey Indenyl catalyst. Then we will detail the development of the 2-methyl-3-phenylindenyl Rh(III) catalyst that has been the cornerstone of the stereoselective chemistry developed in the Blakey group over the last 5 years. One of the main bottlenecks to synthesizing the flagship Blakey catalyst is in the resolution of the precursor racemate. We will discuss work to develop a method to enantioselectively synthesize indenyl planar chiral complexes and another project to provide a small library of electronically biased complexes to probe new reactivity.

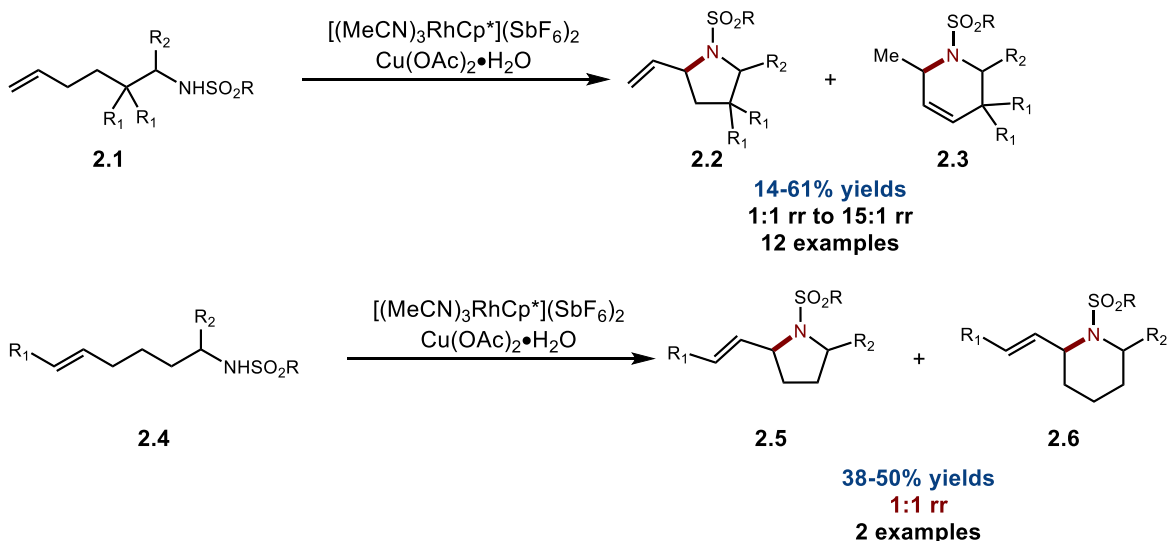
2.1 Recent Advances in Rh and Ir Catalyzed Allylic C–H Functionalization

Until the last decade, allylic functionalization has largely been driven by Pd catalysis which was pioneered by White and colleagues, but was limited to terminal olefins at the time.^{40–45} However, rhodium and iridium catalysis has been important in recent allylic C–H activation advances to access different nucleophiles and less activated olefins. Significant contributions from Blakey, Rovis, and Glorius have enabled allylic amination, amidation, etherification, alkylation, and arylation with activated and unactivated olefins.^{46–55}

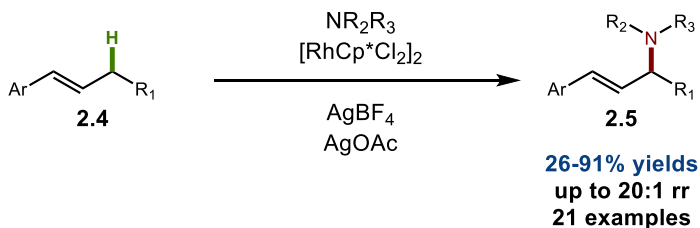
Seminal publications from Cossy and Tanaka laid the foundation for Group IX allylic C–H functionalization by exploring intramolecular amination reactions. In 2012,

Cossy and coworkers realized an intramolecular allylic amination reaction utilizing a rhodium pentamethylcyclopentadienyl (Cp^*) catalyst (Scheme 2.1).⁵⁶ A few substrates from the Cossy report included internal olefins, and while the regioselectivity for these reactions was nonexistent, it did pave the way for others to develop regioselective functionalizations of internal olefins. Later, Tanaka and coworkers led mechanistic investigations into Rh catalyzed amination, revealing it proceeded through a π -allyl intermediate.⁵⁷ In 2017, the Blakey group built upon this foundation and reported a Rh(III) catalyzed intermolecular amination of a series of activated internal olefins (Scheme 2.1).⁴⁶ In addition to being the first reported Rh catalyzed intermolecular allylic amination, a variety of amine nucleophiles were explored, and asymmetric olefins exhibited modest to

Cossy 2012



Blakey 2017

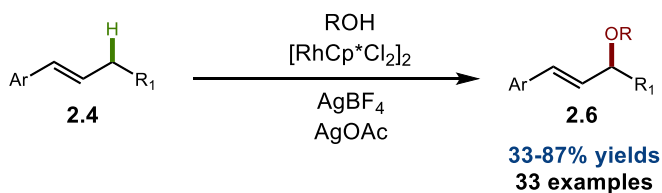


Scheme 2.1 The intramolecular allylic amination reported by Cossy in 2012, and the intermolecular allylic amination of internal olefins from Blakey 2017.

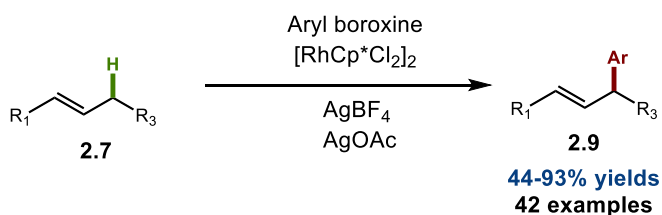
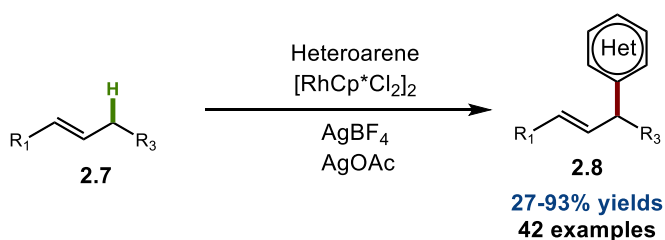
excellent regioselectivity. Jeganmohan provided an analogous study in 2019 that mirrored the earlier disclosure from the Blakey group.⁵⁸

Later, the Blakey group reported an intermolecular allylic etherification (Scheme 2.2).⁴⁷ The etherification was effective with internal olefins, was applicable to a variety of alcohols in decent to good yields and demonstrated exclusive selectivity for the conjugated olefin products. While this etherification method tolerated stereogenic alcohols, little to no diastereoselectivity was observed. Glorius explored allylic C–H arylation in 2018 and 2019 (Scheme 2.2).^{50,51} In their initial study, the Glorius group were only able to engage electron rich heteroaromatic aryl groups in intermolecular allylic functionalization of internal and external olefins.⁵⁰ Later, the Glorius group accessed more mundane aryl groups in allylic functionalization by utilizing aryl boroxines instead of

Blakey Etherification - 2018



Glorius Arylation - 2018, 2019

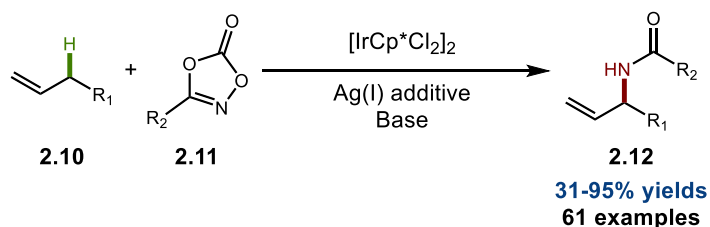


Scheme 2.2 The Blakey etherification procedure and the Glorius arylation methods.

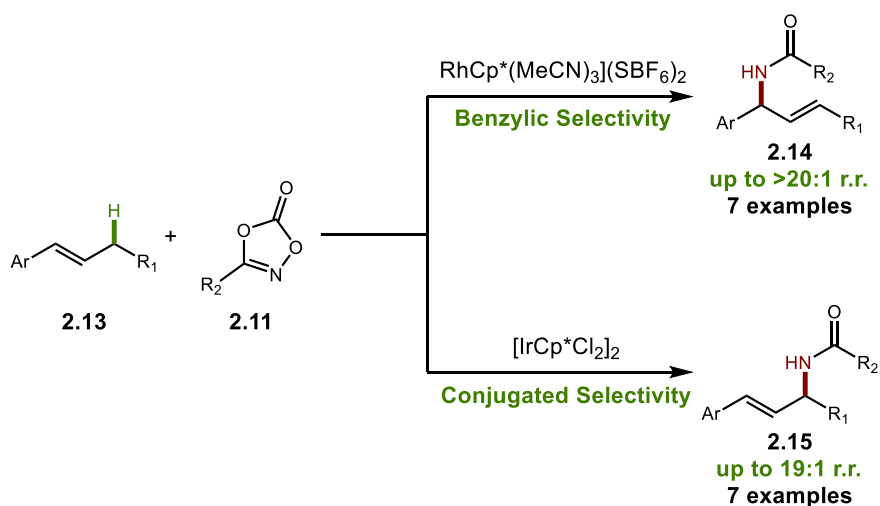
relying on C–H activation of the aryl fragment.⁵¹ These initial publications exemplified how effective

The use of dioxazolones as amidating reagents marked a shift in the field of Group IX allylic functionalization. Popularized by the Chang group,⁵⁹ dioxazolones (**2.11**, Scheme 2.3) removed the requirement for external oxidants, with the N–O bond functioning as an internal oxidant and were found to enable inner sphere nucleophilic addition. Several groups reported on the activity of dioxazolones in Rh and Ir catalyzed allylic amidations. In 2019, Rovis and Glorius independently reported on Ir catalyzed allylic amidation of terminal olefins and observed good yields and excellent regioselectivity for a range of olefins and dioxazolones coupling partners.^{52,54} Notably,

Glorius and Rovis - Independent Publications 2019



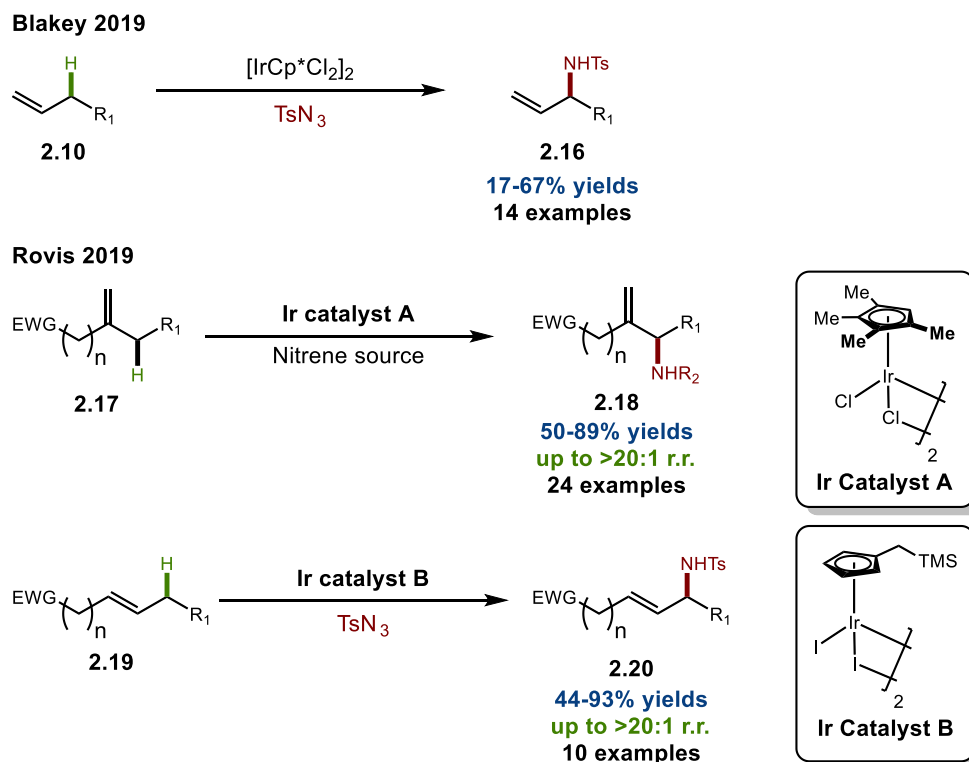
Blakey - 2019



Scheme 2.3 Regioselective Rh and Ir catalyzed allylic C–H amidation reactions disclosed in 2019.

protected amines, silyl ethers, alkyl ethers, halides, and nitriles were tolerated functional groups. While the Glorius group investigated a few internal olefins in their report, the Blakey group disclosed a closer study into the Rh/Ir catalyzed amidation of internal olefins.⁴⁸ The Blakey group found that Rh catalysis was selective for the benzylic functionalized products, while Ir was selective for the conjugated products. However, the Ir catalyst bias was not enough to overcome inherent selectivity for the benzylic functionalized products in some cases, and only resulted in reduced regioselectivity when compared to the Rh reaction.

Tosyl azide was another nitrenoid precursor that was explored in the context of allylic functionalization. Concurrent reports from the Blakey and Rovis groups evaluated a variety of terminal olefins and found moderate to good yields and exclusive selectivity



Scheme 2.4 The regioselective sulfamidation of terminal olefins from the Blakey Group, and the highly regioselective functionalizations disclosed by the Rovis Group.

for the branched olefin product.^{49,55} The Rovis group were able to identify a subtle electronic effect due to distal electron withdrawing groups to significantly influence regioselectivity. In the case of 1,1-disubstituted olefins, distal electronic groups were able to direct functionalization to the furthest allylic carbon center. While this effect was also observed in 1,2-substituted olefins, less hindered Cp ligands were needed to improve selectivity and yield.

Up to this point, there have been a range of regioselective functionalizations of activated and unactivated olefins. However, an enantioselective C–H functionalization reaction had not been disclosed with Rh or Ir catalysis. The Blakey group turned to catalyst development to address this problem.

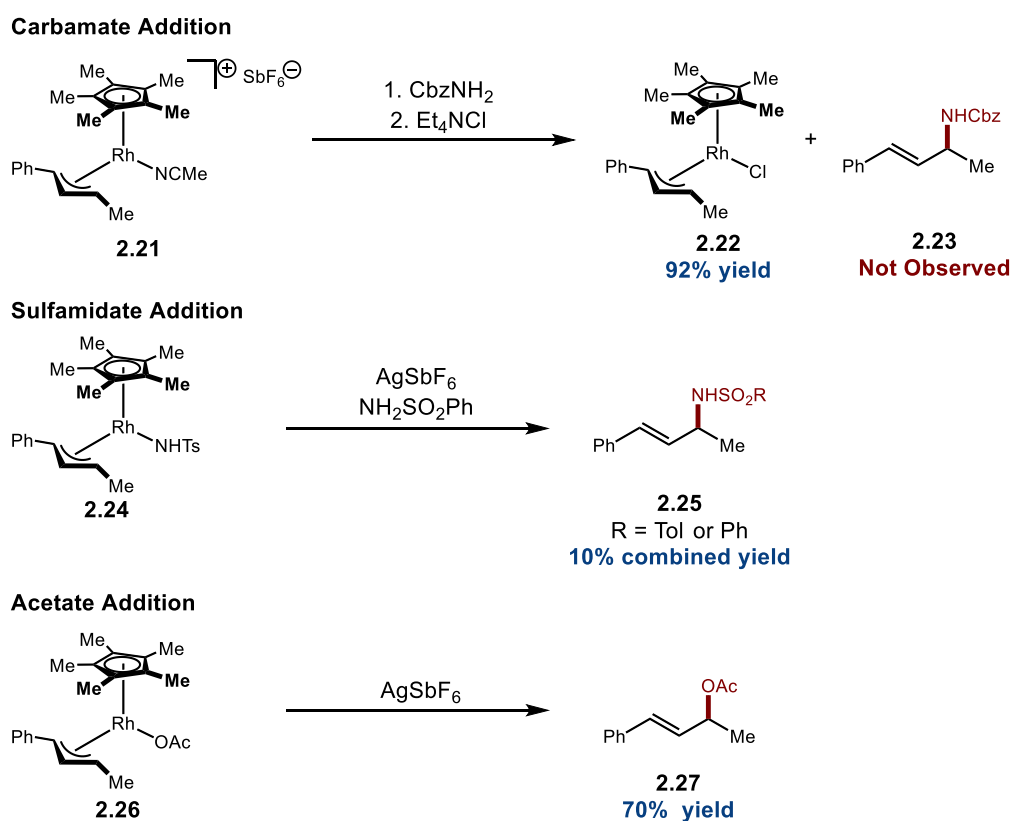
2.2 The Development of the Blakey Indenyl Catalyst

2.2.1 Mechanistic Insight into Allylic Functionalization using External Oxidants

While significant developments were made in Rh and Ir catalyzed allylic C–H functionalization before 2020, a stereoselective version of these reactions had not been discovered. Previous efforts by Dr. Jacob Burman to use chiral Cp catalysts in allylic C–H functionalization proved ineffective. The Blakey group sought to overcome this challenge, but first more mechanistic insight was required. Work conducted by the Blakey, Baik, and Macbeth groups reported their investigations into the amination mechanism in 2020.⁶⁰

Firstly, reaction rate experiments determined allylic amination with Cbz-NH and 1,3-diphenylpropene to be first order in Rh and olefin, and inversely proportionate to carbamate concentration. Kinetic isotope experiments determined allylic functionalization

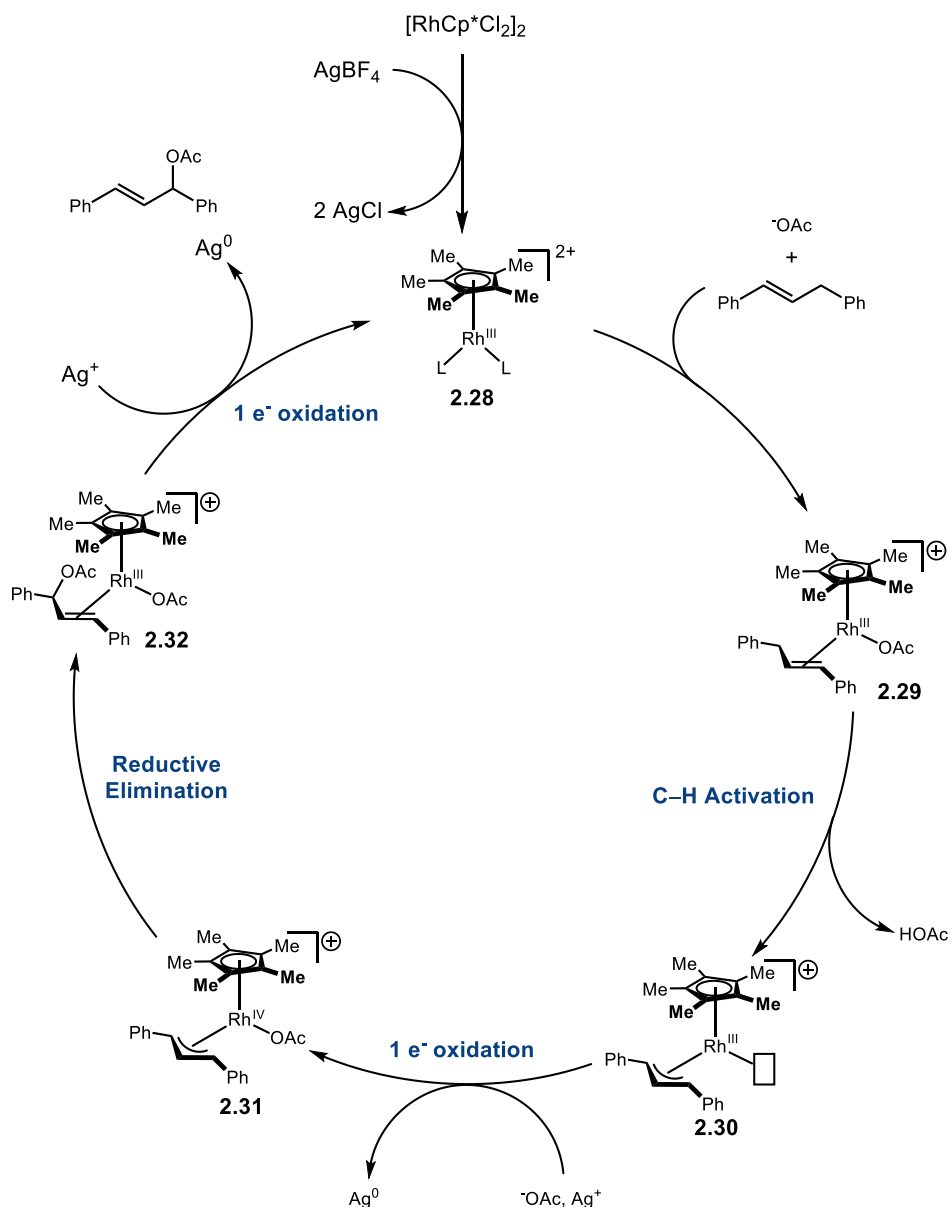
to be the rate-determining step (with a KIE of $k_H/k_D = 2.6$). Next, several π -allyl complexes were synthesized to observe reactivity with carbamate, sulfonamide, and acetates. Complexes **2.21** and **2.24** displayed little to no reactivity in the presence of carbamates or sulfonamides, which are known to form allylic functionalization products. However, complex **2.26** efficiently delivered the requisite allylic acetate in the presence of Ag(I) oxidant. Density functional theory (DFT) studies revealed the Rh(III) was more likely to be oxidized to Rh(IV) and reductively eliminate than oxidize to Rh(V) or directly eliminate from Rh(III) to Rh(I). Computation experiments also revealed the allylic acetate could readily undergo S_N1 substitution to deliver the aminated product.



Scheme 2.5 Reactivity of several Rh π -allyl complexes to determine the initial reductive elimination product.

The combination of experimental and computational studies helped elucidate the mechanism proposed by Blakey and coworkers (Scheme 2.6).⁶⁰ Halide abstraction

provides cationic catalyst **2.28**. Subsequent olefin coordination and irreversible C–H cleavage delivers π -allyl complex **2.30**. Single electron oxidation and coordination delivers acetate complex **2.31**. Facile reductive elimination delivers the allylic acetate, which then undergoes off-metal S_N1 substitution to deliver the allylic amination product. Given that the key bond forming step occurs off-metal, developing a stereoselective version of these reactions would be impossible from a catalyst development standpoint.



Scheme 2.6 The catalytic cycle proposed by Blakey and coworkers.

However, the exploration of dioxazolones in allylic functionalization revealed a new reaction paradigm. The dioxazolone reagent contains an internal oxidant in the N–O bond, which allows for oxidation to the Rh(V) nitrenoid, which readily undergoes reductive elimination. With the inclusion of dioxazolones, the development of chiral catalysts to enact allylic functionalization became an attractive prospect.

2.2.2 Development of the Blakey Indenyl Catalyst

Rh and Ir catalyzed allylic functionalization has largely been conducted by derivatives of cyclopentadienyl complexes. When the Blakey group sought to develop enantioselective allylic functionalization reactions, they naturally looked to existing chiral Cp catalyst scaffolds. Many chiral Cp Rh and Ir complexes have been synthesized over the last decade (Figure 2.1). The most popular of these catalysts were the Cramer complexes (**2.33** and **2.35**), which required 8-9 steps to access.^{61,62} The Rovis and Ward

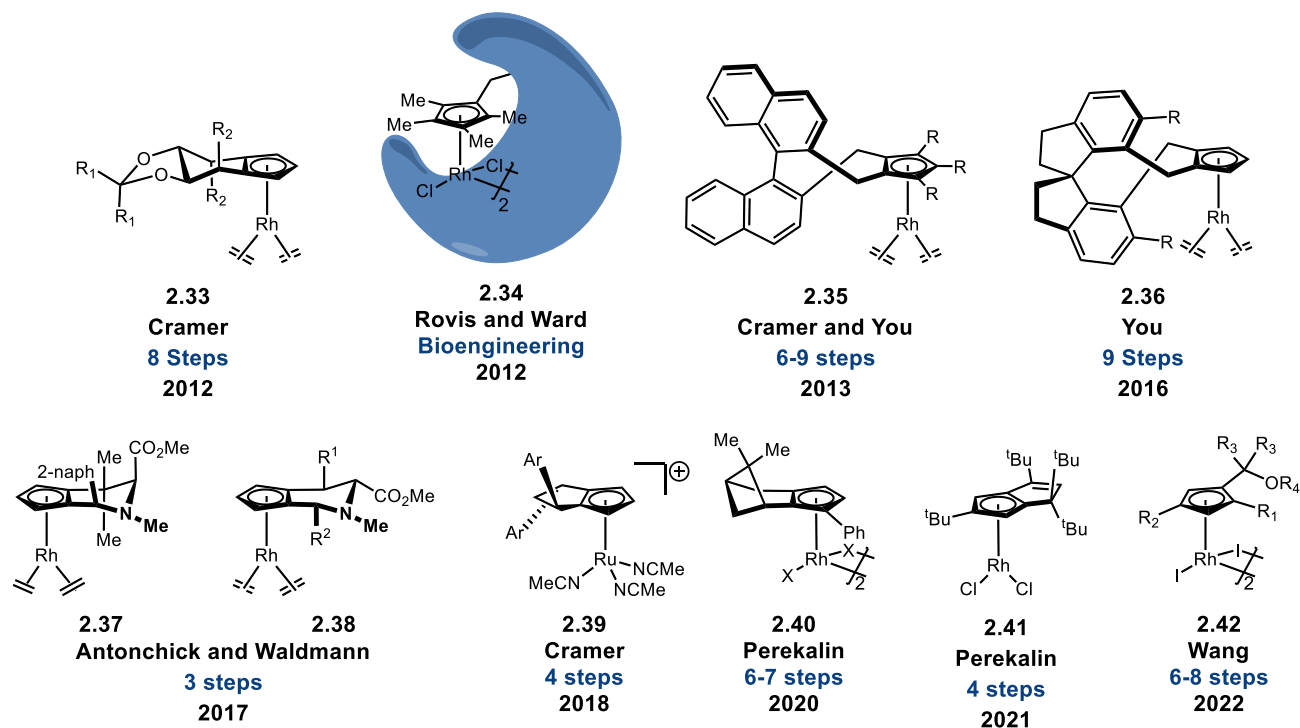
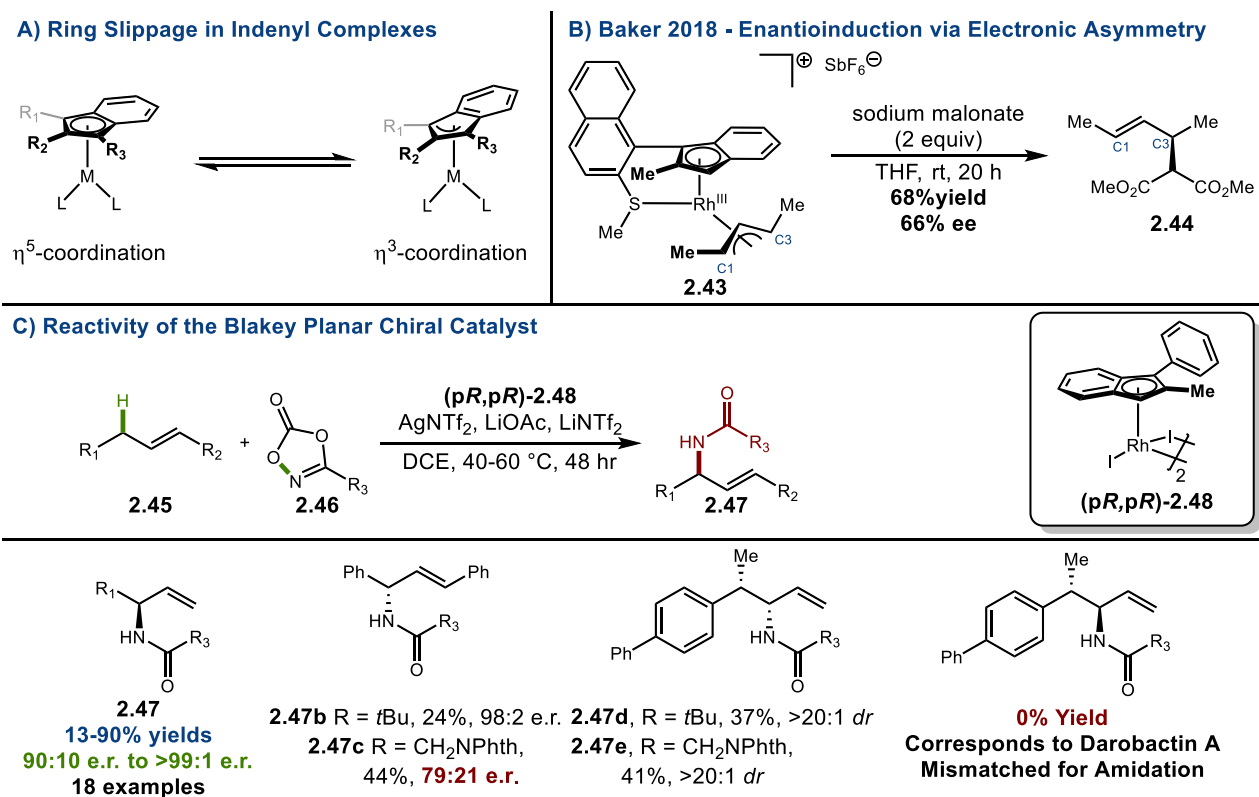


Figure 2.1 A selection of chiral Cp catalysts used in stereoselective transformations over the last decade.

construct **2.34** required bioengineering techniques and while readily evolvable, it was not universally easy to prepare.⁶³ Significant contributions from Cramer,⁶⁴ You,^{65,66} Antonchick, Waldmann,⁶⁷ Perekalin,^{68–70} Wang⁷¹ have built the chiral Cp catalyst catalog into a true library. However, given the relative difficulty in accessing some chiral Cp catalysts, and the desire to probe new reaction space, the Blakey group looked for an alternative to existing Cp scaffolds.

Indenyl ligands are an exciting alternative to Cp ligands due to the expanded π -system allowing for ring slippage from the η^5 to η^3 coordination modes (Scheme 2.7, A). This ring slippage allows for much faster reaction rates in ligand association (especially at congested metal centers).^{72–74} This ring slippage also results in electronic asymmetry



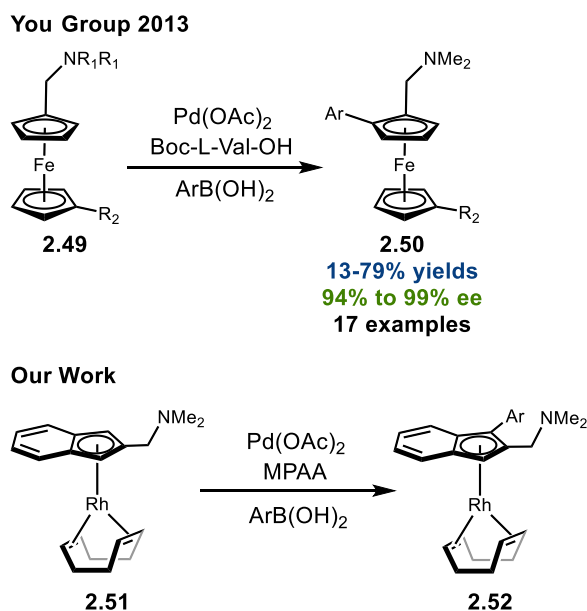
Scheme 2.7 A) Demonstration of indenyl ring slippage. B) Baker Enantioinduction Study. C) Reactivity of Blakey Planar Chiral Indenyl Catalyst

int the indenyl complex. The Blakey group hypothesized that this electronic asymmetry could be leveraged into stereoselective reactions. The 2018 study from Baker *et al.* demonstrated that planar chiral π -allyl complex **2.43** could undergo malonate addition and was able to transfer stereochemical information to the resulting allylic malonate **2.44** (Figure 2.2, B).⁷⁵ While this reaction was stoichiometric and had moderate enantioselectivity, it established that indenyl ligands could transfer asymmetry to π -allyl substrates. The Blakey group sought to pare down the synthetic complexity of the Baker complex to reduce the overall synthetic steps and free a coordination site for inner-sphere nucleophilic addition. Ultimately, the Blakey group removed the chiral sulfinyl group and replaced the naphthyl substituent with phenyl to arrive at 2-methyl-3-phenylindenyl complex **2.48**.⁷⁶

While the Baker complex indicated outer sphere nucleophilic addition would result in enantioinduction, the Blakey group assumed that forcing an inner-sphere addition would increase catalyst control over stereoselectivity. This hypothesis was proven right when catalyst **2.48** was applied towards allylic amidation using dioxazolones.⁷⁶ The new indenyl catalyst displayed excellent enantioselectivity across an array of olefins and dioxazolone nucleophiles. The enantioselective amidation led us to look at potential amino acid targets to apply our chemistry. While this was exciting reactivity, the catalyst did struggle with some internal olefins and olefins with alpha chiral centers. In the case of darobactin A, an exciting peptide natural product, the catalyst system was unable to produce the desired diastereomer in a model study due to a mismatch scenario. We attempted to address these obstacles, as well as probe new reactivity, through a new round of catalyst development.

2.3 Enantioselective Synthesis of Planar Chiral Rhodium Catalysts

The main choking point of the synthesis of planar chiral catalyst **2.48** was the dependence on chiral HPLC to provide enantiopure complex. New HPLC methods must be developed for each catalyst variant and small quantities of eluent are loaded onto the chiral column to ensure sufficient separation of the enantiomers. These constraints made systematic variation of the precursor complex a time-consuming process. Therefore, we aimed to develop a concise synthesis of Rh(III) complexes that enabled modularity and precluded the need for chiral HPLC. The enantioselective arylation of ferrocenyl complexes disclosed by the You Group was an attractive methodology to begin our exploration into enantioselective catalyst generation due to its cheap chiral ligand, a mono-protected amino acid (MPAA), and high enantioinduction (Scheme 2.8).⁷⁷ While You and coworkers only utilized protected valine, they adapted chemistry from the Jin-

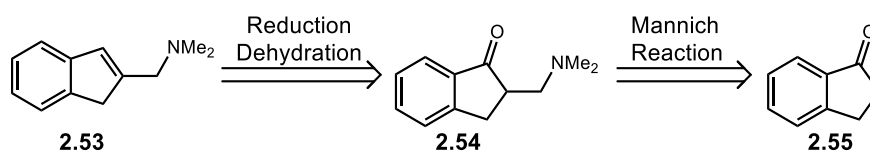


Scheme 2.8 Our plan to adapt the You group's enantioselective arylation of transition metal complexes.

Quan Yu group which explored several MPAA's in a range of transformations.^{78–80} This inspired us to revise our synthetic approach of our Rh(III) complexes. By incorporating an amine directing group to the indenyl scaffold, we envisioned engaging prochiral rhodium complexes in enantioselective functionalization to deliver a library of rhodium indenyl catalysts and circumvent the need for chiral HPLC.

2.3.1 Synthesis

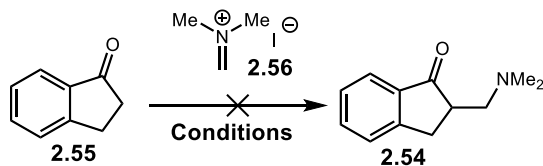
In order to investigate enantioselective arylation, we first needed to synthesize our ligand bearing a directing group. Tertiary amines were the directing group of choice in the enantioselective functionalization of ferrocenes disclosed by You, so dimethylamino ligand **2.53** was chosen as our target indene. The indene would be readily accessible from reduction and subsequent dehydration of the indanone **2.54**. And aminomethylation of indanone **2.55** would be achieved through Mannich aminoalkylation.



Scheme 2.9 Retrosynthesis of the N,N-dimethylaminomethyl indene ligand.

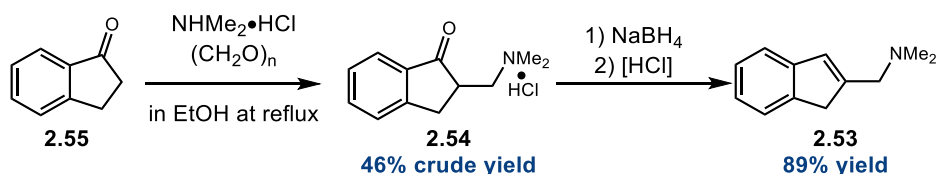
We employed traditional Mannich alkylation procedures using preformed Eschenmoser's salt to no avail (Table 2.1). Although the aminomethylation of indanone was known, commercial and freshly prepared Eschenmoser's salt (**2.56**) did not provide the desired indanone **2.54**.⁸¹ We also attempted deprotonation with LHMDS to engage the resultant enolate in aminoalkylation, but only recovered indanone **2.55** (Table 2.1, Entries 3 and 5). Fortunately, preceded in-situ generation of the desired iminium ion with HCl and paraformaldehyde delivered the hydrochloride salt of **2.54** in 85% crude

yield (Scheme 2.10).^{82,83} The crude ammonium salt was reduced with NaBH₄ then dehydrated under acidic conditions to deliver the desired indene **2.53** in 48% yield.



Entry	Reagents	Solvent	Temperature
1	N/A	MeCN	82 °C
2	N/A	MeCN	110 °C
3	LHMDS	THF	-72 °C to rt
4	<chem>CN(C)C=O</chem>	MeCN	82 °C
5	LHMDS <chem>CN(C)C=O</chem>	THF	-72 °C to rt

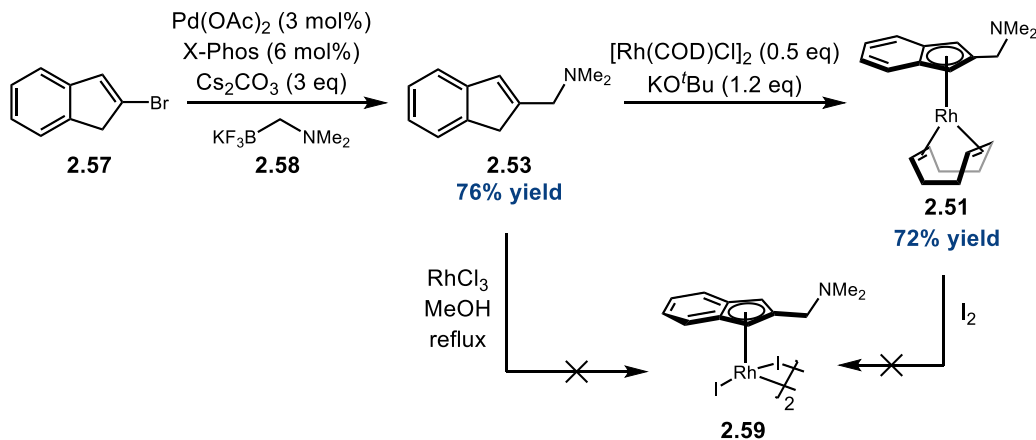
Table 2.1 Unsuccessful Mannich Reactions with pre-prepared Eschenmoser's salt



Scheme 2.10 Synthesis of 2-(N,N-dimethylaminomethyl)indene via Mannich alkylation

Concurrently, we investigated cross coupling for more direct access to the indenyl ligand **2.53**. Using 2-bromoindene as our starting point, we could ideally arrive at our ligand in one step. We identified Suzuki-Miyaura coupling as an attractive route. A Molander study revealed that XPhos was a privileged Buchwald ligand that enabled facile coupling of vinyl bromides and aminomethyl trifluoroborates.⁸⁴ Coupling of 2-bromoindene **2.57** and trifluoroboronate salt **2.58** delivered **2.53** in good yield (Scheme 2.11). With the dimethylaminoindenyl ligand in hand we attempted complexation with rhodium. Unfortunately, direct complexation with RhCl₃ was not accessible. At the time

our methodology for complexing indenyl ligands utilized organolithium bases. While we did not observe successful complexation with $n\text{BuLi}$, treatment of **2.53** with KO^tBu and $[\text{Rh}(\text{COD})\text{Cl}]_2$ delivered the Rh(I) COD complex **2.51** in good yield. In subsequent syntheses of 2-methyl-3-phenyl Rh(I) COD complex, KO^tBu was also found to be more productive than the current $n\text{BuLi}$ protocol. Next we attempted to oxidize the Rh(I) COD species to the more stable Rh(III). We were not able to isolate the Rh(III) complex, and instead saw a significant number of degradation products. There is precedent for the oxidation and iodination of tertiary amines, which could lead to deleterious side reactions.



Scheme 2.11 Direct synthesis of indenyl ligand and complexation onto Rh(I).

We attempted the directed C–H arylation on the Rh(I) monomer but did not observe any arylated Rh(I) complex. Without a convenient method to oxidize the Rh center, we looked for alternate routes towards catalyst development.

2.3.2 Conclusion

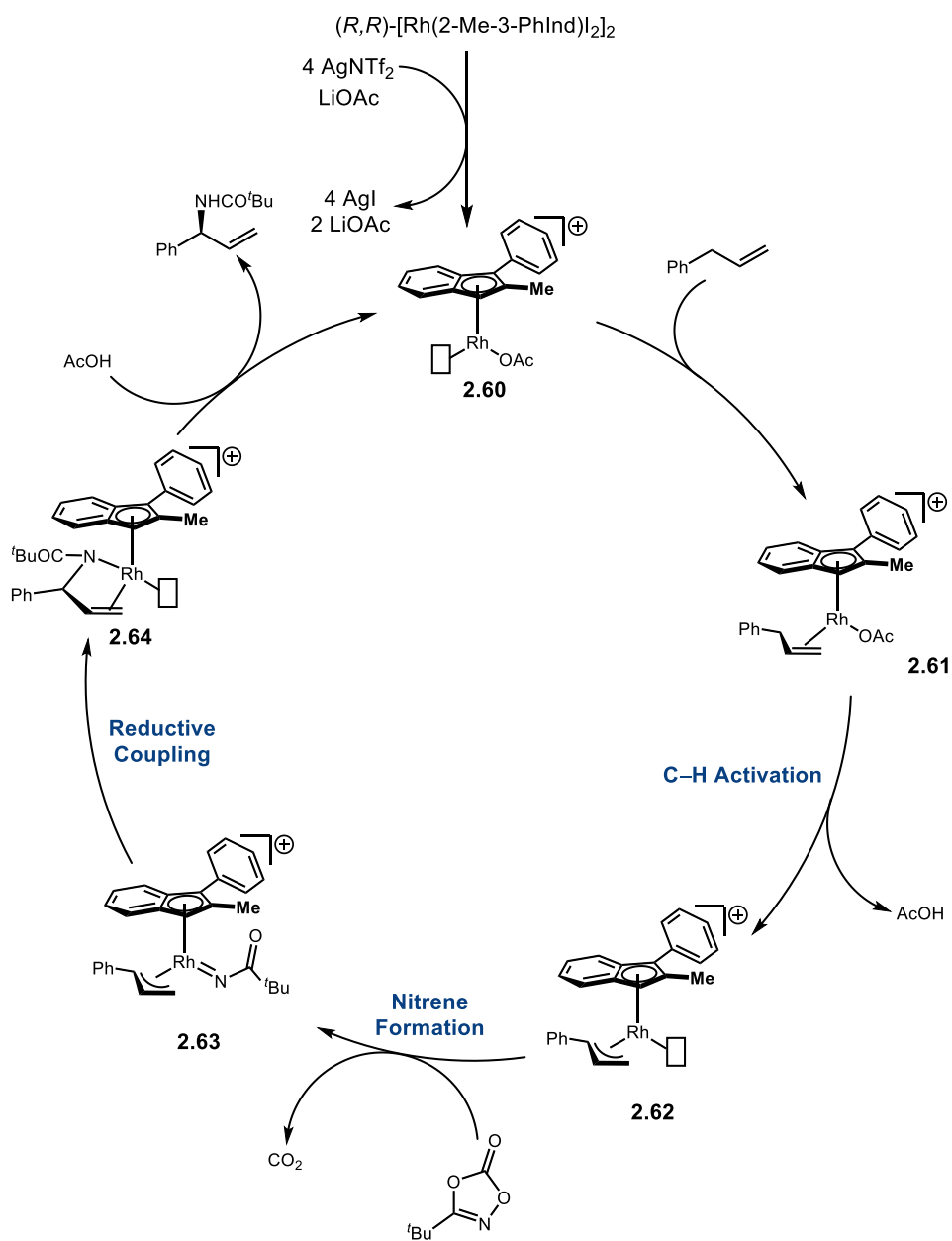
Enantioselective functionalization of transition metal complexes is a complex problem. The ability to deliver a catalog of planar chiral complexes from a precursor complex via enantioselective functionalization represents a powerful methodology in

planar chiral catalyst design that precludes the need for intensive resolution methods such as chiral HPLC. However, the practical limitations of first complexing a ligand with a directing group and the potential of the directing group to interfere with ensuing catalysis makes this strategy less palatable. Research within the Blakey group has turned towards new methods to deliver enantiopure complex in an efficient manner. The original strategy of complexing achiral ligand is currently the best method of providing rhodium indenyl complexes. However, instead of chiral HPLC to resolve the enantiomeric complexes, the group is now looking at utilizing labile chiral ligands such as MPAAAs, chiral diamines or labile ligands such as sodium *S*-Salox. Forming diastereomeric complexes with these labile ligands, then carrying out achiral chromatography and reconstituting the planar chiral complex, has been shown to be an effective strategy in planar chiral catalyst synthesis *vide supra* (Chapter 1.1. Synthesis and Chiral Resolution of Planar Chiral Complexes).

2.4 Exploration of Electronic Effects in the Planar Chiral Indenyl Scaffold

While progress towards efficient syntheses of Rh(III) indenyl complexes was ongoing, improving the reactivity of the Rh(III) indenyl catalyst remained a primary goal. During our studies in enantioselective complex synthesis, the Blakey group and the Baik group elucidated the mechanism of the C–H amidation using experimental and computational methods (Scheme 2.12).⁷⁶ The catalytic cycle begins with generation of cationic complex **2.60**. Subsequent olefin coordination and concerted metalation and deprotonation (CMD), which was supported to be the rate and enantio- determining step, delivers π -allyl complex **2.62**. Dioxazolone readily coordinates to the π -allyl complex and

rapidly undergoes oxidative nitrene formation to form **2.63**. The reactive Rh(V) nitrene undergoes reductive C–N bond formation to form **2.64**, and protonation releases the chiral amide product and reconstitutes catalyst **2.60**. Given the electronic asymmetry that is responsible for the excellent reactivity of catalyst **2.48**, we hypothesized that electronic



Scheme 2.12 Proposed catalytic cycle for allylic C–H amidation.

differentiation in the catalyst would have a pronounced effect on reactivity and possibly open new areas for our indenyl catalyst scaffold.

2.4.1 Synthesis

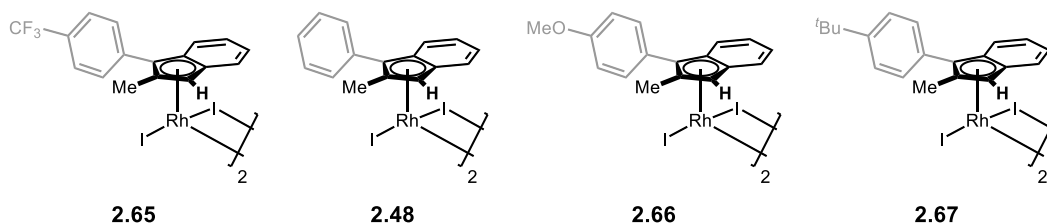
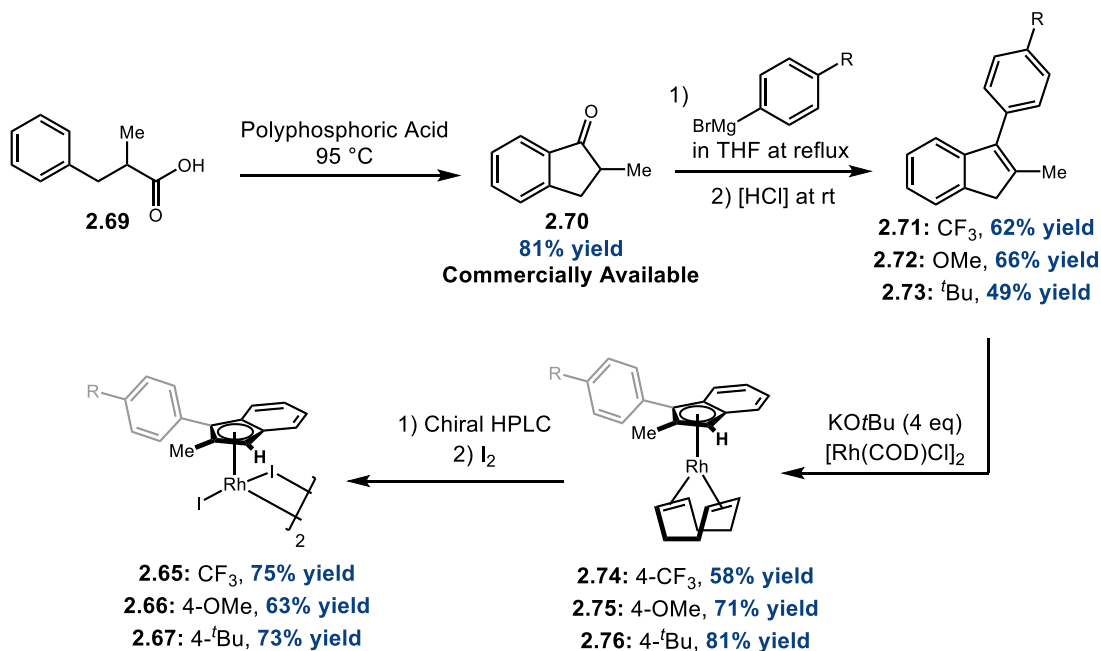


Figure 2.2 A suite of electronically biased indenyl complexes.

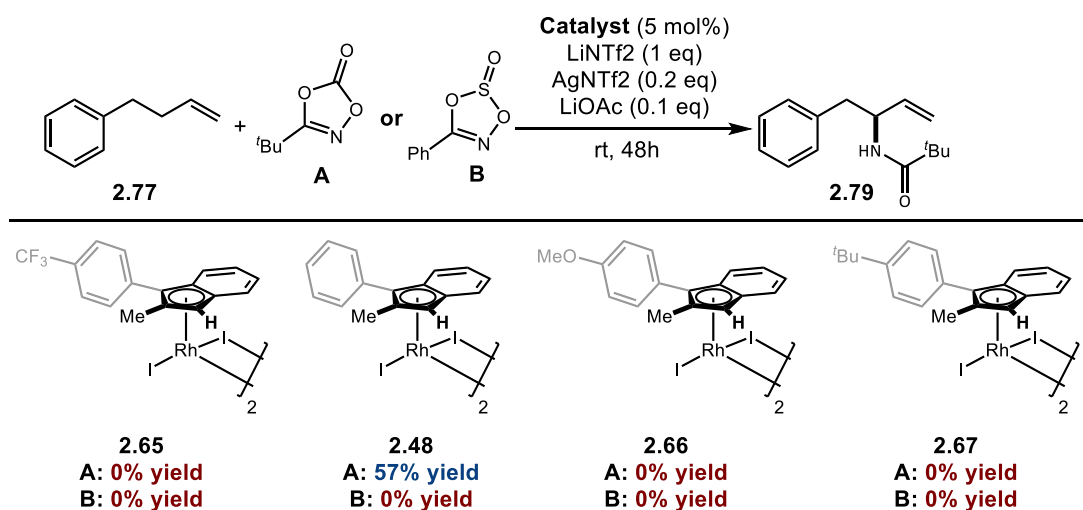
In order to probe the electronic biases in indenyl catalysis, we envisioned delivering several complexes with electronically differentiated ligands that minimized steric interference at the metal (Figure 2.2). We applied the synthetic route used to deliver **2.48**, with the appropriate Grignards, to arrive at our desired complexes (Scheme 2.13). 2-methyl-1-indanone **2.70** was furnished from the cyclization of α -methylhydrocinnamic



Scheme 2.13 Synthesis of 4'-substituted 2-Me-3-Phenyl indenyl complexes.

acid **2.69** using polyphosphoric acid. While **2.70** is commercially available, only indanone prepared in lab was productive in later steps. The indenenes **2.71-73** were obtained via arylation with freshly prepared Grignards and subsequent acid mediated dehydration. Indene complexation proceeded in good order to provide Rh(I) COD monomers **2.74-76**. Enantiopure Rh(I) COD monomers were obtained through chiral resolution on preparatory chiral HPLC. The enantiopure COD monomers were oxidized to the Rh(III) dimers **2.65-2.67** with iodine. It is noteworthy that extensive washing of the crude iodide dimers with diethyl ether was necessary to remove excess iodine and cyclooctadiene.

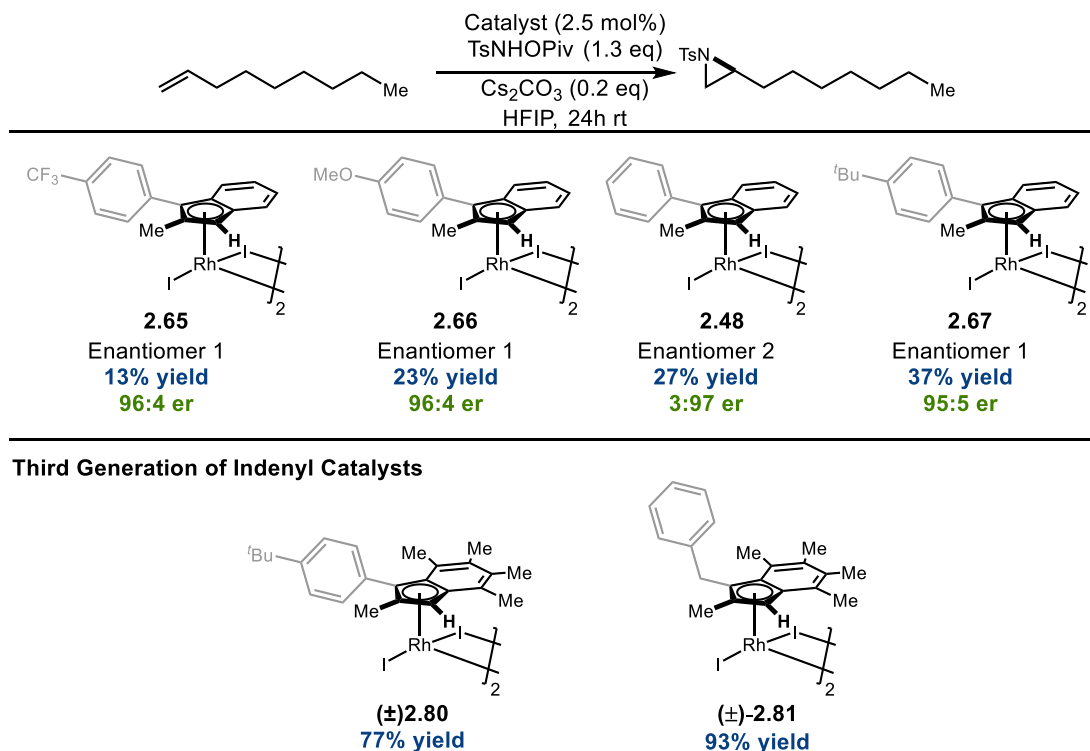
The amidation of 4-phenylbutene was used as the benchmark reaction for assessing catalyst performance in allylic amidation (Figure 2.3). This study began with the evaluation of the Rh(III) complexes. Our original Rh(III) catalyst **2.48** had the best performance, while both the electron deficient complex **2.65** and the electron rich complexes **2.66** and **2.67** yielded no product. The reaction was also evaluated with respect to the amidation reagent. The Chang group evaluated the activity of several amidation reagents in the functionalization of 2-phenylpyridine.⁵⁹ The main feature of



Scheme 2.14 Evaluation of electronically biased ligands and nitrene precursors in allylic C–H amidation.

dioxazolones was their ability to function as an internal oxidant. Several heterocycles can function in this manner, namely 1,3,2,4-dioxathiazole-2-oxides (Scheme 2.14, **B**). Dioxathiazole-2-oxides have been shown to need higher temperatures than dioxazolones for equivalent yields.⁵⁹ Unfortunately, the dioxathiazole-2-oxide was unproductive in allylic amidation at 20 °C, 60 °C and 80 °C.

While the performance of the Rh(III) indenyl catalysts in allylic C-H amidation was disappointing, the catalysts revealed a trend in a different reaction class. Patrick Gross evaluated the performance of the Rh(III) indenyl catalysts in allylic aziridination (Scheme 2.15). Using the small library of Rh(III) complexes, Patrick discovered that the Rh(III) indenyl complexes were able to catalyze enantioselective aziridination in unactivated olefins. More excitingly, we saw an increase in reactivity with increasingly electron rich ligands, which supports the idea that electronics can be fine-tuned to improve yields. With



Scheme 2.15. Planar chiral indenyl catalysts and their performance in aziridination reactions.

this foundation, Patrick Gross developed the next generation of more electron-rich catalysts, **2.80** and **2.81**, that resulted in improved yields. While the poly methylated complexes have yet to be resolved, given the impressive stereinduction in two reaction classes with a range of indenyl ligands, we are confident that resolution of complexes **2.80** and **2.81** will deliver highly selective reactions as well.

2.4.2 Conclusions

Electronics play an important role in the reactivity of planar chiral indenyl complexes. The original aim of this project was to increase the reactivity of the planar chiral indenyl catalysts in enantioselective amidation. Unfortunately, increasing electron density led to catalyst incompetence in the realm of allylic amidation. However, electron-rich catalysts led to improved yields in aziridination reactions. These results show that electronics are a fine dial with which we can optimize reactions. The trend of the earlier indenyl catalysts became the foundation of a new project in the area of aziridination led by Patrick Gross. Given the inability of chiral HPLC to resolve the enantiomers of poly-methylated indenyl complexes, alternative resolution techniques remain a critical research point.

2.5 Experimental Details

General Information: ^1H and ^{13}C nuclear magnetic resonance spectra (NMR) were recorded on a Varian 400 INOVA spectrometer (^1H 400 MHz, ^{13}C 126 MHz), a Varian 400 VNMR spectrometer (^1H 400 MHz, ^{13}C 100 MHz), a Varian INOVA 500 spectrometer (^1H 500 MHz, ^{13}C 126MHz), a Varian INOVA 600 spectrometer (^1H 600Hz, ^{13}C 151MHz), a Bruker 600 spectrophotometer (600 Mhz ^1H , 151 Mhz ^{13}C) at room temperature in CDCl_3 unless otherwise indicated. Chemical shifts were reported in ppm and coupling constants (J) in Hz. Multiplicities were indicated with the following abbreviations: s = singlet, d = doublet, t = triplet, q = quartet, qn = quintet, m = multiplet, br = broad. Analytical thin-layer chromatography was carried out on glass-backed Silicycle TLC plates and visualized with UV light, and ethanolic p-anisaldehyde or KMnO_4 unless otherwise indicated. Flash chromatography was done with Silicycle SiliaFlash[®] F60 silica gel (40- 63 μm) or Alumina as indicated on a Biotage Isolera One system. Silica gel column chromatography was done using Silicycle SiliaFlash[®] F60 silica gel (40- 63 μm).

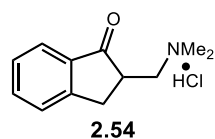
Reactions were conducted under nitrogen atmosphere using Schlenk technique unless otherwise stated. Anhydrous tetrahydrofuran (THF), diethyl ether (Et_2O), dichloromethane (DCM), hexanes, and toluene were obtained by passage over activated alumina using *Glass Contours* solvent system. Anhydrous DMF, DMSO and 1,4-dioxane were obtained from Dry-Seal EMD Millipore, subjected to degassing and stored over 4Å molecular sieves. Solvents for work-up and chromatography were obtained from commercial suppliers without additional purification. Reactive or hydroscopic salts (NHMDS, KHMDS, LDA, KO^tBu, LiOAc LiCl, LiNTf₂ and AgNTf₂) were stored and weighed in a N_2 filled glovebox. Organometallic compounds ($[\text{Rh}(\text{COD})\text{Cl}]_2$, $[\text{Ir}(\text{COD})\text{Cl}]_2$, **2.51**, **2.65**, **2.66**, **2.67**) were stored and weighed in a N_2 glovebox. All other reagents were purchased from Ambeed, MilliporeSigma, Strem Chemicals, Oakwood Chemicals, Matrix Scientific or TCI.

High Performance Liquid Chromatography (HPLC) was performed on an Agilent 1100 series HPLC utilizing CHIRALCEL[®] OD-H 4.6 x 150 mm analytical column or on an Agilent 1260 Infinity II series HPLC CHIRALCEL[®] OD-H 4.6 x 150 mm analytical column.

Semi-preparative HPLC was performed on an Agilent 1260 Infinity II series preparative HPLC using a CHIRALCEL® OD-H 20 x 250 mm column.

Procedures

2.54: 2-((dimethylamino)methyl)-indan-1-one • HCl. Prepared according to Schaverien *et al.*⁸¹



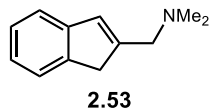
Into a 15 mL vial was placed 1-indanone (9.57 mmol), paraformaldehyde (13.4 mmol) and dimethylamine hydrochloride (13.4 mmol). Then 3 mL of absolute ethanol were added followed by 2 drops of 12M HCl. The reaction was placed on a heating block at 90 °C and stirred for 3h. The reaction was cooled, and off-white precipitate was filtered and washed with hexanes and diethyl ether, then dried under vacuum. (4.45 g, 53% purity).

¹H NMR: (CDCl₃, 600 MHz) δ 12.12 (br s, 1H), 9.57 (br s, 1H, dimethylamine HCl) 7.70 (d, *J* = 7.8 Hz, 1H), 7.61 (dd, *J* = 7.2Hz, 7.8 Hz, 1H), 7.50 (d, *J* = 7.2 Hz, 1H), 7.37 (dd, *J* = 7.2 Hz, 7.8 Hz, 1H), 3.74 – 3.70 (m, 1H), 3.63 – 3.59 (m, 1H), 3.38 – 3.27 (m, 2H), 3.22 – 3.19 (m, 1H), 2.97 (d, *J* = 4.8 Hz), 2.93 (d, *J* = 4.8 Hz), 2.68 (t, *J* = 5.4 Hz, 6H, dimethylamine HCl)

Safety Note for Paraformaldehyde: While solid paraformaldehyde is easier to handle than non-polymeric liquid formaldehyde, it is still quite hazardous. Paraformaldehyde is a potent sensitizer and represents a significant respiratory hazard due to fine dust particles and its ability to off-gas monomeric formaldehyde. To accommodate these hazards, all paraformaldehyde was measured in the hood and quickly added to the reaction vessel. All equipment used to measure paraformaldehyde was thoroughly cleaned and waste materials were disposed of in solid waste. Below is a link to the sds for paraformaldehyde.

<https://www.fishersci.com/store/msds?partNumber=O4042500&productDescription=PARAFORMALDEHYDE+R+500G&vendorId=VN00033897&countryCode=US&language=en>

2.53: 2-(N,N-dimethylaminomethyl)-1H-indene

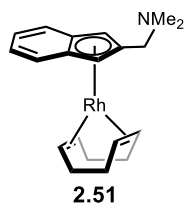


Procedure 1: To crude **2.54** (2.36 g, 10mmol) was added THF (80 mL) then the reaction was cooled to 0 °C. Sodium borohydride (0.99 g, 26.2 mmol) was added portion wise, and the reaction allowed to warm to room temperature. After 6 hours, the reaction was diluted with DI water and extracted with ethyl acetate (3 x 40 mL). The combined organics were concentrated via rotary evaporation. The resultant residue was diluted in 12 M HCl (23 mL) and glacial acetic acid (55 mL) and heated to 80 °C for 2 hours. The reaction cooled to room temperature then quenched with 3M NaOH (414 mL) and the aqueous layer was extracted with ethyl acetate (3 x 150mL). The organic layer was concentrated and provided **2.53** as a dark brown oil (1.64 g, 89% yield).

Procedure 2 (Adapted from Molander *et al.*)⁸⁴: To an oven-dried 50 mL round bottom flask equipped with condenser and stir bar, was added potassium (N,N-dimethylaminomethyl)trifluoroborate (0.51 g, 3.08 mmol), 2-bromo-1H-indene (0.50 g, 2.56 mmol), Pd(OAc)₂ (0.02 g, 0.08 mmol), X-Phos (0.07 g, 0.15 mmol) and Cs₂CO₃ (2.51 g, 7.69 mmol). Then the atmosphere was exchanged with N₂ (3 x 5 minutes). Then 10 mL of dry THF were added followed by 1 mL of DI H₂O. The reaction stirred for 48 hours and then was diluted with DI H₂O. The organics were extracted with DCM (6 x 10mL). The combined organic fractions were dried with Na₂SO₄ then concentrated via rotary evaporation. The residue was purified on alumina via column chromatography to afford **13** as a dark brown oil (0.34 g, 76% yield).

¹H NMR: (CDCl₃, 600 MHz) δ 7.45 (d, *J* = 7.2 Hz, 1H), 7.35 (d, *J* = 7.8 Hz, 1H), 7.27 (t, *J* = 7.2 Hz, 1H), 7.18 (t, *J* = 7.2 Hz, 1H). 6.72 (s, 1H), 3.45 (s, 2H), 3.38 (s, 2H), 2.31 (s, 6H). **¹³C NMR**: (CDCl₃, 151 MHz) δ 146.85, 144.75, 143.72, 129.79, 126.30, 124.33, 123.70, 120.52, 60.07, 45.40, 40.28. **HRMS**: (+ESI) calculated for C₁₂H₁₆N [M+H]⁺ 174.1277, found 174.1277.

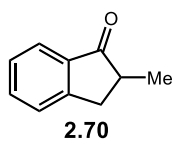
2.51: 1,5-cyclooctadiene(η⁵-2-(N,N-dimethylaminomethyl)inden-1H-yl)rhodium(I)



A vial containing $[\text{Rh}(\text{COD})\text{Cl}]_2$ (0.050 g, 0.10 mmol) and KO^tBu (0.028 g, 0.25 mmol) was removed from the box. Indene **2.53** (0.037 g, 0.21 mmol) was weighed into an oven-dried vial then sealed and the atmosphere was exchanged with N_2 3 times over 5 minute cycles. Then dry THF (1 mL) was added to the indene and the indene solution was transferred to the reaction vial containing $[\text{Rh}(\text{COD})\text{Cl}]_2$ and KO^tBu . The reaction stirred at room temperature for 24 hours. The crude reaction mixture was reduced via rotary evaporation then the residue was purified on silica via column chromatography to afford **2.51** as a yellow solid in 72% yield.

^1H NMR: (CDCl_3 , 500 MHz) δ 7.16 (dd, $J = 6.6, 3.0$ Hz, 2H), 7.03 (dd, $J = 6.0, 3.0$ Hz, 2H), 5.15 (s, 2H), 3.96 (s, 4H), 3.57 (s, 2H), 2.28 (s, 6H), 1.86 – 1.80 (m, 4H), 1.74 – 1.68 (m, 4H). **^{13}C NMR:** (CDCl_3 , 151 MHz) δ 128.69, 122.31, 119.10, 113.41 (d, $J_{\text{C-Rh}} = 2.4$ Hz), 109.28 (d, $J_{\text{C-Rh}} = 5.6$ Hz), 77.83 (d, $J_{\text{C-Rh}} = 4.4$ Hz), 67.940, 67.851 (d, $J_{\text{C-Rh}} = 13.4$ Hz), 58.359, 44.941, 31.372. **HRMS** (-ESI) calculated for $\text{C}_{20}\text{H}_{26}\text{N}^{103}$ $[\text{M-H}]^-$ 383.1148, found 383.1171.

2.70: 2-methyl-1-indanone: Prepared following a procedure from Gilmore, and the Blakey catalyst synthesis.^{76,85}



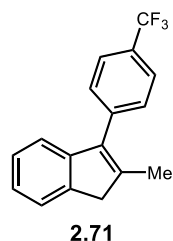
To a flame-dried 250 mL round-bottom flask was added α -methylhydrocinnamic acid (5.04 g, 30.7 mmol) and 100 mL polyphosphoric acid. The flask was sealed, and the atmosphere exchanged with N_2 (3 x 3 minutes). The reaction was then placed a heating block at 95 °C and the reaction stirred for 22 h. The reaction was added to a 1L Erlenmeyer with ice and was quenched with solid K_2CO_3 . Once quenched the organics were extracted with EtOAc (4 x 500 mL). The combined organics were washed with 1M NaOH (2 x 500 mL) and dried with MgSO_4 . The organics were reduced via rotary evaporation then further evacuated under low pressure. Indanone **27** was obtained as a dark red oil in 81% yield. Spectroscopic data matches previously reported spectra.⁷⁶

¹H NMR: (CDCl₃, 600 MHz) δ 7.76 (d, *J* = 6.6 Hz, 1H), 7.60 – 7.57 (m, 1H), 7.45 (dd, *J* = 7.7, 1.2 Hz, 1H), 7.38 – 7.36 (m, 1H), 3.40 (dd, *J* = 17.7, 9.0 Hz, 1H), 2.75 – 2.69 (m, 1H), 1.32 (dd, 7.2, 0.9 Hz, 3H)

General procedure A for the synthesis of indenenes 2.71-73

To prepare the Grignard solution, ground magnesium turnings (4.4 eq) were added to a round bottom flask equipped with a stir bar and condenser, then flame-dried under vacuum. The flask was allowed to cool to room temperature then THF (0.22M) was added followed by arylbromide (2.2 eq). The septum was quickly opened and I₂ (0.05 g, 0.22 mmol) was added. The reaction was heated to reflux overnight. After 18 hours, the reaction was cooled to room temperature and cannulated into another flask equipped with a condenser and stir bar to remove excess magnesium.

Indenyl Preparation: 2-methyl-1-indanone **2.70** (1.0 eq) was added to the flask containing Grignard solution (2.2 eq, 0.22 M) via syringe and the reaction was heated to 85 °C. After 24 hours, the reaction was quenched with 10 mL of DI H₂O. Then 10 mL of concentrated HCl was added followed by 10 mL of Et₂O and the reaction stirred at room temperature for 18 hours. The organics were extracted with EtOAc (3 x 20 mL), then the combined organic fractions were washed with sat. NaHCO₃ (3 x 50 mL) and washed with brine (1 x 50 mL). The organics were dried with MgSO₄. The organic residue was purified via column chromatography to deliver the requisite indene.



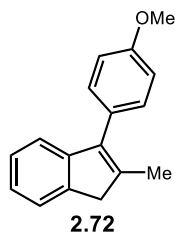
2.71: 2-methyl-3-(4-(trifluoromethyl)phenyl)-1H-indene

General procedure A was applied to indanone **2.70** (0.29 g, 2.0 mmol) and 1-bromo-4-(trifluoromethyl)benzene (0.62 mL, 4.4 mmol). Column chromatography (0% to 2% EtOAc in hexanes on silica) delivered **2.56** as a white solid (0.29 g, 62% yield).

¹H NMR (600 MHz, CDCl₃) δ 7.73 (d, *J* = 8.2 Hz, 2H), 7.52 (d, *J* = 8.2 Hz, 1H), 7.49 – 7.44 (m, 1H), 7.28 – 7.22 (m, 1H), 7.22 – 7.14 (m, 2H), 3.50 (s, 2H), 2.15 (s, 3H). **¹³C NMR** (151 MHz, CDCl₃) δ 145.83, 142.42, 142.17, 139.47, 137.69, 129.59, 129.14 (q, *J* = 32.2 Hz), 126.47, 125.55 (q, *J* = 3.7 Hz), 124.49, 124.47 (q, *J* = 271.9 Hz), 123.70,

43.40, 14.95. **¹⁹F NMR** (564 MHz, CDCl₃) δ -62.40. **HRMS** (+APCI) calculated for C₁₇H₁₄F₃ [M+H]⁺ 275.10421, found 275.10404.

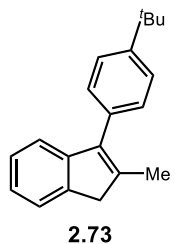
2.72: 3-(4-methoxyphenyl)-2-methyl-1H-indene



General procedure A was applied to indanone **2.70** (0.50, 3.4 mmol) and 1-bromo-4-(methoxy)benzene (0.86 mL, 6.8 mmol). Column chromatography (0% to 5% EtOAc in hexanes on silica) delivered **2.72** as an orange-yellow solid (0.54 g, 66% yield).

¹H NMR (600 MHz, CDCl₃) δ 7.44 (d, *J* = 7.3 Hz, 1H), 7.36 (d, *J* = 8.4 Hz, 2H), 7.25 (d, *J* = 4.2 Hz, 2H), 7.17 – 7.13 (m, 1H), 7.02 (d, *J* = 8.6 Hz, 2H), 3.88 (s, 3H), 3.45 (s, 2H), 2.15 (s, 3H). **¹³C NMR** (151 MHz, CDCl₃) δ 158.69, 146.71, 142.55, 140.15, 138.25, 130.37, 127.95, 126.26, 124.01, 123.49, 119.36, 113.99, 55.41, 43.14, 15.00. **HRMS** (+APCI) calculated for C₁₇H₁₇O [M+H]⁺ 237.12739, found 237.12732.

2.73: 3-(4-*tert*-butylphenyl)-2-methyl-1H-indene



General procedure A was applied to indanone **2.70** (0.50, 3.4 mmol) and 1-bromo-4-(*tert*-butyl)benzene (1.2 mL, 6.8 mmol). Column chromatography (0% to 5% EtOAc in Hexanes on silica) delivered **2.73** as a white solid (0.44 g, 49% yield).

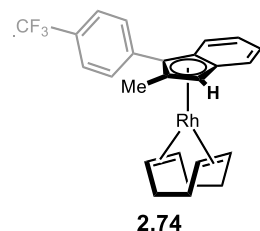
¹H NMR (600 MHz, CDCl₃) δ 7.49 (d, *J* = 8.3 Hz, 2H), 7.44 (d, *J* = 7.3 Hz, 1H), 7.36 (d, *J* = 8.3 Hz, 2H), 7.29 (d, *J* = 7.5 Hz, 1H), 7.24 (t, *J* = 7.4 Hz, 1H), 7.16 (dt, *J* = 7.3, 1.2 Hz, 1H), 3.46 (s, 2H), 2.17 (s, 3H), 1.40 (s, 9H). **¹³C NMR** (151 MHz, CDCl₃) δ 149.85, 146.63, 142.58, 140.45, 138.50, 132.56, 128.89, 126.22, 125.40, 123.98, 123.47, 119.56, 43.25, 34.76, 31.56, 15.10. **HRMS** (+APCI) calculated for C₂₀H₂₃ [M+H]⁺ 263.17943, found 263.17932.

General procedure B for the synthesis of Rh(I) Monomers 2.74-2.76

An oven-dried 4 mL vial was charged with the appropriate indene (2.1 eq) and the atmosphere was exchanged with nitrogen (3 x 5 minutes). Then [Rh(COD)Cl]₂ (1 eq) and KO^tBu (2.5 eq) was removed from the box in a 7 mL vial and placed under nitrogen

balloon. To the vial containing indene, dry THF (0.13 M) was added and the indene solution was transferred to the reaction vial containing $[\text{Rh}(\text{COD})\text{Cl}]_2$ and KO^tBu via syringe. The reaction stirred for 18 hours at room temperature, then the reaction mixture was reduced via rotary evaporation and the residue was purified via column chromatography on silica.

2.74: 1,5-cyclooctadiene(η^5 -2-methyl-3-(4-trifluoromethylphenyl)inden-1H-yl)rhodium(I)

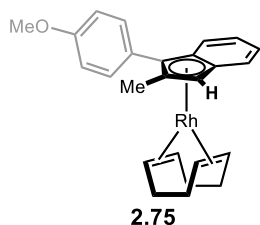


Procedure B was applied to indene **2.71** (175 mg, 0.64 mmol), $[\text{Rh}(\text{COD})\text{Cl}]_2$ (150 mg, 0.30 mmol), and KO^tBu (85 mg, 0.76 mmol). Column chromatography (100% Hexanes) afforded **2.74** as a yellow solid (221 mg, 75% yield).

^1H NMR (600 MHz, C_6D_6) δ 7.45 (d, $J = 8.2$ Hz, 2H), 7.27 (d, $J = 7.8$ Hz, 2H), 7.19 (ddt, $J = 9.2, 8.2, 1.1$ Hz, 2H), 7.11 – 7.05 (m, 2H), 4.62 (s, 1H), 3.82 (qd, $J = 4.8, 2.2$ Hz, 2H), 3.62 (ddd, $J = 8.0, 5.6, 2.5$ Hz, 2H), 2.23 (d, $J = 1.3$ Hz, 3H), 1.87 – 1.77 (m, 4H), 1.71 – 1.60 (m, 4H). **^{13}C NMR** (151 MHz, C_6D_6) δ 139.67, 129.68, 125.73 (q, $J = 3.8$ Hz), 124.32 (q, $J = 271.6$ Hz), 123.57, 122.78, 119.77, 117.37, 112.81 (d, $J_{\text{C-Rh}} = 2.1$ Hz), 112.49 (d, $J_{\text{C-Rh}} = 2.8$ Hz), 108.08 (d, $J_{\text{C-Rh}} = 5.0$ Hz), 94.09 (d, $J_{\text{C-Rh}} = 3.8$ Hz), 77.50 (d, $J_{\text{C-Rh}} = 4.8$ Hz), 72.51 (d, $J_{\text{C-Rh}} = 13.7$ Hz), 69.67 (d, $J_{\text{C-Rh}} = 13.7$ Hz), 31.78, 31.64, 14.69. **^{19}F NMR** (564 MHz, C_6D_6) δ -61.98. **HRMS** (+APCI) calculated for $\text{C}_{25}\text{H}_{24}\text{F}_3\text{Rh}$ $[\text{M}]^+$ 484.08797, found 484.0894.

Chiral Resolution: Analytical HPLC (Chiracel AD-H column 0% 2-propanol in hexanes, 1.0 mL/min) (**2.74 E1**): $t_1 = 4.6$ min, (**2.74 E2**): $t_2 = 7.1$ min, **Semi-prep HPLC** (20 x 250 mm Chiracel OD-H column, 0% 2-Propanol in Hexanes, 20 mL/min 500 μL injections of 22 mg/mL solutions were made to resolve the complex.

2.75: 1,5-cyclooctadiene(η^5 -3-(4-methoxyphenyl)-2-methylinden-1H-yl)rhodium(I)

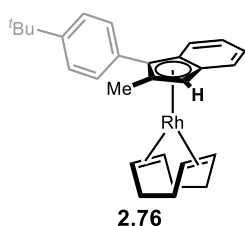


Procedure B was applied to indene **2.72** (175 mg, 0.64 mmol), $[\text{Rh}(\text{COD})\text{Cl}]_2$ (150 mg, 0.30 mmol), and KO^tBu (85 mg, 0.76 mmol). Column chromatography (5% EtOAc in Hexanes) afforded **2.75** as a yellow solid (229 mg, 63% yield).

$^1\text{H NMR}$ (600 MHz, C_6D_6) δ 7.43 – 7.39 (m, 1H), 7.38 (d, $J = 8.2$ Hz, 2H), 7.25 – 7.21 (m, 1H), 7.13 – 7.08 (m, 2H), 6.88 (d, $J = 8.2$ Hz, 2H), 4.68 (s, 1H), 3.94 (td, $J = 7.5, 3.4$ Hz, 2H), 3.77 (tt, $J = 7.6, 3.1$ Hz, 2H), 3.37 (s, 3H), 2.38 (s, 3H), 1.96 – 1.83 (m, 4H), 1.78 – 1.65 (m, 4H). **$^{13}\text{C NMR}$** (151 MHz, C_6D_6) δ 158.78, 130.77, 127.43, 123.15, 122.41, 119.66, 117.96, 114.42, 112.97 (d, $J_{\text{C-Rh}} = 2.3$ Hz), 112.07 (d, $J_{\text{C-Rh}} = 2.7$ Hz), 107.69 (d, $J_{\text{C-Rh}} = 5.0$ Hz), 96.06 (d, $J_{\text{C-Rh}} = 3.7$ Hz), 76.77 (d, $J_{\text{C-Rh}} = 4.9$ Hz), 72.03 (d, $J_{\text{C-Rh}} = 13.7$ Hz), 69.12 (d, $J_{\text{C-Rh}} = 13.8$ Hz), 54.86, 31.91, 31.78, 14.82. **HRMS** (+APCI) calculated for $\text{C}_{25}\text{H}_{27}\text{ORh} [\text{M}]^+$ 446.11115, found 446.1111.

Chiral Resolution: Analytical HPLC (Chiracel AD-H column 0% 2-propanol in hexanes, 1.0 mL/min) (**2.75 E1**): $t_1 = 4.6$ min, (**2.75 E2**): $t_2 = 7.1$ min, **Semi-prep HPLC** (20 x 250 mm Chiracel OD-H column, 0% 2-Propanol in Hexanes, 20 mL/min 500 μL injections of 22 mg/mL solutions were made to resolve the complex

2.76: 1,5-cyclooctadiene(η^5 -3-(4-*tert*-butylphenyl)-2-methylinden-1H-yl)rhodium(I)



Procedure B was applied to indene **2.73** (100 mg, 0.38 mmol), $[\text{Rh}(\text{COD})\text{Cl}]_2$ (89 mg, 0.18 mmol), and KO^tBu (51 mg, 0.45 mmol). Column chromatography (100% hexanes) provided **2.76** as a yellow solid (139 mg, 81% yield).

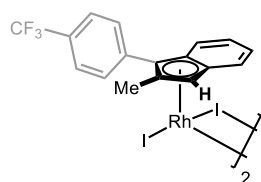
$^1\text{H NMR}$ (600 MHz, C_6D_6) δ 7.47 – 7.45 (m, 2H), 7.45 – 7.41 (m, 1H), 7.41 – 7.37 (m, 2H), 7.24 – 7.20 (m, 1H), 7.12 – 7.06 (m, 2H), 4.67 (s, 1H), 3.94 (dp, $J = 7.2, 3.0$ Hz, 2H), 3.77 (ddt, $J = 7.8, 6.2, 1.9$ Hz, 2H), 2.40 (d, $J = 1.4$ Hz, 3H), 1.92 – 1.82 (m, 4H), 1.75 – 1.63 (m, 4H), 1.29 (s, 9H). **$^{13}\text{C NMR}$** (151 MHz, C_6D_6) δ 149.19, 132.57, 129.47, 125.77, 123.18, 122.43, 119.68, 113.04 (d, $J_{\text{C-Rh}} = 2.3$ Hz), 112.18 (d, $J_{\text{C-Rh}} = 2.7$ Hz), 107.81 (d, $J_{\text{C-Rh}} = 5.0$ Hz), 96.04 (d, $J_{\text{C-Rh}} = 3.8$ Hz), 76.95 (d, $J_{\text{C-Rh}} = 4.9$ Hz), 72.09 (d, $J_{\text{C-Rh}} = 13.8$

Hz), 69.19 (d, $J_{C-Rh} = 13.6$ Hz), 34.62, 31.81 (d, $J_{C-Rh} = 2.2$ Hz), 31.50, 14.91. **HRMS** (+APCI) calculated for $C_{28}H_{33}Rh [M]^+$ 472.163, found 472.16426.

Chiral Resolution: Analytical HPLC (Chiracel AD-H column 0% 2-propanol in hexanes, 1.0 mL/min) (**2.76 E1**): $t_1 = 4.6$ min, (): $t_2 = 7.1$ min, **Semi-prep HPLC** (20 x 250 mm Chiracel OD-H column, 0% 2-Propanol in Hexanes, 20 mL/min 500 μ L injections of 22 mg/mL solutions were made to resolve the complex 18

General Procedure C for the synthesis of Rh(III) dimers 2.65-67

To a 20 mL scintillation vial was added Rh(I) COD monomer (1 eq) and I_2 (2.5 eq), followed by 5 mL of dry Et_2O . The vial was capped and stirred at room temperature for 24 hours. Black precipitate formed in the reaction was filtered and washed thoroughly with Et_2O . The washed precipitate was placed under low pressure to remove residual solvents to afford pure Rh(III) complex.

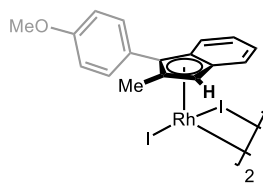


2.65

2.65: (η^5 -2-methyl-3-(4-trifluoromethylphenyl)inden-1H-yl)rhodium(III) diiodide dimer

General Procedure C was applied to Rh(I) complex **2.74** (49 mg, 0.10 mmol) and I_2 (64 mg, 0.25 mmol). Filtration afforded **2.65** as a black solid (37 mg, 58% yield).

1H NMR (600 MHz, $DMSO-d_6$) δ 8.06 (d, $J = 8.0$ Hz, 4H), 7.88 (d, $J = 8.0$ Hz, 4H), 7.71 (d, $J = 8.5$ Hz, 2H), 7.63 (t, $J = 7.5$ Hz, 2H), 7.59 (t, $J = 7.6$ Hz, 2H), 7.44 (d, $J = 8.4$ Hz, 2H), 6.54 (s, 2H), 2.27 (s, 6H). **^{13}C NMR** (151 MHz, $DMSO-d_6$) δ 134.06, 133.73, 132.67, 129.01 (q, $J = 31.9$ Hz), 127.62, 125.39, 125.31 (q, $J = 4.0$ Hz), 124.18 (q, $J = 272.1$ Hz), 112.10 (d, $J_{C-Rh} = 5.4$ Hz), 107.09 (d, $J_{C-Rh} = 3.7$ Hz), 104.34 (d, $J_{C-Rh} = 4.1$ Hz), 92.91 (d, $J_{C-Rh} = 5.6$ Hz), 78.28 (d, $J_{C-Rh} = 6.7$ Hz), 13.46. **^{19}F NMR** (565 MHz, $DMSO-d_6$) δ -61.09. **HRMS** (+APCI) calculated for $C_{17}H_{12}F_3^{127}I_3^{103}Rh [M-C_{17}H_{12}IRh]^-$ 756.70857, found 756.70865

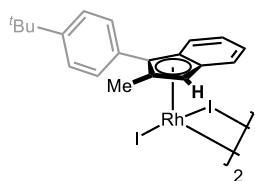


2.66

2.66: (η^5 -3-(4-methoxyphenyl)-2-methylinden-1H-yl)rhodium(III) diiodide dimer

General Procedure C was applied to Rh(I) complex **2.75** (47 mg, 0.12 mmol) and I₂ (66 mg, 0.29 mmol). Filtration supplied **2.66** as a black solid (50 mg, 80% yield).

¹H NMR: **¹H NMR** (600 MHz, DMSO-d₆) δ 7.80 (d, J = 8.7 Hz, 4H), 7.70 – 7.65 (m, 2H), 7.58 (tt, J = 6.7, 5.2 Hz, 4H), 7.47 – 7.41 (m, 2H), 7.06 (d, J = 8.7 Hz, 4H), 6.43 (s, 2H), 3.83 (s, 6H), 2.23 (s, 6H). **¹³C NMR** (151 MHz, DMSO-d₆) δ 159.64, 133.48, 132.35, 132.21, 127.83, 125.55, 120.95, 113.98, 110.83 (d, J_{C-Rh} = 5.4 Hz), 107.29 (d, J_{C-Rh} = 3.9 Hz), 103.45 (d, J_{C-Rh} = 4.7 Hz), 95.23 (d, J_{C-Rh} = 5.6 Hz), 77.58 (d, J_{C-Rh} = 7.2 Hz), 55.23, 13.58. **HRMS** (+APCI) calculated for C₁₇H₁₄OI₂Rh [M-C₁₇H₁₆OI₂Rh]⁻ 590.81725, found 590.81689.



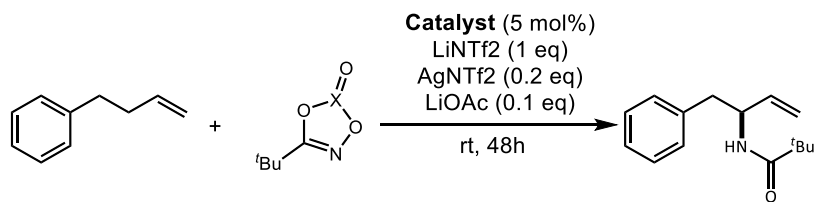
2.67

2.67: (η^5 -3-(4-*tert*-butylphenyl)-2-methylinden-1H-yl)rhodium(III) diiodide dimer

General Procedure C was applied to Rh(I) complex **2.76** (32 mg, 0.09 mmol) and I₂ (56 mg, 0.22 mmol). Filtration delivered **2.67** as a black solid (36 mg, 66% yield).

¹H NMR: **¹H NMR** (600 MHz, DMSO-d₆) δ 7.79 (d, J = 8.3 Hz, 4H), 7.68 (dd, J = 8.4, 1.2 Hz, 2H), 7.62 – 7.58 (m, 2H), 7.58 – 7.55 (m, 2H), 7.51 (d, J = 8.0 Hz, 4H), 7.45 (d, J = 8.5 Hz, 2H), 6.44 (s, 2H), 2.25 (s, 6H), 1.34 (s, 18H). **¹³C NMR** (151 MHz, DMSO-d₆) δ 151.29, 133.48, 130.55, 127.75, 125.67, 125.28, 111.32 (d, J_{C-Rh} = 5.7 Hz), 107.36 (d, J_{C-Rh} = 3.8 Hz), 103.62 (d, J_{C-Rh} = 4.5 Hz), 94.93 (d, J_{C-Rh} = 5.9 Hz), 77.63 (d, J_{C-Rh} = 7.0 Hz), 34.59, 31.03, 13.74. **HRMS** (+APCI) calculated for C₂₀H₂₁IRh [M- C₂₀H₂₁I₃Rh]⁺ 490.97375, found 490.9738

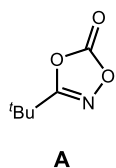
General procedure for amidation of 4-phenylbutene



A 4 mL vial containing Rh(III) catalyst (0.005 mmol), LiOAc (0.010 mmol), LiNTf₂ (0.100 mmol) and AgNTf₂ (0.020 mmol) was removed from a nitrogen filled glove-box and placed under nitrogen balloon. To the reaction vial was added 4-phenylbutene stock solution (0.25 mL, 0.4M) via syringe. Then stock solution of amidation reagent (0.25 mL, 0.8M) was added via syringe and the reaction stirred for 48 at room temperature. The reaction mixture was filtered through a pad of celite and the residue was purified via column chromatography to afford a white solid. ¹H NMR spectra matches previously reported data.⁷⁶

¹H NMR: (CDCl₃, 600 MHz) δ 7.30 – 7.28 (m, 2H), 7.23 – 7.20 (m, 1H), 7.19 – 7.16 (m, 2H), 5.85 (ddd, *J* = 17.1, 10.5, 5.2 Hz, 1H), 5.46 (d, *J* = 8.2, 1H), 5.11 – 5.06 (m, 2H), 4.80 – 4.74 (m, 1H), 2.92 (dd, *J* = 13.7, 6.6 Hz, 1H), 2.83 (dd, *J* = 13.7, 6.8 Hz, 1H), 1.11 (s, 9H).

Nitrene Precursor A: 3-(tert-butyl)-1,4,2-dioxazol-5-one. Prepared according to previously reported procedures.⁴⁸

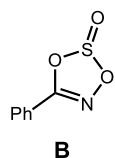


CDI (3.81 g, 23.5 mmol) was removed from the box in a sealed 250 mL round bottom flask and placed under nitrogen balloon. The reaction flask was charged with 40 mL MeCN. The flask was briefly opened to add pivalic acid (2.00 g, 19.6 mmol) and stirred for 2 hours. Then the flask was briefly opened, and hydroxylamine hydrochloride was added (1.70 g, 24.5 mmol) and the reaction stirred overnight under a balloon of nitrogen. Then the septum was briefly opened and CDI (4.76 g, 29.4 mmol) was added quickly and the reaction stirred at room temperature for 2 hours. The reaction was quenched with 1 M HCl (50 mL) and the organics were extracted with DCM (3 x 50 mL). The combined organic fractions were dried with Na₂SO₄ and reduced via rotary evaporation. The crude hydroxamic acid was filtered through a pad of celite,

and washed with DCM to deliver the dioxazolone (2.38 g, 85% yield). The ^1H NMR matches previously reported data.

^1H NMR: (CDCl_3 , 400 MHz) δ 1.34 (s, 9H)

Nitrene Precursor B: 5-phenyl-1,3,2,4-dioxathiazole 2-oxide. Prepared according to previously reported procedures.^{59,86}



CDI (8.19 g, 8.19 mmol) was removed from the box in a sealed 250 mL round bottom flask and placed under nitrogen balloon. The reaction flask was charged with 50 mL THF. The flask was briefly opened to add benzoic acid (1.00 g, 12.3 mmol) and stirred for 2 hours. Then the flask was briefly opened, and hydroxylamine hydrochloride was added (1.14g, 16.4 mmol) and the reaction stirred overnight under a balloon of nitrogen. The reaction was quenched with 5% aqueous NaHSO_4 and the organics were extracted with EtOAc 3 times. The combined organic fractions were dried with Na_2SO_4 and reduced via rotary evaporation. The N-hydroxybenzamide was purified via column chromatography (0% - 5% MeOH in DCM) to deliver a white solid (0.50 g, 45% yield). ^1H NMR matches previously reported spectral data.⁸⁶

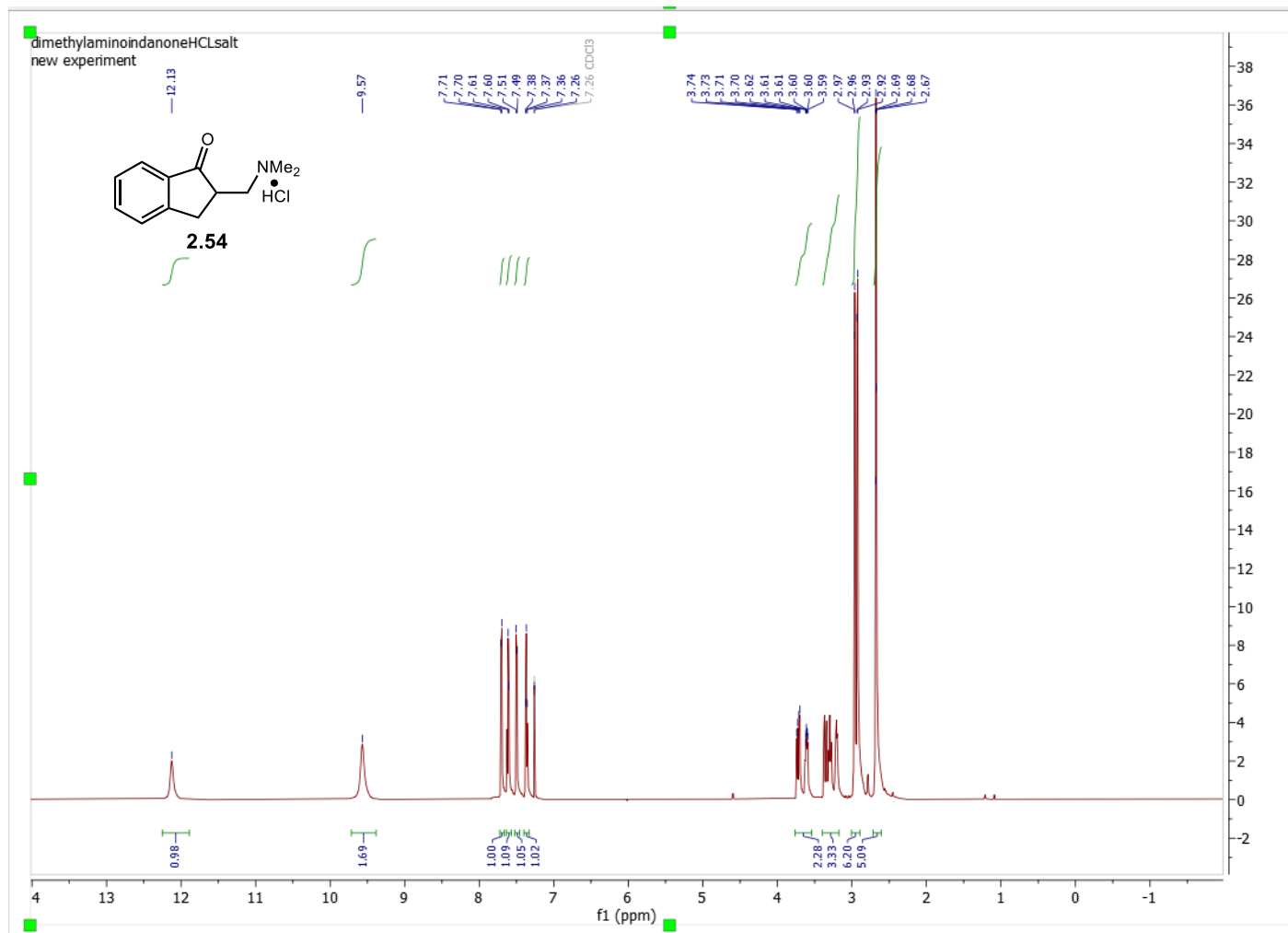
^1H NMR: (DMSO, 400 MHz) δ 11.22 (s, 1H), 9.04 (s, 1H), 7.78 – 7.70 (m, 2H), 7.55 – 7.48 (m, 1H), 7.45 (t, $J = 7.3$ Hz, 2H).

An oven-dried round-bottom flask was charged with crude hydroxamic acid (0.45 g, 3.28 mmol) and placed under nitrogen balloon. Dry DCM (15 mL) was added to the reaction flask followed by thionyl chloride (0.95 mL, 13.1 mmol). The reaction stirred overnight at room temperature. The reaction mixture was filtered and reduced under rotary evaporation to provide dioxathiazole-2-oxide product (0.54 g, 90% yield) as a yellow oil. ^1H NMR matches previously reported spectral data.⁵⁹

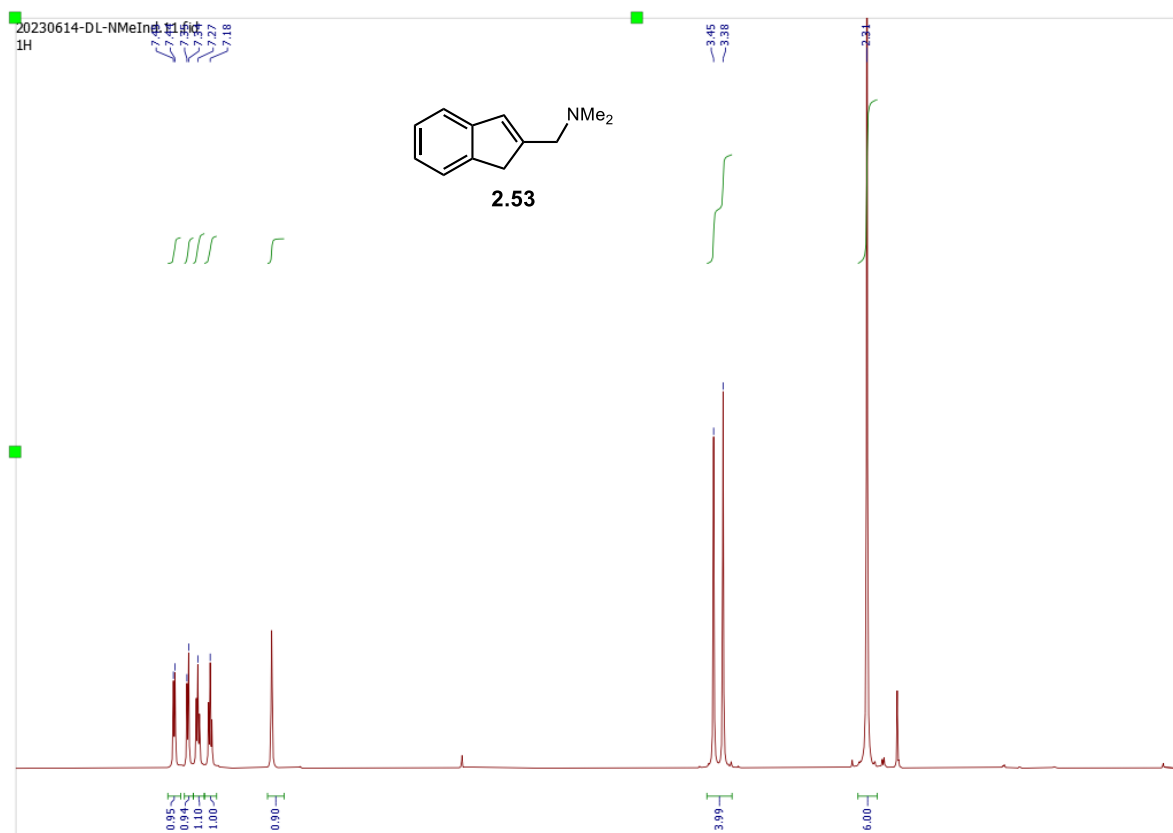
^1H NMR: (CDCl_3 , 400 MHz) δ 7.96 – 7.90 (m, 2H), 7.64 – 7.57 (m, 1H), 7.52 (t, $J = 7.6$ Hz, 2H)

2.6 Spectral Data

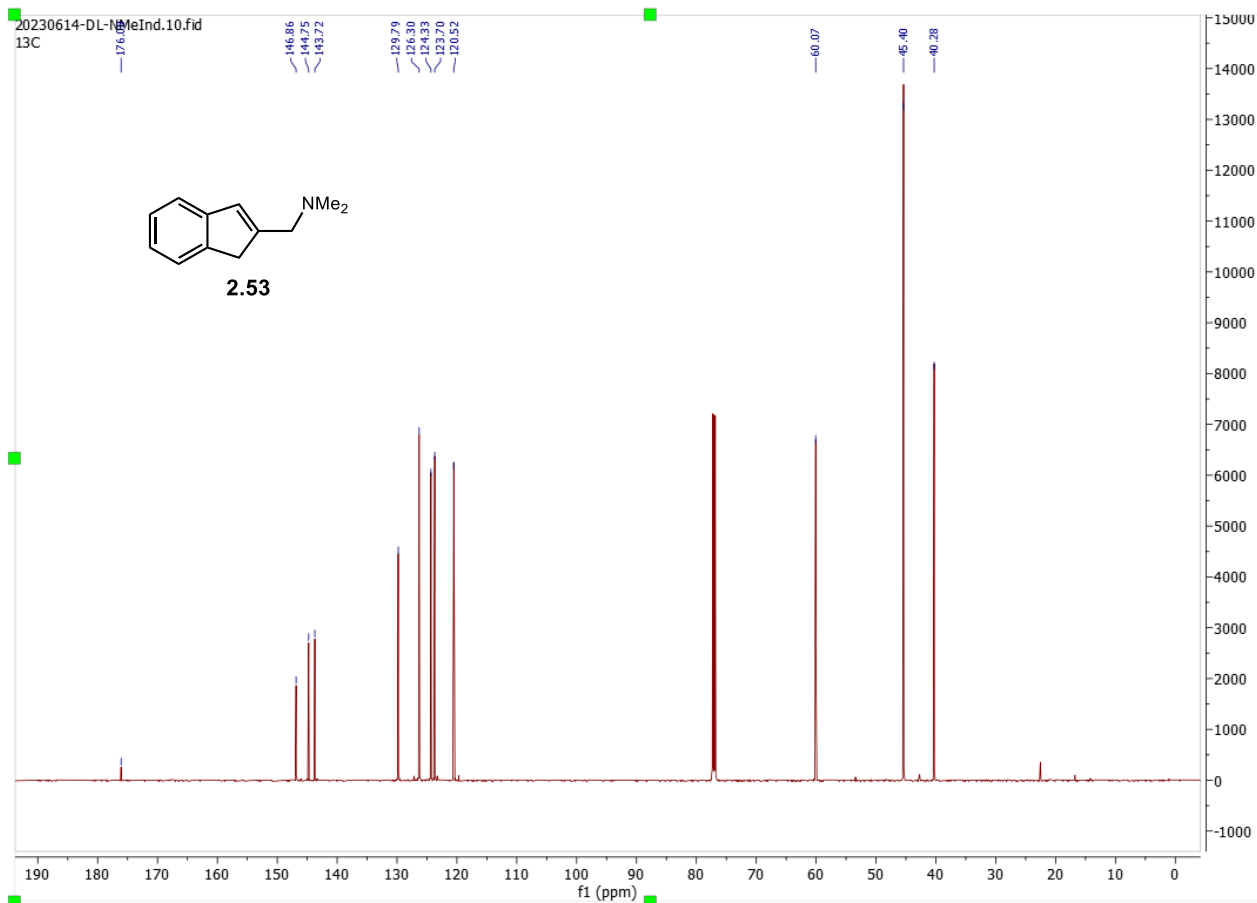
2.54: ^1H NMR (600 MHz, CDCl_3)



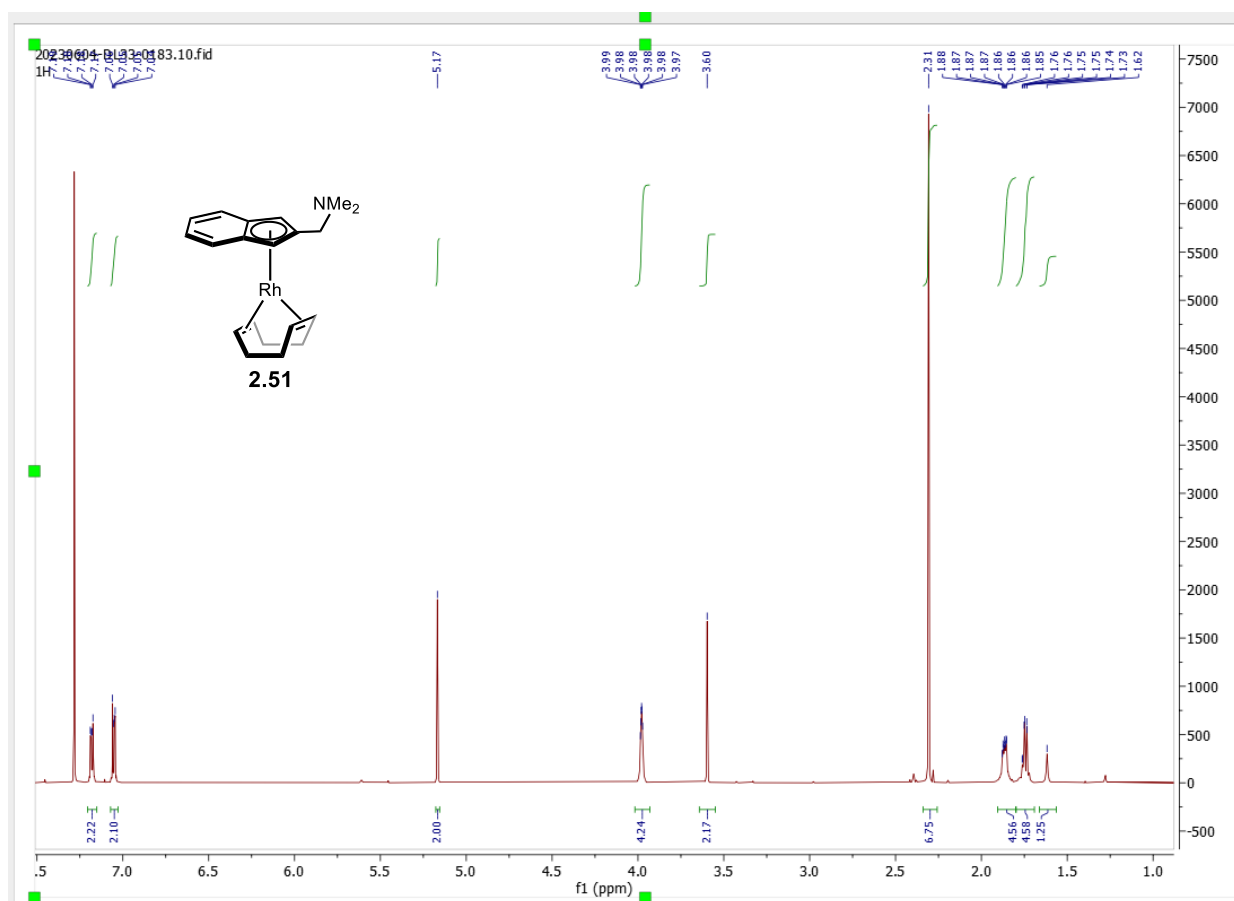
2.53: ^1H NMR (600 MHz, CDCl_3)



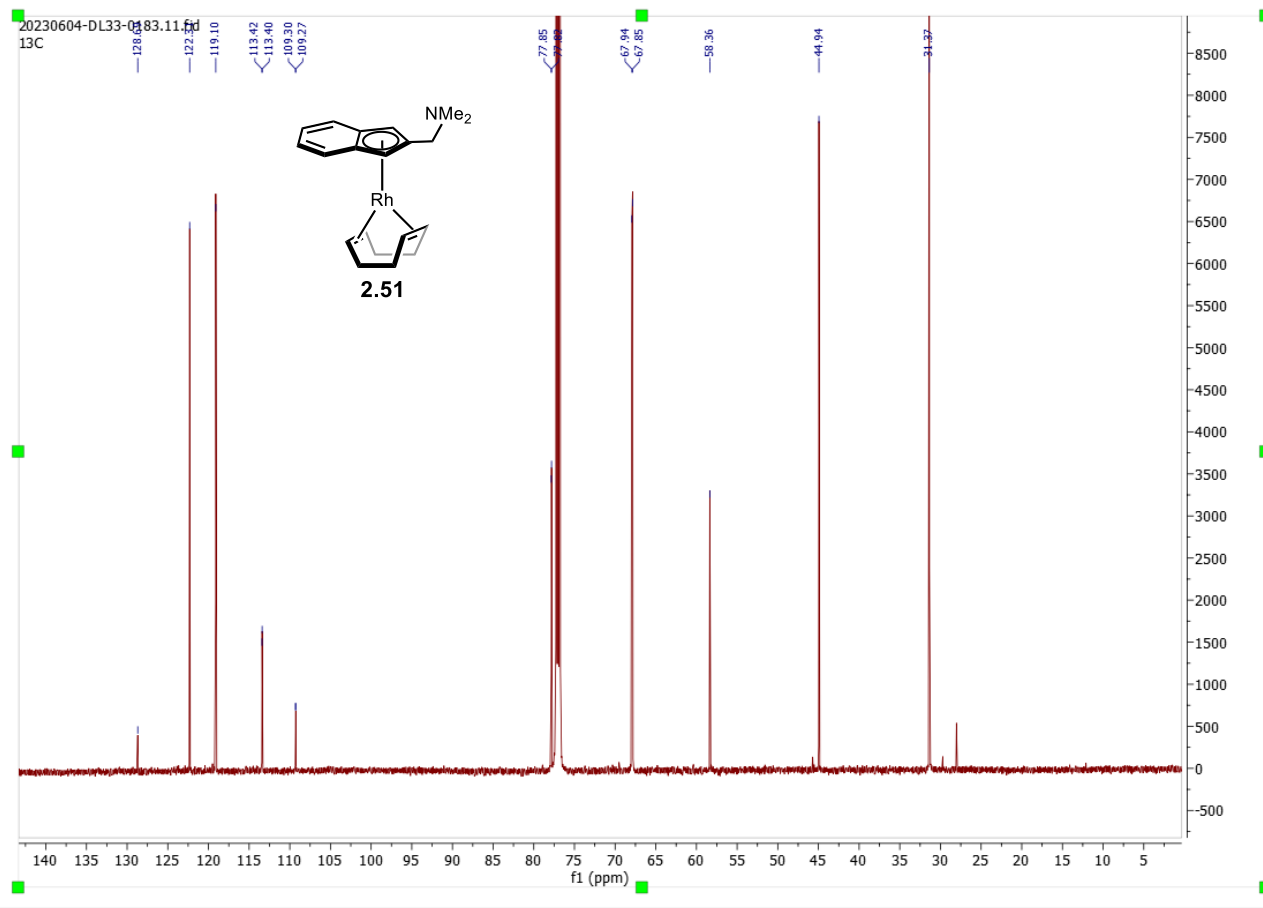
2.53 ^{13}C NMR (151MHz, CDCl_3)



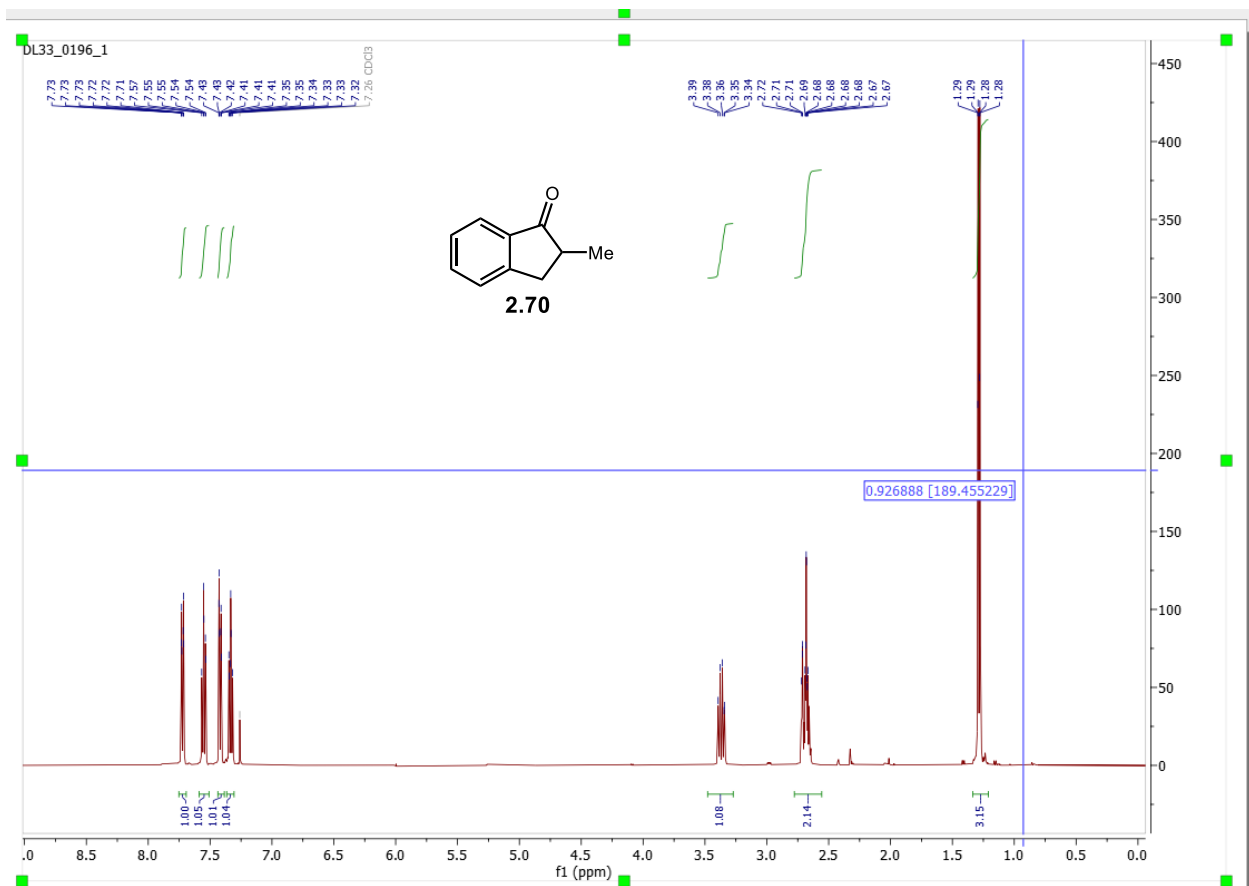
2.51 ¹H NMR (600 MHz, CDCl₃)



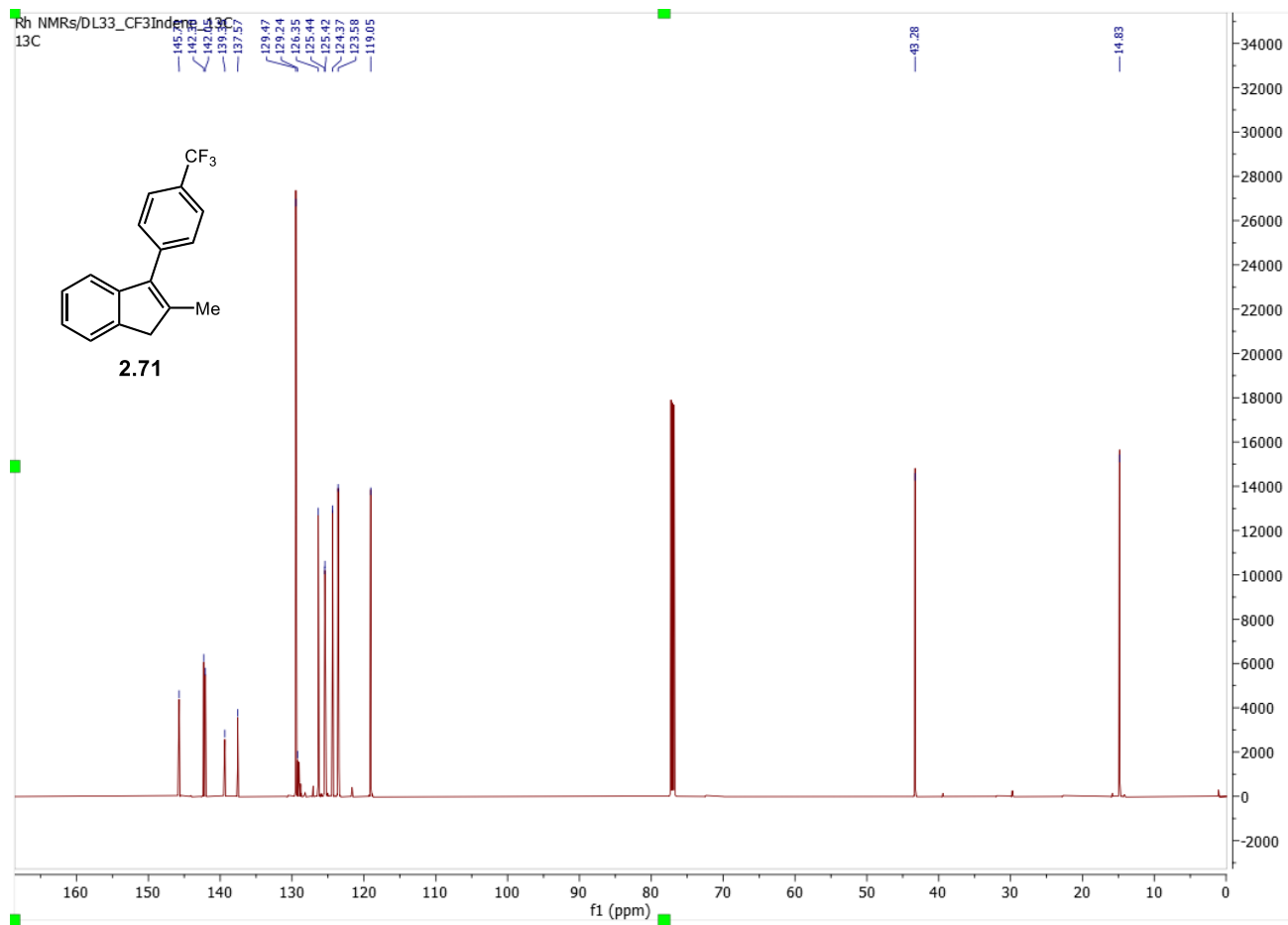
2.51: ^{13}C NMR (151MHz, CDCl_3)



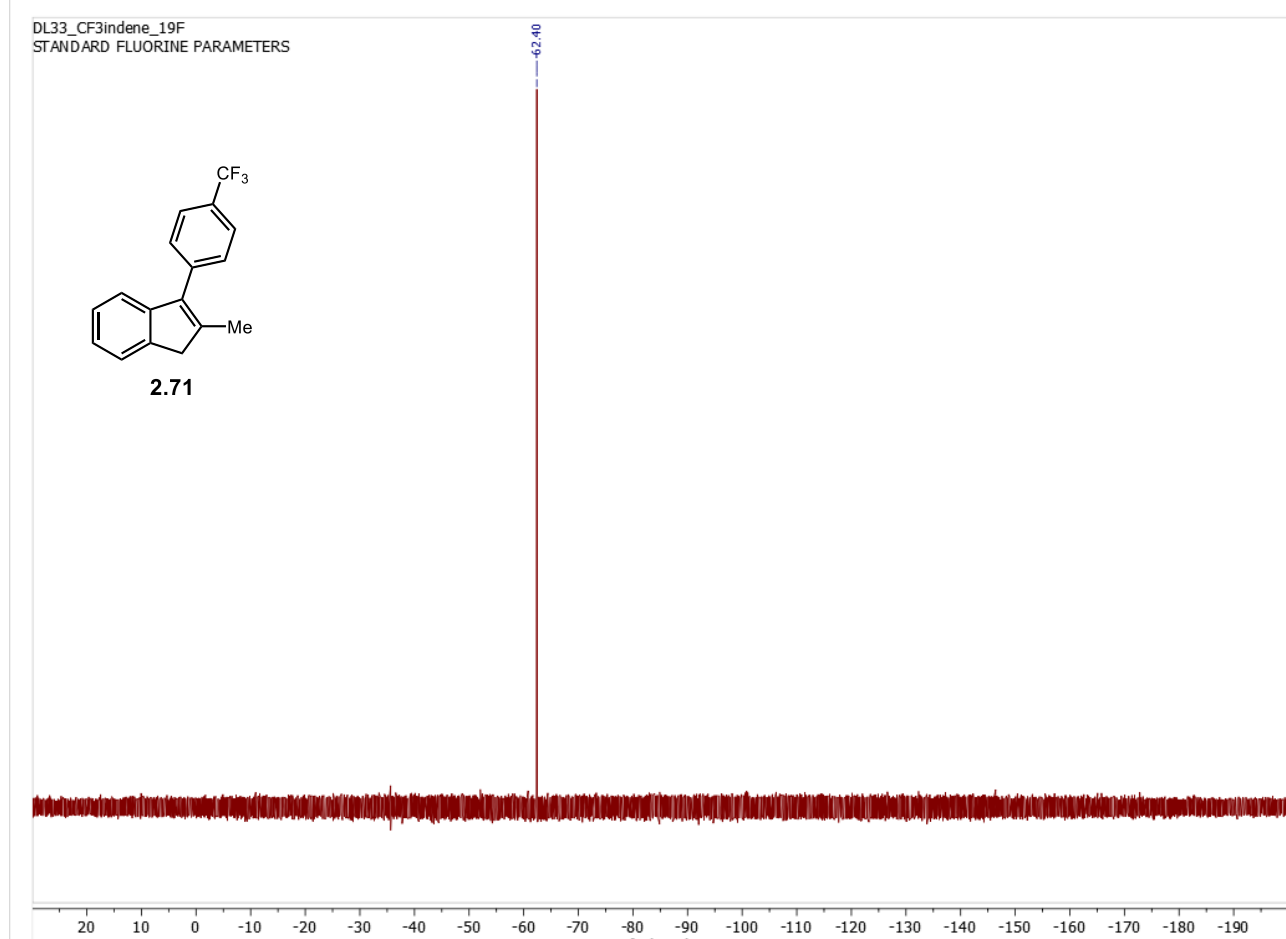
2.70 ¹H NMR (600 MHz, CDCl₃)



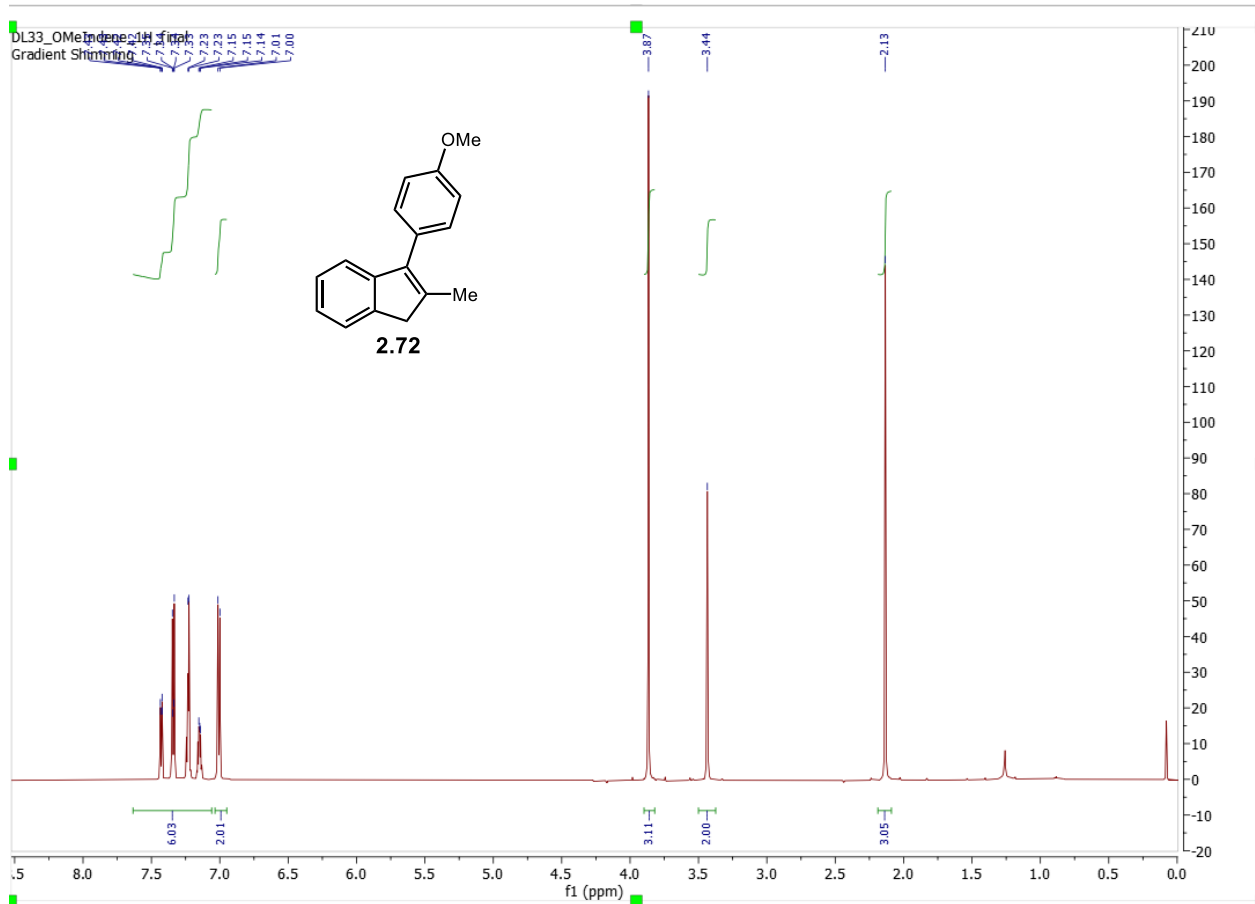
2.71 ¹³C NMR (600MHz, CDCl₃)



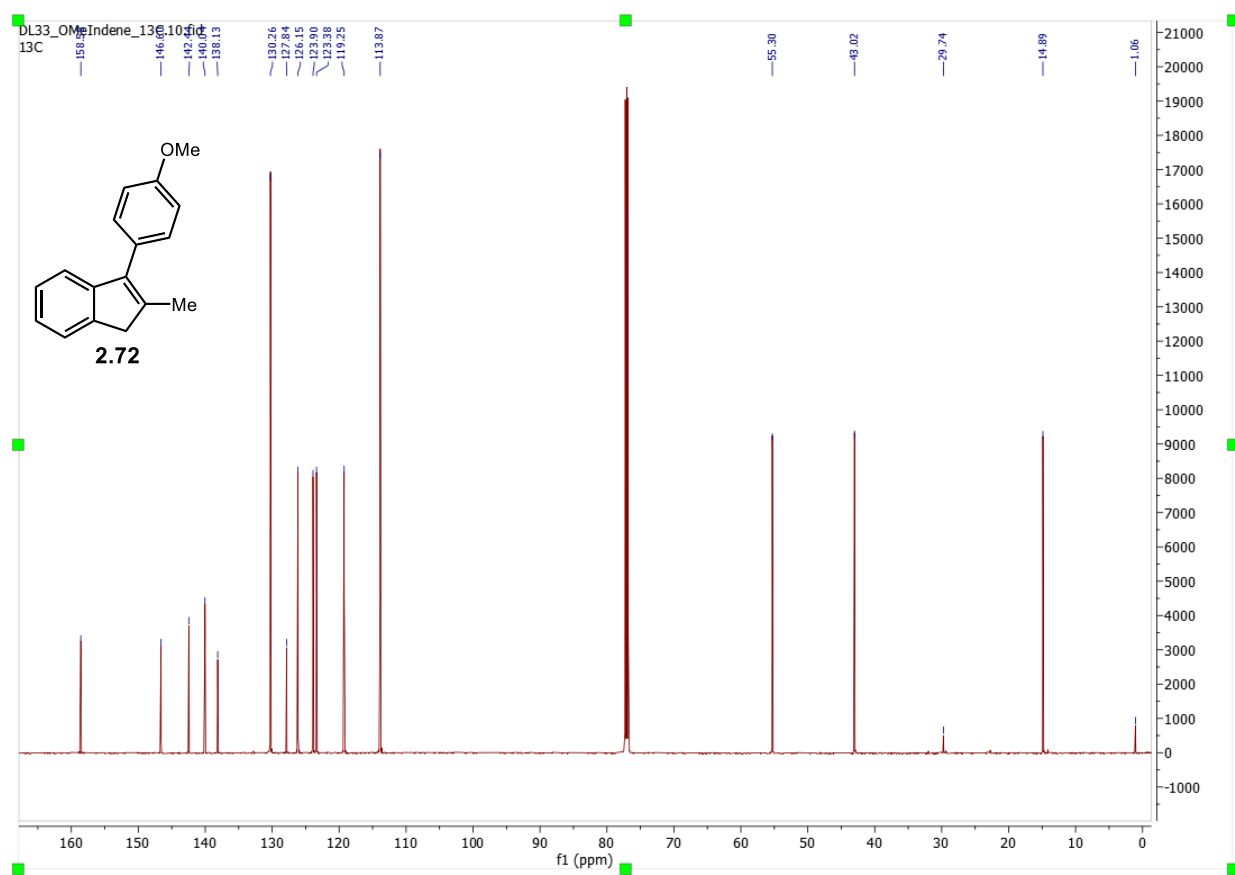
2.71: ^{19}F NMR (564 MHz, CDCl_3)



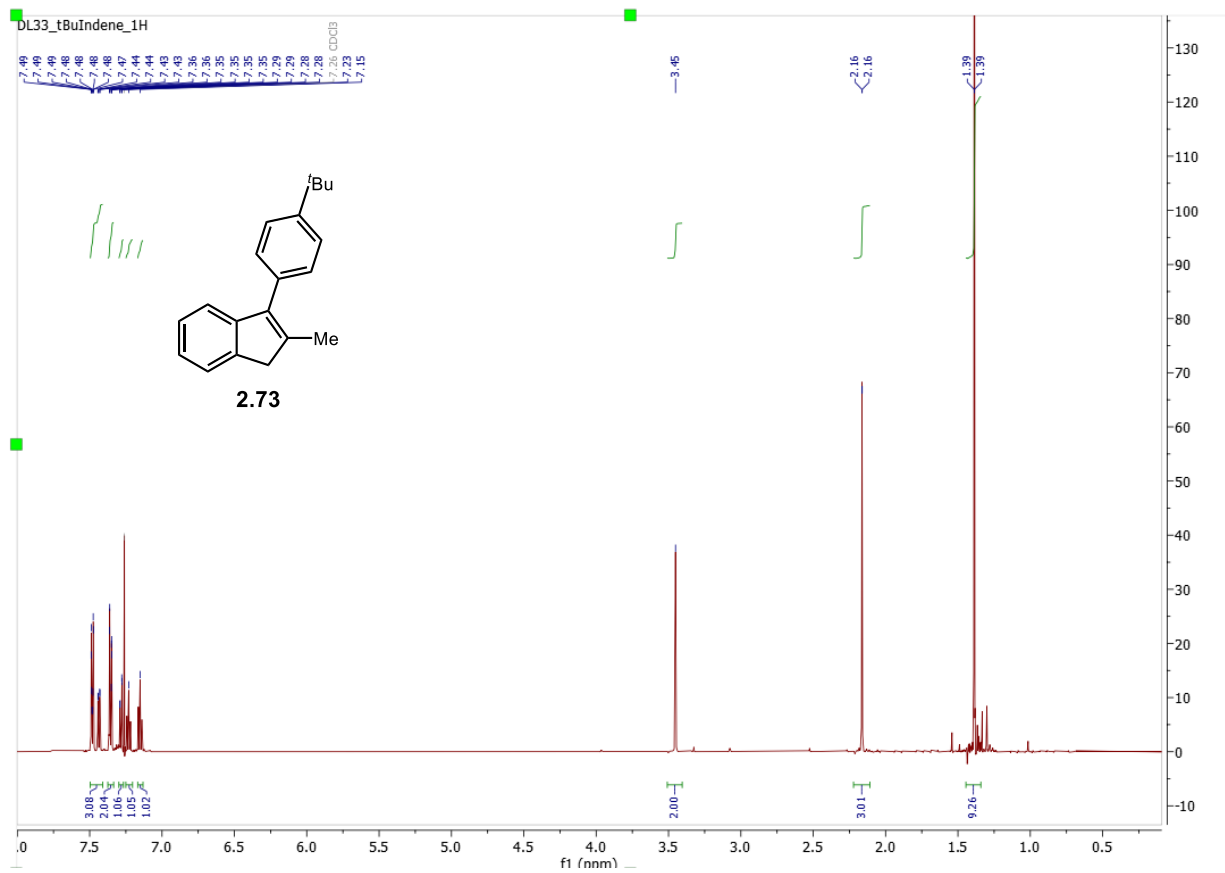
2.72: ^1H NMR, (600 MHz, CDCl_3)



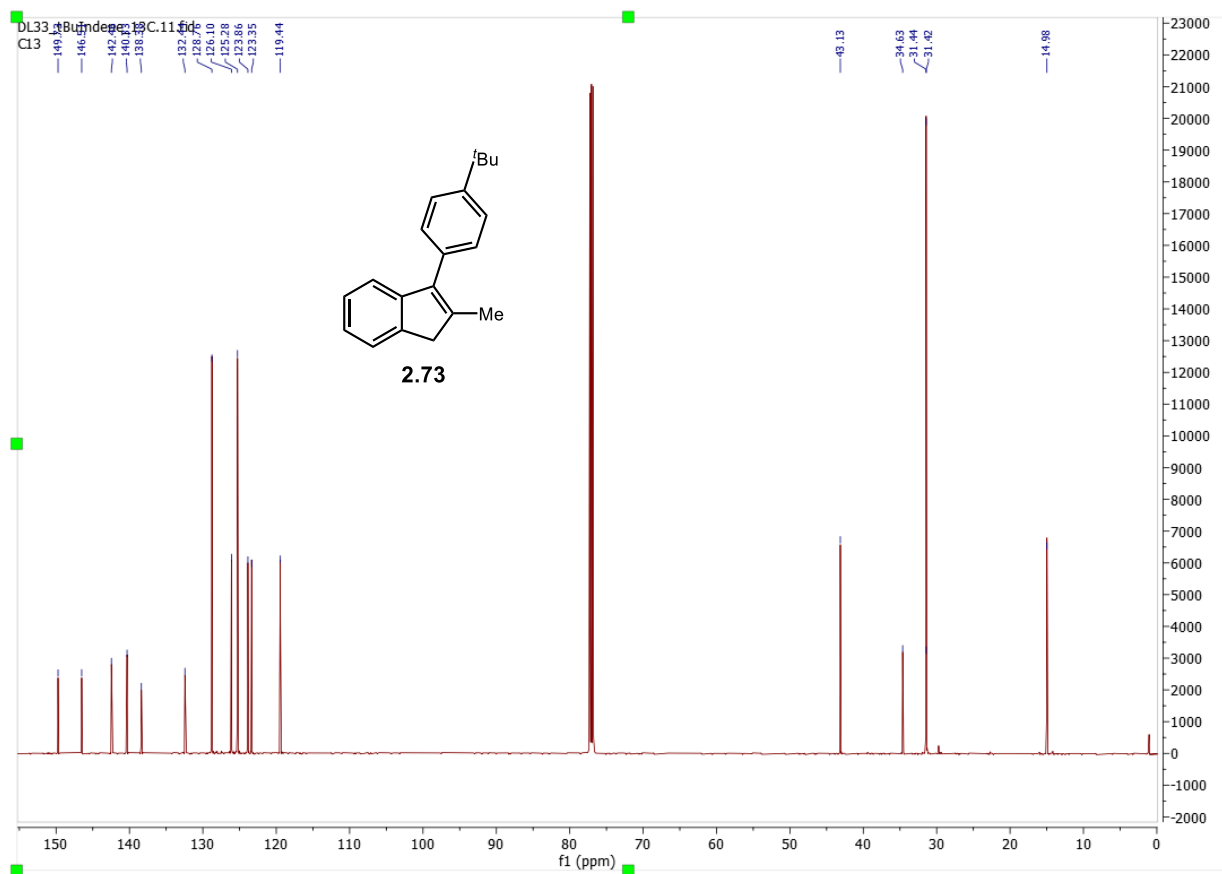
2.72: ^{13}C NMR (151 MHz, CDCl_3)



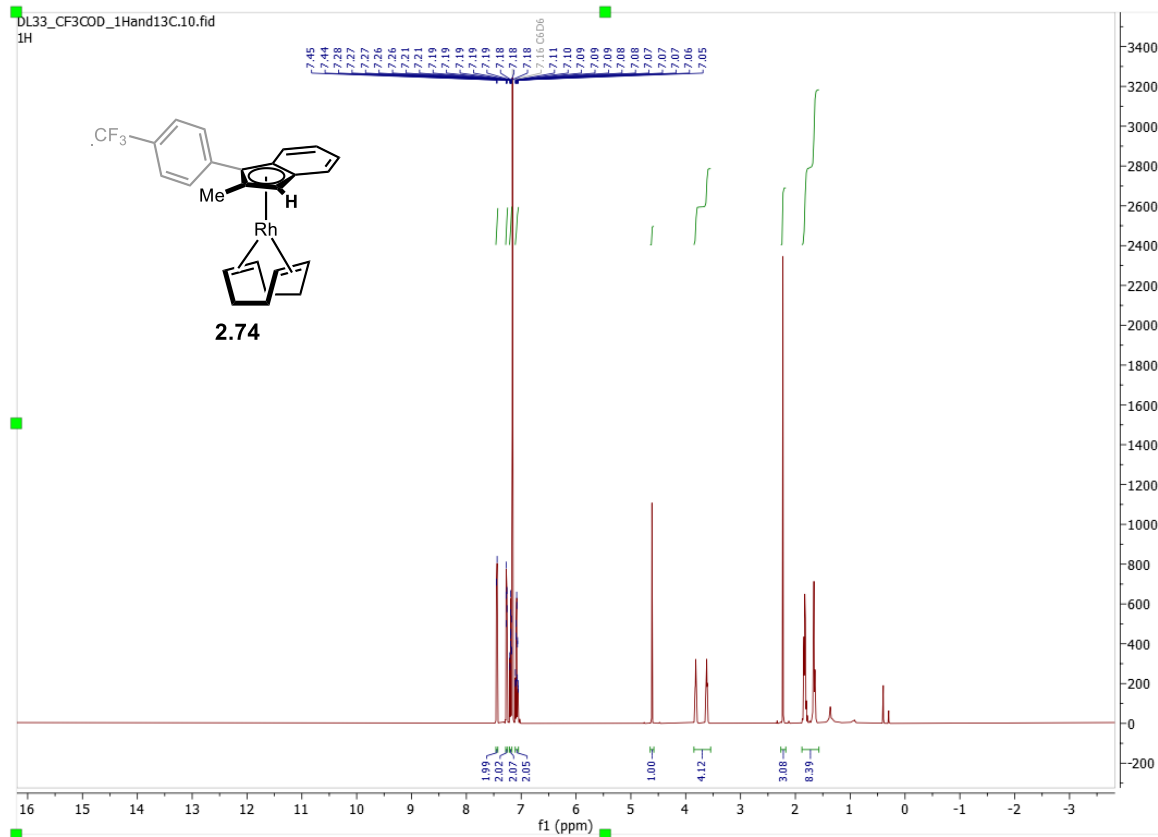
2.73: ^1H NMR (600 MHz, CDCl_3)



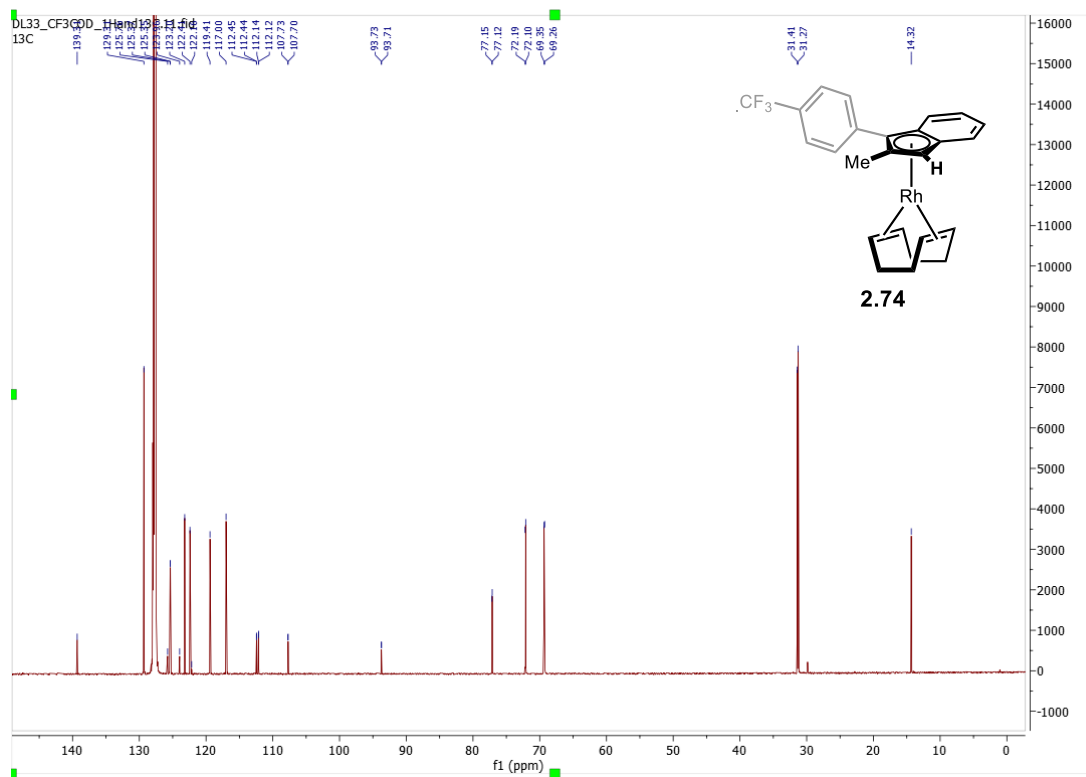
2.73: ^{13}C NMR (151 MHz, CDCl_3)



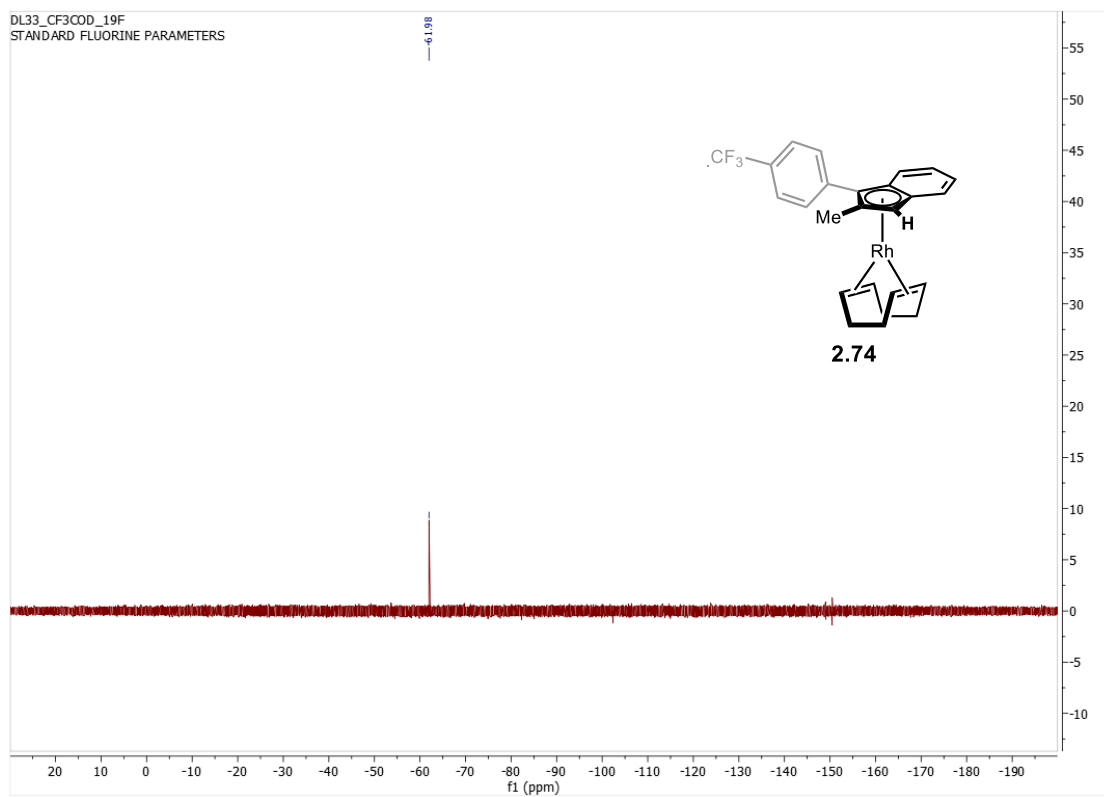
2.74: ^1H NMR (600 MHz, C_6D_6)

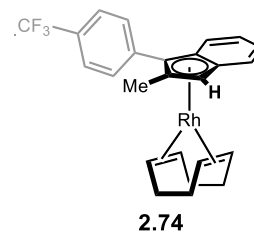


2.74: ^{13}C NMR (151 MHz, C_6D_6)



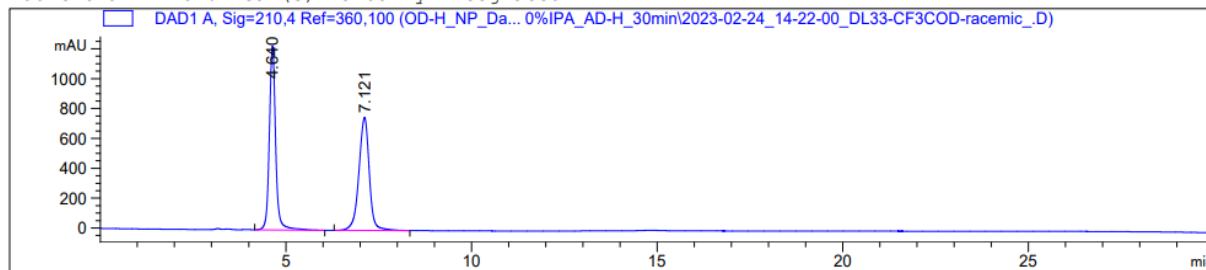
2.74: ^{19}F NMR (564 MHz, C_6D_6)





2.74: HPLC Traces to determine Enantiomeric Purity

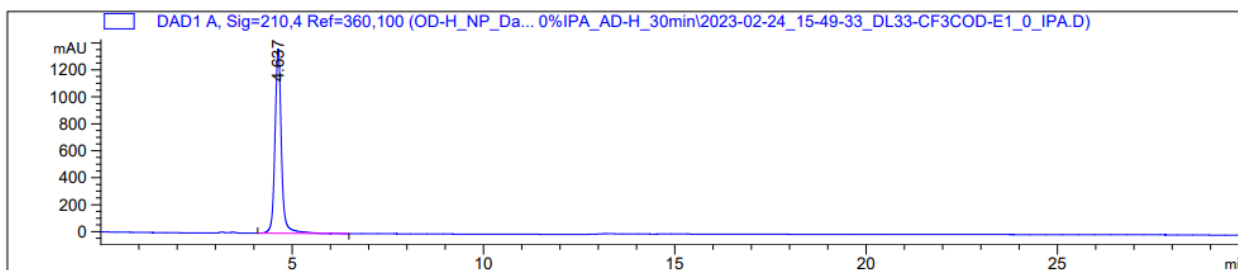
Racemic Trace



Signal 1: DAD1 A, Sig=210,4 Ref=360,100

Peak #	RetTime [min]	Type	Width [min]	Area [mAU*s]	Height [mAU]	Area %
1	4.640	BB	0.1801	1.45736e4	1230.82532	49.7977
2	7.121	BB	0.2922	1.46920e4	754.39130	50.2023

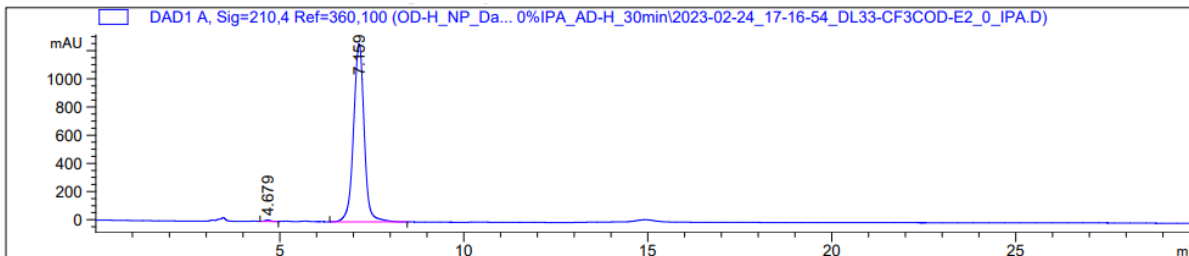
Enantiomer 1 Trace



Signal 1: DAD1 A, Sig=210,4 Ref=360,100

Peak #	RetTime [min]	Type	Width [min]	Area [mAU*s]	Height [mAU]	Area %
1	4.637	BV R	0.1774	1.61073e4	1367.97742	100.0000

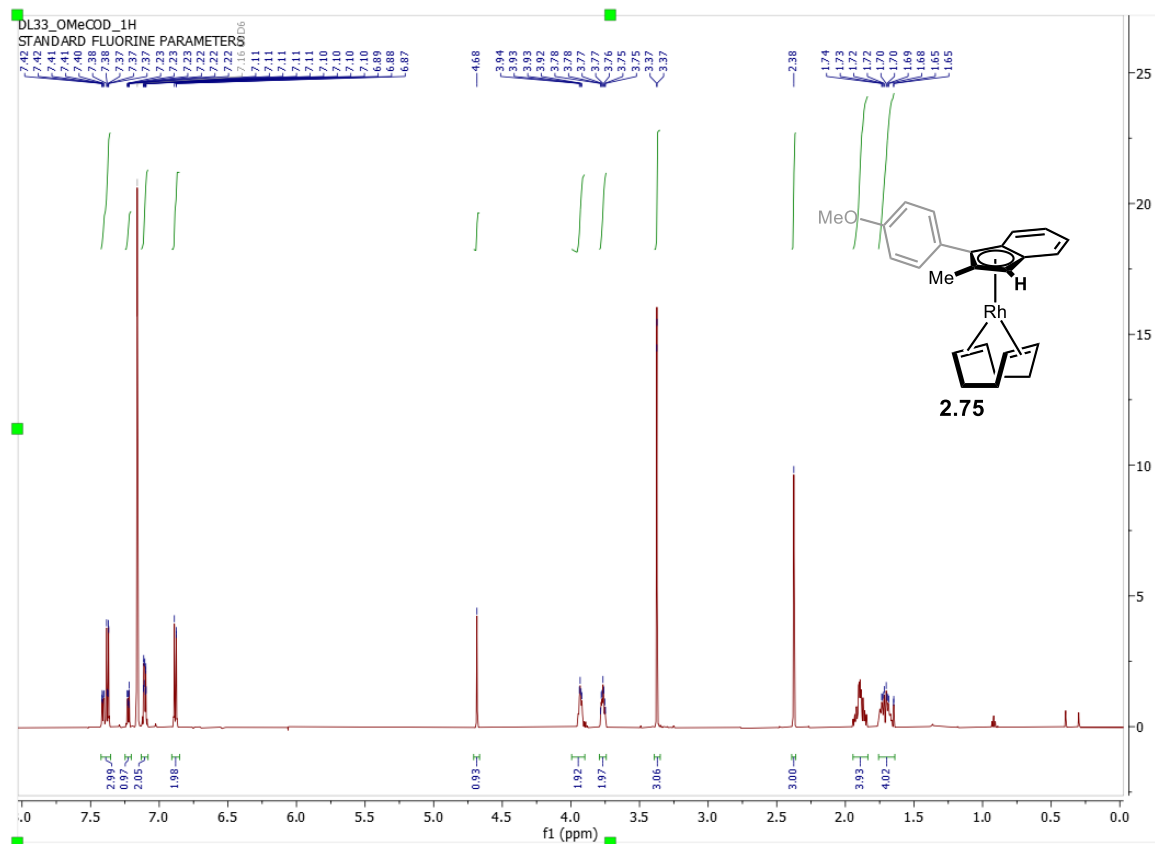
Enantiomer 2 Trace



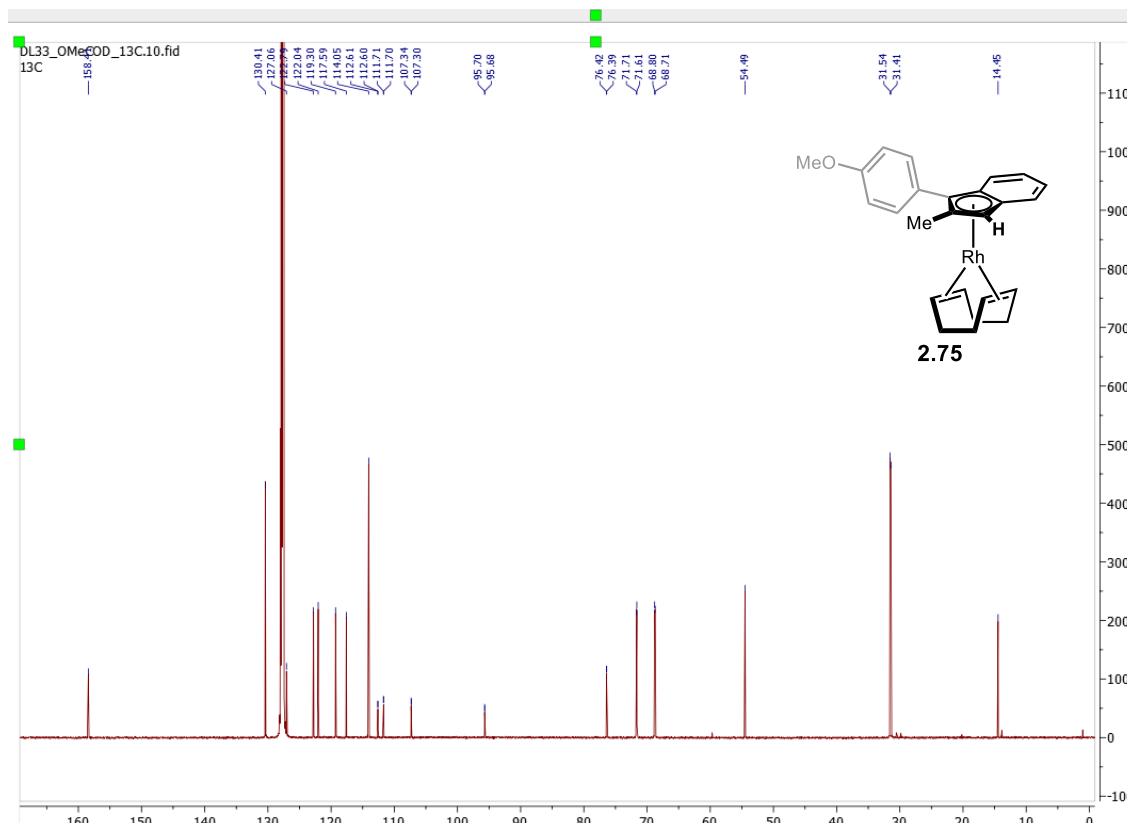
Signal 1: DAD1 A, Sig=210,4 Ref=360,100

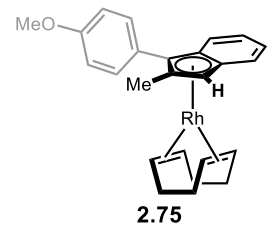
Peak #	RetTime [min]	Type	Width [min]	Area [mAU*s]	Height [mAU]	Area %
1	4.679	VB	0.1346	104.69446	9.32031	0.4106
2	7.159	BB	0.3003	2.53954e4	1264.67896	99.5894

2.75: ^1H NMR (600 MHz, C_6D_6)



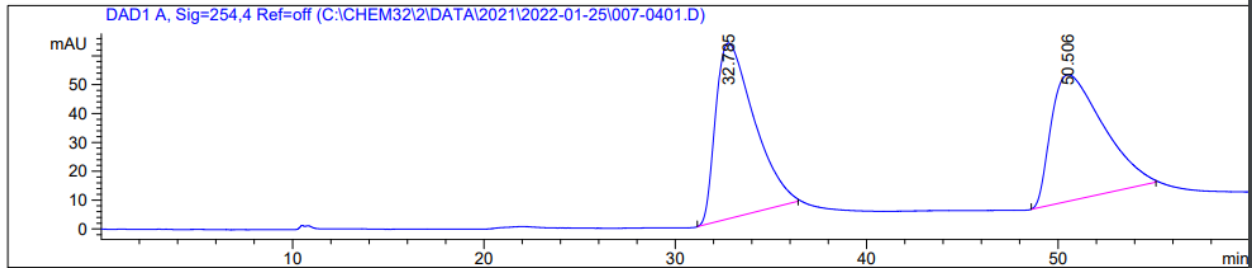
2.75: ^{13}C NMR (151MHz, C_6D_6)





2.75: HPLC Traces to Determine Enantiomeric Purity

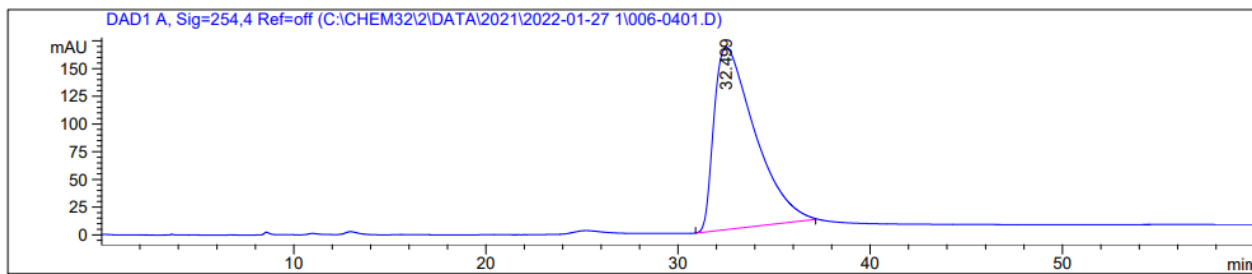
Racemic Trace



Signal 1: DAD1 A, Sig=254,4 Ref=off

Peak #	RetTime [min]	Type	Width [min]	Area [mAU*s]	Height [mAU]	Area %
1	32.785	BB	1.9017	8497.05078	60.90253	50.7854
2	50.506	BB	2.2075	8234.23340	43.87610	49.2146

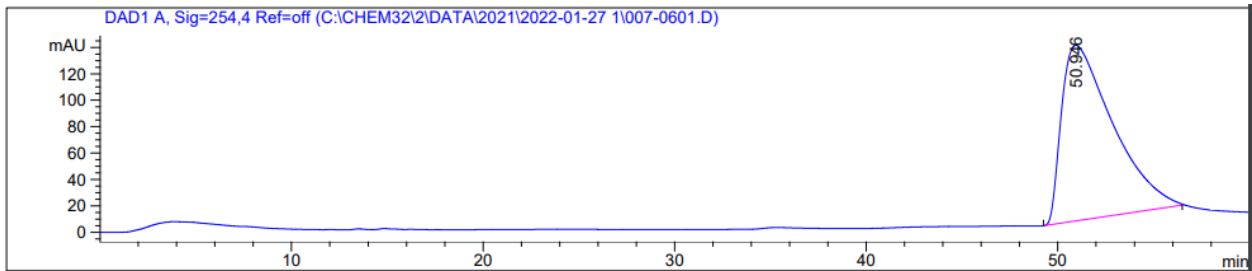
Enantiomer 1



Signal 1: DAD1 A, Sig=254,4 Ref=off

Peak #	RetTime [min]	Type	Width [min]	Area [mAU*s]	Height [mAU]	Area %
1	32.499	BB	2.0821	2.42883e4	164.54539	100.0000

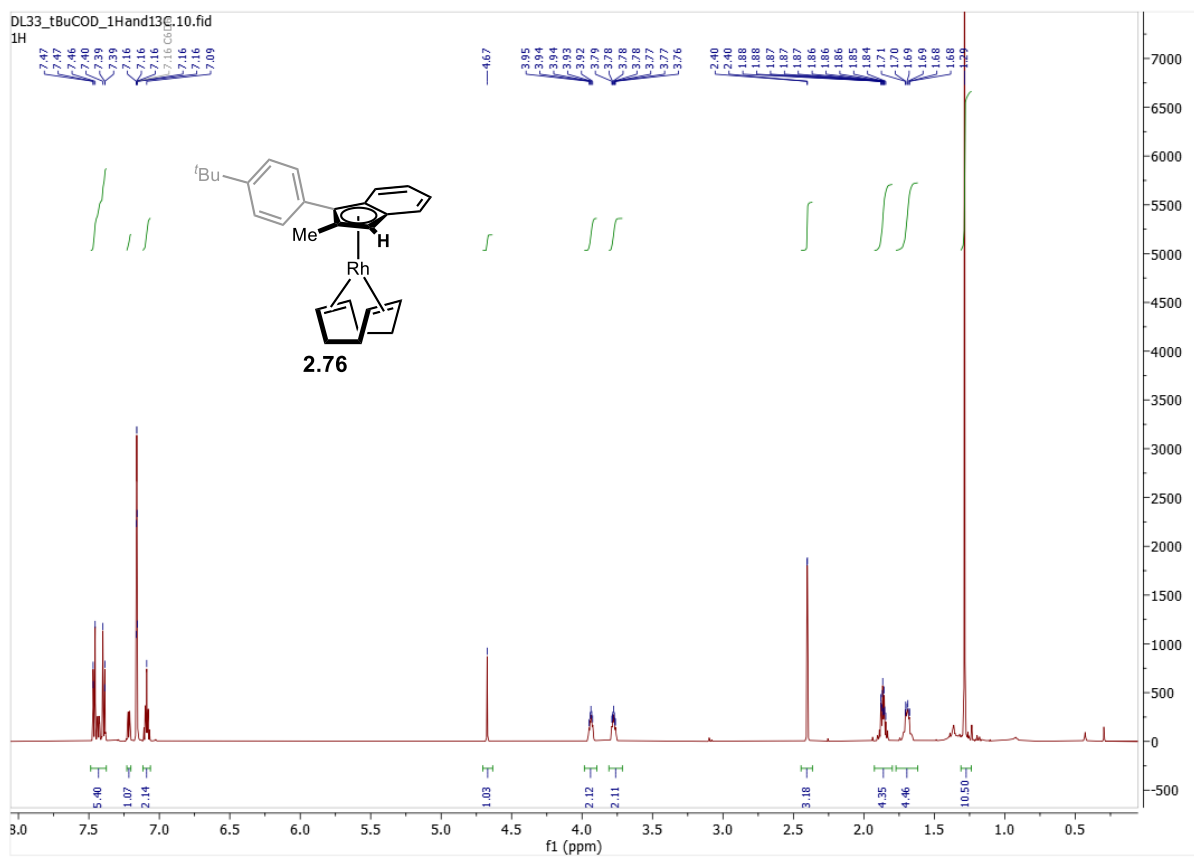
Enantiomer 2



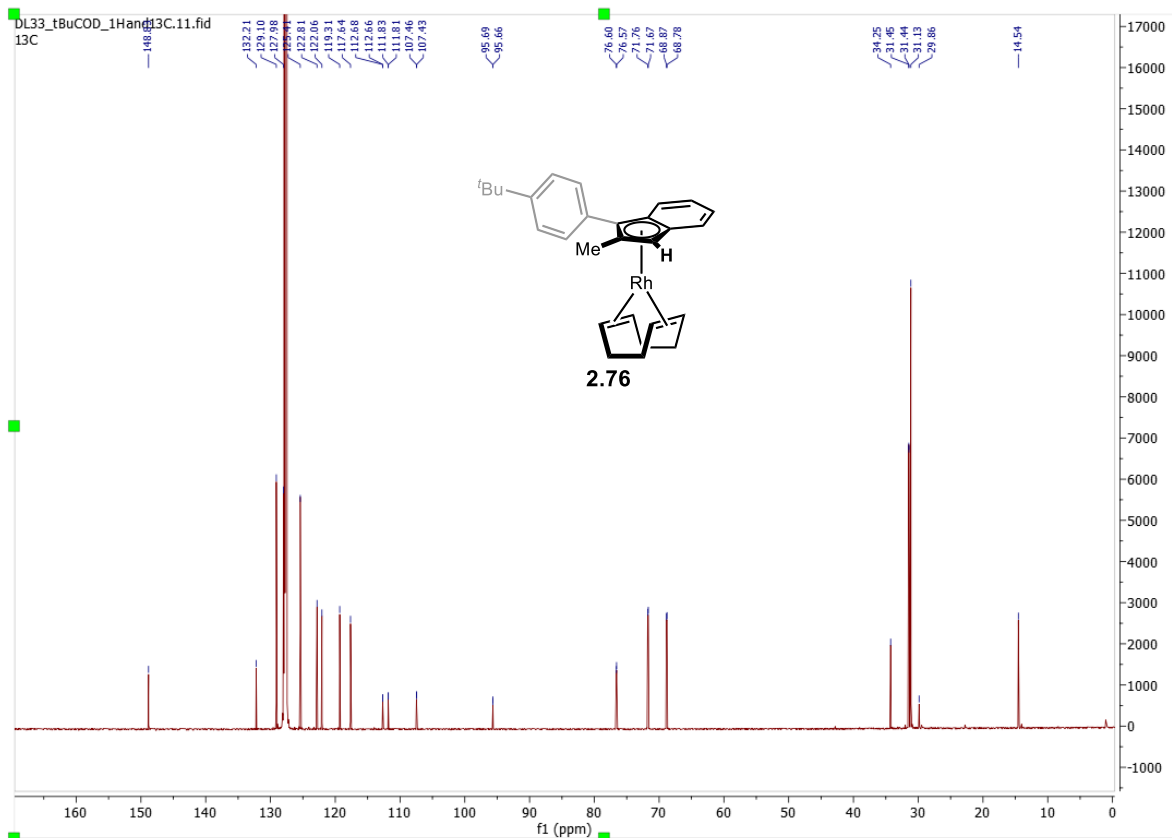
Signal 1: DAD1 A, Sig=254,4 Ref=off

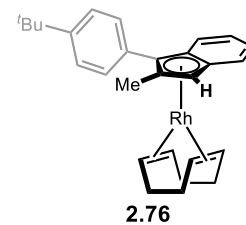
Peak #	RetTime [min]	Type	Width [min]	Area [mAU*s]	Height [mAU]	Area %
1	50.946	BB	2.4440	2.47072e4	133.08168	100.0000

2.76: ^1H NMR (600MHz, C_6D_6)



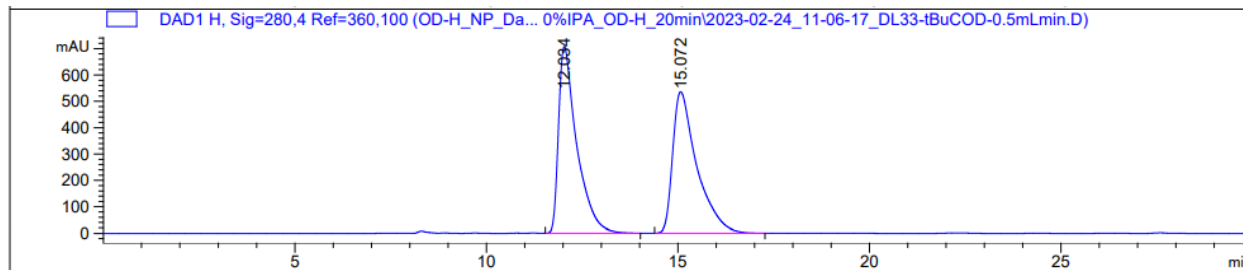
2.76: ^{13}C NMR (151 MHz, C_6D_6)





2.76: HPLC Traces to Determine Enantiomeric Purity

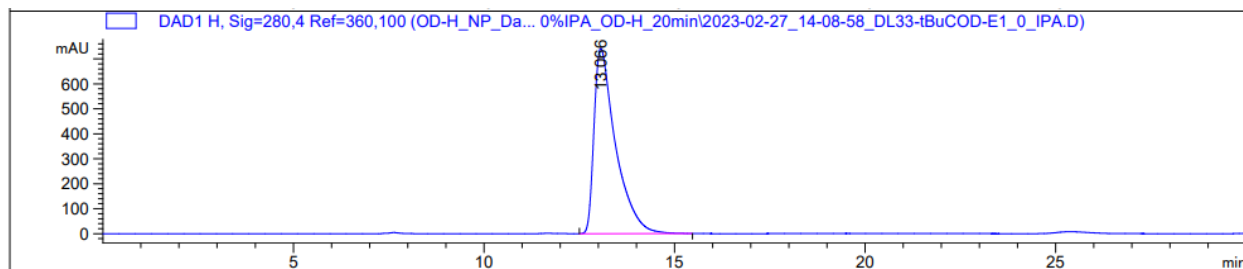
Racemic Trace



Signal 8: DAD1 H, Sig=280,4 Ref=360,100

Peak #	RetTime [min]	Type	Width [min]	Area [mAU*s]	Height [mAU]	Area %
1	12.034	BB	0.4545	2.33193e4	706.56873	49.9360
2	15.072	BB	0.5452	2.33790e4	535.66266	50.0640

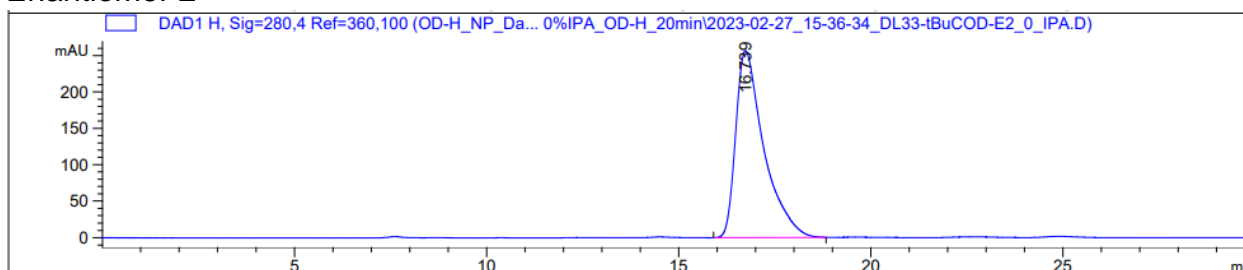
Enantiomer 1



Signal 8: DAD1 H, Sig=280,4 Ref=360,100

Peak #	RetTime [min]	Type	Width [min]	Area [mAU*s]	Height [mAU]	Area %
1	13.066	BB	0.5203	2.91352e4	741.71021	100.0000

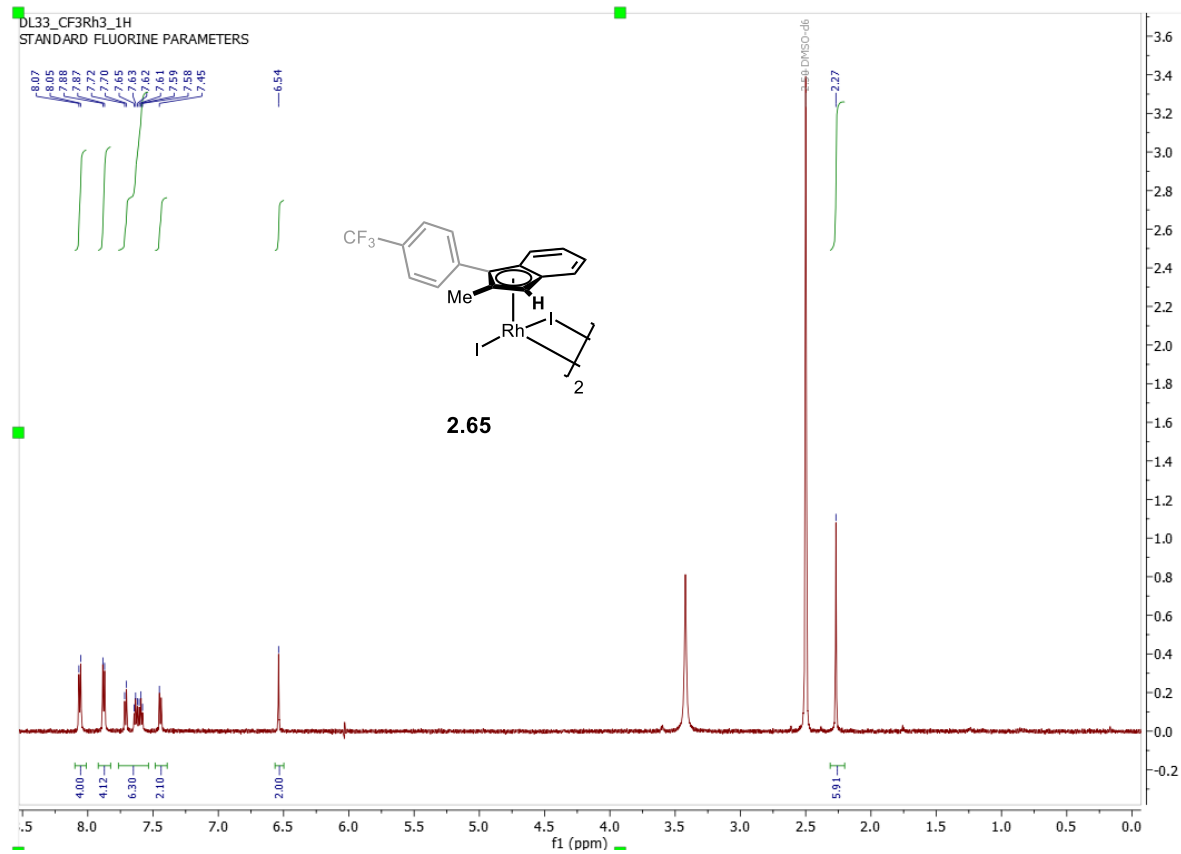
Enantiomer 2



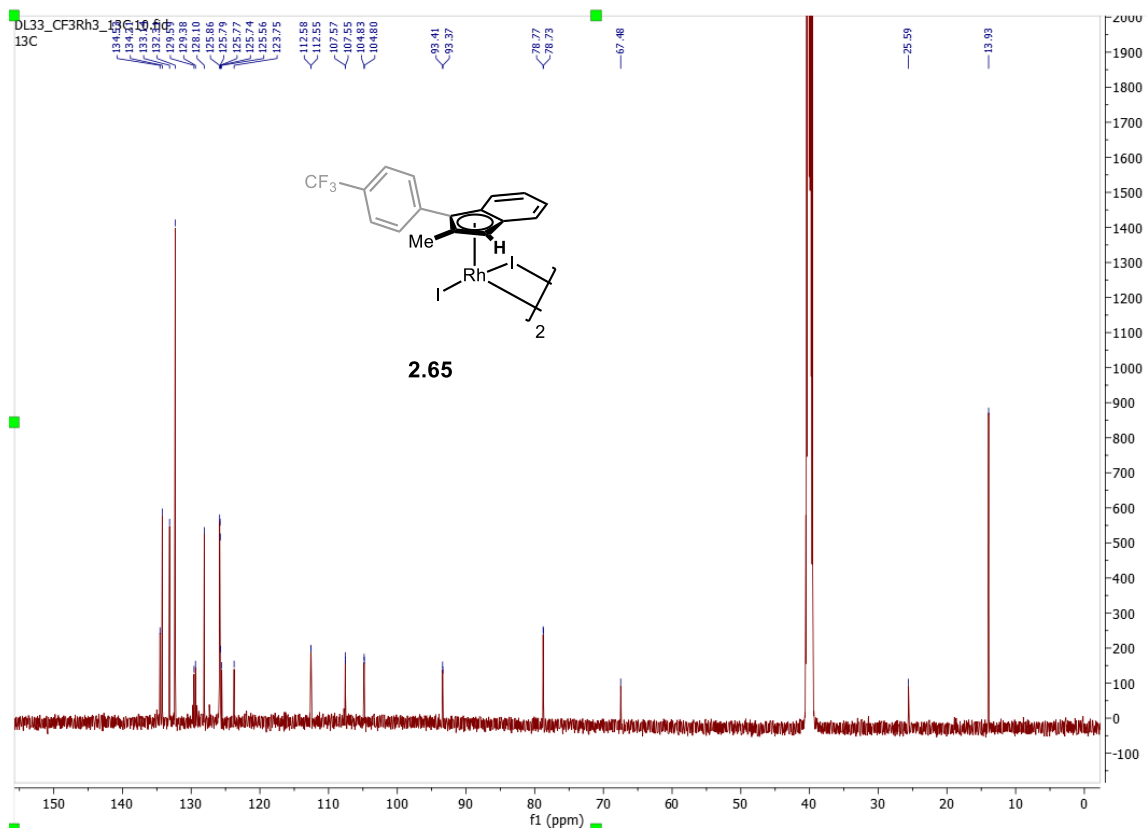
Signal 8: DAD1 H, Sig=280,4 Ref=360,100

Peak #	RetTime [min]	Type	Width [min]	Area [mAU*s]	Height [mAU]	Area %
1	16.739	BB	0.6018	1.29895e4	256.50885	100.0000

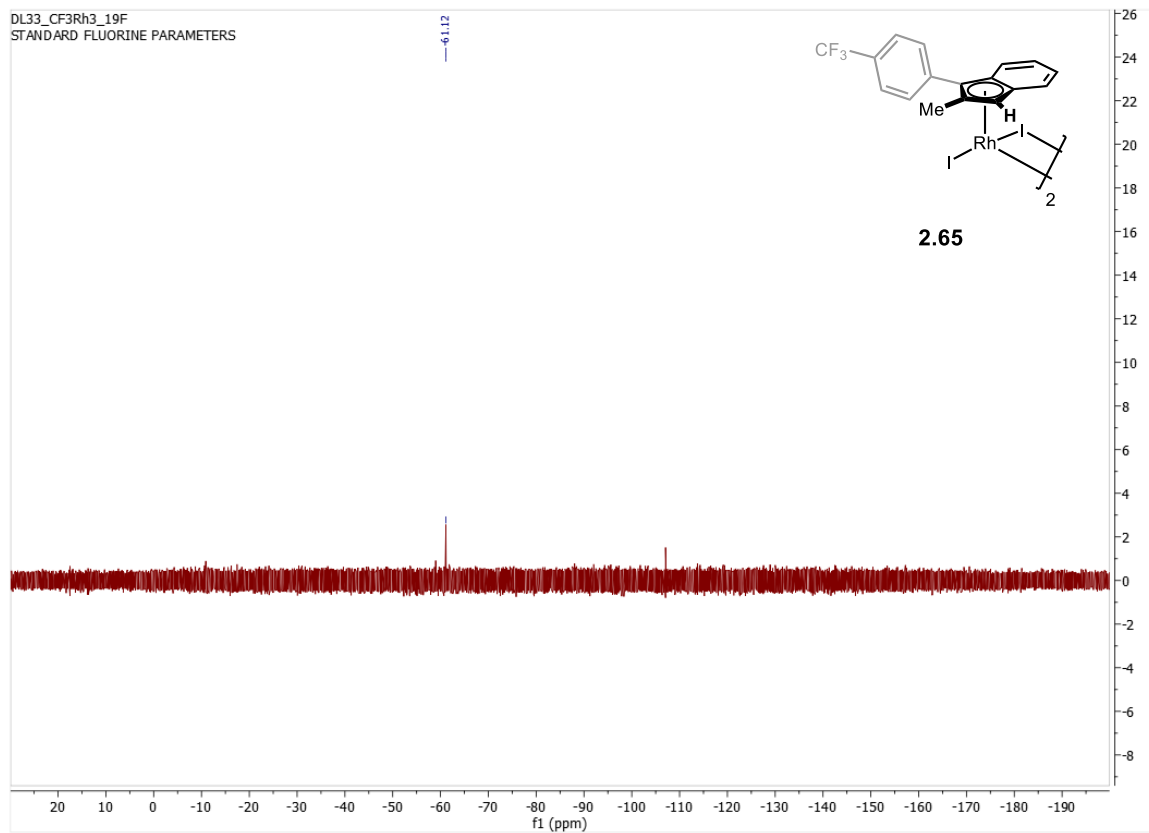
2.65: ^1H NMR (600 MHz, $\text{DMSO-}d_6$)



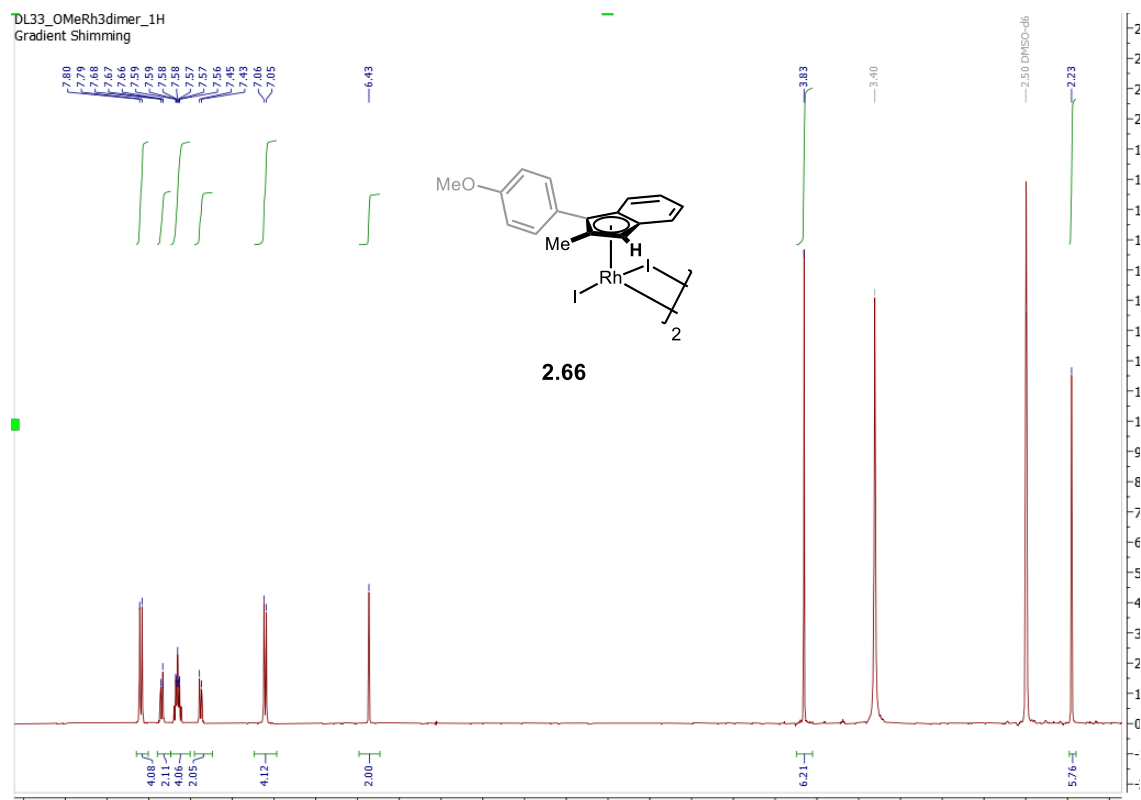
2.65: ^{13}C NMR (151 MHz, $\text{DMSO-}d_6$)



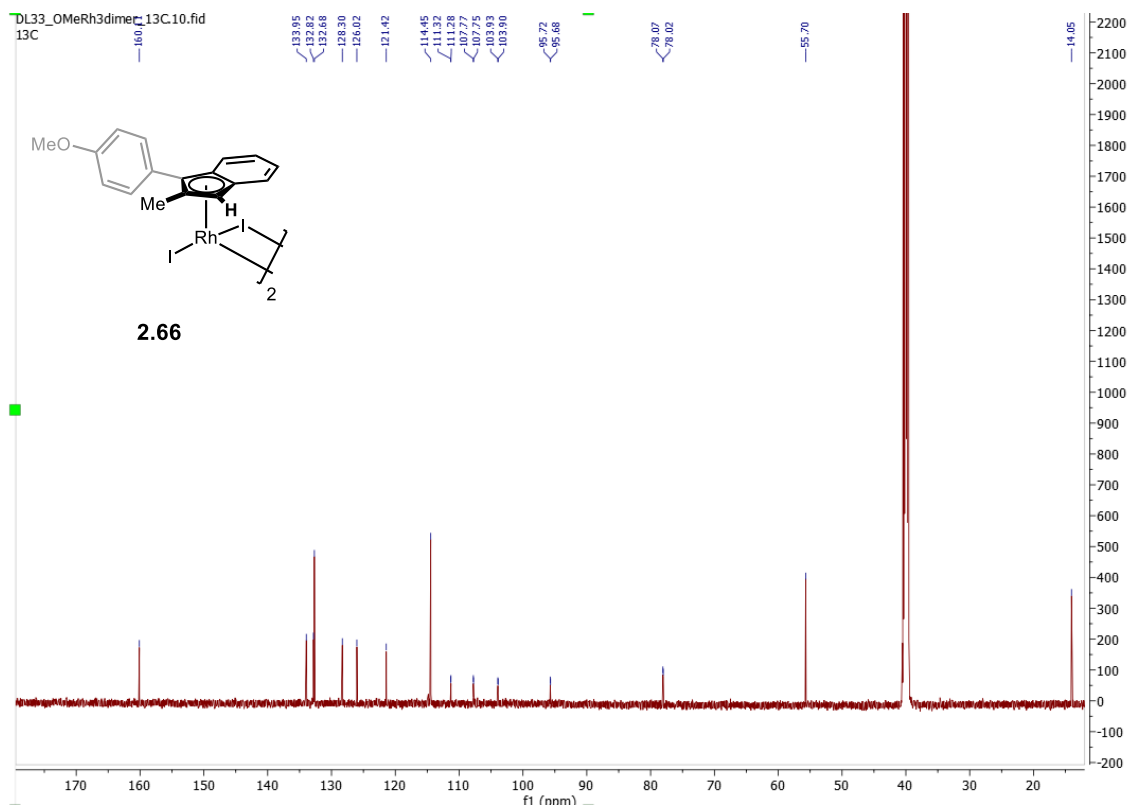
2.65: ^{19}F NMR (564 MHz, $\text{DMSO-}d_6$)



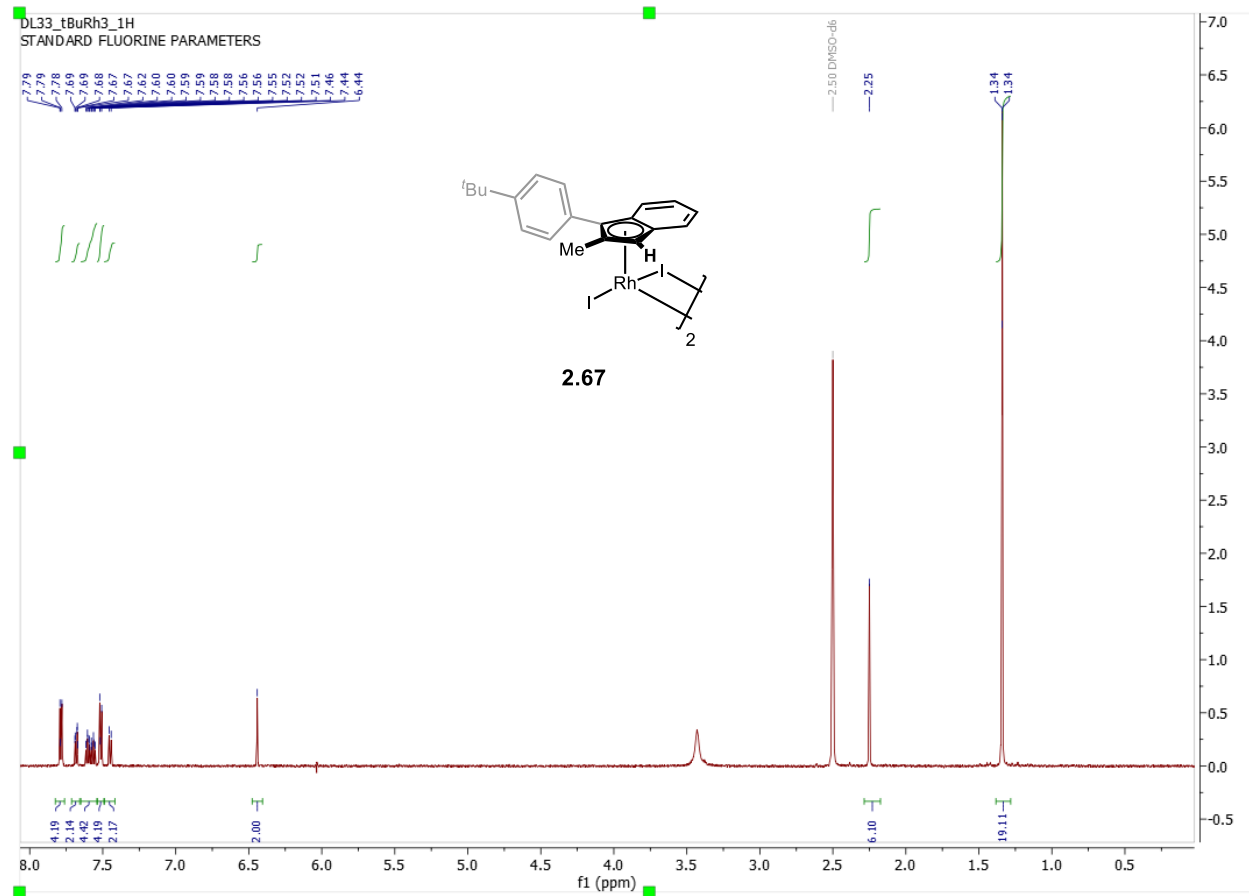
2.66: ^1H NMR (600 MHz, $\text{DMSO-}d_6$)



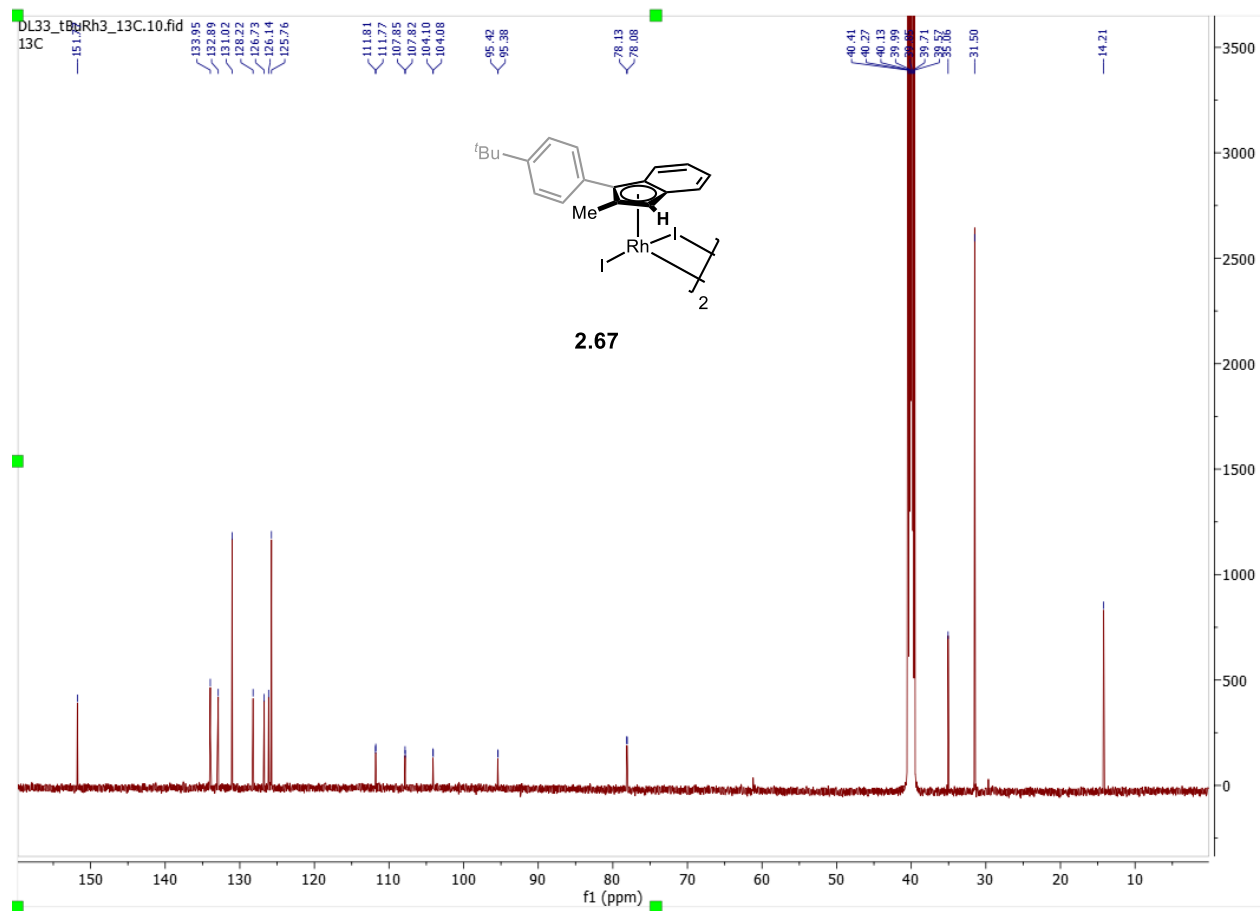
2.66: ^1H NMR (151 MHz, $\text{DMSO-}d_6$)



2.67: ^1H NMR (600 MHz, $\text{DMSO-}d_6$)



2.67: ^{13}C NMR (151MHz, DMSO- d_6)



2.7 References

- (40) Chen, M. S.; White, M. C. A Sulfoxide-Promoted, Catalytic Method for the Regioselective Synthesis of Allylic Acetates from Monosubstituted Olefins via C–H Oxidation. *J. Am. Chem. Soc.* **2004**, *126* (5), 1346–1347. <https://doi.org/10.1021/ja039107n>.
- (41) Chen, M. S.; Prabakaran, N.; Labenz, N. A.; White, M. C. Serial Ligand Catalysis: A Highly Selective Allylic C–H Oxidation. *J. Am. Chem. Soc.* **2005**, *127* (19), 6970–6971. <https://doi.org/10.1021/ja0500198>.
- (42) Covell, D. J.; White, M. C. A Chiral Lewis Acid Strategy for Enantioselective Allylic C–H Oxidation. *Angew. Chem. Int. Ed.* **2008**, *47* (34), 6448–6451. <https://doi.org/10.1002/anie.200802106>.
- (43) Young, A. J.; White, M. C. Catalytic Intermolecular Allylic C–H Alkylation. *J. Am. Chem. Soc.* **2008**, *130* (43), 14090–14091. <https://doi.org/10.1021/ja806867p>.
- (44) Reed, S. A.; Mazzotti, A. R.; White, M. C. A Catalytic, Brønsted Base Strategy for Intermolecular Allylic C–H Amination. *J. Am. Chem. Soc.* **2009**, *131* (33), 11701–11706. <https://doi.org/10.1021/ja903939k>.
- (45) Ammann, S. E.; Liu, W.; White, M. C. Enantioselective Allylic C–H Oxidation of Terminal Olefins to Isochromans by Palladium(II)/Chiral Sulfoxide Catalysis. *Angew. Chem. Int. Ed.* **2016**, *55* (33), 9571–9575. <https://doi.org/10.1002/anie.201603576>.

- (46) Burman, J. S.; Blakey, S. B. Regioselective Intermolecular Allylic C–H Amination of Disubstituted Olefins via Rhodium/ π -Allyl Intermediates. *Angew. Chem. Int. Ed.* **2017**, *56* (44), 13666–13669. <https://doi.org/10.1002/anie.201707021>.
- (47) Nelson, T. A. F.; Blakey, S. B. Intermolecular Allylic C–H Etherification of Internal Olefins. *Angew. Chem. Int. Ed.* **2018**, *57* (45), 14911–14915. <https://doi.org/10.1002/anie.201809863>.
- (48) Burman, J. S.; Harris, R. J.; Farr, C. M. B.; Bacsa, J.; Blakey, S. B. Rh(III) and Ir(III)Cp* Complexes Provide Complementary Regioselectivity Profiles in Intermolecular Allylic C–H Amidation Reactions. *ACS Catal.* **2019**, 5474–5479. <https://doi.org/10.1021/acscatal.9b01338>.
- (49) Kazerouni, A. M.; Nelson, T. A. F.; Chen, S. W.; Sharp, K. R.; Blakey, S. B. Regioselective Cp*Ir(III)-Catalyzed Allylic C–H Sulfamidation of Allylbenzene Derivatives. *J. Org. Chem.* **2019**, *84* (20), 13179–13185. <https://doi.org/10.1021/acs.joc.9b01816>.
- (50) Lerchen, A.; Knecht, T.; Koy, M.; Ernst, J. B.; Bergander, K.; Daniliuc, C. G.; Frank Glorius, and; Lerchen, A.; Knecht, T.; Koy, M.; B Ernst, D. J.; Bergander, D.; GDaniliuc, D.; lorius, D. Non-Directed Cross-Dehydrogenative (Hetero)Arylation of Allylic C(Sp³)–H Bonds Enabled by C–H Activation. *Angew. Chem. Int. Ed.* **2018**, *57* (46), 15248–15252. <https://doi.org/10.1002/ANIE.201807047>.
- (51) Knecht, T.; Pinkert, T.; Dalton, T.; Lerchen, A.; Glorius, F. CpRh III -Catalyzed Allyl-Aryl Coupling of Olefins and Arylboron Reagents Enabled by C(Sp³)-H Activation.

ACS Catal. **2019**, *9* (2), 1253–1257.

https://doi.org/10.1021/ACSCATAL.8B04677/SUPPL_FILE/CS8B04677_SI_001.PDF.

(52) Knecht, T.; Mondal, S.; Ye, J.-H.; Das, M.; Glorius, F. Intermolecular, Branch-Selective, and Redox-Neutral Cp*Ir^{III}-Catalyzed Allylic C–H Amidation. *Angew. Chem. Int. Ed.* **2019**, *58* (21), 7117–7121. <https://doi.org/10.1002/anie.201901733>.

(53) Pinkert, T.; Wegner, T.; Mondal, S.; Glorius, F. Intermolecular 1,4-Carboamination of Conjugated Dienes Enabled by Cp*RhIII-Catalyzed C–H Activation. *Angew. Chem. Int. Ed.* **2019**, *58* (42), 15041–15045.

<https://doi.org/10.1002/ANIE.201907269>.

(54) Lei, H.; Rovis, T. Ir-Catalyzed Intermolecular Branch-Selective Allylic C–H Amidation of Unactivated Terminal Olefins. *J. Am. Chem. Soc.* **2019**, *141* (6), 2268–2273. <https://doi.org/10.1021/jacs.9b00237>.

(55) Lei, H.; Rovis, T. A Site-Selective Amination Catalyst Discriminates between Nearly Identical C–H Bonds of Unsymmetrical Disubstituted Alkenes. *Nat. Chem.* **2020**, *12* (8), 725–731. <https://doi.org/10.1038/S41557-020-0470-Z>.

(56) Cochet, T.; Bellosta, V.; Roche, D.; Ortholand, J. Y.; Greiner, A.; Cossy, J. Rhodium(III)-Catalyzed Allylic C–H Bond Amination. Synthesis of Cyclic Amines from ω -Unsaturated N-Sulfonylamines. *Chem. Commun.* **2012**, *48* (87), 10745–10747.

<https://doi.org/10.1039/c2cc36067e>.

(57) Shibata, Y.; Kudo, E.; Sugiyama, H.; Uekusa, H.; Tanaka, K. Facile Generation and Isolation of π -Allyl Complexes from Aliphatic Alkenes and an Electron-Deficient

Rh(III) Complex: Key Intermediates of Allylic C–H Functionalization. *Organometallics* **2016**, *35* (10), 1547–1552. <https://doi.org/10.1021/acs.organomet.6b00143>.

(58) Sihag, P.; Jeganmohan, M. Iridium(III)-Catalyzed Intermolecular Allylic C-H Amidation of Internal Alkenes with Sulfonamides. *J. Org. Chem.* **2019**, *84* (20), 13053–13064. <https://doi.org/10.1021/ACS.JOC.9B02047>.

(59) Park, Y.; Park, K. T.; Kim, J. G.; Chang, S. Mechanistic Studies on the Rh(III)-Mediated Amido Transfer Process Leading to Robust C-H Amination with a New Type of Amidating Reagent. *J. Am. Chem. Soc.* **2015**, *137* (13), 4534–4542. <https://doi.org/10.1021/JACS.5B01324>.

(60) Harris, R. J.; Park, J.; Nelson, T. A. F.; Iqbal, N.; Salgueiro, D. C.; Bacsa, J.; Macbeth, C. E.; Baik, M. H.; Blakey, S. B. The Mechanism of Rhodium-Catalyzed Allylic C-H Amination. *J. Am. Chem. Soc.* **2020**, *142* (12), 5842–5851. <https://doi.org/10.1021/JACS.0C01069>.

(61) Ye, B.; Cramer, N. Chiral Cyclopentadienyl Ligands as Stereocontrolling Element in Asymmetric C-H Functionalization. *Science* **2012**, *338* (6106), 504–506. <https://doi.org/10.1126/science.1226938>.

(62) Ye, B.; Cramer, N. A Tunable Class of Chiral Cp Ligands for Enantioselective Rhodium(III)-Catalyzed C-H Allylations of Benzamides. *J. Am. Chem. Soc.* **2013**, *135* (2), 636–639. <https://doi.org/10.1021/JA311956K>.

(63) Hyster, T. K.; Knörr, L.; Ward, T. R.; Rovis, T. Biotinylated Rh(III) Complexes in Engineered Streptavidin for Accelerated Asymmetric C-H Activation. *Science* **2012**, *338* (6106), 500–503. <https://doi.org/10.1126/science.1226132>.

- (64) Mas-Roselló, J.; Herraiz, A. G.; Audic, B.; Laverny, A.; Cramer, N. Chiral Cyclopentadienyl Ligands: Design, Syntheses, and Applications in Asymmetric Catalysis. *Angew. Chem. Int. Ed.* **2021**, *60* (24), 13198–13224.
<https://doi.org/10.1002/ANIE.202008166>.
- (65) Cui, W. J.; Wu, Z. J.; Gu, Q.; You, S. L. Divergent Synthesis of Tunable Cyclopentadienyl Ligands and Their Application in Rh-Catalyzed Enantioselective Synthesis of Isoindolinone. *J. Am. Chem. Soc.* **2020**, *142* (16), 7379–7385.
<https://doi.org/10.1021/JACS.0C02813>.
- (66) Zheng, J.; Cui, W. J.; Zheng, C.; You, S. L. Synthesis and Application of Chiral Spiro Cp Ligands in Rhodium-Catalyzed Asymmetric Oxidative Coupling of Biaryl Compounds with Alkenes. *J. Am. Chem. Soc.* **2016**, *138* (16), 5242–5245.
<https://doi.org/10.1021/JACS.6B02302>.
- (67) Jia, Z.-J.; Merten, C.; Gontla, R.; Daniliuc, C. G.; Antonchick, A. P.; Waldmann, H. General Enantioselective C–H Activation with Efficiently Tunable Cyclopentadienyl Ligands. *Angew. Chem. Int. Ed.* **2017**, *56* (9), 2429–2434.
<https://doi.org/10.1002/anie.201611981>.
- (68) Trifonova, E. A.; Ankudinov, N. M.; Mikhaylov, A. A.; Chusov, D. A.; Nelyubina, Y. V.; Perekalin, D. S. A Planar-Chiral Rhodium(III) Catalyst with a Sterically Demanding Cyclopentadienyl Ligand and Its Application in the Enantioselective Synthesis of Dihydroisoquinolones. *Angew. Chem. Int. Ed.* **2018**, *57* (26), 7714–7718.
<https://doi.org/10.1002/anie.201801703>.

- (69) Pototskiy, R. A.; Kolos, A. V.; Nelyubina, Y. V.; Perekalin, D. S. Rhodium Catalysts with a Chiral Cyclopentadienyl Ligand Derived from Natural R-Myrtenal. *Eur. J. Org. Chem.* **2020**, 2020 (37), 6019–6025. <https://doi.org/10.1002/EJOC.202001029>.
- (70) Kolos, A. V.; Nelyubina, Y. V.; Sundararaju, B.; Perekalin, D. S. Synthesis of Overloaded Cyclopentadienyl Rhodium(III) Complexes via Cyclotetramerization of Tert-Butylacetylene. *Organometallics* **2021**, 40 (22), 3712–3719. <https://doi.org/10.1021/ACS.ORGANOMET.1C00403>.
- (71) Yan, X.; Jiang, J.; Wang, J.; Yan, J. X.; Jiang, J.; Wang, J. A Class of Readily Tunable Planar-Chiral Cyclopentadienyl Rhodium(III) Catalysts for Asymmetric C–H Activation. *Angew. Chem. Int. Ed.* **2022**, 61 (23), e202201522. <https://doi.org/10.1002/ANIE.202201522>.
- (72) Marder, T. B.; Calabrese, J. C.; Roe, D. C.; Tulip, T. H. The Slip-Fold Distortion of η -Bound Indenyl Ligands. Dynamic NMR and X-Ray Crystallographic Studies of (η -Indenyl)RhL₂ Complexes. *Organometallics* **1987**, 6 (9), 2012–2014. <https://doi.org/10.1021/OM00152A041>.
- (73) Westcott, S. A.; Kakkar, A. K.; Stringer, G.; Taylor, N. J.; Marder, T. B. Flexible Coordination of Indenyl Ligands in Sandwich Complexes of Transition Metals. Molecular Structures of $[(\eta\text{-C}_9\text{R}_7)_2\text{M}]$ (M = Fe, R = H, Me; M = Co, Ni, R = H): Direct Measurement of the Degree of Slip-Fold Distortion as a Function of *d*-Electron Count. *J. Organomet. Chem.* **1990**, 394 (1–3), 777–794. [https://doi.org/10.1016/0022-328X\(90\)87268-I](https://doi.org/10.1016/0022-328X(90)87268-I).

- (74) O'Connor, J. M.; Casey, C. P. Ring-Slippage Chemistry of Transition Metal Cyclopentadienyl and Indenyl Complexes. *Chem. Rev.* **1987**, *87* (2), 307–318.
<https://doi.org/10.1021/cr00078a002>.
- (75) Baker, R. W. Asymmetric Induction via the Structural Indenyl Effect. *Organometallics* **2018**, *37* (3), 433–440.
<https://doi.org/10.1021/acs.organomet.7b00841>.
- (76) Farr, C. M. B.; Kazerouni, A. M.; Park, B.; Poff, C. D.; Won, J.; Sharp, K. R.; Baik, M. H.; Blakey, S. B. Designing a Planar Chiral Rhodium Indenyl Catalyst for Regio- And Enantioselective Allylic C-H Amidation. *J. Am. Chem. Soc.* **2020**, *142* (32), 13996–14004. <https://doi.org/10.1021/JACS.0C07305>.
- (77) Gao, D.-W.; Shi, Y.-C.; Gu, Q.; Zhao, Z.-L.; You, S.-L. Enantioselective Synthesis of Planar Chiral Ferrocenes via Palladium-Catalyzed Direct Coupling with Arylboronic Acids. *J. Am. Chem. Soc.* **2013**, *135* (1), 86–89. <https://doi.org/10.1021/ja311082u>.
- (78) Musaev, D. G.; Kaledin, A.; Shi, B. F.; Yu, J. Q. Key Mechanistic Features of Enantioselective C-H Bond Activation Reactions Catalyzed by [(Chiral Mono-N-Protected Amino Acid)-Pd(II)] Complexes. *J. Am. Chem. Soc.* **2012**, *134* (3), 1690–1698. <https://doi.org/10.1021/JA208661V>.
- (79) Shi, B. F.; Mangel, N.; Zhang, Y. H.; Yu, J. Q. PdII-Catalyzed Enantioselective Activation of C(Sp²)-H and C(Sp³)-H Bonds Using Monoprotected Amino Acids as Chiral Ligands. *Angew. Chem. Int. Ed.* **2008**, *47* (26), 4882–4886.
<https://doi.org/10.1002/anie.200801030>.

- (80) Wasa, M.; Engle, K. M.; Lin, D. W.; Yoo, E. J.; Yu, J. Q. Pd(II)-Catalyzed Enantioselective C-H Activation of Cyclopropanes. *J. Am. Chem. Soc.* **2011**, *133* (49), 19598–19601. <https://doi.org/10.1021/JA207607S>.
- (81) Schaverien, C. J.; Ernst, R.; Schut, P.; Dall'Occo, T. Ethylene Bis(2-Indenyl) Zirconocenes: A New Class of Diastereomeric Metallocenes for the (Co)Polymerization of α -Olefins. *Organometallics* **2001**, *20* (16), 3436–3452. <https://doi.org/10.1021/OM010160Z>.
- (82) Komatsu, S.; Sone, H.; Koike, T.; Kawahama, S.; Process for preparation of norbornene derivatives. WO2010146951A1, 2010.
- (83) Schaverien, C. J.; Ernst, R.; Schut, P.; Dall'Occo, T. Ethylene Bis(2-Indenyl) Zirconocenes: A New Class of Diastereomeric Metallocenes for the (Co)Polymerization of α -Olefins. *Organometallics* **2001**, *20* (16), 3436–3452. <https://doi.org/10.1021/OM010160Z>.
- (84) Molander, G. A.; Gormisky, P. E.; Sandrock, D. L. Scope of Aminomethylations via Suzuki–Miyaura Cross-Coupling of Organotrifluoroborates. *J. Org. Chem.* **2008**, *73* (6), 2052–2057. <https://doi.org/10.1021/jo800183q>.
- (85) Gilmore, R. C. Cyclization of Aryl-Aliphatic Esters with Phosphorus Pentoxide in Phosphoric Acid. *J. Am. Chem. Soc.* **1951**, *73* (12), 5879–5880. <https://doi.org/10.1021/ja01156a521>.
- (86) Hoshino, Y.; Okuno, M.; Kawamura, E.; Honda, K.; Inoue, S. Base-Mediated Rearrangement of Free Aromatic hydroxamic Acids (ArCO–NHOH) to Anilines. *Chem. Commun.* **2009**, *17*, 2281–2283. <https://doi.org/10.1039/B822806J>.

Chapter 3. Ribosomally Synthesized and Post-translationally Modified Peptides containing C–O and C–C Crosslinks

Ribosomally synthesized and post-translationally modified peptides (RiPPs) are a rapidly growing class of natural products that often exhibit useful bioactivities. Advances in bioinformatic techniques over the last decade have allowed for targeted identification of novel RiPPs. Two subsets of this family of natural products are RiPPs containing C–O or RiPPs containing C–C crosslinks. We are focusing on these crosslinks primarily because of their presence in darobactin A, which will be the subject of a later chapter. These crosslinks often occur between side-chain moieties and complicate the de novo syntheses of natural products when present. Due to the Blakey Group interest in synthesizing RiPP natural products containing these crosslinks, we will discuss the general biosynthesis of RiPP natural products. Then we will focus on the chemical syntheses of RiPPs containing alkyl-aryl C–O crosslinks, and RiPPs with C–C crosslinks containing tryptophan given their relevance in the synthesis of darobactin A.

3.1 The Generic Biosynthesis of Ribosomally Synthesized and Post-translationally Modified Peptides

Ribosomally synthesized and post-translationally modified peptides (RiPPs) are classified by the mechanism of their biosynthesis and are distinct from more well-known natural products such as non-ribosomally synthesized peptides (NRPs). The recent boom in RiPP discovery in the last two decades has largely been due to advances in bioinformatic techniques, such as new genome mining tools.^{87,88} Given the importance of

biosynthesis to the classification of RiPPs, we are going to outline the basic structure of natural RiPP production.

A typical RiPP polypeptide will consist of a leader peptide, core peptide, and sometimes include a signal peptide or recognition sequence (Figure 3.1). All RiPPs begin as a single precursor peptide, which consists of a leader peptide (LP) and a core peptide, with an optional follower peptide. The leader peptide has several functions; it aids in recognition for subsequent post-translational enzymes, it can increase activity of requisite post-translational modification (PTM) enzymes and inhibit activation of the core peptide as its being modified, and it can help impose the correct order as modifications are enacted.⁸⁹ The core peptide contains what will become the RiPP natural product and is where the post-translational modifications take place. In some cases, a follower peptide can be included after the core peptide and replaces the functionality of the leader peptide.

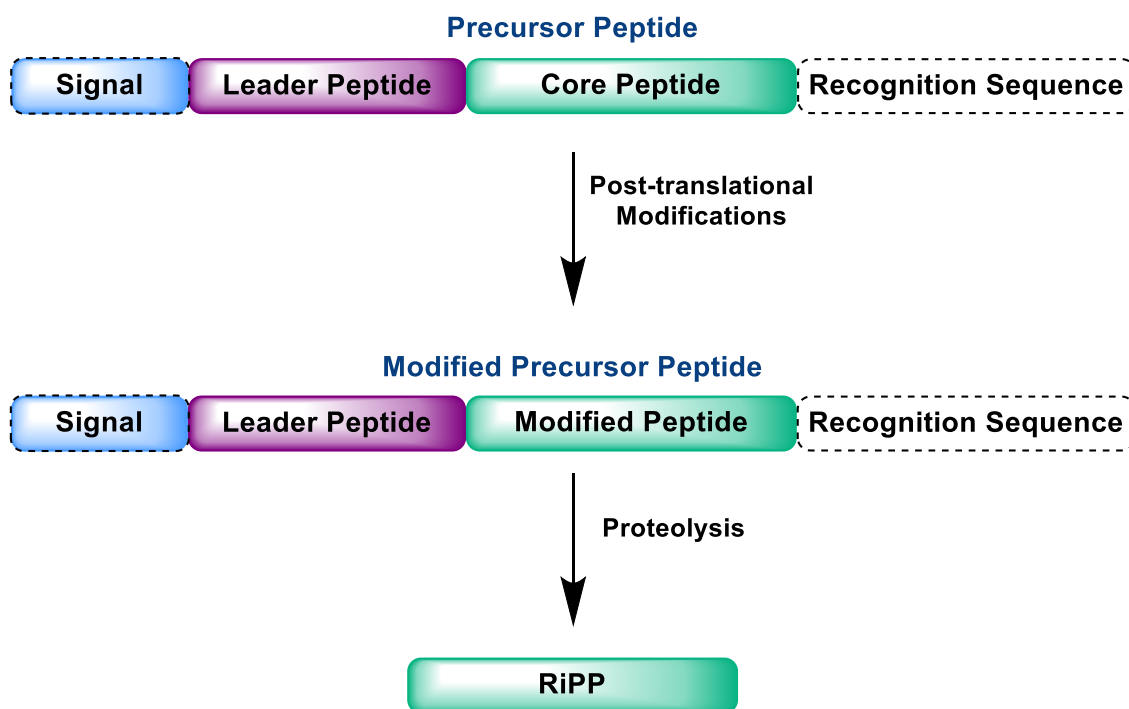


Figure 3.1 Generic RiPP Biosynthesis

Signal peptides are an optional eukaryotic moiety that can direct the peptide to the organelle where it will be modified. It is also noteworthy that a single precursor can contain multiple core peptides, each preceded by recognition sequences.

RiPP biosynthesis begins with ribosomal precursor peptide translation. Then post-translational enzymes (often encoded just downstream of the precursor peptide in the genome) modify the core region, using recognition sequences to guide their modifications. The modified peptide is then excised, delivering the RiPP natural product. Common modifications include macrocyclization, epimerization, methylation, oxygenation and halogenation.⁸⁷ Macrocyclization is a growing area of interest due to the ability of macrocyclic peptides to exhibit pharmacological activity similar to small molecules while maintaining the specificity often associated with peptides.^{90,91} While certain modes of macrocyclization are relatively easy to access, such as head-to-tail cyclization and disulfide bridging, side chain crosslinks remain relatively challenging to synthesize. Through the lens of chemical synthesis, the most inaccessible side chain crosslinks are C–C containing crosslinks, but certain C–O crosslinks remain challenging as well. We will now outline interesting RiPPs containing these crosslinks.

3.2 Chemical Synthetic Approaches towards Ribosomally Synthesized and Post-translationally Modified Peptides containing C–O and C–C Crosslinks

The biosyntheses of RiPPs containing C–O and C–C crosslinks are often elegant in contrast to chemical syntheses. However, biosynthetic yields of RiPP natural products are often found wanting, especially in the case of RiPPs with exciting bioactivities such as darobactin A. While side-chain crosslinks vastly complicate synthesis of macrocyclic RiPPs, the synthetic community has developed an array of approaches to overcome these obstacles. In preparation for developing a synthesis of darobactin A, we are going

to discuss prior approaches to synthesize alkyl-aryl C–O crosslinks and alkyl-aryl C–C crosslinks containing tryptophan which are the two macrocyclic linkages in the RiPP natural product.

3.2.1 Synthetic Approaches towards forging Alkyl-Aryl C–O Crosslinks in RiPPs

Chemical Syntheses of Ustiloxin D

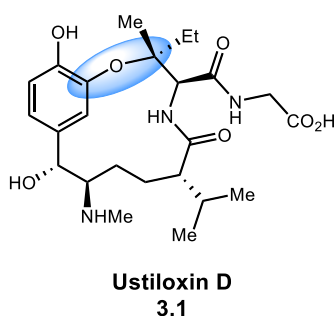
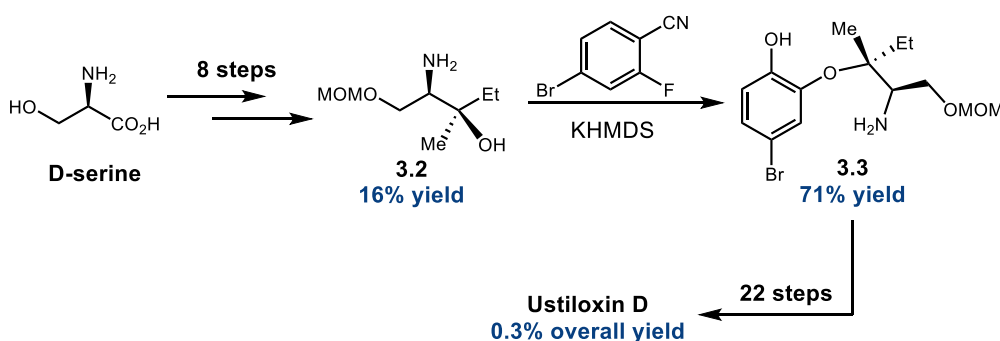


Figure 3.2 The macrocyclic RiPP Ustiloxin

Methodology for delivering C–O crosslinks has been developed over the last 20 years to synthesize a number of RiPPs.^{92–95} Alkyl-aryl C–O linkages have been one of the more challenging moieties to build into a synthesis and maintain concise step count. The dikaritins are a class of fungal RiPPs that feature phenolic C–O crosslinks between a tyrosine side chain and the side chain of another amino acid.⁸⁸ The ustiloxins are dikaritins that have been isolated from the false smut balls caused by *Ustilaginoidea virens* infecting rice panicles.^{96–98} Ustiloxin D, has been the subject of several chemical syntheses due to its relative molecular simplicity and good bioactivity, and provides a great case study in the development of forging C–O crosslinks in the context of RiPP natural products.^{99–103}

The first synthesis of ustiloxin D was conducted by the Joullié group in 2002 (Scheme 3.1).⁹⁹ In order to apply their crosslinking reaction, Joullié and coworkers

needed chiral alcohol **3.2**, which was accessed in 8 steps from D-serine. The key ethereal crosslink was forged via nucleophilic aromatic substitution (S_NAr) in good yield, early in the synthesis (**3.3**, Scheme 3.1). Unfortunately, 22 additional steps were required to deliver the RiPP natural product. Protecting group manipulations and establishing the phenolic functionalization were major factors impeding the initial synthesis reported by the Joullié group. While S_NAr was shown to be competent in RiPP alkyl-aryl ether synthesis, the seminal total synthesis of ustiloxin D left much room for improvement.

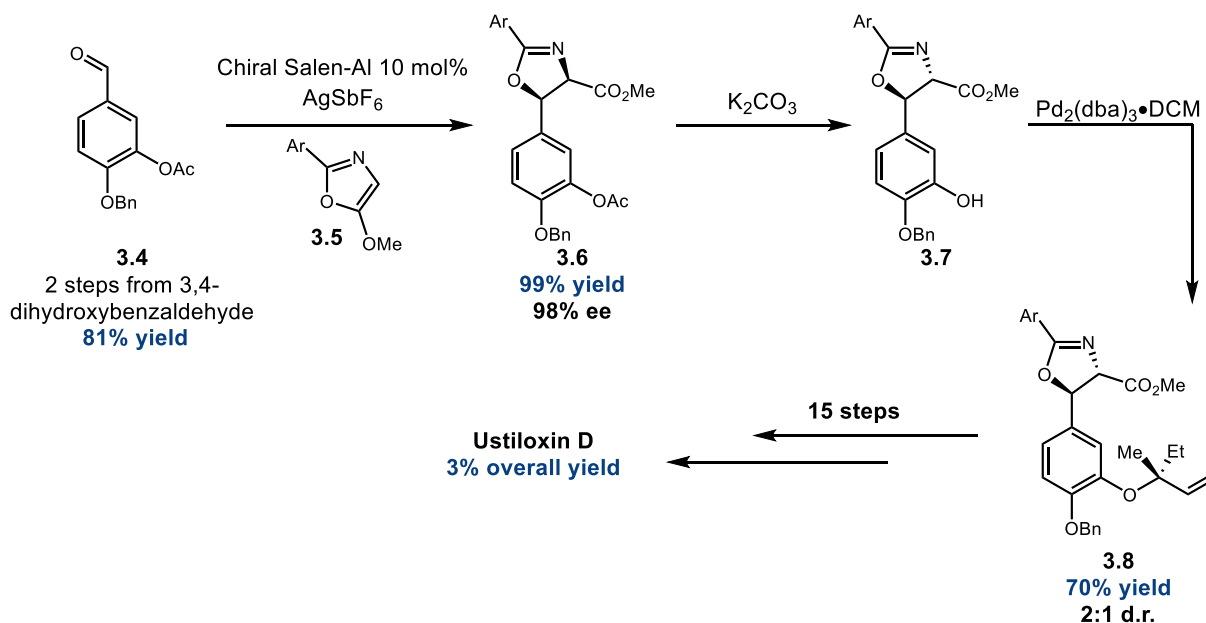


Scheme 3.1 The first total synthesis of ustiloxin D by Joullié and coworkers.

Later, the Wandless group delivered a 20-step synthesis of ustiloxin D (Scheme 3.2).¹⁰⁰ While the Wandless synthesis utilized a similar strategy in C–O crosslink formation, with early forging of the C–O bond, their approach differed significantly in the details. The synthesis began with converting 3,4-dihydroxybenzaldehyde into chiral oxazoline **3.6** in 3 steps and great enantioselectivity. However, during deprotection of the phenol to set the stage for forging the C–O crosslink, the basic conditions inverted the stereochemistry at the imine chiral center to deliver **3.7**. Fortunately, this epimerization delivered the requisite stereochemistry that corresponds to ustiloxin D. Allylic substitution was used to deliver the alkyl-aryl crosslink, but even with a chiral phosphine ligand only 2:1 diastereoselectivity was observed. The remaining 14 steps occurred without complication to deliver ustiloxin B in 3% overall yield. Wandless demonstrated that

disguising the tyrosine amino acid fragment as an oxazoline and the use of allylic substitution to forge the C–O crosslink cut a significant number of steps that Joullié and coworkers needed to properly functionalize the central benzyl ring and carry out protecting group manipulations. However, the issues with diastereoselectivity did inspire investigations targeted at improving selectivity throughout the synthesis.

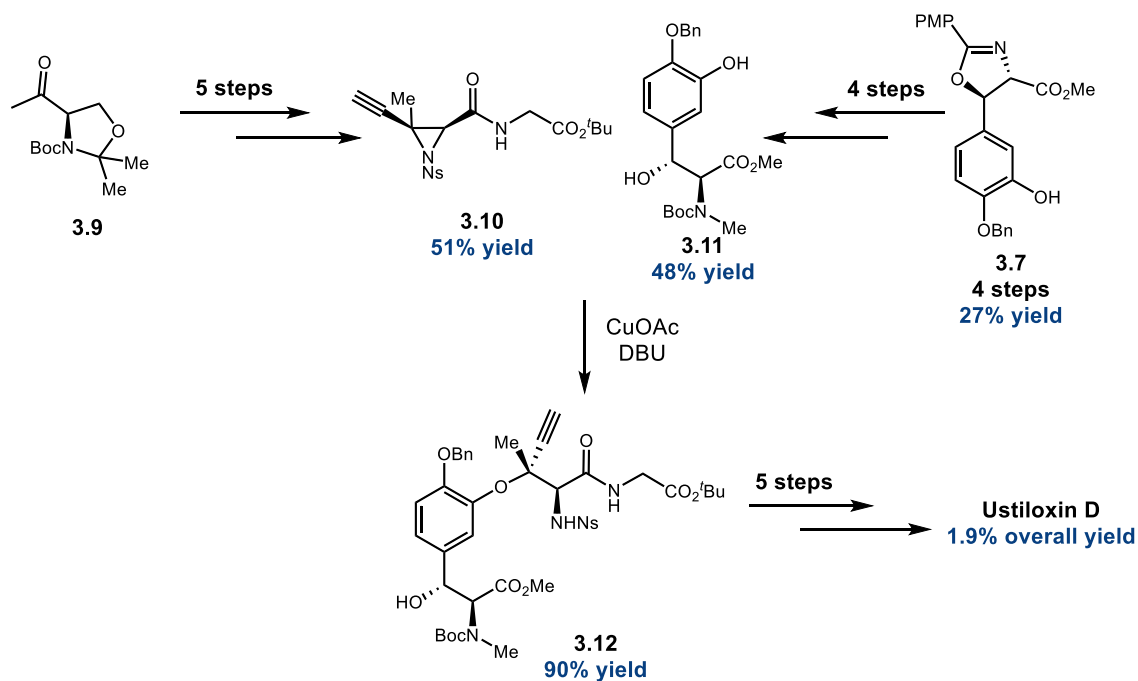
Wandless 2003



Scheme 3.2 The Wandless synthesis of ustiloxin D

Joullié and coworkers' second synthesis of ustiloxin D marked a change in strategy when considering C–O crosslinks.¹⁰² Instead of forging the crosslink in the first half of the synthesis, advanced intermediates were prepared for a late-stage coupling. The synthesis began with preparing tri-substituted aziridine **3.10** in a highly diastereoselective fashion over 5 steps from oxazolidine **3.9**. Tyrosine derivative **3.11** was prepared in four steps from the chiral oxazoline **3.7** disclosed by Wandless. With both coupling partners in hand, the Joullié group engaged phenol **3.11** in a copper catalyzed aziridine ring opening in an S_N2 fashion to forge the key C–O crosslink in good yield and forming

advanced intermediate **3.12** as a single stereoisomer. Only five more steps and ustiloxin D was made in 1.9% yield, which was slightly improved on the Wandless synthesis when considering isomeric purity.



Scheme 3.3 The improved convergent synthesis of ustiloxin D from Joullié and coworkers

Other dikaritins have since been synthesized, but they largely use the methodology and strategies established for the synthesis of ustiloxin D.^{93,95}

3.2.2 Synthetic Approaches towards RiPPs with C–C Crosslinks containing Trp

There are quite a few RiPPs containing C–C crosslinks. While we will only focus on a subset of these RiPPs that utilize a tryptophan moiety to build its crosslinks, our 2022 review details the isolation and syntheses of all C–C crosslinked RiPPs discovered before 2023.¹⁰⁴

3.2.2.1 Chemical Syntheses of Celogentin C

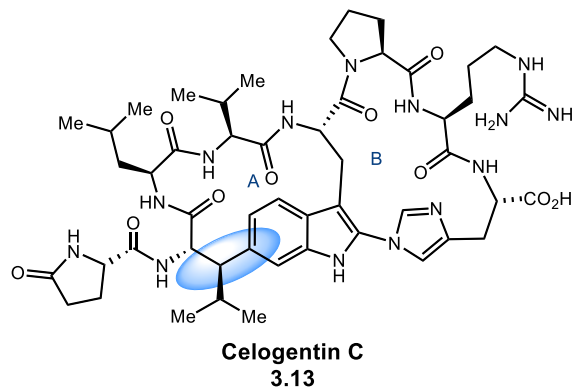
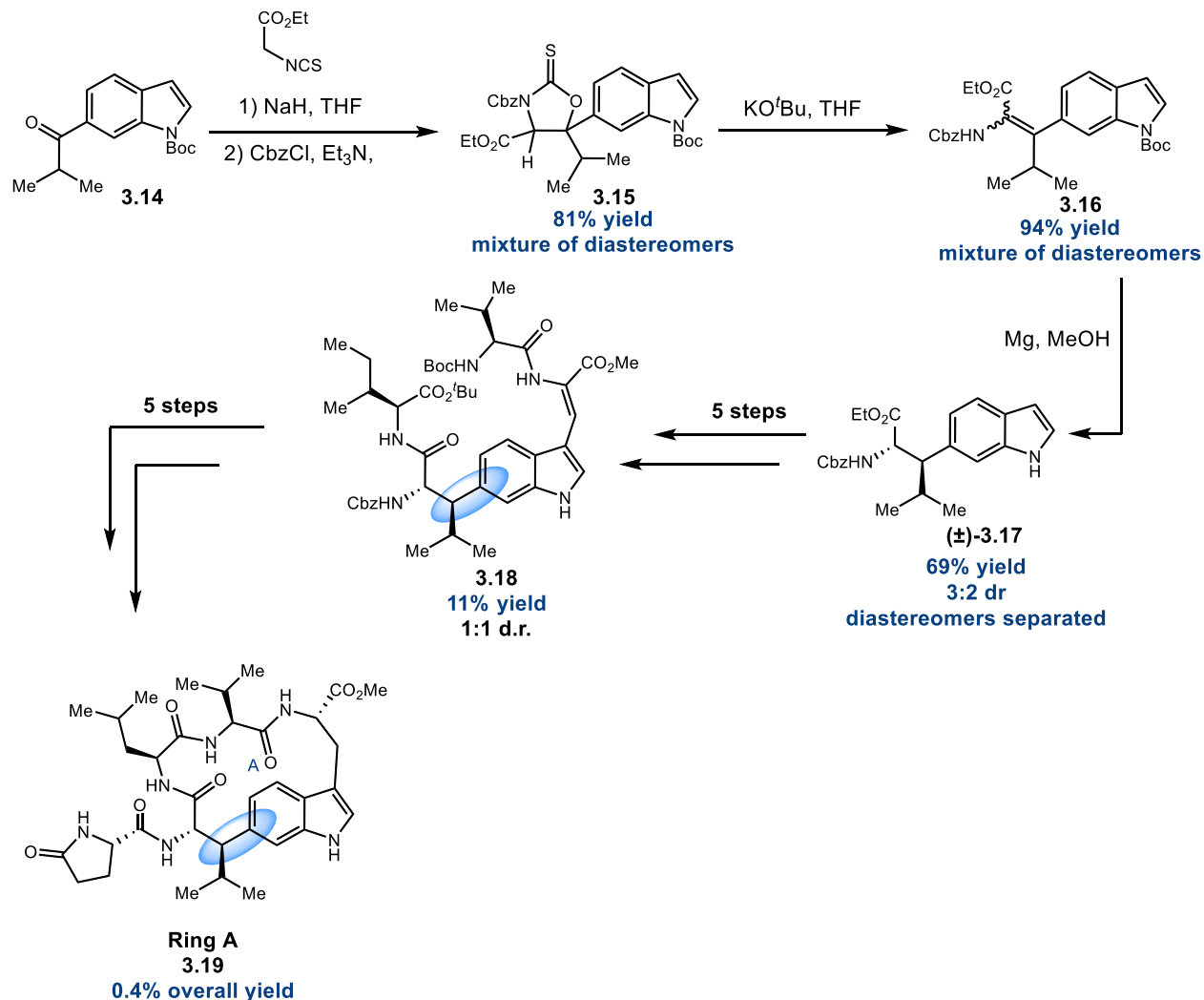


Figure 3.3 The structure of celogentin C.

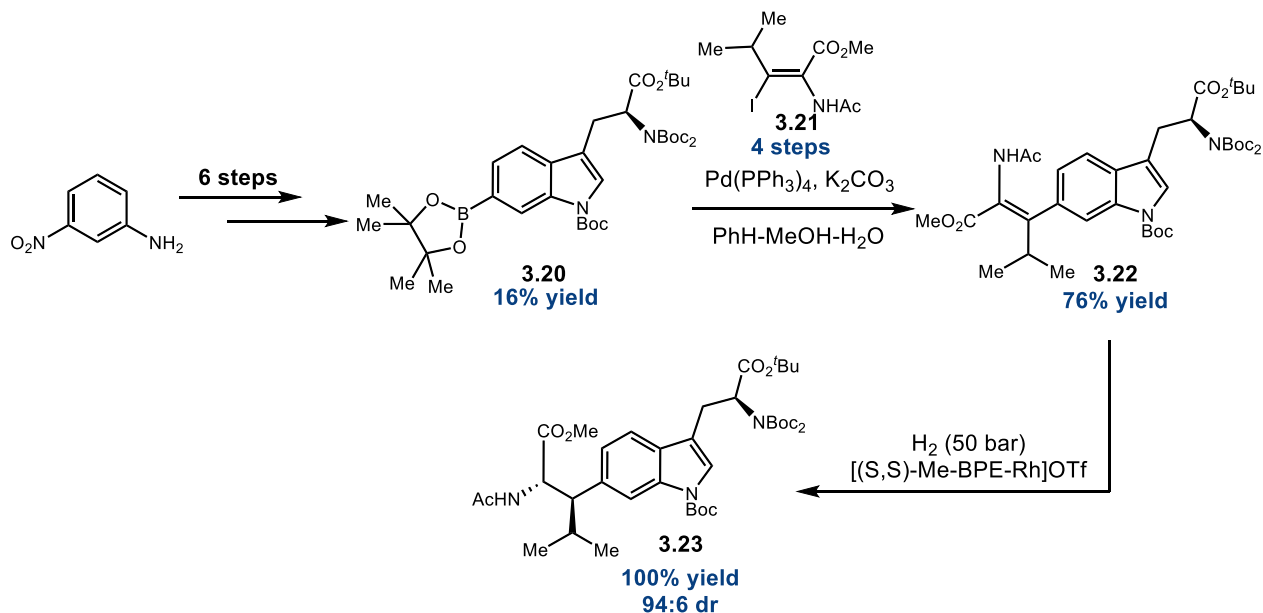
Celogentin C is a bi-macrocyclic RiPP that possesses potent anti-mitotic activity and was studied as a potential anti-tumor agent.¹⁰⁵ Celogentin C possesses a central tryptophan residue with a C–C crosslink to a leucine and a C – N crosslink to histidine. There have been many synthetic investigations into the chemical synthesis of celogentin C. The first approach to deliver the western macrocycle was reported by Moody in 2006 (Scheme 3.4).¹⁰⁶ While Moody and coworkers were able to purchase indole **3.14** bearing the C–C crosslink, much of their synthetic ingenuity was needed to transform the feedstock indole into the complex celogentin C subunit. Swift conversion of the ketone to oxazolidine-2-thione **3.15** and subsequent basic mediated elimination of carbonyl sulfide delivered olefin **3.16** in good yield. Unfortunately, the Moody group were forced to carry a mixture of inseparable diastereomers through these steps. They then reduced the olefin which enabled separation of the diastereomers but given the achiral nature of the reductant they generated racemic **3.17**, which was again carried forward. After elaboration of the linear peptide, diastereomers were separated and the correct stereoisomer cyclized to form the western ring of celogentin C (**3.19**). This initial



Scheme 3.4 The first synthesis of the A ring of celogentin C by Moody and coworkers.

exploration from Moody was instrumental in guiding synthetic strategy in later celogentin C syntheses, but their methods of forming the chiral architecture surrounding the C–C crosslink needed improvement.

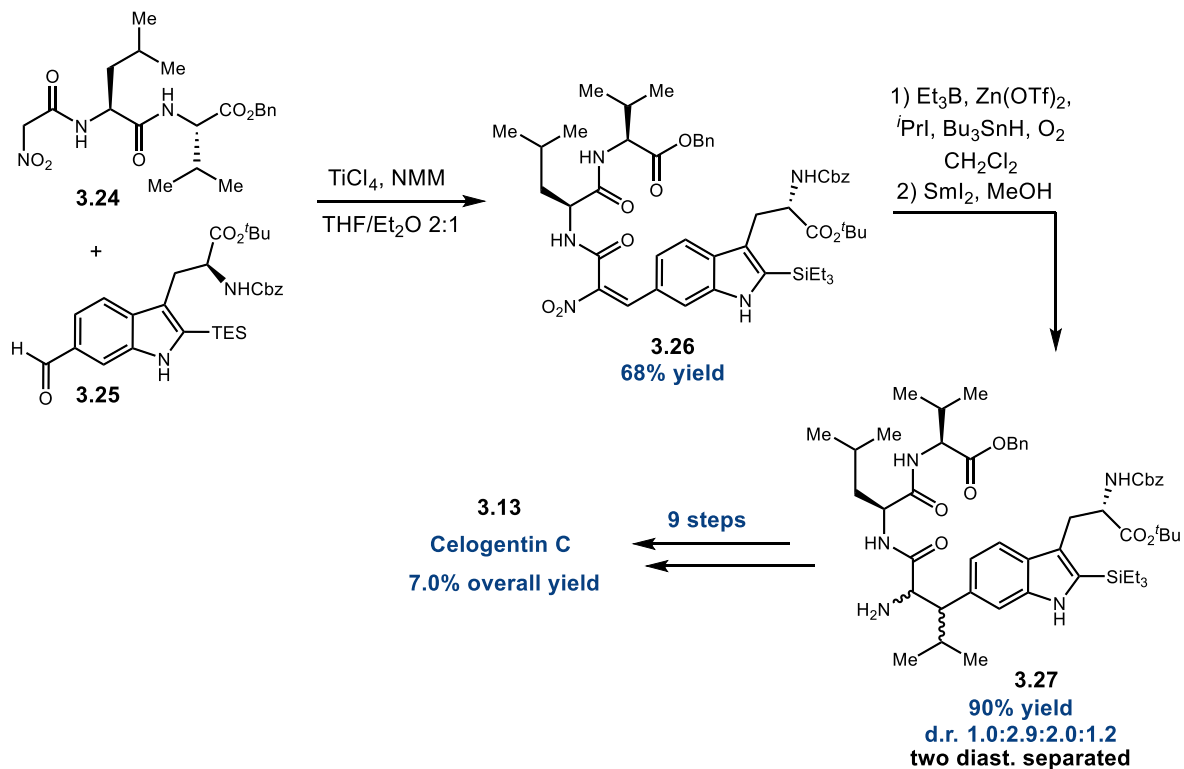
Seeing the need to improve the stereoselectivity of the Moody synthesis, Campagne delivered an alternate approach to the central tryptophan residue (Scheme 3.5).¹⁰⁷ By coupling pure vinyl iodide **3.21** with borylated Trp residue **3.20**, they were able to produce olefin **3.21** in good yield via Suzuki-Miyaura coupling. Subsequent



Scheme 3.5 Synthesis of the central tryptophan residue by Campagne *et al.* using Suzuki-Miyaura coupling

hydrogenation with a chiral Rh catalyst, delivered key tryptophan residue **3.23** quantitatively, with excellent diastereoselectivity. While this approach eliminated the issues with establishing the stereochemistry around the C–C crosslink, the requisite intermediates **3.20** and **3.21** required lengthy syntheses.

Castle and coworkers reported the first total synthesis of celogentin C (Scheme 3.7).^{108,109} They utilized a strategy similar to Moody's approach to forge the western macrocycle. In the Castle synthesis, they utilize a Knoevenagel condensation to couple functionalized tryptophan **3.25** and tripeptidyl fragment **3.24** to deliver advanced olefin intermediate **3.26** in only three linear steps. Radical conjugate addition chemistry developed by the Castle group was able to introduce the isopropyl moiety and subsequent reduction of the nitro group delivered a partially separable mixture of isomers **3.27**. Over the next nine steps, the desired diastereomer was eventually separated and celogentin C was obtained in 14 steps and 7% overall yield from simple amino acid starting materials.

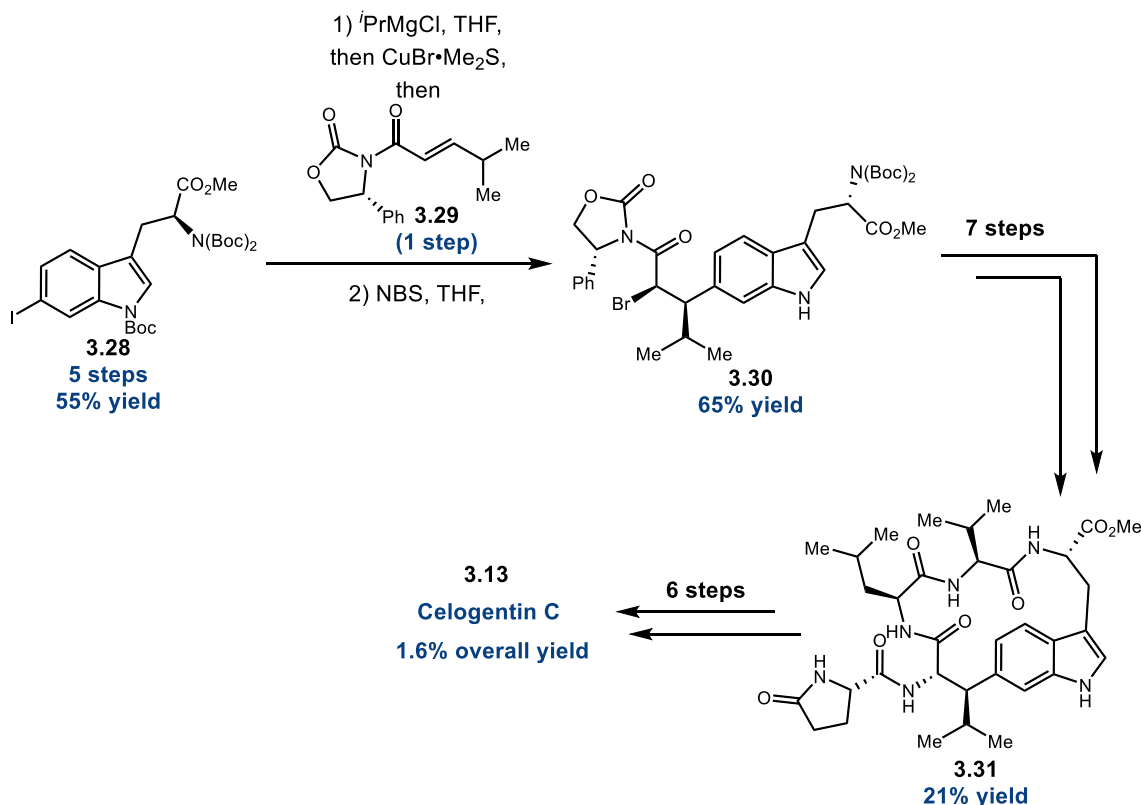


Scheme 3.6 Castle's total synthesis of celogentin C

The Castle synthesis utilized convergent methods to deliver the C–C crosslink efficiently, and although it struggles with diastereomeric purity, the conciseness of the synthesis balanced many of its weaknesses.

Jia and coworkers published their synthesis of celogentin C within a month of Castle's report (Scheme 3.7).¹¹⁰ Similar to previous strategies for celogentin C, the Jia synthesis utilized advanced intermediates for cross-coupling to forge the C–C crosslink. Trp fragment **3.28** and acylated Evans type auxiliary **3.29** to form the key C–C crosslink. While iodinated tryptophan **3.28** was synthesized in five steps, the Michael addition occurred with high diastereoselectivity and decent yield. Another seven steps delivered the western macrocycle and another six steps delivered celogentin C in 1.6% overall

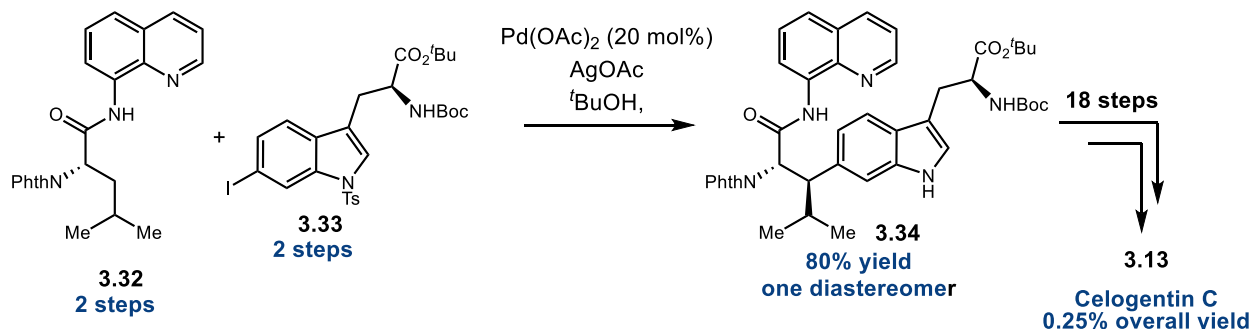
yield. While the overall yield was lower, when considering the stereoselectivity of the synthetic route, the Jia synthesis comes out slightly ahead of the Castle synthesis.



Scheme 3.7 Synthesis of the celogentin C crosslink via Michael addition by Jia and coworkers

Chen and coworkers were able to deliver a truly innovative construction of the C–C crosslink.¹¹¹ They were able to synthesize leucine residue **3.32** with an 8-aminoquinoline directing group and 6-iodotryptophan **3.33** in two steps each. With the coupling partners in hand, Chen and coworkers were able to utilize directed C–H functionalization to arylate at the β -position to furnish **3.34** with exclusive selectivity for the stereoisomer depicted. Unfortunately, the sleek C–H functionalization was not indicative of the rest of the Chen synthesis. Another 18 steps were needed to convert the dipeptide into the bimacrocyclic natural product. However, this did reveal the 8-

aminoquinoline directed functionalization as a powerful tool which for C–C crosslink formation and would be used in the chemical synthesis of other RiPP natural products.



Scheme 3.8 The total synthesis of celogentin C using directed C–H activation

3.2.2.2 Chemical Synthesis of Streptide

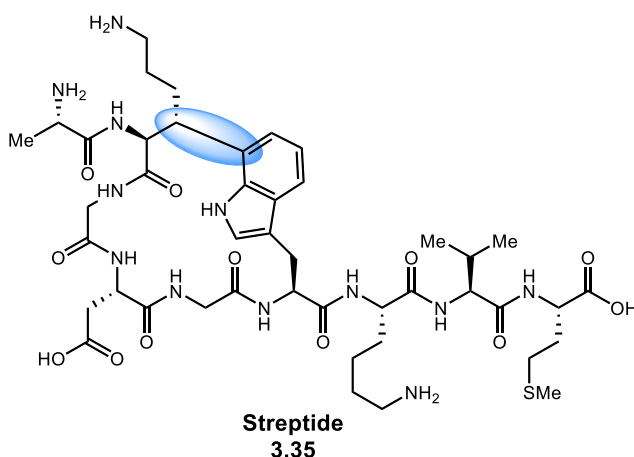
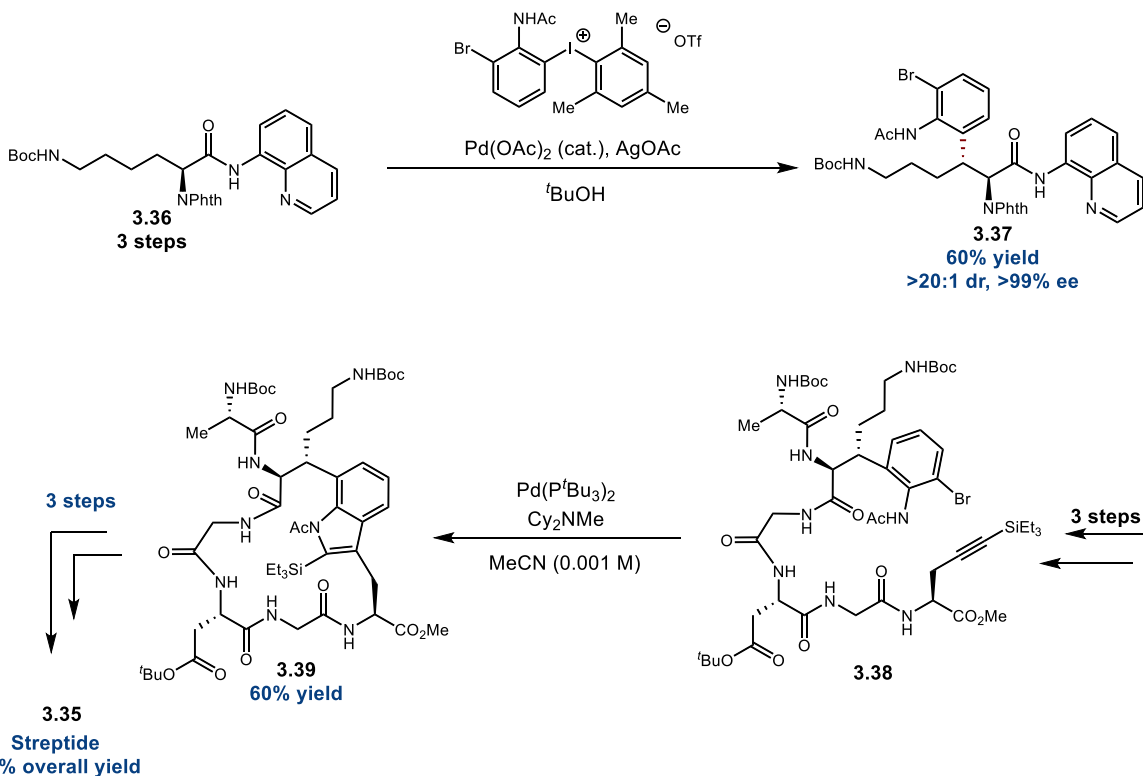


Figure 3.4 The structure of streptide

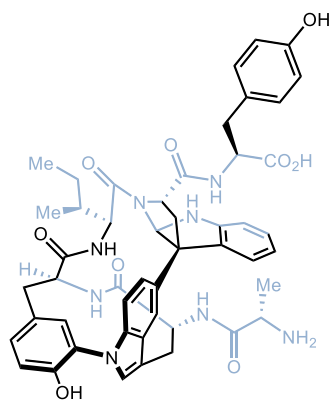
Streptide is a macrocyclic RiPP that contains a Lys-Trp alkyl-aryl C–C crosslink with unknown bioactivity.¹¹² Boger and coworkers disclosed their synthesis of streptide in 2019.¹¹³ Inspired by the Chen synthesis of celogentin C years prior, the Boger group forged the C–C crosslink utilizing an 8-aminoquinoline directed C–H functionalization of protected lysine **3.36**. The arylation proceeded in good yield and excellent stereoselectivity to deliver **3.37**, but instead of coupling a full tryptophan derivative, as in the Chen synthesis, the Boger group coupled N-acetyl-2-bromoaniline. Only three more

steps were required to elaborate the peptide chain and introduce the propargyl glycine residue, which primed the linear peptide for cyclization. An intramolecular Larock annulation was utilized to couple the pendant alkyne and 2-bromoacetamide which simultaneously generated the central indole residue and closed the macrocycle in good yield. Although the Larock required stoichiometric Pd for efficient conversion, given the difficult cyclization and generation of a single atropisomer, that fault was overshadowed by the efficiency of the overall synthesis. This clever use of the Larock annulation would influence other syntheses of functionalized tryptophan residues and cyclizing peptide scaffolds containing tryptophan. After forming the macrocycle, only three more steps were required to deliver streptide in 8.6% overall yield.



Scheme 3.9 Boger's synthesis of the streptide C–C crosslink via C–H arylation

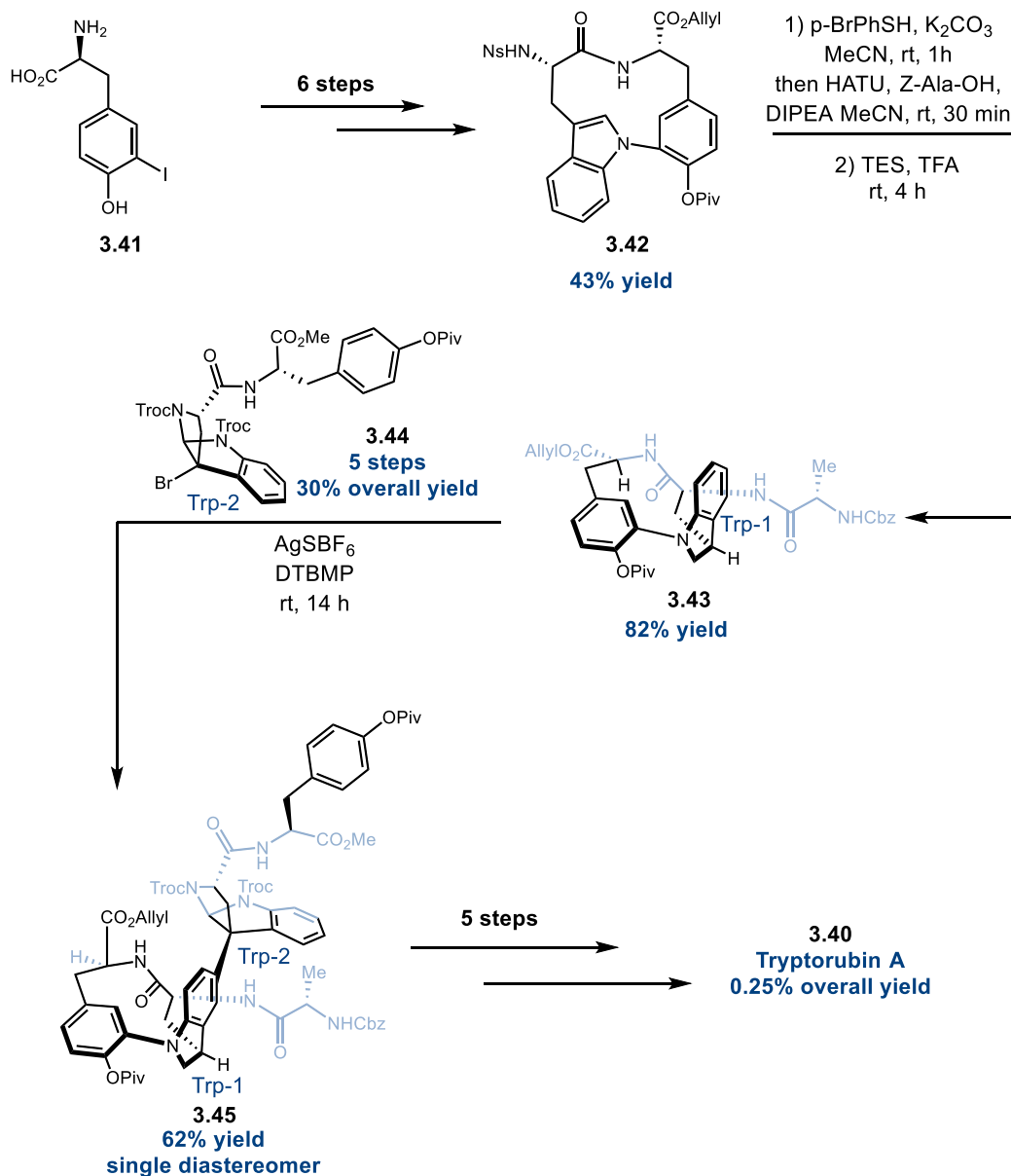
3.2.2.3 Chemical Synthesis of Tryptorubin A



Tryptorubin A
3.40

Figure 3.5 The structure of Tryptorubin A, a fused tri-macrocyclic RiPP

Tryptorubin A is a densely functionalized tri-macrocyclic RiPP natural product with a C–N crosslink between Trp-Tyr and the first observed alkyl-aryl C–C crosslink between two tryptophan residues.¹¹⁴ The Baran group undertook the synthesis of tryptorubin A due to its sheer molecular complexity (Scheme 3.10).¹¹⁵ The synthesis began with converting commercially available 2-iodotyrosine into tripeptide macrocycle **3.42** in 6 steps. The subsequent reduction of the indole to the indoline was necessary to prevent atropisomerism when exposed to peptide coupling conditions, which enabled the synthesis of **3.43** in good yield and isomeric purity. Friedel-Crafts arylation of **3.43** was initiated by Ag(I) bromide abstraction of fused tryptophan derived dipeptide **3.44**, which readily forged the C–C crosslink. The resultant arylated indoline was converted to tryptorubin A in five additional steps and 0.25% overall yield. This synthesis from the Baran group showcased that existing methodology can be quite potent in delivering complex macrocyclic RiPP natural products relatively late in the synthesis.



Scheme 3.10 Baran's synthesis of tryptorubin A. They utilized a Friedel-Crafts to build the C–C crosslink.

3.2.3 Chemical Syntheses of Darobactin A

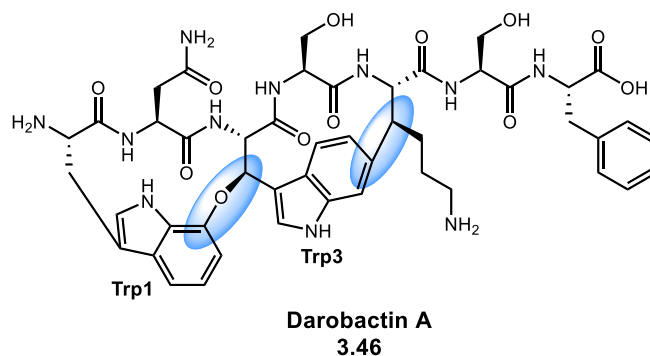
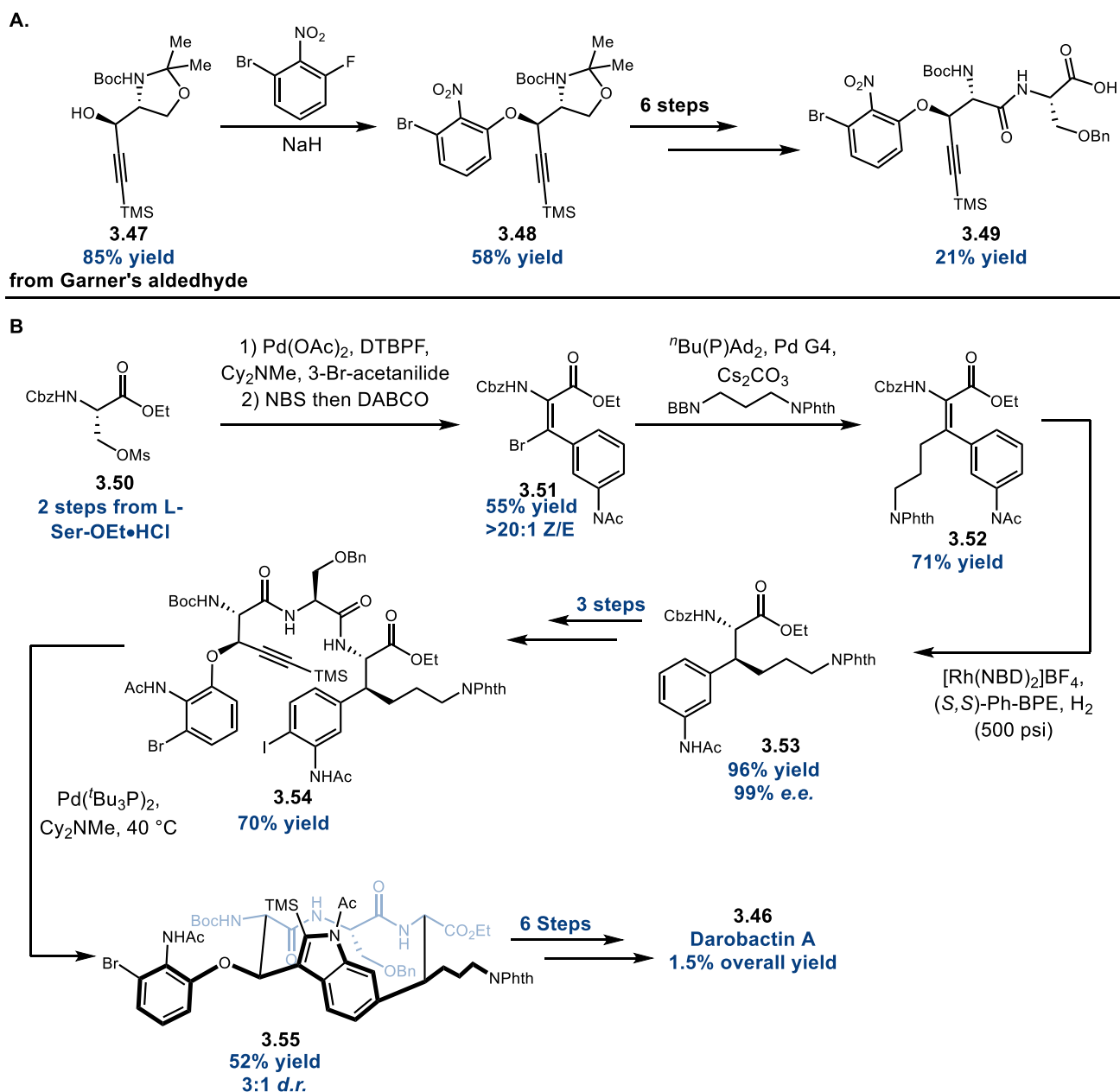


Figure 3.6 The heptapeptide darobactin A

Darobactin A is an exciting bi-macrocyclic RiPP, isolated from the nematophilic bacteria *Photorhabdus khanii* HGB1456.¹¹⁶ The heptapeptide contains both a C–O crosslink between Trp¹ and Trp³ and a C–C crosslink between Trp³ and Lys⁵. These crosslinks lock darobactin A into a strained bi-macrocyclic conformation which is critical to its bioactivity. Darobactin A displayed potent antimicrobial activity towards pathogenic gram-negative bacteria, while exhibiting tolerance to less harmful bacteria found in eukaryotes.¹¹⁶ Its reactivity profile is interesting, but its mode of action is what made darobactin A a hot target. Darobactin A binds to the lateral gate of BamA, a transmembrane protein that assists in embedding other transmembrane proteins.¹¹⁷ Due to its competitive inhibition, darobactin A prevents native substrates from binding and significantly impedes bacterial outer membrane function resulting in cell death. Many of darobactin A's interactions with BamA occur along the peptide backbone, which indicates there may be ample opportunity for derivatization with the amino acid sidechains, to improve bioactivity.¹¹⁷ With an impressive profile, and the desire to study analogs of the natural product, several groups began working on chemical syntheses of darobactin A.

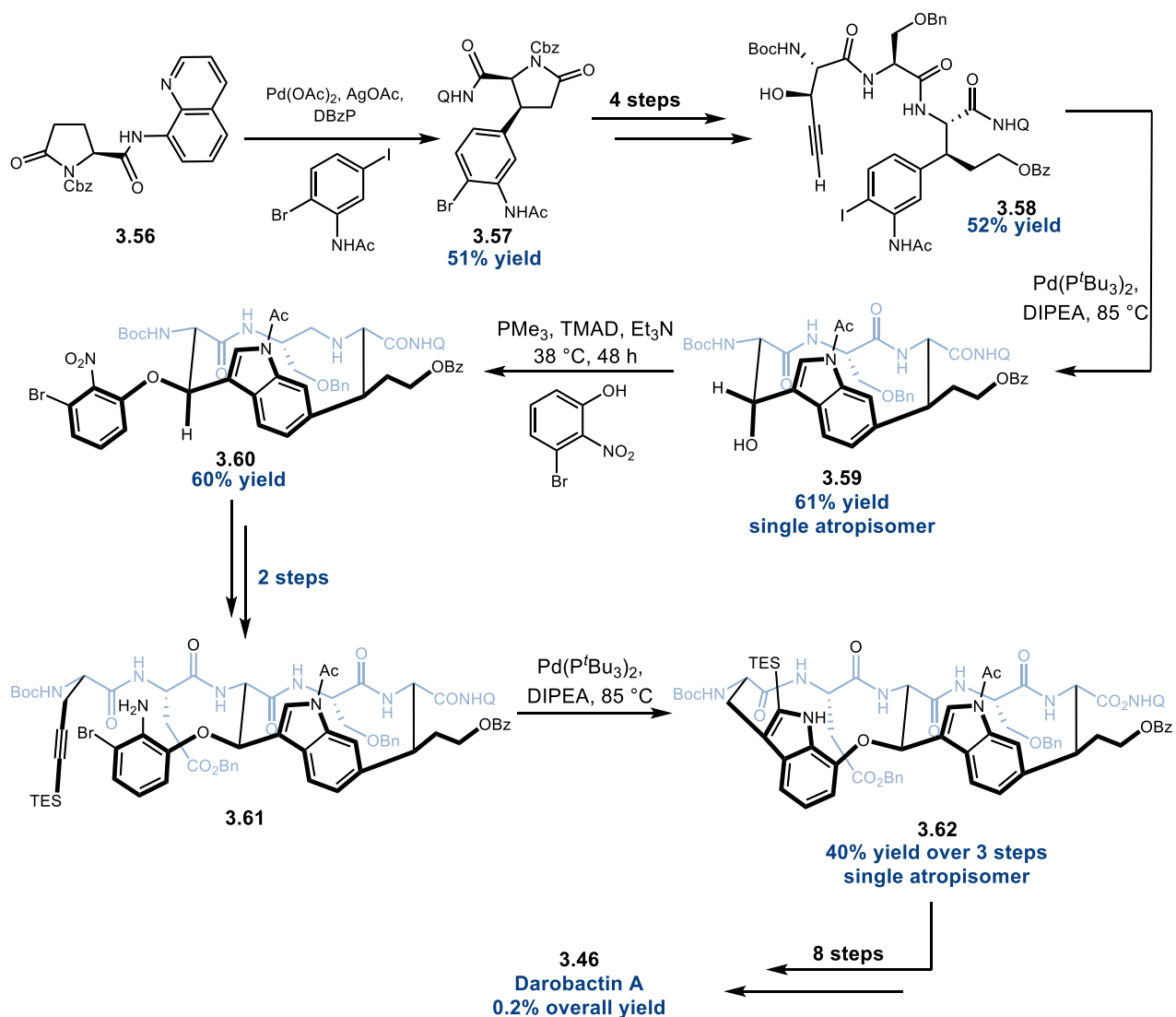
While our work towards the synthesis of darobactin A began in 2020, there have been two syntheses reported since then.^{118,119} The first synthesis was reported by Sarlah in collaboration with Merck (Scheme 3.11).¹¹⁸ The C–O crosslink was synthesized via a S_NAr reaction to deliver **3.48**, which was carried forward to peptide coupling intermediate **3.49** (Scheme 3.11, A). The linear synthesis began with Heck coupling to forge the C–C



Scheme 3.11 The Sarlah synthesis of darobactin A.

crosslink, followed by bromination to deliver vinyl bromide **3.51** primed for Suzuki-Miyaura cross coupling. The subsequent cross coupling reaction proceeded in good yield, and forceful hydrogenation was able to convert the tetra-substituted olefin into lysine derivative **3.53**, with the requisite stereochemistry. Elaboration of the peptide chain incorporated the ethereal fragment **3.49**, which contained the 2-bromoacetamide for future Larock cyclization. The first macrocyclic Larock annulation delivered the eastern macrocyclic good yield with some diastereoselectivity for the natural atropisomer. Another round of peptide couplings set the stage for the second Larock cyclization which occurred in decent yield with exclusivity for the correct atropisomer. Global deprotection then delivered darobactin A in 1.5% overall yield and 16 steps.

The Baran synthesis followed a similar synthetic strategy of forging the C–C crosslink then elaborating the linear peptide to set the stage for subsequent macrocyclizations (Scheme 3.12).¹¹⁹ In contrast to the Sarlah synthesis, Baran and coworkers utilized the 8-aminoquinoline directed arylation to forge the C–C crosslink by installing 2-bromoacetamide to deliver **3.57**. In four steps, they elongated the peptide chain to include a pendant alkyne for Larock cyclization which proceeded in good yield with exclusivity for the natural atropisomer. After the first macrocyclization, the Baran



Scheme 3.12 The Baran synthesis of darobactin A.

group subjected **3.59** to Mitsunobu substitution to forge the C–O crosslink. In another two steps, intermediate **3.61** was primed for another Larock annulation. The Baran group found that when the eastern macrocycle was generated first, it would later guide the western macrocyclization and so they were able to complete both Larock cyclizations with exclusive diastereoselectivity for the natural atropisomer. In eight more steps, the Baran group delivered darobactin A in 0.2% overall yield.

3.3 Conclusions

There have been significant advancements in the synthesis of RiPPs containing C–O and C–C crosslinks. In the realm of C–O crosslink formation; nucleophilic addition with stereo-defined coupling partners has been shown to be a reliable method for creating ethereal crosslinks in the context of RiPP synthesis, while establishing stereochemistry while forging the C – O bond was much more challenging to carry out effectively. There have been many syntheses of RiPPs with tryptophan containing C–C crosslinks. A common thread among these syntheses was that forging the C–C crosslink with the tryptophan moiety intact was much more difficult than appending an aryl fragment that would eventually become the tryptophan fragment. Challenging RiPP macrocyclic scaffolds often required new methodology to effect efficient syntheses. Several groups utilized the relatively recently reported 8-aminoquinoline directed C–H arylation in the context of peptidyl substrates as an efficient method to forge C–C crosslinks. Despite these advances in methodology, RiPP chemical syntheses have remained stagnant in strategic development. The difficult crosslinks are forged in the beginning of the synthetic route and peptide chains are elongated from that fragment, then cyclization events take place. While this strategy eliminates a lot of risk when forging the crosslink, it often results

in longer syntheses. We will detail our efforts in developing robust methodology for forging C–O or C–C crosslinks to alleviate the risk of late stage synthesis of RiPP crosslinks in the following chapter.

3.4. References

- (87) Arnison, P. G.; Bibb, M. J.; Bierbaum, G.; Bowers, A. A.; Bugni, T. S.; Bulaj, G.; Camarero, J. A.; Campopiano, D. J.; Challis, G. L.; Clardy, J.; Cotter, P. D.; Craik, D. J.; Dawson, M.; Dittmann, E.; Donadio, S.; Dorrestein, P. C.; Entian, K.-D.; Fischbach, M. A.; Garavelli, J. S.; Göransson, U.; Gruber, C. W.; Haft, D. H.; Hemscheidt, T. K.; Hertweck, C.; Hill, C.; Horswill, A. R.; Jaspars, M.; Kelly, W. L.; Klinman, J. P.; Kuipers, O. P.; Link, A. J.; Liu, W.; Marahiel, M. A.; Mitchell, D. A.; Moll, G. N.; Moore, B. S.; Müller, R.; Nair, S. K.; Nes, I. F.; Norris, G. E.; Olivera, B. M.; Onaka, H.; Patchett, M. L.; Piel, J.; Reaney, M. J. T.; Rebuffat, S.; Ross, R. P.; Sahl, H.-G.; Schmidt, E. W.; Selsted, M. E.; Severinov, K.; Shen, B.; Sivonen, K.; Smith, L.; Stein, T.; Süssmuth, R. D.; Tagg, J. R.; Tang, G.-L.; Truman, A. W.; Vederas, J. C.; Walsh, C. T.; Walton, J. D.; Wenzel, S. C.; Willey, J. M.; Van Der Donk, W. A. Ribosomally Synthesized and Post-Translationally Modified Peptide Natural Products: Overview and Recommendations for a Universal Nomenclature. *Nat. Prod. Rep.* **2013**, *30*, 108-160. <https://doi.org/10.1039/c2np20085f>.
- (88) Montalbán-López, M.; Scott, T. A.; Ramesh, S.; Rahman, I. R.; van Heel, A. J.; Viel, J. H.; Bandarian, V.; Dittmann, E.; Genilloud, O.; Goto, Y.; Grande Burgos, M. J.; Hill, C.; Kim, S.; Koehnke, J.; Latham, J. A.; Link, A. J.; Martínez, B.; Nair, S. K.; Nicolet, Y.; Rebuffat, S.; Sahl, H.-G.; Sareen, D.; Schmidt, E. W.; Schmitt, L.; Severinov, K.; Süssmuth, R. D.; Truman, A. W.; Wang, H.; Weng, J.-K.; van Wezel, G. P.; Zhang, Q.; Zhong, J.; Piel, J.; Mitchell, D. A.; Kuipers, O. P.; van der Donk, W. A. New Developments in RiPP Discovery, Enzymology and Engineering. *Nat. Prod. Rep.* **2020**, *38*, 130-239. <https://doi.org/10.1039/d0np00027b>.
- (89) Oman, T. J.; Van Der Donk, W. A. Follow the Leader: The Use of Leader Peptides to Guide Natural Product Biosynthesis. *Nat. Chem. Biol.* **2010**, *6* (1), 9–18. <https://doi.org/10.1038/nchembio.286>.
- (90) Matsson, P.; Doak, B. C.; Over, B.; Kihlberg, J. Cell Permeability beyond the Rule of 5. *Adv. Drug Deliv. Rev.* **2016**, *101*, 42–61. <https://doi.org/10.1016/j.addr.2016.03.013>.
- (91) Degoey, D. A.; Chen, H. J.; Cox, P. B.; Wendt, M. D. Beyond the Rule of 5: Lessons Learned from AbbVie's Drugs and Compound Collection. *J. Med. Chem.* **2018**, *61* (7), 2636–2651. <https://doi.org/10.1021/ACS.JMEDCHEM.7B00717>.
- (92) Li, P.; Evans, C. D.; Wu, Y.; Cao, B.; Hamel, E.; Joullié, M. M. Evolution of the Total Syntheses of Ustiloxin Natural Products and Their Analogues. *J. Am. Chem. Soc.* **2008**, *130* (7), 2351–2364. <https://doi.org/10.1021/JA710363P>.
- (93) Grimley, J. S.; Sawayama, A. M.; Tanaka, H.; Stohlmeyer, M. M.; Woiwode, T. F.; Wandless, T. J. The Enantioselective Synthesis of Phomopsin B. *Angew. Chem. Int. Ed.* **2007**, *46* (43), 8157–8159. <https://doi.org/10.1002/ANIE.200702537>.

- (94) Taichi, M.; Yamazaki, T.; Kimura, T.; Nishiuchi, Y. Total Synthesis of Marinostatin, a Serine Protease Inhibitor Isolated from the Marine Bacterium *Pseudoalteromonas sagamiensis*. *Tetrahedron Lett.* **2009**, *50* (20), 2377–2380. <https://doi.org/10.1016/J.TETLET.2009.02.213>.
- (95) Shabani, S.; White, J. M.; Hutton, C. A. Total Synthesis of the Putative Structure of Asperipin-2a and Stereochemical Reassignment. *Org. Lett.* **2020**, *22* (19), 7730–7734. <https://doi.org/10.1021/ACS.ORGLETT.0C02884>.
- (96) Koiso, Y.; Natori, M.; Iwasaki, S.; Sato, S.; Sonoda, R.; Fujita, Y.; Yaegashi, H.; Sato, Z. Ustiloxin: A Phytotoxin and a Mycotoxin from False Smuth Balls on Rice Panicles. *Tetrahedron Lett.* **1992**, *33* (29), 4157–4160. [https://doi.org/10.1016/S0040-4039\(00\)74677-6](https://doi.org/10.1016/S0040-4039(00)74677-6).
- (97) Koiso, Y.; Li, Y.; Iwasaki, S.; Hanaka, K.; Kobayashi, T.; Sonoda, R.; Fujita, Y.; Yaegashi, H.; Sato, Z. Ustiloxins, Antimitotic Cyclic Peptides From False Smut Balls on Rice Panicles Caused by *Ustilagoideae Virens*. *J. Antibiot.* **1994**, *47* (7), 765–773. <https://doi.org/10.7164/ANTIBIOTICS.47.765>.
- (98) Koiso, Y.; Morisaki, N.; Yamashita, Y.; Mitsui, Y.; Shirai, R.; Hashimoto, Y.; Iwasaki, S. Isolation and Structure of an Antimitotic Cyclic Peptide, Ustiloxin F: Chemical Interrelation with a Homologous Peptide, Ustiloxin B. *J. Antibiot.* **1998**, *51* (4), 418–422. <https://doi.org/10.7164/ANTIBIOTICS.51.418>.
- (99) Cao, B.; Park, H.; Joullié, M. M. Total Synthesis of Ustiloxin D. *J. Am. Chem. Soc.* **2002**, *124* (4), 520–521. <https://doi.org/10.1021/JA017277Z>.
- (100) Tanaka, H.; Sawayama, A. M.; Wandless, T. J. Enantioselective Total Synthesis of Ustiloxin D. *J. Am. Chem. Soc.* **2003**, *125* (23), 6864–6865. <https://doi.org/10.1021/JA035429F>.
- (101) Sawayama, A. M.; Tanaka, H.; Wandless, T. J. Total Synthesis of Ustiloxin D and Considerations on the Origin of Selectivity of the Asymmetric Allylic Alkylation. *J. Org. Chem.* **2004**, *69* (25), 8810–8820. <https://doi.org/10.1021/JO048854F>.
- (102) Li, P.; Evans, C. D.; Joullié, M. M. A Convergent Total Synthesis of Ustiloxin D via an Unprecedented Copper-Catalyzed Ethynyl Aziridine Ring-Opening by Phenol Derivatives. *Org. Lett.* **2005**, *7* (23), 5325–5327. <https://doi.org/10.1021/OL052287G>.
- (103) Brown, A. L.; Churches, Q. I.; Hutton, C. A. Total Synthesis of Ustiloxin D Utilizing an Ammonia-Ugi Reaction. *J. Org. Chem.* **2015**, *80* (20), 9831–9837. <https://doi.org/10.1021/ACS.JOC.5B01519>.
- (104) Laws, D.; Plouch, E. V.; Blakey, S. B. Synthesis of Ribosomally Synthesized and Post-Translationally Modified Peptides Containing C-C Cross-Links. *J. Nat. Prod.* **2022**, *85* (10), 2519–2539. <https://doi.org/10.1021/ACS.JNATPROD.2C00508>.

- (105) Kobayashi, J.; Suzuki, H.; Shimbo, K.; Takeya, K.; Morita, H. Celogentins A-C, New Antimitotic Bicyclic Peptides from the Seeds of *Celosia Argentea*. *J. Org. Chem.* **2001**, *66* (20), 6626–6633. <https://doi.org/10.1021/jo0103423>.
- (106) Bentley, D. J.; Slawin, A. M. Z.; Moody, C. J. Total Synthesis of Stephanotic Acid Methyl Ester. *Org. Lett.* **2006**, *8* (10), 1975–1978. <https://doi.org/10.1021/OL060153C>.
- (107) Michaux, J.; Retaillea, P.; Campagne, J. M. Synthesis of the Central Tryptophan-Leucine Residue of Celogentin C. *Synlett* **2008**, *10*, 1532–1536. <https://doi.org/10.1055/s-2008-1078411>.
- (108) Ma, B.; Litvinov, D. N.; He, L.; Banerjee, B.; Castle, S. L. Total Synthesis of Celogentin C**. *Angew. Chem. Int. Ed.* **2009**, *48* (33), 6104–6107. <https://doi.org/10.1002/anie.200902425>.
- (109) Ma, B.; Banerjee, B.; Litvinov, D. N.; He, L.; Castle, S. L. Total Synthesis of the Antimitotic Bicyclic Peptide Celogentin C. *J. Am. Chem. Soc.* **2010**, *132* (3), 1159–1171. <https://doi.org/10.1021/ja909870g>.
- (110) Hu, W.; Zhang, F.; Xu, Z.; Liu, Q.; Cui, Y.; Jia, Y. Stereocontrolled and Efficient Total Synthesis of (-)-Stephanotic Acid Methyl Ester and (-)-Celogentin C. *Org. Lett.* **2010**, *12* (5), 956–959. <https://doi.org/10.1021/OL902944F>.
- (111) Feng, Y.; Chen, G. Total Synthesis of Celogentin C by Stereoselective C-H Activation. *Angew. Chem. Int. Ed.* **2010**, *49* (5), 958–961. <https://doi.org/10.1002/anie.200905134>.
- (112) Schramma, K. R.; Bushin, L. B.; Seyedsayamdost, M. R. Structure and Biosynthesis of a Macrocyclic Peptide Containing an Unprecedented Lysine-to-Tryptophan Crosslink. *Nat. Chem.* **2015**, *7* (5), 431–437. <https://doi.org/10.1038/nchem.2237>.
- (113) Isley, N. A.; Endo, Y.; Wu, Z.-C.; Covington, B. C.; Bushin, L. B.; Seyedsayamdost, M. R.; Boger, D. L. Total Synthesis and Stereochemical Assignment of Streptide. *J. Am. Chem. Soc.* **2019**, *141* (43) 17361–17369. <https://doi.org/10.1021/jacs.9b09067>.
- (114) Wyche, T. P.; Ruzzini, A. C.; Schwab, L.; Currie, C. R.; Clardy, J. Tryptorubin A: A Polycyclic Peptide from a Fungus-Derived Streptomycete. *J. Am. Chem. Soc.* **2017**, *139* (37), 12899–12902. <https://doi.org/10.1021/jacs.7b06176>.
- (115) Reisberg, S. H.; Gao, Y.; Walker, A. S.; Helfrich, E. J. N.; Clardy, J.; Baran, P. S. Total Synthesis Reveals Atypical Atropisomerism in a Small-Molecule Natural Product, Tryptorubin A. *Science*, **2020**, *367* (6476), 458–463. <https://doi.org/10.1126/science.aay9981>.
- (116) Imai, Y.; Meyer, K. J.; Iinishi, A.; Favre-Godal, Q.; Green, R.; Manuse, S.; Caboni, M.; Mori, M.; Niles, S.; Ghiglieri, M.; Honrao, C.; Ma, X.; Guo, J. J.;

Makriyannis, A.; Linares-Otoya, L.; Böhringer, N.; Wuisan, Z. G.; Kaur, H.; Wu, R.; Mateus, A.; Typas, A.; Savitski, M. M.; Espinoza, J. L.; O'Rourke, A.; Nelson, K. E.; Hiller, S.; Noinaj, N.; Schäberle, T. F.; D'Onofrio, A.; Lewis, K. A New Antibiotic Selectively Kills Gram-Negative Pathogens. *Nature* **2019**, *576* (7787), 459–464. <https://doi.org/10.1038/s41586-019-1791-1>.

(117) Kaur, H.; Jakob, R. P.; Marzinek, J. K.; Green, R.; Imai, Y.; Bolla, J. R.; Agustoni, E.; Robinson, C. V.; Bond, P. J.; Lewis, K.; Maier, T.; Hiller, S. The Antibiotic Darobactin Mimics a β -Strand to Inhibit Outer Membrane Insertase. *Nature* **2021**, *593* (7857), 125–129. <https://doi.org/10.1038/s41586-021-03455-w>.

(118) Nesic, M.; Ryffel, D. B.; Maturano, J.; Shevlin, M.; Pollack, S. R.; Donald R. Gauthier, Jr.; Trigo-Mouriño, P.; Zhang, L.-K.; Schultz, D. M.; Dunn, J. M. M.; Campeau, L.-C.; Patel, N. R.; Petrone, D. A.; Sarlah, D. Total Synthesis of Darobactin A. *J. Am. Chem. Soc.* **2022**, *144* (31), 14026–14030. <https://doi.org/10.1021/JACS.2C05891>.

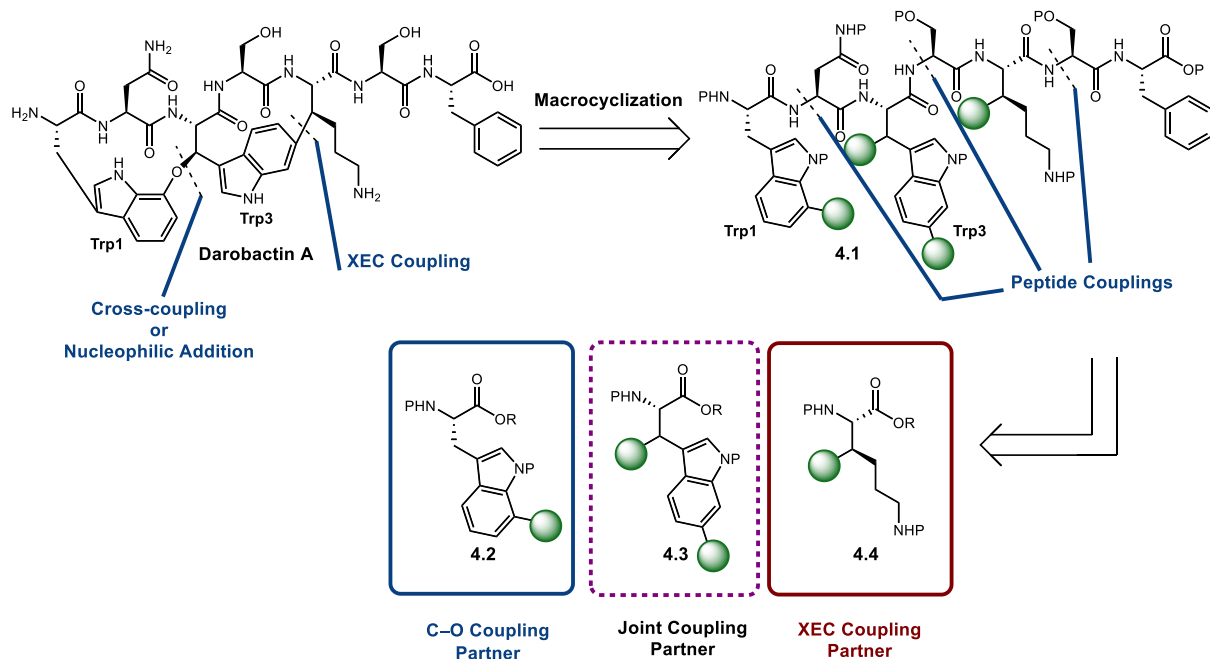
(119) Lin, Y.-C.; Schneider, F.; Eberle, K. J.; Chiodi, D.; Nakamura, H.; Reisberg, S. H.; Chen, J.; Saito, M.; Baran, P. S. Atroposelective Total Synthesis of Darobactin A. *J. Am. Chem. Soc.* **2022**, *144* (32), 14458–14462. <https://doi.org/10.1021/JACS.2C05892>.

Chapter 4. Progress Towards the Synthesis of the Western Macrocycle of Darobactin A

In this chapter we will discuss our work towards developing a synthesis of darobactin A. We will begin with our retrosynthetic strategy focused on developing robust methods for crosslink formation. Then we will discuss chemistry to deliver functionalized amino acid residues for use in C–O crosslinking reactions. Finally, we will evaluate methods of forging the western C–O crosslink between Trp¹ and Trp³ found in darobactin A.

4.1 Synthetic Strategy towards the Total Synthesis of Darobactin A

When we began developing our synthetic strategy towards the total synthesis of darobactin A, we sought to diverge from existing strategic approaches towards RiPPs with macrocyclic side-chain crosslinks. As shown in the previous chapter, RiPP chemical syntheses typically began with forging the side chain crosslink. Given that these crosslinks represent the majority of synthetic complexity, this was a great way to offset risk in longer total syntheses. However, this approach usually elongates the forward route. To reduce this risk, we sought to develop or adapt crosslinking methodology that would be compatible in the context of peptide chemistry, where plenty of extraneous functional groups surround the desired position for crosslink formation. We focused on identifying methodology that could be adapted to synthesize the C–O crosslink between Trp¹ and Trp³, while fellow graduate students Eleda Plouch and Mark Maust investigated a cross electrophile coupling (XEC) to form the eastern C–C crosslink between Trp³ and Lys⁵.

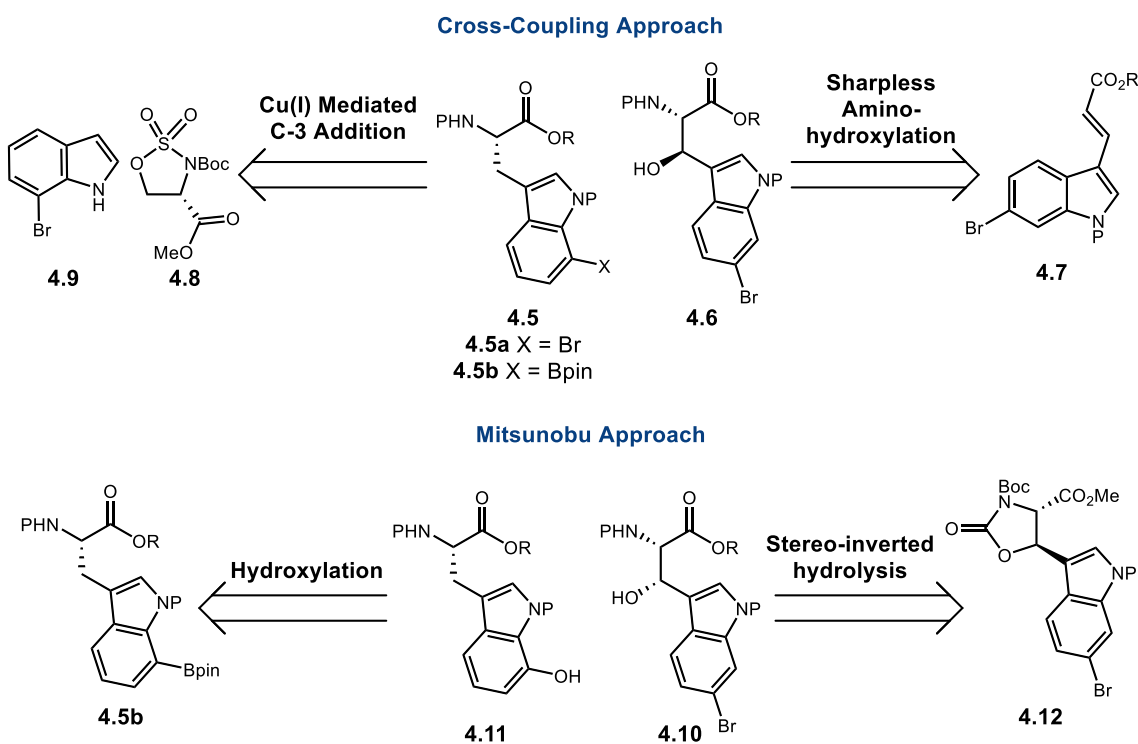


Scheme 4.1 Our retrosynthetic analysis of darobactin A.

In the ideal retrosynthetic pathway, we envisioned two macrocyclic disconnections to arrive at the linear peptide **4.1** from darobactin A (Scheme 4.1). The linear peptide would need to contain key functionalizations at the indicated positions. Peptide coupling disconnections would provide the functionalized amino acids **4.2-4**, in a convergent approach. These amino acids would have different functionality depending on the proposed chemistry of our forward route. Another consideration when developing our route is that **4.3**, the central tryptophan residue, would need to contain functional groups that would correspond both with C–O bond formation and Trp–Lys coupling. We considered several methodologies to apply our functionalized amino acids. The aforementioned XEC was identified for construction of the eastern macrocycle. In order to utilize this methodology, we would need a 6-bromo tryptophan and β -bromolysine. We decided to probe both metal mediated cross-coupling and nucleophilic Mitsunobu addition approaches to the western macrocycle. With these methods under consideration, we

identified our target amino acid fragments (Figure 4.1). While β -bromolysine is integral to this synthesis, Eleda Plouch and Mark Maust were focused on delivering that moiety.

We developed two retrosynthetic routes for our amino acids used in constructing the western macrocycle (Scheme 4.2). In a cross-coupling approach, we would need a 7-functionalized tryptophan, while erythro- β -hydroxy-tryptophan (**4.6**, Scheme 2) also bearing the 6-bromo group, would be needed as the coupling partner. In an Ullman-type coupling we would need the 7-bromotryptophan (**4a**, Scheme 4.2). Alternatively, in a Chan-Lam coupling we would need the 7-boryl tryptophan (**4.5b**, Scheme 4.2). At first glance, the multiple aryl bromides would render the Ullman coupling useless, but if the XEC is done beforehand, removing the 6-bromo group, this remains a viable strategy. Both the 7-bromo and 7-boryl tryptophans are accessible from C-3 addition of 7-bromoindole to sulfamidate **4.8**. The erythro- β -hydroxy-tryptophan would be delivered via



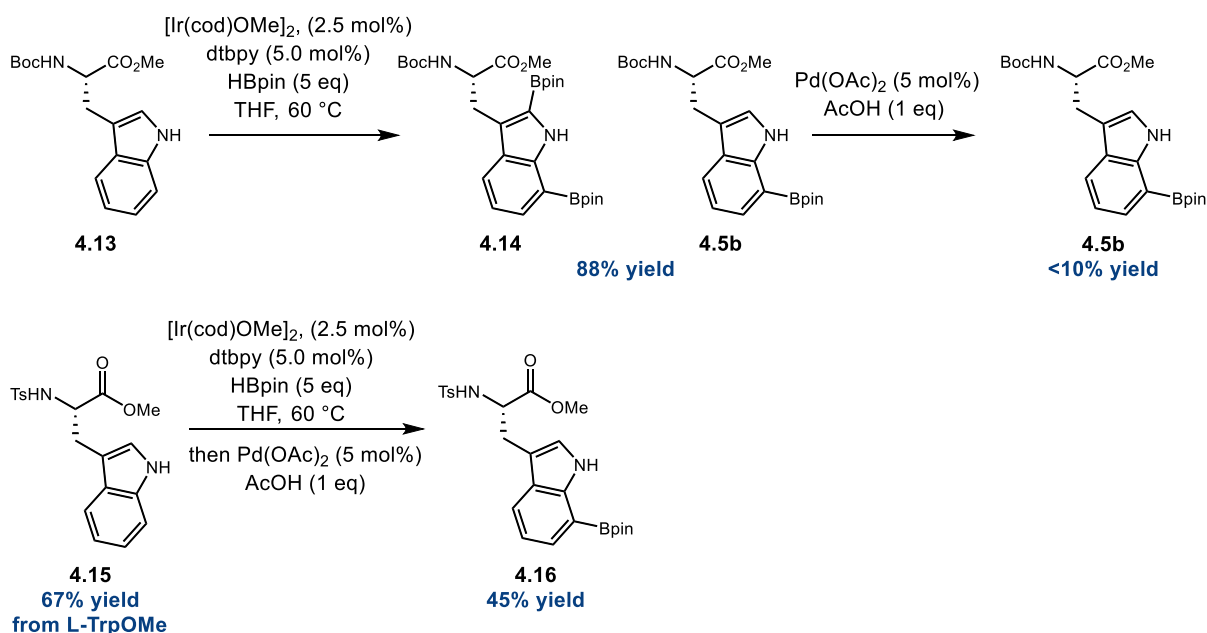
Scheme 4.2 Retrosynthetic analysis of amino acid fragments

Sharpless aminohydroxylation. In another realm entirely, nucleophilic addition was considered for the coupling of these two fragments. In that case 7-OH tryptophan **4.11** would engage *threo*- β -hydroxy tryptophan **4.10** in a Mitsunobu style substitution. The 7-OH tryptophan would be accessed from hydroxylation of **4.5b** while the *threo*-hydroxy tryptophan would be delivered from hydrolysis of oxazolidinone **4.12**. Having reduced our retrosynthetic pathway to commercially accessible materials, we began investigating our forward route.

4.2 Synthesis of Amino Acid Fragments

4.2.1 Synthesis of 7-substituted *L*-Tryptophan derivatives

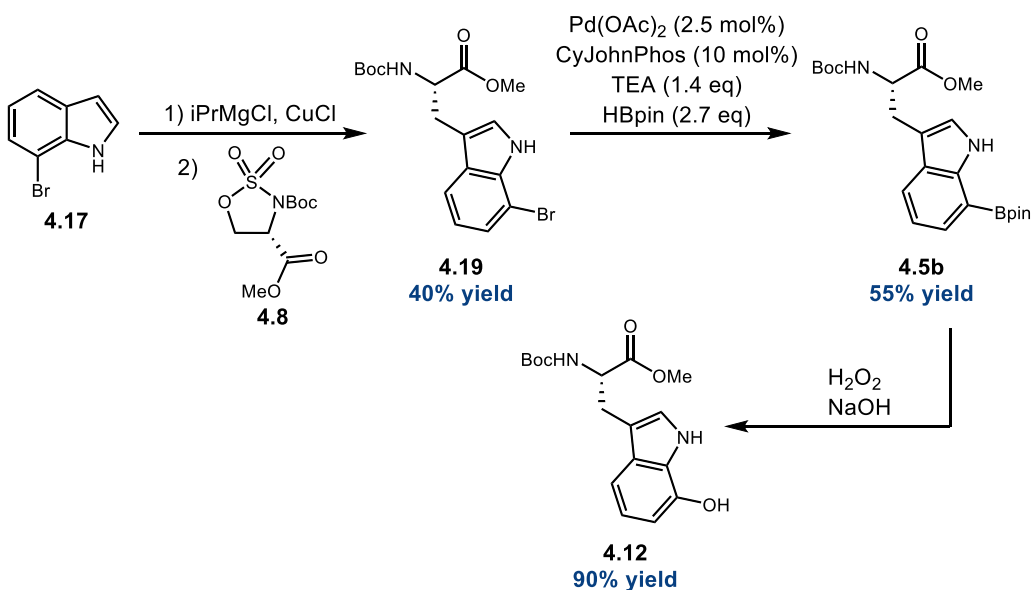
The first 7-substituted tryptophan residue we sought out was 7-borylated *L*-tryptophan derivative **4.5b** for use in Chan-Lam coupling. Movassaghi and coworkers have previously disclosed the Ir catalyzed, regioselective C7-borylation of indoles including *L*-tryptophan.¹²⁰ The indole nitrogen would direct Ir to borylate the neighboring



Scheme 4.3 The synthesis of 7-Bpin-*L*-Trp via directed borylation

carbons, then given indole C2 is more reactive than C7, regioselective deborylation via Pd(OAc)₂ and AcOH would provide the desired C7 substituted tryptophan. While the diborylation of tryptophan occurred in up to 88% yield, we struggled to effect selective deborylation retaining a mixture of borylated species. We exchanged the Boc protecting group for the more acid tolerant tosyl and were able to obtain the mono pinacolboronate ester (Bpin) product in 45% yield via acidification with trifluoroacetic acid. However, we saw a less time intensive way to deliver the mono borylated product through Miyaura coupling with 7-bromotryptophan.

To access the 7-bromo-L-tryptophan we utilized the C-3 selective alkylation of indoles disclosed by Bartoccini *et al.* (Scheme 4.4).¹²¹ We found that the addition of 7-bromoindole into sulfamidate **4.8** delivered 7-bromo-L-tryptophan **4.19** in moderate yield, however we made several modifications to the procedure. We found that iPrMgCl performed better in the deprotonation/activation of C-3 of indole, and excess indole delivered a cleaner reaction. 7-bromo-L-tryptophan underwent facile Miyaura coupling to



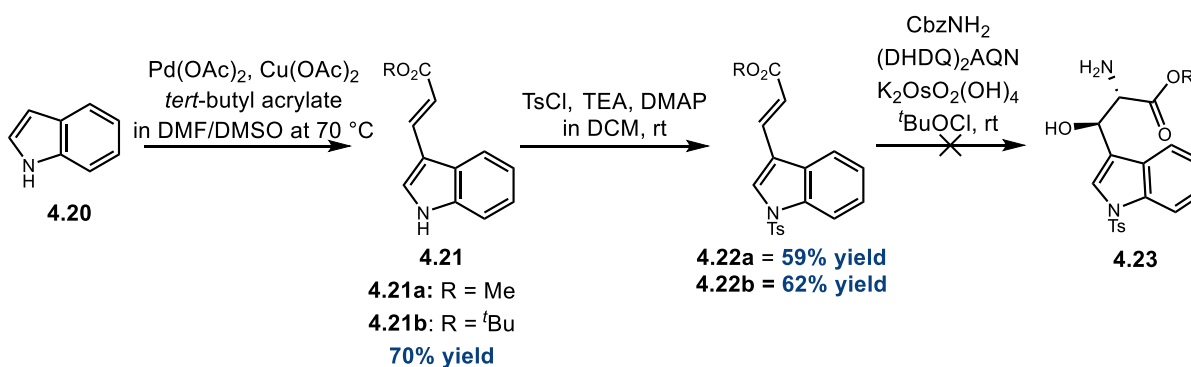
Scheme 4.4 Generation of the 7-substituted L-tryptophan derivatives

provide the 7-Bpin Trp **4.5b** in good yield.¹²² Lastly, we synthesized 7-hydroxy-*L*-tryptophan for use as an oxygen nucleophile in Mitsunobu studies. The oxidation of the 7-Bpin-tryptophan went smoothly and swiftly to deliver the 7-hydroxytryptophan derivative **4.12** under basic conditions.¹²³

4.2.2 Synthesis of erythro- β -hydroxytryptophan

Transition metal mediated coupling of β -hydroxy-*L*-Tryptophan was an attractive reaction paradigm for macrocyclization because we would not have to set point chirality as we also established planar chirality in the form of atropisomerism. To evaluate typical cross-coupling reactions such as Ullman or Chan-Lam coupling, we needed the *erythro*- β -hydroxy-*L*-tryptophan derivative. Unfortunately, the synthesis of this amino acid derivative was not as straightforward as the 7-substituted *L*-tryptophans.

Initially we aimed to utilize precedented stereoselective Sharpless amino-hydroxylation of conjugated olefin **4.22** (Scheme 4.5).¹²⁴ While this would have been a direct method to the 1,2-aminoalcohol, with excellent enantioselectivity and diastereoselectivity, neither the methyl nor *tert*-butyl ester were productive in the amino-hydroxylation. We tried fresh Os reagent and biscinchona alkaloid to no avail. Also, fresh



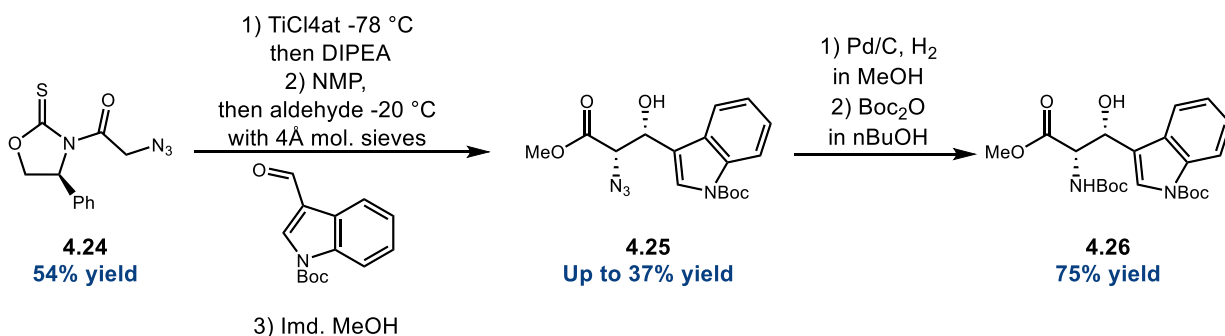
Scheme 4.5 Our attempts at Sharpless amino-hydroxylation of indolyl acrylates

preparation of *tert*-butyl hypochlorite did not turn on reactivity. With no luck in the direct amino-hydroxylation, we turned to chiral auxiliaries to provide our desired diastereomer.

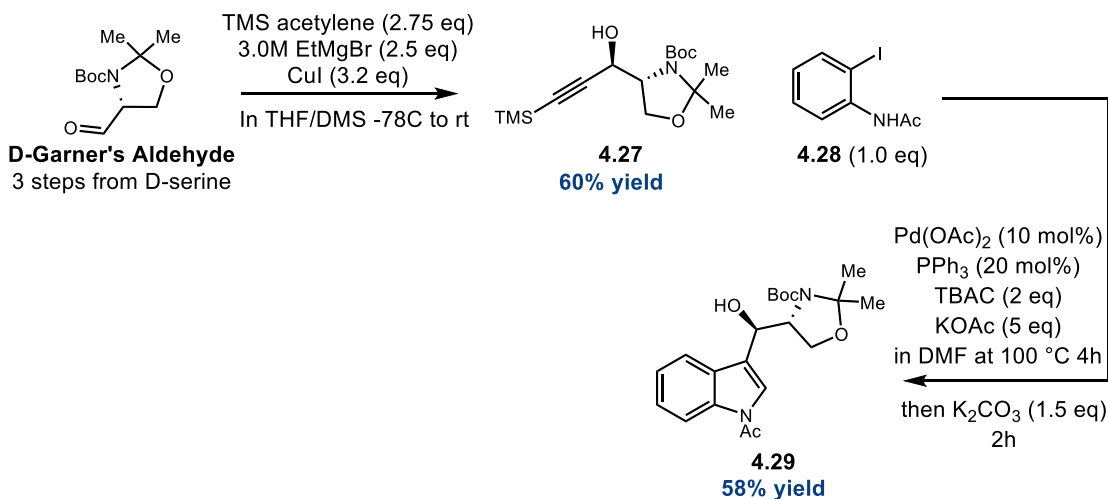
We identified the diastereoselective aldol reaction reported by Franck and coworkers as a promising alternative to the Sharpless aminohydroxylation.¹²⁵ The chelation controlled, TiCl₄ mediated aldol delivered great selectivity for the *syn*- α -amino- β -hydroxy acid in the presence of Evans' auxiliary **4.24**. Given that we wished to obtain the opposite enantiomer of aldol product, we synthesized the (S)-4-phenyloxazolidine-2-thione. Acylation with 2-azidoacetic acid occurred in good yield, with necessary precautions to handle the low molecular weight azide. The first aldol reaction with the acylated chiral auxiliary proceeded in poor yield. However, distillation of TiCl₄ and the addition of molecular sieves improved the yield from 9% to 37% yield. **4.25** was conveniently converted into protected amine **4.26**, to serve as a suitable Chan-Lam reagent. Unfortunately, we experienced an incident after one instance in purification of the aldol product, where most likely the chiral auxiliary decomposed on silica and 2-azidoacetic acid was recovered from flash chromatography which exploded in my hands after being disturbed. Ultimately, I made a full recovery due to proper use of personal protective equipment, but in an abundance of caution, we ceased all work with the chiral auxiliary and 2-azidoacetic acid. Given our inability to access the acylated oxazolidine-2-

thiones, we were unable to generate racemic aldol products to verify enantiopurity of the final azide.

Without the Evans auxiliary, we looked for alternate routes to the *erythro*- β -hydroxytryptophan derivative. Garner's aldehyde has long been used to access β -hydroxy-1,2 aminols in good yields and diastereoselectivities, with routine d.r.'s of 20:1 and d.r.'s on the low end around 11:1.¹²⁶ Several groups have utilized alkyne addition to Garner's aldehyde as a route to β -hydroxy amino acids.^{118,127} Also the pendant alkyne would provide a handle for future synthesis of the eastern macrocycle, but we also converted a portion to the indole. Alkyne addition occurred in decent yield and selectivity for the *syn*- β -hydroxyaminol **4.27**, verified by comparison with previous ¹H NMR and optical rotation (Scheme 4.7). Larock annulation was productive,¹²⁸ although subsequent



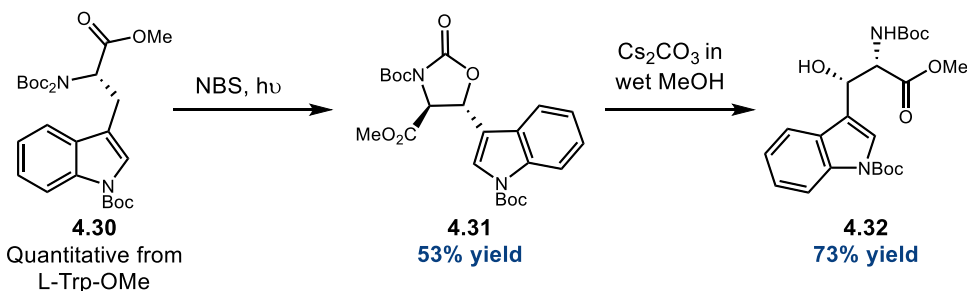
Scheme 4.6 Asymmetric aldol using Evans's auxiliary



Scheme 4.7 The synthesis of *erythro*- β -hydroxy-L-tryptophan utilizing Garner's aldehyde treatment with K₂CO₃ was necessary to desilylate the indole so that the Larock product could be purified. With two *erythro*- β -hydroxy derivatives for testing in coupling reactions, we were ready to begin screening C–O coupling reactions.

4.2.3 Synthesis of *threo*- β -hydroxytryptophan

The last tryptophan derivative needed was a *threo*- β -hydroxytryptophan to engage in Mitsunobu type chemistry. Crich *et al.* provided a succinct method to deliver *threo*- β -hydroxy derivatives of β -aryl amino acids.¹²⁹ Triple *tert*-butylcarbamate (Boc) protection of L-tryptophan was carried out in quantitative yield. Subjection of the tri-Boc protected amino acid to radical benzylic bromination under heat, conveniently converted tryptophan

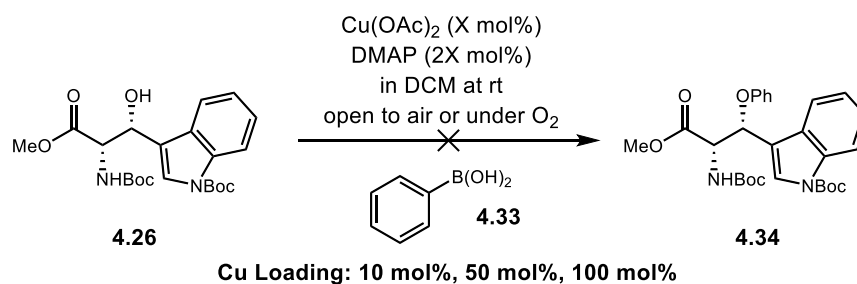


Scheme 4.8 Synthesis of *threo*- β -hydroxy-L-tryptophan

4.30 into oxazolidinone **4.31**. Presumably this reaction proceeded through a carbocation which was rapidly quenched upon thermal cleavage of the *tert*-butyl moiety of the di-Boc protected amine, allowing for good to excellent stereocontrol of the resultant oxazolidinone. Cs₂CO₃ catalyzed hydrolysis of the oxazolidinone provided the *threo*- β -hydroxytryptophan **4.32** in good yield.

4.3 Exploration of C–O Crosslinking Methods

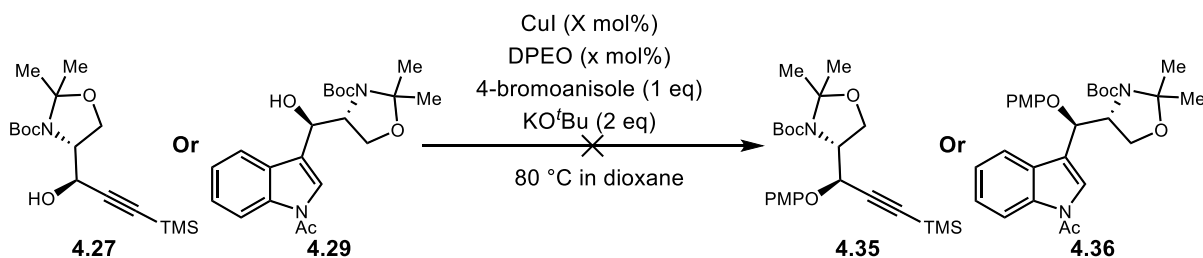
With our requisite amino acid fragments in hand, we were prepared to evaluate a variety of reactions in competency forging the C–O crosslink. Chan-Lam etherification was the first reaction we explored. Although alkyl-aryl Chan-Lam couplings are not known for their consistency, Molander *et al.* published a useful procedure for coupling serine or threonine, which gave convinced us this coupling may be efficacious.¹³⁰ While we did not have much of **4.26** given the explosive nature of its intermediates, we were able to test several Chan-Lam couplings before exhausting our supply. Unfortunately, the Chan-Lam coupling with phenyl boronic acid was not productive under a small range of conditions. We conducted our catalytic experiments under air and oxygen balloon but saw no conversion to the alkyl-aryl ether. Using stoichiometric Cu did not result in conversion



Scheme 4.9: Chan-Lam couplings attempted with *erythro*- β -hydroxy tryptophan

either. We found that we could not reproduce literature results with L-serine, and so we abandoned the Chan-Lam coupling procedure.

Still optimistic about the potential for cross-coupling we looked towards an Ullman-type coupling disclosed by Ma, in which oxalic diamides and *tert*-butoxide enabled the coupling of aliphatic alcohols with aryl bromides.¹³¹ The oxalic diamide ligand was easily synthesized, but neither the *tert*-butoxide or oxalic diamide procedures delivered coupled product. We increased the catalyst loading to 1 eq, and reaction time to up to 2 days with alkyne **4.27**. We were able to recover a significant amount of starting material except in the case of the 48h run at 80 °C, where we began to lose alkyne to degradation. We attempted similar conditions with indole **4.29**, but unfortunately, we observed no reactivity. In contrast to the Chan-Lam couplings, the Ma coupling was consistent with literature compounds but was unproductive with our substrates.



Entry	Alcohol	Cu(I) Loading	DPEO Loading	Base eq	Time
1	4.27	10 mol%	20 mol%	1.2 eq	24 h
2	4.27	100 mol%	200 mol%	3 eq	24 h
3	4.27	100 mol%	200 mol%	3 eq	48 h
4	4.29	10 mol%	20 mol%	1.2 eq	24 h
5	4.29	10 mol%	20 mol%	1.2 eq	24 h
6	4.29	50 mol%	100 mol%	2 eq	24 h
7	4.29	100 mol%	200 mol%	3 eq	24 h

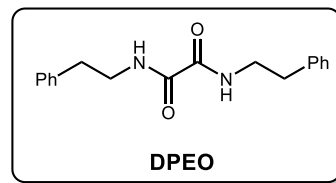
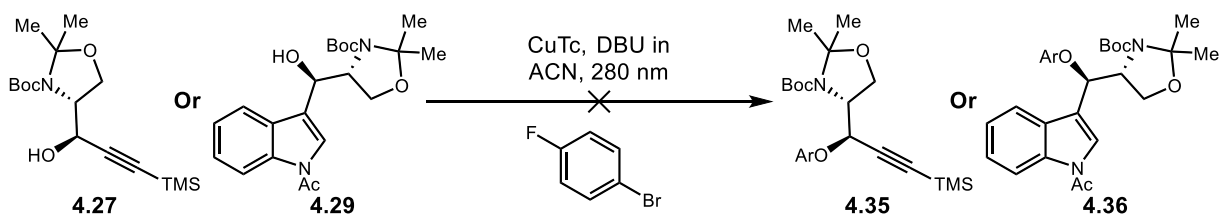


Table 4.1 Exploration of Ullman type cross-coupling utilizing DPEO ligand

Eventually, we began considering light promoted cross coupling methodologies. Initially we were attracted to the Ritter etherification disclosed in 2022.¹³² The Ritter protocol involved directly exciting the aryl halide via UV irradiation, which would undergo homolysis to deliver the aryl radical. The Cu(I) reagent then couples the nucleophile and aryl radical. While we were skeptical of this reaction's performance with tryptophan as the aryl halide, the scope did include 5-bromoindole and Boc-protected amines, indicating it could have some compatibility with our system. Unfortunately, **4.28** or **4.29** were not suitable partners in the UV light promoted cross coupling. Our 280 nm LED set up was able to carry out the coupling with previously disclosed aryl bromides and alcohols, encouraging the thought that our alcohols are simply incompatible. Given that the majority of alcohols in the Ritter report are primary or simple secondary alcohols, it is possible the steric demands of the nearby N-Boc and/or indole ring shut down reactivity.



Scheme 4.10 Unproductive UV light mediated cross-coupling

The last cross-coupling method we investigated was the blue light promoted Ni catalyzed cross coupling from Xue and coworkers as a potential C–O bond forging reaction.¹³³ We applied Ni catalyst **4.38** towards the arylation of alkyne **4.27** and tryptophan derivative **4.29**. Surprisingly, we saw a small conversion to product **4.39** with 5% catalyst loading. Unfortunately, higher catalyst loadings only slightly improved conversion and stoichiometric loading resulted in degradation of the alkyne. It was quite intriguing that despite changing catalyst loading we remained around 10% yield. The

tryptophan derived β -alcohol **4.29** was entirely unproductive, not even achieving the meager yields seen with the alkyne. It is hard to posit what exactly was impeding the coupling. The system performed as desired on literature substrates in quantitative yield, suggesting that the alkyne was inhibiting the reaction in some fashion. Lewis basic functionality such as the carbamate should not interfere as Xue and coworkers report several Boc protected amines that were compatible. With another methodology crossed off our list, we turned to nucleophilic addition reactions.

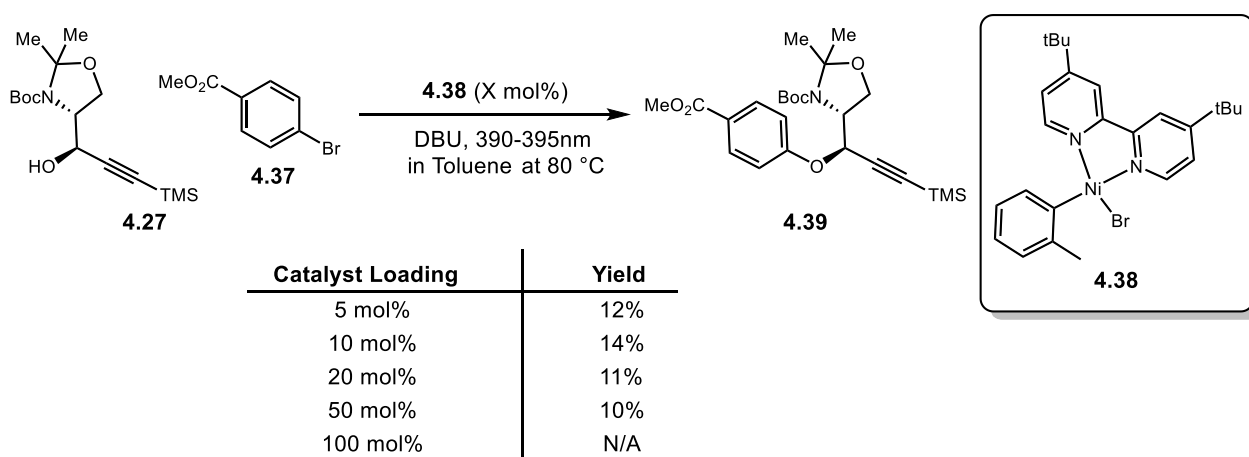
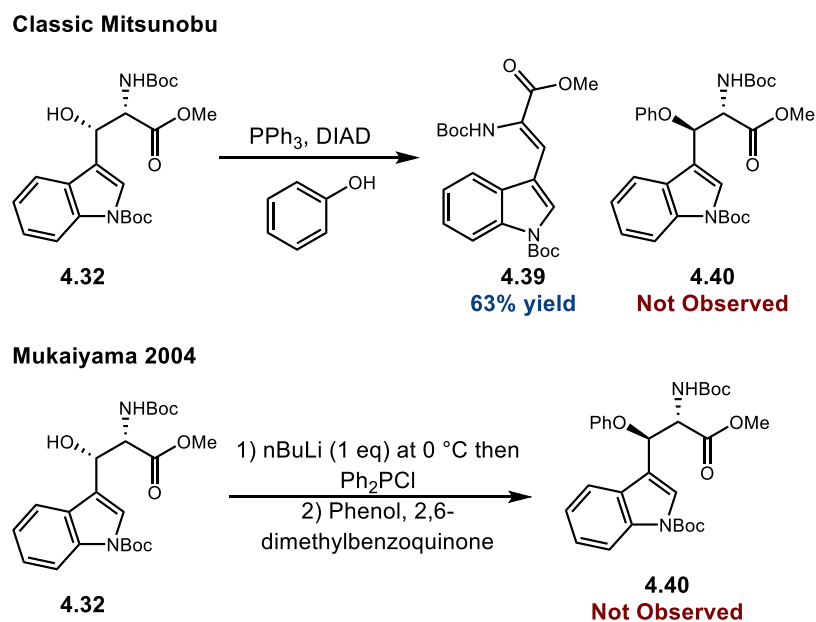


Table 4.2 The effect of catalyst loading on blue light promoted arylation

Due to the electronics of the indole ring, S_NAr was sadly off the table. Although has been proven effective in RiPP synthesis, we doubt an electron rich indole ring would undergo S_NAr easily. Instead, we turned to the classic method for etheral bond formation. The Mitsunobu has been proven in several RiPP syntheses as described earlier, however the system we designed was demanding. We sought to invert the β -alcohol, with a substantial electron withdrawing group two carbons away, and do this chemistry at a benzylic carbon. These concerns were founded when Mitsunobu conditions resulted in clean elimination to the α,β -unsaturated ester. We tried a Mitsunobu inspired protocol from Mukaiyama in which an alkoxydiphenylphosphine is generated,

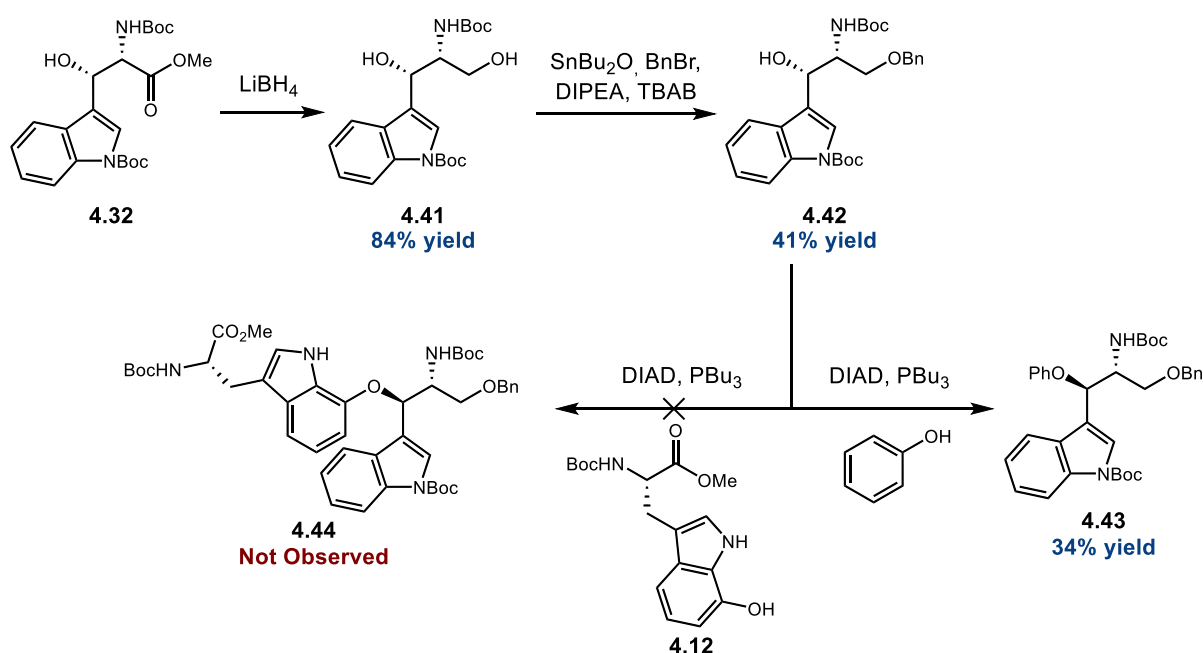
then reduction of dimethyl benzoquinone provides a phenoxide to deprotonate the desired phenol for nucleophilic addition.¹³⁴ While we observed crude alkoxydiphenylphosphine, we were unable to push the substitution reaction forward.



Scheme 4.11 Initial Mitsunobu attempts

In another effort to reduce the driving force for elimination, we reduced the ester and selectively benzyl protected the primary alcohol, so that elimination would not longer yield. Lithium borohydride was essential for the clean conversion to diol **4.41** (lithium aluminum hydride also deprotected the indole nitrogen),^{135,136} and subsequent tin-catalyzed benzylation selectively provided protected diol **4.42**.¹³⁷ With **4.42** in hand we re-approached Mitsunobu coupling with phenol. Fortunately, we saw a moderate amount of coupling product **4.43** in our test system. We also applied the Mitsunobu to 7-OH-L-tryptophan **4.12**, but were unable to see conversion to the alkyl-aryl ether. While we were concerned about steric congestion by protecting the indole nitrogen, that is the logical next move. While we did not see N-alkylation, it is possible that the free nitrogen makes

the phenolic tryptophan much less stable as we observed rapid decomposition at room temperature on the bench top, and **4.12** had to be stored in the freezer to preserve purity.



Scheme 4.12 Alternate pathway to enable Mitsunobu reactivity

4.4 Conclusions

We envisioned a concise synthesis of darobactin A, where a range of amino acid fragments could be joined in peptide coupling to deliver a linear peptide with the requisite coupling partners for macrocyclization. With our synthetic strategy established, we delivered several 7-substituted tryptophans and β -hydroxy tryptophans in hopes of engaging them in C–O crosslink formation. We tested Chan-Lam coupling, Ullman coupling, light-promoted couplings, and Mitsunobu substitutions. Unfortunately, only light-promoted coupling and Mitsunobu reactions delivered any alkyl-aryl ether products in test systems. And while the Mitsunobu was the more optimistic of these reactions it was not successful in a more rigorous test with 7-OH-L-tryptophan. These

findings suggest that C–O crosslinking is a challenging problem, especially for whole amino acid substrates. In the future we think that a potential method could be developed by adapting Mitsunobu reactivity to more stable tryptophan derivatives. As of today, the state of the art in RiPP C–O crosslink formation involves coupling relatively simple substrates and building out the aryl fragment to the aryl-amino acid moiety.

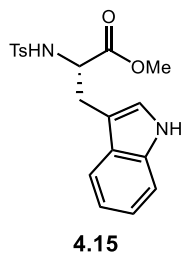
4.5 Experimental Details

General Information: ^1H and ^{13}C nuclear magnetic resonance spectra (NMR) were recorded on a Varian 400 INOVA spectrometer (^1H 400 MHz, ^{13}C 126 MHz), a Varian 400 VNMR spectrometer (^1H 400 MHz, ^{13}C 100 MHz), a Varian INOVA 500 spectrometer (^1H 500 MHz, ^{13}C 126MHz), a Varian INOVA 600 spectrometer (^1H 600Hz, ^{13}C 151MHz), a Bruker 600 spectrophotometer (600 Mhz ^1H , 151 Mhz ^{13}C) at room temperature in CDCl_3 unless otherwise indicated. Chemical shifts were reported in ppm and coupling constants (J) in Hz. Multiplicities were indicated with the following abbreviations: s = singlet, d = doublet, t = triplet, q = quartet, qn = quintet, m = multiplet, br = broad. Analytical thin-layer chromatography was carried out on glass-backed Silicycle TLC plates and visualized with UV light, and ethanolic p-anisaldehyde or KMnO_4 unless otherwise indicated. Flash chromatography was done with Silicycle SiliaFlash[®] F60 silica gel (40- 63 μm) or Alumina as indicated on a Biotage Isolera One system. Silica gel column chromatography was done using Silicycle SiliaFlash[®] F60 silica gel (40- 63 μm). Optical rotations were taken using the Rudolph Research Analytical Autopol IV.

Reactions were conducted under nitrogen atmosphere using Schlenk technique unless otherwise stated. Anhydrous tetrahydrofuran (THF), diethyl ether (Et_2O), dichloromethane (DCM), hexanes, and toluene were obtained by passage over activated alumina using *Glass Contours* solvent system. Anhydrous DMF, DMSO and 1,4-dioxane were obtained from Dry-Seal EMD Millipore, subjected to degassing and stored over 4Å molecular sieves. Solvents for work-up and chromatography were obtained from commercial suppliers without additional purification. Reactive or hydroscopic salts (NHMDS, KHMDS, LDA, KO^tBu , LiOAc LiCl, LiNTf_2 and AgNTf_2) were stored and weighed in a N_2 filled glovebox. All other reagents were purchased from Ambeed, MilliporeSigma, Strem Chemicals, Oakwood Chemicals, Matrix Scientific or TCI.

Procedures

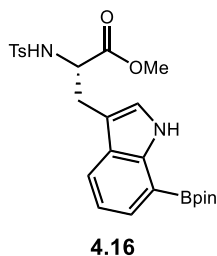
4.15: Methyl tosyl-L-tryptophanoate: Prepared according to Kinderman *et al.*¹³⁸



To a flame-dried round bottom flask *L*-TrpOMe • HCl (1.00 g, 3.9 mmol) was added and the atmosphere exchanged with nitrogen (3 x 5 min). DCM added to the reaction flask followed by triethylamine (1.15 mL, 8.2 mmol) and the reaction lowered to 0 °C ice bath. The septum was briefly opened and TsCl (0.82 g, 4.3 mmol) was added. The reaction was allowed to warm to room temperature over 5 hours. The reaction was diluted with DCM and DI water. Then the aqueous layer was extracted with DCM (3 x 10 mL). The combined organics were washed with sodium bicarbonate and dried with magnesium sulfate. The solvent was removed via rotary evaporation and the crude residue was purified via flash chromatography (40% EtOAc in hexanes). ¹H NMR data matches literature data.¹³⁸

¹H NMR (CDCl₃, 600 MHz) δ 8.03 (br s, 1H), 7.61 (d, *J* = 8.4 Hz, 2H), 7.44 (d, *J* = 8.4 Hz, 1H), 7.33 (d, *J* = 8.4 Hz, 1H), m (7.19 – 7.16, 3H), 7.07 (t, *J* = 7.8 Hz, 1H), 7.04 (br s, 1H), 5.06 (d, *J* = 8.4 Hz), 4.25 (dt, *J* = 9 Hz, 5.4 Hz, 1H), 3.43 (s, 3H), 3.24 (d, *J* = 5.4 Hz, 2H), 2.38 (s, 3H) ppm.

4.16: Methyl N-tosyl-7-Bpin-*L*-tryptophanoate

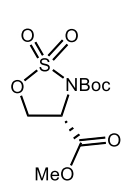


A flask containing [Ir(COD)Cl]₂ (2.5 mol%) was removed from the glove box. It was charged with 4,4'-di-*tert*-butyl-2,2'-bipyridine (5 mol%), bis(pinacolato)diboron (2.0 eq) and *L*-tryptophan derivative (1 eq). The atmosphere was exchanged with nitrogen (3 x 5 minutes). Then THF (0.1 M) was added to the reaction mixture and lowered to a 60 °C heating block. The reaction stirred overnight. The reaction was diluted with EtOAc and washed with DI water

(3 x 10 mL), then the organics were dried with Na₂SO₄ and solvents were removed via rotary evaporation. The organic residue was then dissolved in AcOH and Pd(OAc)₂ was added and the reaction stirred overnight to ensure C-2 deborylation. The reaction mixture was diluted with EtOAc and filtered through celite. The organics were then washed with sodium bicarbonate and dried with sodium sulfate. The solvents were removed via rotary evaporation and the organic residue was purified via flash chromatography (10% EtOAc in hexanes to 30% EtOAc in hexanes) to deliver a white solid.

¹H NMR: (CDCl₃, 600 MHz) δ 9.10 (br s, 1H), 7.61 (dd, *J* = 7.2 Hz, 1H, 1H), 7.58 (d, *J* = 8.4 Hz, 2H), 7.54 (d, *J* = 8.4 Hz, 1H), 7.15 (d, *J* = 7.2 Hz, 1H), 7.08 – 7.06 (m, 2H), 5.09 (d, *J* = 8.4 Hz, 1H), 4.24 (dt, *J* = 9 Hz, 5.4 Hz, 1H), 3.43 (s, 3H), 3.24 (d, *J* = 5.4 Hz, 2H), 2.36 (s, 3H), 1.40 (s, 12H) ppm. **¹³C NMR:** (CDCl₃, 151 MHz) ¹³C NMR (151 MHz, CDCl₃) δ 171.65, 143.41, 141.27, 136.61, 129.48, 129.46, 127.08, 126.10, 123.33, 122.08, 119.18, 108.43, 83.88, 56.10, 52.40, 29.34, 25.02, 21.53 ppm.

4.8: 3-(tert-butyl) 4-methyl (S)-1,2,3-oxathiazolidine-3,4-dicarboxylate 2,2-dioxide.

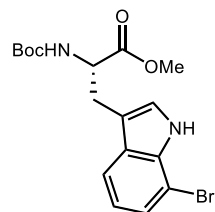


Prepared according to previous procedures.¹³⁹

¹H NMR: (CDCl₃, 600 MHz) δ 4.82 – 4.68 (m, 3H), 3.84 (s, 3H), 1.56 (s, 9H)

4.19: methyl (S)-3-(7-bromo-1H-indol-3-yl)-2-((tert-butoxycarbonyl)amino)propanoate.

Procedure adapted from Loach *et al.*¹²⁰



A flame-dried flask, equipped with a stir bar and 4Å molecular sieves was charged with CuCl (0.74 g, 7.47 mmol) and removed from the glove box.

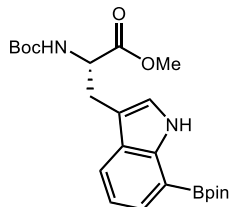
The septum was briefly opened and 7-bromoindole (1.74 g, 8.9 mmol)

was added and the septum closed and the reaction vessel was purged and the

atmosphere exchanged with nitrogen (3 x 5 minutes). Dry DCM (10mL) was added to the reaction vessel and the flask was lowered to a 0 °C ice bath. *i*PrMgCl (3.56 mL, 2.0 M, 7.11 mmol) was added slowly over 10 minutes, then the reaction was stirred at 0 °C for an additional 30 minutes to ensure thorough transmetalation. After 30 minutes the reaction was cooled to -20°C and sulfamidate **4.8** was added in DCM (3 mL) over 1 hour. Then the reaction was allowed to warm to room temperature overnight. After 16 hours, the reaction was diluted with DCM and cooled to 0 °C. The reaction was quenched via dropwise addition of 2 M citric acid (15 mL). After complete addition of citric acid the reaction was stirred at room temperature for 10 minutes, then filtered through a pad of Celite and washed with DCM. The resultant mixture was extracted with DCM (3 x 15 mL) and the organics were dried via magnesium sulfate. The solvent was removed via rotary evaporation and the organic residue was purified via flash chromatography to deliver **4.19** as a light brown solid (0.57 g, 40% yield). The ¹H NMR matched previously reported spectra.

¹H NMR: (CDCl₃, 600 MHz) δ 8.23 (br s, 1H), 7.49 (d, *J* = 7.8 Hz, 1H), 7.34 (d, *J* = 7.2 Hz, 1H), 7.07 (br s, 1H), 7.00 (t, *J* = 7.8 Hz, 1H), 5.06 (d, *J* = 8.4 Hz 1H), 4.66 – 4.63 (m, 1H), 3.31 – 3.32 (m, 2H), 1.43 (s, 9H)

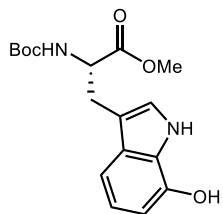
4.5b: methyl (S)-2-((tert-butoxycarbonyl)amino)-3-(7-(4,4,5,5-tetramethyl-1,3,2-dioxaborolan-2-yl)-1H-indol-3-yl)propanoate. Adapted from the borylation procedure from Mentzel *et al.*¹²²



A flame dried flask equipped with a stir bar was charged with 7-BrTrp **4.19** (1.00 g, 2.52 mmol), Pd(OAc)₂ (14 mg, 0.06 mmol), and CyJohnPhos (88 mg, 0.25 mmol) and the atmosphere was exchanged with nitrogen (3 x 5 minutes). Then freshly distilled dioxane (3 mL, 0.8M) was added at room temperature. Triethylamine (0.5 mL, 3.6 mmol) and HBpin (0.97 mL, 6.7 mmol) were added via syringe and the flask was sealed with electric tape and copper wire and lowered to a 80 °C heating block. The bromide was consumed within 1 hour confirmed by TLC and the reaction was removed from heat. Once the reaction reached room temperature, it was quenched with DI water and extracted with DCM (3 x 10 mL). The combined organics were dried with sodium sulfate and filtered. Once the solvents were removed via rotary evaporation, the crude boronate ester was purified via flash chromatography, 0 to 20% EtOAc hexanes to deliver a vivid yellow solid (0.62 g, 55% yield). The ¹H NMR matched previously reported spectra.¹²⁰

¹H NMR: (CDCl₃, 600 MHz) δ 9.13 (s, 1H), 7.67 (d, *J* = 7.8 Hz, 1H), 7.64 (d, *J* = 7.2 Hz, 1H), 7.13 (t, *J* = 7.2 Hz, 1H), 7.05 (s, 1H), 5.05 (d, *J* = 8.4 Hz, 1H), 4.63 (d, *J* = 7.2 Hz, 1H), 3.67 (s, 3H), 3.30 (d, *J* = 5.4 Hz, 2H), 1.42 (s, 9H), 1.39 (s, 12H)

4.12: Methyl (S)-2-((tert-butoxycarbonyl)amino)-3-(7-hydroxy-1H-indol-3-yl)propanoate.
Adapted from Iqbal *et al.*¹²³

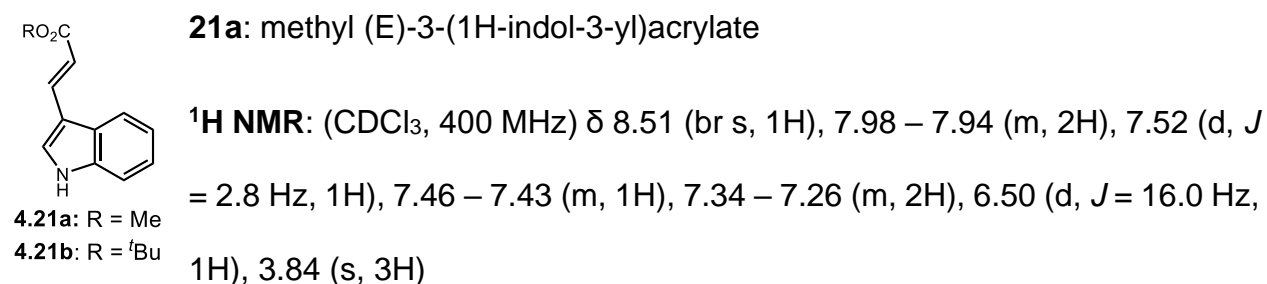


To **4.5b** (0.86 g, 1.9 mmol) in a round bottom flask was added THF (20 mL, 0.1M). Soon after, a solution of 50% H₂O₂ (1.0 mL, ~18 mmol) was added, followed by a solution of 1M NaOH (1.94 mL, 1.9 mmol). The

reaction stirred at room temperature for 15 minutes, after which, TLC indicated the reaction was complete. The reaction was diluted with Et₂O (40 mL), and washed with DI water then brine. The organic phase was dried with sodium sulfate and concentrated. The crude product was purified on flash chromatography, (35% EtOAc in hexanes) to yield a brown solid.

¹H NMR: (CDCl₃, 600 MHz) δ 8.50 (s, 1H), 7.12 – 7.05 (m, 1H), 6.95 – 6.85 (m, 2H), 6.59 (d, *J* = 7.8 Hz, 1H), 6.42 (br s, 1H), 5.22 (d, *J* = 8.4 Hz, 1H), 4.66 – 4.64 (m, 1H), 3.68 (s, 3H), 3.21 – 3.29 (m, 2H), 1.41 (s, 9H) **¹³C NMR** (CDCl₃, 151 MHz) δ 173.04, 155.52, 141.98, 129.68, 126.11, 122.62, 120.08, 111.06, 110.30, 106.71, 80.20, 75.19, 54.29, 52.37, 28.28, 24.80. **HRMS** (-ESI) calculated for C₁₇H₂₂N₂O₅Cl [M+Cl]⁻ 369.1222, found 369.12192.

Indole acrylates **21** were prepared according to the procedure from Grimster *et al.*¹⁴⁰ The ¹NMR spectra for **21a-b** match previously reported values.^{140,141}

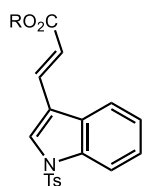


21b: *tert*-butyl (E)-3-(1H-indol-3-yl)acrylate

¹H NMR: (CDCl₃, 600 MHz) δ 8.44 (br s, 1H), 7.95 (d, *J* = 7.8 Hz, 1H), 7.85 (dd, *J* = 15.6 Hz, 0.6 Hz), 7.49 (d, *J* = 2.4 Hz, 1H), 7.43 (d, *J* = 7.2 Hz, 1H), 7.32 – 7.25 (m, 2H), 6.43 (d, *J* = 15.6 Hz, 1H), 1.58 (s, 9H)

The indolyl acrylates were tosyl protected following the procedure from Oikawa *et al.*¹⁴²

¹H NMR match previously reported values.^{143,144}



22a: methyl (E)-3-(N-tosyl-indol-3-yl)acrylate

¹H NMR: (CDCl₃, 400 MHz) δ 8.03 (d, *J* = 8.0 Hz), 7.86 – 7.79 (m, 5H), 7.42 – 4.32 (m, 2H), 7.24 – 7.26 (m, 2H), 6.52 (d, *J* = 16.2 Hz, 1H), 3.82 (s, 3H), 2.35 (s, 3H)

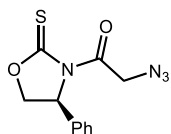
4.22a: R = Me

4.22b: R = ^tBu

22b: *tert*-butyl (E)-3-(N-tosyl-indol-3-yl)acrylate

¹H NMR: (CDCl₃, 400 MHz) δ 7.99 (d, *J* = 8.4 Hz, 1H), 7.81 – 7.77 (m, 4H), 7.68 (d, *J* = 16.2 Hz, 1H), 7.37 (t, *J* = 7.2 Hz, 1H), 7.31 (t, *J* = 7.8 Hz, 1H), 7.26 – 7.22 (m, 2H), 6.44 (d, *J* = 16.2 Hz, 1H), 2.35 (s, 3H), 1.54 (s, 9H)

4.24: (S)-2-azido-1-(4-phenyl-2-thioxooxazolidin-3-yl)ethan-1-one. Acylated chiral



auxiliary was prepared according to Moore *et al.*¹⁴⁵ The ¹H NMR spectra matches previously reported data.

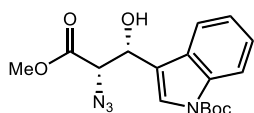
¹H NMR: (CDCl₃, 600 MHz) δ 7.42 – 7.35 (m, 3H), 7.32 – 7.30 (m, 2H), 5.71 (dd, *J* = 8.4 Hz, 3 Hz), 4.93 – 4.82 (m, 3H), 4.55 (dd, *J* = 9.0 Hz, 3 Hz)

Safety Note: Preparation of 2-azidoacetic acid

When following the procedure for synthesizing 2-azidoacetic acid, the reaction mixture was cooled to 0 °C behind a blast shield when adding sodium azide and working up the reaction mixture. When removing excess solvent from the crude product, the rotary evaporator was cooled to 0 °C and the mixture was not evaporated to dryness. The crude

2-azidoacetic acid was obtained in mixtures of 30 – 50% in diethyl ether and used the same day as synthesized. No incidents were experienced following these procedures.

4.25: *tert*-butyl 3-((1*R*,2*S*)-2-azido-1-hydroxy-3-methoxy-3-oxopropyl)-1*H*-indole-1-carboxylate.

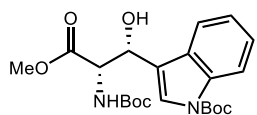


To a flame dried rbf was added **4.24** (100 mg, 0.38 mmol) and the atmosphere was exchanged with nitrogen (3 x 10 minutes), then DCM (3mL, 0.1M) was added and the reaction lowered to -78 °C bath. TiCl₄ (44 μL, 0.40 mmol), that has been distilled and stored in a Schlenk flask over molecular sieves, was added via syringe. Distilled diisopropylethylamine (73μL, 0.42 mmol) was added via syringe, and the reaction mixture turned black. Soon after, distilled N-methylpyrrolidone was added and allowed to stir for 15 minutes. Then N-Boc-indole-3-carbaldehyde (140 mg, 0.57 mmol) in DCM was added dropwise and the reaction was moved to a -20 °C bath. The reaction stirred for 2 hours at this temperature until TLC indicated the acyl azide had been consumed. The reaction was quenched with ammonium chloride, extracted with cold ether (4 x 10 mL). Then the organics were washed successively with 1M HCl, DI water and brine, then dried with magnesium sulfate and concentrated via rotary evaporation. The crude material was then dissolved in MeOH, and imidazole was added. After 1.5 hours TLC indicated the aldol intermediate was consumed and the reaction was quenched with DI water and extracted with EtOAc (3 x 10 mL). The organics were concentrated and then purified via flash chromatography to afford **4.25** as a yellow oil (252 mg, 37% yield).

¹H NMR: (CDCl₃, 600 MHz) δ 8.17 (d, *J* = 7.8 Hz, 1H), 7.70 (s, 1H), 7.60 (dt, *J* = 7.8 Hz, 1.2 Hz, 1H), 7.36 – 7.34 (m, 1H), 7.28 – 7.25 (m, 1H), 5.51 (ddd, *J* = 5.7 Hz, 4.2 Hz, 0.6 Hz, 1H), 4.30 (d, *J* = 3.6 Hz, 1H), 3.82 (s, 3H), 2.56 (d, *J* = 5.4 Hz, 1H), 1.68 (s, 9H) **¹³C NMR:** (CDCl₃, 151 MHz) δ 169.03, 149.48, 135.61, 127.94, 124.92, 123.95, 122.90, 119.04, 119.00, 115.59, 84.19, 68.69, 66.16, 53.04, 28.20. **HRMS:** (-ESI) calculated for [C₁₈H₁₆ON₈³⁵Cl]⁻ 395.11411, found 395.11232.

Safety Note: Working up the TiCl₄ Mediated Aldol: While this procedure was followed numerous times, one incident resulted in the injury of a graduate student when material that was not the aldol product was removed from the rotary evaporator and exploded in the researcher's hands. We hypothesize that this was hydrolyzed chiral auxiliary and 2-azidoacetic acid which is a suspected energetic. We halted further operation of this procedure to avoid any future incidences.

4.26: *tert*-butyl 3-((1*R*,2*S*)-2-((*tert*-butoxycarbonyl)amino)-1-hydroxy-3-methoxy-3-oxopropyl)-1*H*-indole-1-carboxylate. Procedure adapted from Shao and Goodman.¹⁴⁶



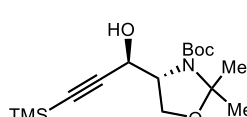
To a oven-dried vial **4.25** (85 mg, 0.24 mmol) and Pd/C (50 mg, 10% w/w, 0.02 mmol) were quickly added and the septa resealed. The vial

was evacuated, then dry MeOH was added, and the atmosphere was exchanged with hydrogen. The reaction stirred at room temperature until TLC indicated the reaction was complete after 5 hours, and the reaction was filtered through celite. The organics were concentrated via rotary evaporation and the resultant residue was dissolved in nBuOH

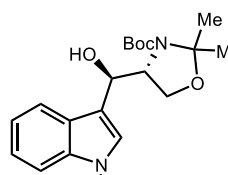
and Boc₂O (62 mg, 0.28 mmol) was added and the reaction stirred overnight. The Boc-protected tryptophan was obtained as a yellow oil (46 mg, 75% yield).

¹H NMR: (CDCl₃, 600 MHz) δ 8.14 (br s, 1H), 7.68 – 7.55 (m, 2H), 7.33 (t, *J* = 7.8 Hz, 1H), 7.26 – 7.24 (m, 1H), 5.52 (s, 1H), 5.42 (d, *J* = 9.0 Hz, 1H), 4.68 (d, *J* = 9.0 Hz, 1H), 3.78 (s, 3H), 2.67 (br s, 1H), 1.66 (s, 9H), 1.36 (s, 9H).

4.27: *tert*-butyl (*R*)-4-((*R*)-1-hydroxy-3-(trimethylsilyl)prop-2-yn-1-yl)-2,2-dimethyloxazolidine-3-carboxylate. Prepared according to Zhang *et al.*¹²⁷ The spectra matched the literature data.

 **¹H NMR:** (DMSO-*d*₆, 600 MHz) δ 5.77 (2d, *J* = 6.0 Hz, 1H), 4.68 (2t, *J* = 4.8 Hz, 1H), 4.10 – 3.94 (m, 2H), 3.86 – 3.77 (m, 1H), 1.53 (s, 3H), 1.45 – 1.35 (m, 12H), 0.12 (s, 9H)

4.27 was converted to the free alkyne as reported and optical rotation was compared to literature value.¹²⁷ [α]_D²² = 38.2°, Lit: [α]_D²⁵ 45.7°

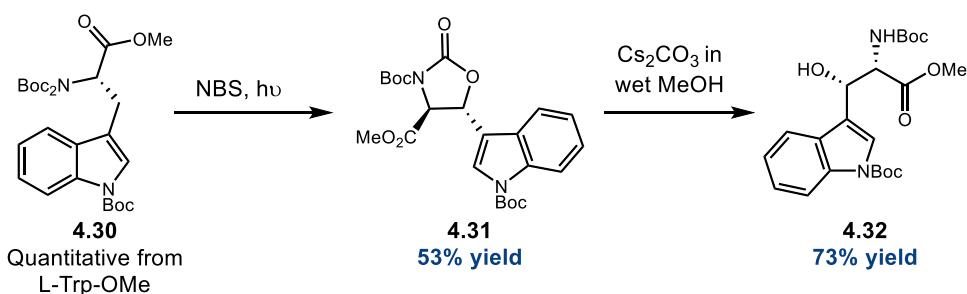
 **4.29:** *tert*-butyl (*R*)-4-((*R*)-(1-acetyl-1H-indol-3-yl)(hydroxy)methyl)-2,2-dimethyloxazolidine-3-carboxylate.

To a flame-dried round bottom equipped with stir bar was added tetrabutylammonium chloride (0.85 g, 3.0 mmol), Pd(OAc)₂(PPh₃)₂ (0.114 mg, 0.15 mmol), N-(2-iodophenyl)acetamide (0.40 g, 1.5 mmol), and KOAc (0.75 g, 7.6 mmol) and the flask was sealed and the atmosphere exchanged with nitrogen (3 x 5 minutes). The reaction was diluted with DMF (10 mL), and then alkyne **4.27** in DMF (5 mL) was added and then the reaction was lowered to a heating block. After 5 hours TLC indicated that the alkyne was consumed and the reaction was diluted with EtOAc (80 mL) and washed

with DI water (3 x 50 mL), then washed with brine (30 mL) and then the organic phase was dried with sodium sulfate. The Larock product was then desilylated to improve chromatography. Crude indole was dissolved in MeOH and 1 eq of K₂CO₃, after two hours no silylated indole remained. Flash chromatography provided **4.29** as a brown foam (0.34 g, 58% yield).

¹H NMR: (CDCl₃, 600 MHz) δ 8.66 (rot.), 8.43 (d, *J* = 12.6 Hz, 2H), 7.42 (dd, *J* = 11.4 Hz, 2.4 Hz, 1H), 7.36 (td, *J* = 12 Hz, 2.4 Hz, 1H), 7.04 (td, *J* = 11.4 Hz, 1.8 Hz, 1H), 53.01 – 4.97 (m, 1H), 4.46 – 4.10 (m, 3H), 3.49 (s, 1H), 2.37 (rot.), 2.26 (s, 3H), 1.68 – 1.49 (m 15 H). **¹³C NMR:** (CDCl₃, 151 MHz) δ 169.04, 153.86, 139.86, 132.33, 130.04, 123.21, 119.93, 110.94, 94.74, 81.63, 64.53, 64.32, 61.76, 28.50, 28.37, 27.18, 24.61, 24.18. (Several rotameric peaks due to N-Boc obfuscate the ¹³C NMR) **HRMS** (+ESI) calculated [M+1]⁺ for C₂₁H₃₀N₂O₅ 389.2071, found 389.2066.

4.30-2 were prepared according to the protocol developed by Crich and Banerjee.¹²⁹ The spectra and optical rotations match the reported values.



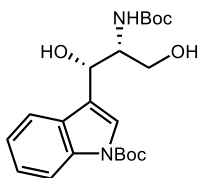
4.30: *tert*-butyl (S)-3-(2-(bis(*tert*-butoxycarbonyl)amino)-3-methoxy-3-oxopropyl)-1H-indole-1-carboxylate. **¹H NMR:** (CDCl₃, 600 MHz) δ 8.11 (br s, 1H), 7.52 (d, *J* = 7.8 Hz, 1H), 7.39 (s, 1H), 7.29 (t, *J* = 7.2 Hz, 1H), 7.22 (t, *J* = 7.2 Hz, 1H), 5.21 (dd, *J* = 10.2 Hz,

4.8 Hz, 1H), 3.77 (s, 3H), 3.52 (dd, $J = 15$ Hz, 4.8 Hz, 1H), 3.36 (dd, $J = 15$ Hz, 10.2 Hz, 1H), 1.64 (s, 9H), 1.32 (s, 18H).

4.31: 3-(*tert*-butyl) 4-methyl (4*S*,5*R*)-5-(1-(*tert*-butoxycarbonyl)-1H-indol-3-yl)-2-oxooxazolidine-3,4-dicarboxylate. **$^1\text{H NMR}$** : (CDCl_3 , 600 MHz) δ 8.21 (d, $J = 8.4$ Hz, 1H), 7.68 (s, 1H), 7.59 (d, $J = 7.8$ Hz, 1H), 7.40 (t, $J = 7.8$ Hz, 1H), 7.31 (t, $J = 7.2$ Hz, 1H), 5.67 (dd, $J = 4.2$ Hz, 1.2 Hz, 1H), 4.84 (d, $J = 3.6$ Hz, 1H), 3.92 (s, 3H), 1.67 (s, 9H), 1.50 (s, 9H). $[\alpha]_{\text{D}}^{22} = 20.26^\circ$, Lit: $[\alpha]_{\text{D}}^{25} = 24.9^\circ$

4.32: *tert*-butyl 3-((1*S*,2*S*)-2-((*tert*-butoxycarbonyl)amino)-1-hydroxy-3-methoxy-3-oxopropyl)-1H-indole-1-carboxylate. **$^1\text{H NMR}$** : (CDCl_3 , 600 MHz) δ 8.14 (s, 1H), 7.68 – 7.61 (m, 2H), 7.32 (t, $J = 7.2$ Hz, 1H), 7.26 – 7.24 (m, 1H), 5.51 (t, $J = 3.6$ Hz, 1H), 5.42 (d, $J = 9.0$ Hz, 1H), 4.68 (d, $J = 9.6$ Hz, 1H), 3.79 (s, 3H), 2.70 (s, 1H), 1.66 (s, 9H), 1.36 (s, 9H). $[\alpha]_{\text{D}}^{22} = -7.01^\circ$, Lit: $[\alpha]_{\text{D}}^{25} = -12.5^\circ$

4.41: *tert*-butyl 3-((1*S*,2*R*)-2-((*tert*-butoxycarbonyl)amino)-1,3-dihydroxypropyl)-1H-indole-1-carboxylate

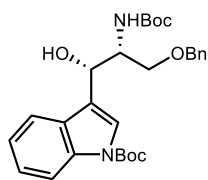


To a flame dried flask equipped with a stir bar, **4.32** (1.65 g, 3.80 mmol) was added and the atmosphere was exchanged with nitrogen (3 x 3 minutes). A solution of LiCl (0.5 M, 15.2 mL, 7.60 mmol) was added via syringe, then the septa was briefly opened and NaBH_4 was added followed by absolute EtOH. The reaction stirred for 12 hours and all the ester was consumed. The reaction was quenched with ammonium chloride and DI water, then extracted with EtOAc (3 x 30 mL) and the combined organic phases were dried with sodium sulfate. The diol was purified via flash chromatography to deliver a white solid (1.30 g, 84% yield).

¹H NMR: (CDCl₃, 600 MHz) δ 8.17 (br s, 1H), 7.64 (m, 2H), 7.34 (t, *J* = 7.2 Hz, 1H), 7.25 (t, *J* = 7.8 Hz, 1H), 5.35 – 5.26 (m, 2H), 4.04 (br s, 1H), 3.92 – 3.86 (m, 2H), 3.27 (br s, 1H), 2.49 (br s, 1H), 1.68 (s, 9H), 1.41 (s, 9H). **¹³C NMR:** (CDCl₃, 151 MHz) δ 156.67, 149.60, 135.75, 128.48, 124.65, 123.38, 122.74, 120.87, 119.48, 115.42, 83.81, 79.95, 68.94, 64.14, 55.82, 28.19. **HRMS:** (-ESI) calculated mass for C₂₁H₃₀O₆N₂³⁵Cl [M+Cl]⁻ 441.1798, found 441.17928.

4.42: *tert*-butyl 3-((1*S*,2*R*)-3-(benzyloxy)-2-((*tert*-butoxycarbonyl)amino)-1-hydroxypropyl)-1*H*-indole-1-carboxylate

An oven-dried vial was charged with tetrabutylammonium bromide (0.26 g, 0.81 mmol), dibutyltin oxide (0.10 g, 0.41 mmol) and **4.41** (1.10 g, 2.71 mmol). The atmosphere was exchanged with nitrogen (3 x 5 minutes), then DIPEA (1.89 mL, 10.8 mmol) and benzyl bromide (1.29 mL, 10.8 mmol) were added via syringe. The reaction vial was sealed with Teflon tape and electrical tape, lowered to a heating block at 80 °C, and stirred overnight. After 16 hours, the reaction was cooled to room temperature and diluted with DCM (20 mL). The organic phase was washed with DI water (30 mL) then washed ammonium chloride (30 mL). The aqueous layers were collected in a separate waste stream and the organics were concentrated via rotary evaporation with adequate ventilation. The residue was purified via column chromatography to yield the benzyl ether in 41% yield (0.55 g, 1.10 mmol).



¹H NMR: (CDCl₃, 600 MHz) δ 8.18 (br s, 1H), 7.66 (d, *J* = 7.8 Hz, 1H), 7.62 (s, 1H), 7.40 – 7.32 (m, 6H), 7.24 (td, *J* = 7.8 Hz, 1.2 Hz, 1H), 7.38 (d, *J* = 8.4 Hz, 1H), 5.28 (s, 1H), 4.56 – 4.51 (m, 2H), 4.17 (br s, 1H), 3.74 – 3.65 (m, 2H), 3.56 (br s, 1H), 1.68 (s, 9H), 1.43 (s, 9H) **¹³C NMR:** (CDCl₃, 151 MHz) δ 156.53, 149.62, 137.52, 135.74, 128.57, 127.75, 124.495, 123.40, 122.65, 120.90, 119.61, 115.32, 83.61, 79.80, 73.65, 71.37, 69.18, 54.50, 28.32, 28.20. **HRMS:** (-ESI) calculated mass for C₂₈H₃₆O₆N₂³⁵Cl [M+Cl]⁻ 531.2267, found 531.2270.

General Procedure for Chan-Lam Couplings

A vial was charged with alcohol **4.26** (30 mg, 0.07 mmol), phenyl boronic acid (8.4 mg, 0.07 mmol), Cu(OAc)₂ • H₂O (1.4 mg, 0.007 mmol), and DMAP (1.7 mg, 0.014 mmol) and the atmosphere was exchanged with oxygen (3 x 5 minutes). The reaction was diluted with DCM and stirred at room temperature overnight. The reaction was concentrated under rotary evaporation and the residue was purified via column chromatography.

General Procedure for Oxalic Diamide Couplings

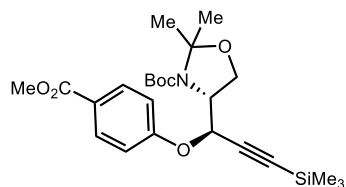
An oven dried vial was equipped with a stir bar and mol. sieves and moved into the glove box. CuI and potassium *tert*-butoxide were added to the vial and removed from the box. The septum was briefly opened and DPEO and aryl bromide were added and the vial resealed and atmosphere exchanged with nitrogen (3 x 5 minutes). Then alcohol (**2.27** or **2.29**) in dioxane was added and the reaction stirred on a 80 °C heating block overnight. Then the reaction was cooled to room temperature, diluted with DI water and extracted with Et₂O x 3. The combined organics were washed with brine x 4, then dried with sodium sulfate. The organics were concentrated and purified via column chromatography.

Procedure for Blue light Promoted Coupling

A vial containing **4.38** was removed from the glove and aryl bromide (if solid), alcohol **4.27** were added to the reaction vial. Then the atmosphere of the vessel was exchanged with nitrogen (3 x 10 minutes). Toluene was added to the reaction vial under nitrogen, followed by DBU and the vial was sealed and placed under 390-95nm light at room temperature overnight.

4.39: *tert*-butyl (*R*)-4-((*R*)-1-(4-(methoxycarbonyl)phenoxy)-3-(trimethylsilyl)prop-2-yn-1-yl)-2,2-dimethyloxazolidine-3-carboxylate

The general procedure for blue light coupling was applied to **4.27** (49 mg, 0.15 mmol), methyl 4-bromobenzoate (32 mg, 0.15 mmol), **4.38** (7.5 mg, 0.015 mmol), and DBU (34 μ L, 0.23 mmol). Alkyl-aryl ether was delivered as a white solid (14% yield).



¹H NMR: (CDCl₃, 600 MHz) δ 8.04 (m, 2H), 7.09 – 7.03 (m, 2H), 5.49 (d, *J* = 6.6 Hz), 5.28 (br s, 1H), 4.36 – 4.10 (m, 3H), 3.89 (s, 3H), 1.66 – 1.48 (m, 19H), 0.14 (s, 9H) **¹³C NMR:** (CDCl₃, 151 MHz) δ 161.034, 131.39, 115.34, 67.94, 64.55, 59.28, 51.85, 29.71, 28.43, 26.66, 25.03, -0.39. **HRMS:** (+ESI) calculated mass for C₂₄H₃₆NO₆Si [M+H]⁺ 462.2306, found 462.2301.

General Procedure for Mitsunobu Coupling

An oven dried vial was charged with a stir bar, desired phenol, alkyl alcohol, (if phosphine was a solid, it was added before atmosphere exchange, (if the phosphine was a liquid it was added after THF addition) and the atmosphere was exchanged with nitrogen (3 x 5

minutes). Then THF is added followed by the desired coupling reagent, in this case we primarily used DIAD. The reaction stirred at room temperature overnight and the crude mixture was concentrated via rotary evaporation and purified via flash chromatography.

4.39: *tert*-butyl (Z)-3-(2-((*tert*-butoxycarbonyl)amino)-3-methoxy-3-oxoprop-1-en-1-yl)-1H-indole-1-carboxylate

The general procedure for Mitsunobu coupling was applied to **4.32** (50 mg, 0.12 mmol), phenol (13 mg, 0.14 mmol), Triphenylphosphine (60 mg, 0.23 mmol), and DIAD (27 μ L, 0.14 mmol). The α,β -unsaturated ester was obtained in 63% yield.

$^1\text{H NMR}$: (CDCl_3 , 400 MHz) δ 8.15 (d, $J = 8.4$ Hz, 1H), 7.94 (s, 1H), 7.71 (d, $J = 7.6$ Hz, 1H), 7.59 (s, 1H), 7.35 (td, $J = 7.8$ Hz, 1.2 Hz, 1H), 7.29 (td, $J = 7.6$ Hz, 1.2 Hz, 1H), 6.20 (br s, 1H), 3.87 (s, 3H), 1.68 (s, 9H), 1.45 (s, 9H) **$^{13}\text{C NMR}$:** (CDCl_3 , 151 MHz) δ 165.904, 149.289, 134.908, 129.565, 127.385, 125.038, 123.211, 122.369, 119.083, 115.336, 114.402, 84.478, 80.951, 52.566, 28.230, 28.156. **HRMS:** (-APCI) calculated for $\text{C}_{22}\text{H}_{27}\text{N}_2\text{O}_6$ $[\text{M}-\text{H}]^-$ 415.1874, found 415.1861.

4.43: *tert*-butyl 3-((1*S*,2*R*)-3-(benzyloxy)-2-((*tert*-butoxycarbonyl)amino)-1-hydroxypropyl)-1H-indole-1-carboxylate

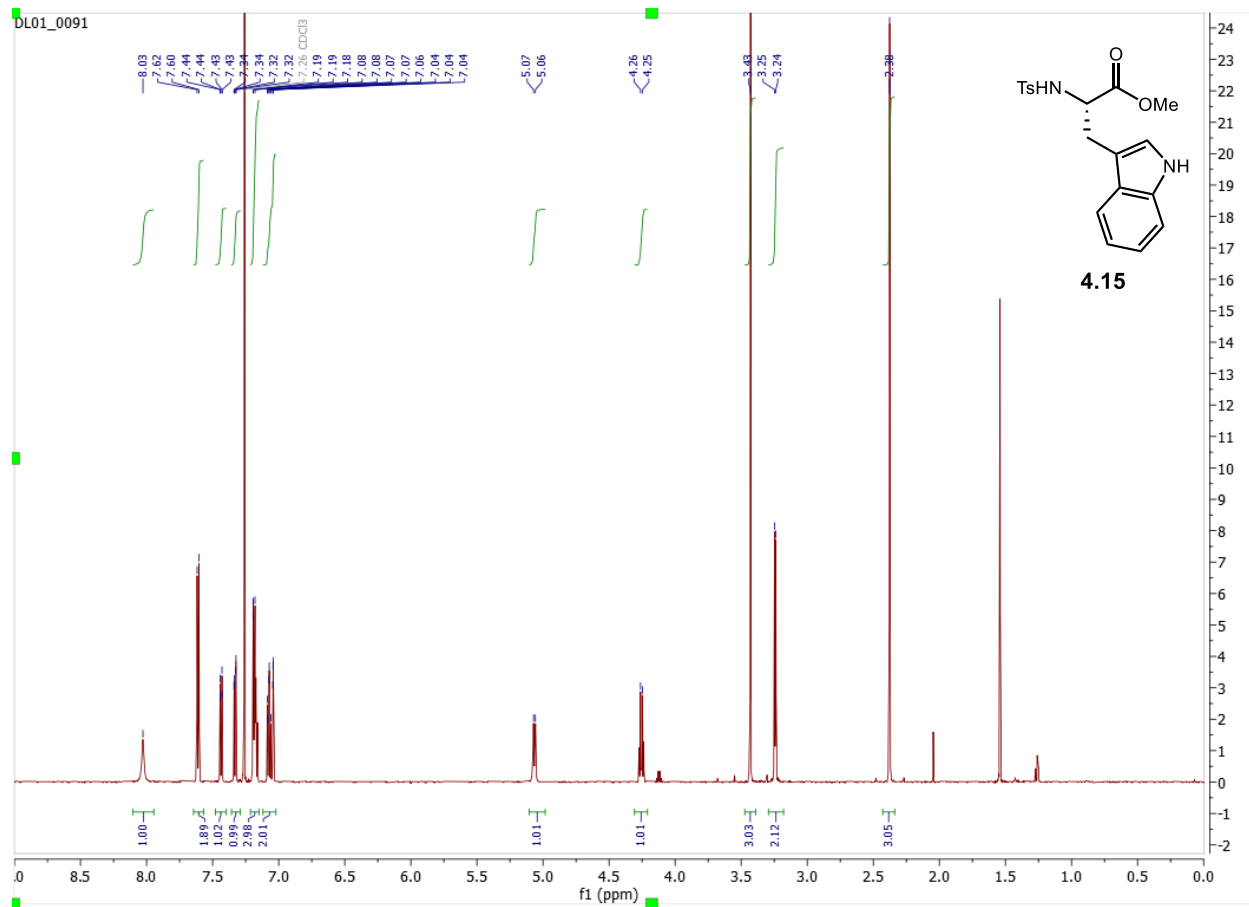
The general procedure for Mitsunobu coupling was applied to **4.42** (100 mg, 0.20 mmol), phenol (21 mg, 0.22 mmol), tributylphosphine (0.15 mL, 0.60 mmol), and DIAD (78 μ L, 0.40 mmol). The desired alkyl aryl ether was obtained in 36% yield.

$^1\text{H NMR}$: (CDCl_3 , 600 MHz) δ 8.12 (s, 1H), 7.83 (d, $J = 7.8$ Hz, 1H), 7.73 (rot.), 7.55 (s, 1H), 7.60 (rot.), 7.34 – 7.19 (m, 9H), 6.93 – 6.90 (m, 3H), 5.73 (2d, $J = 6$ Hz, 1H), 5.05 (d, $J = 9.6$ Hz, 1H), 4.56 – 4.38 (m, 3H), 3.97 – 3.94 (m, 1H), 3.66 – 3.63 (m, 1H), 1.66 (s,

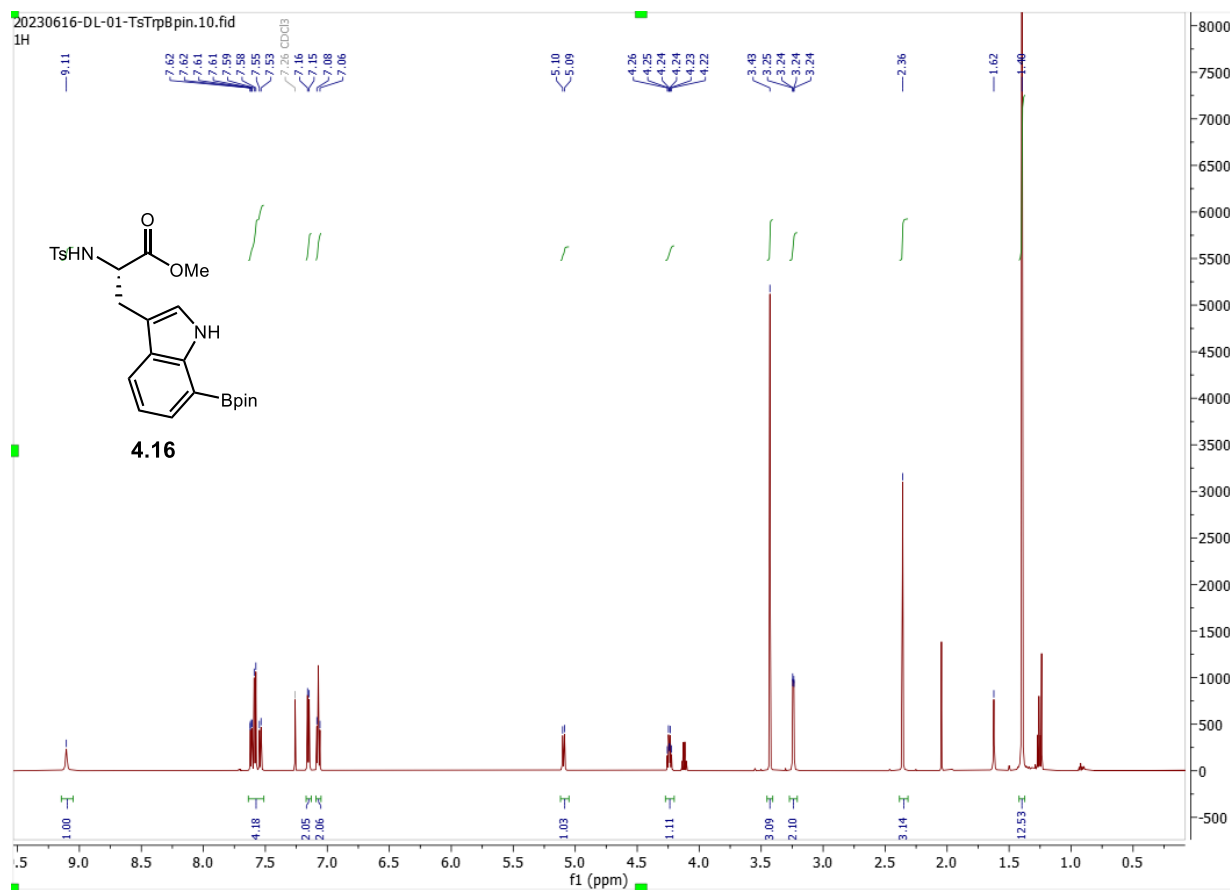
9H) 1.32 (s, 9H). **¹³C NMR:** (CDCl₃, 151 MHz) δ 158.104, 155.283, 149.539, 137.943, 135.597, 129.371, 128.414, 128.360, 127.671, 127.651, 124.553, 122.858, 121.187, 120.182, 117.934, 115.809, 115.721, 115.234, 83.841, 79.297, 74.242, 73.274, 73.098, 69.168, 68.544, 54.182, 28.309, 28.183 **HRMS:** (-ESI) calculated for C₃₄H₄₀O₆N₂³⁵Cl [M+Cl]⁻ 607.2580, found 607.2580.

4.6 Spectral Data

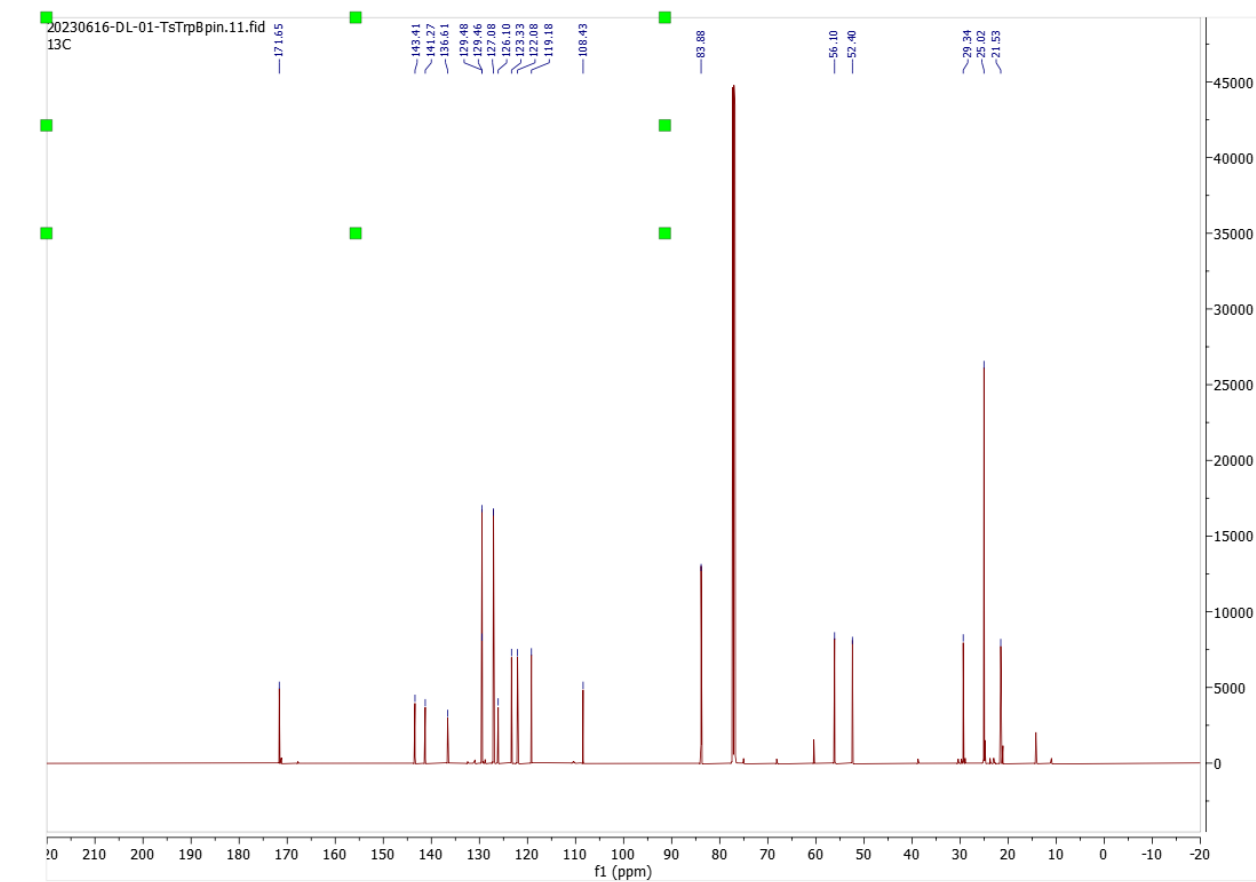
4.15- ¹H NMR 600 MHz, CDCl₃



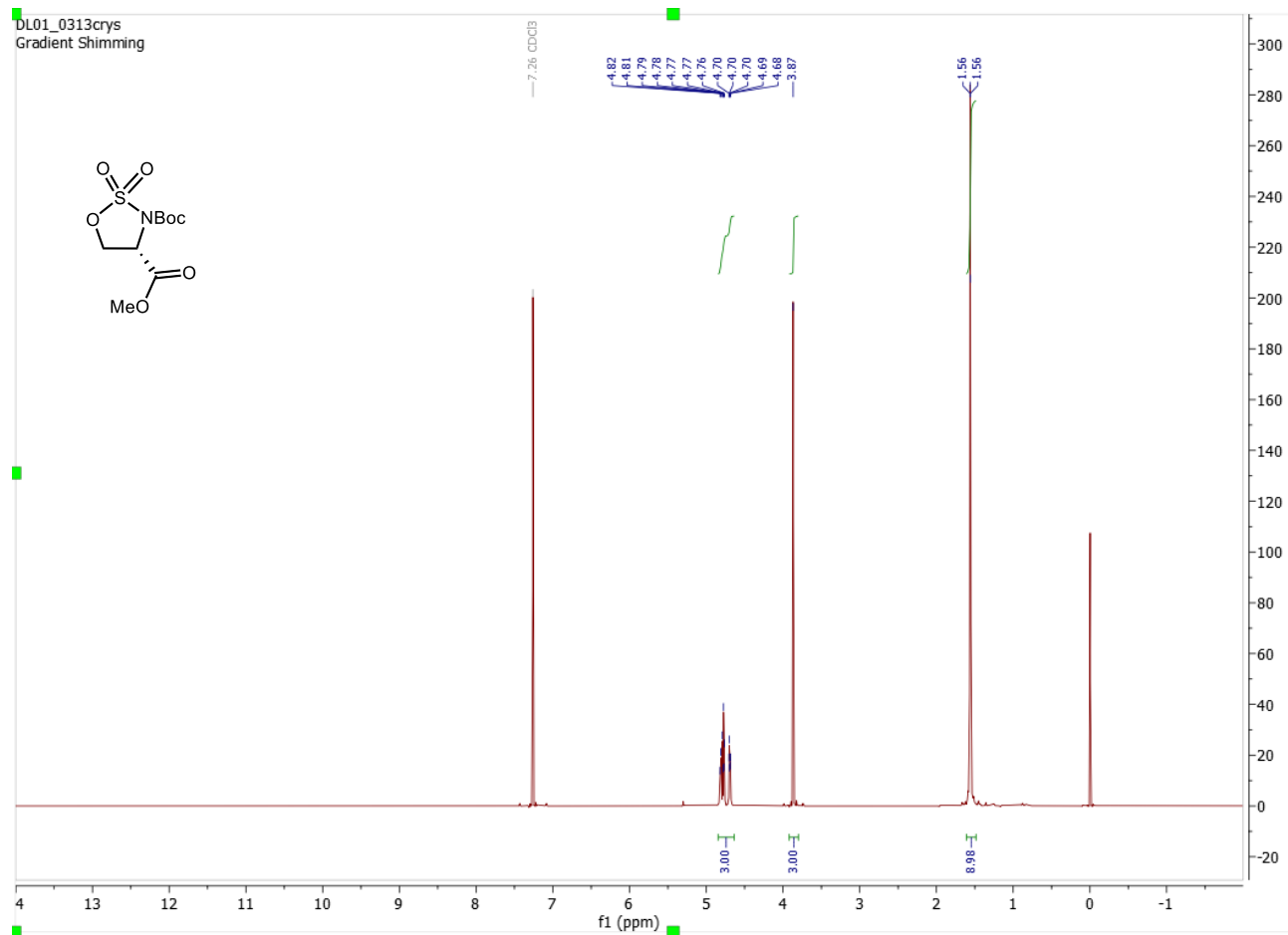
4.16 ¹H NMR (600 MHz, CDCl₃)



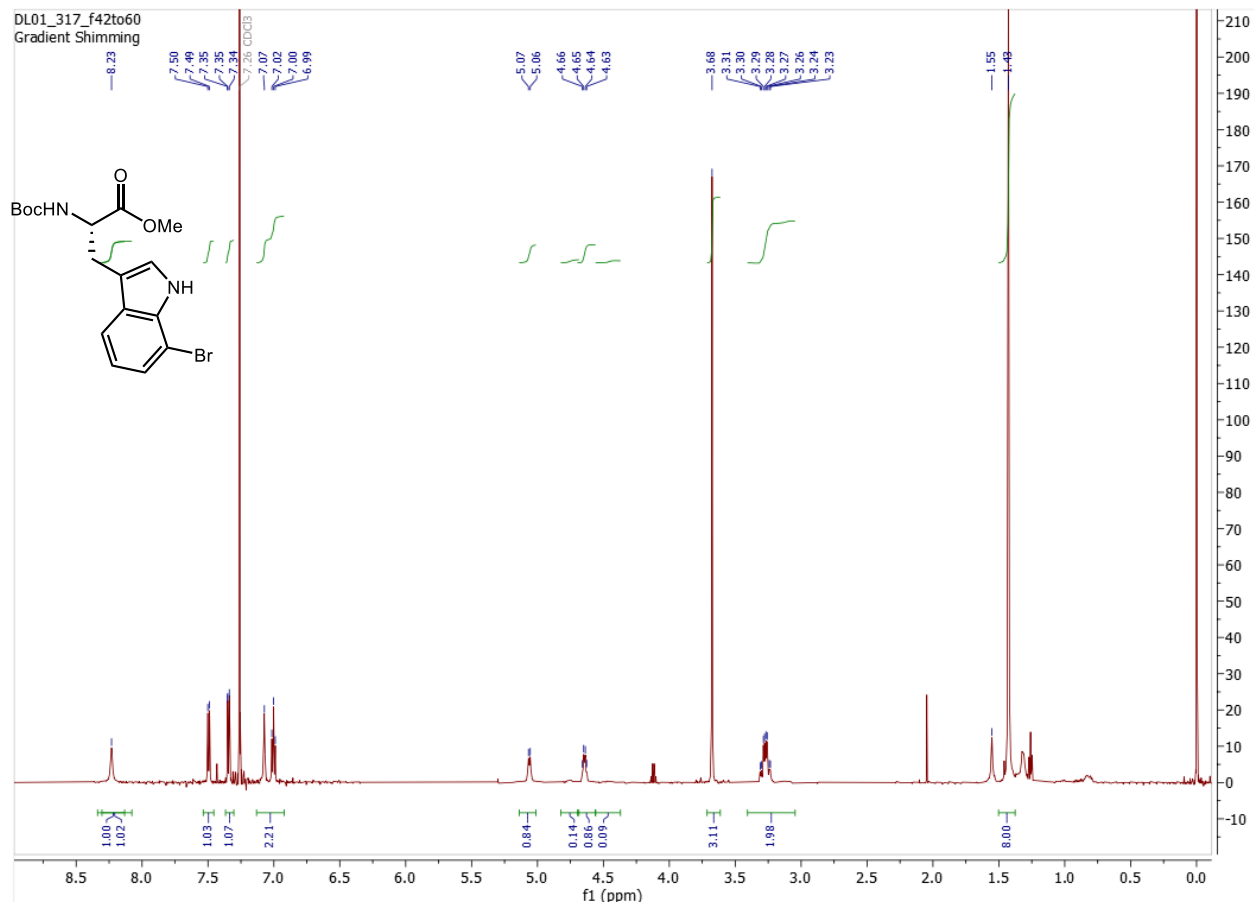
¹³C NMR (151 MHz, CDCl₃)



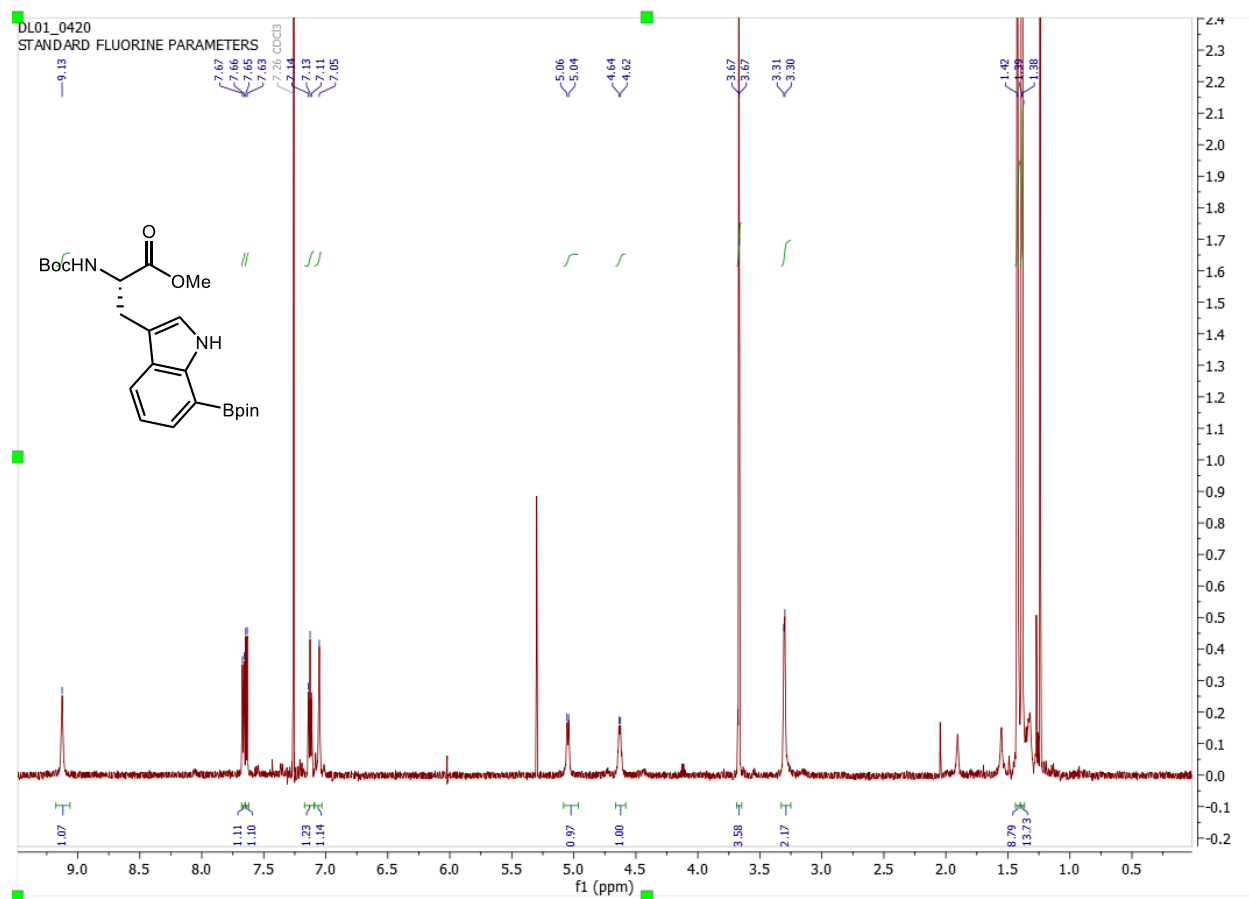
4.8 ^1H NMR (600 MHz, CDCl_3)



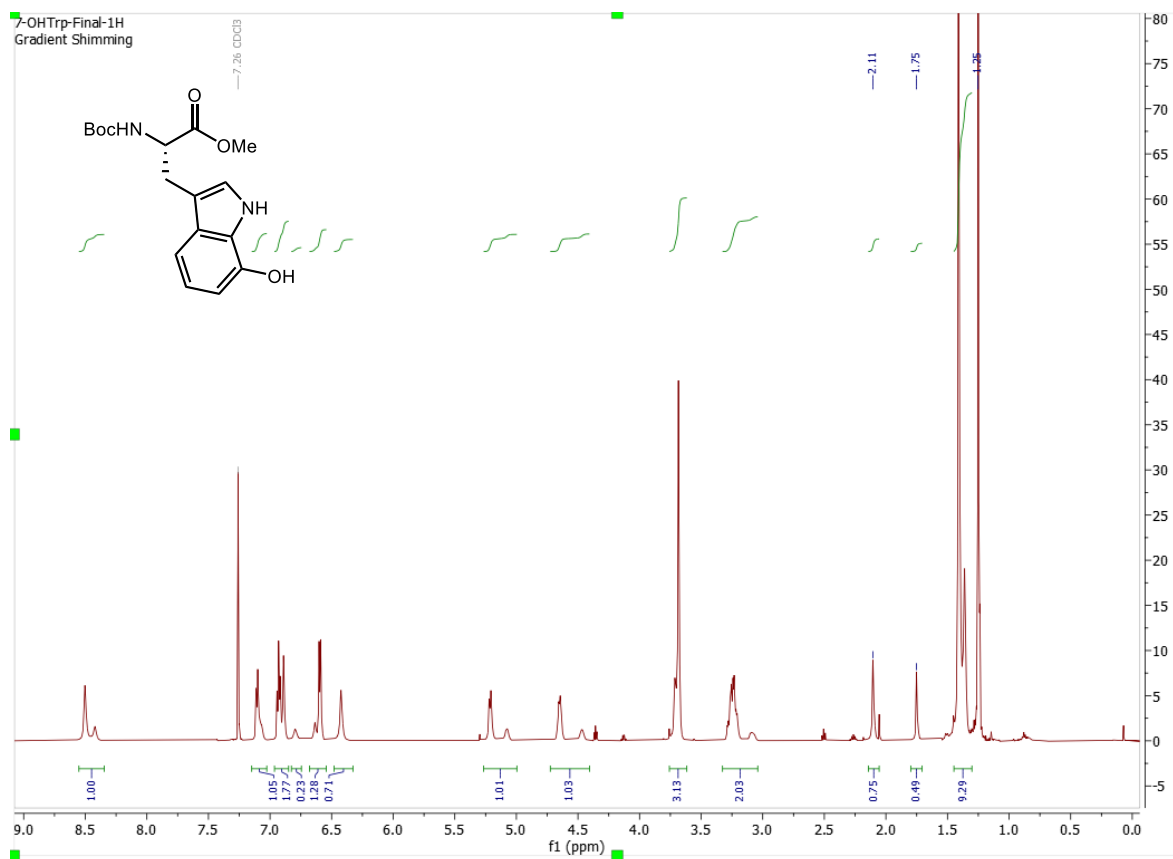
4.19 ¹H NMR (600 MHz, CDCl₃)



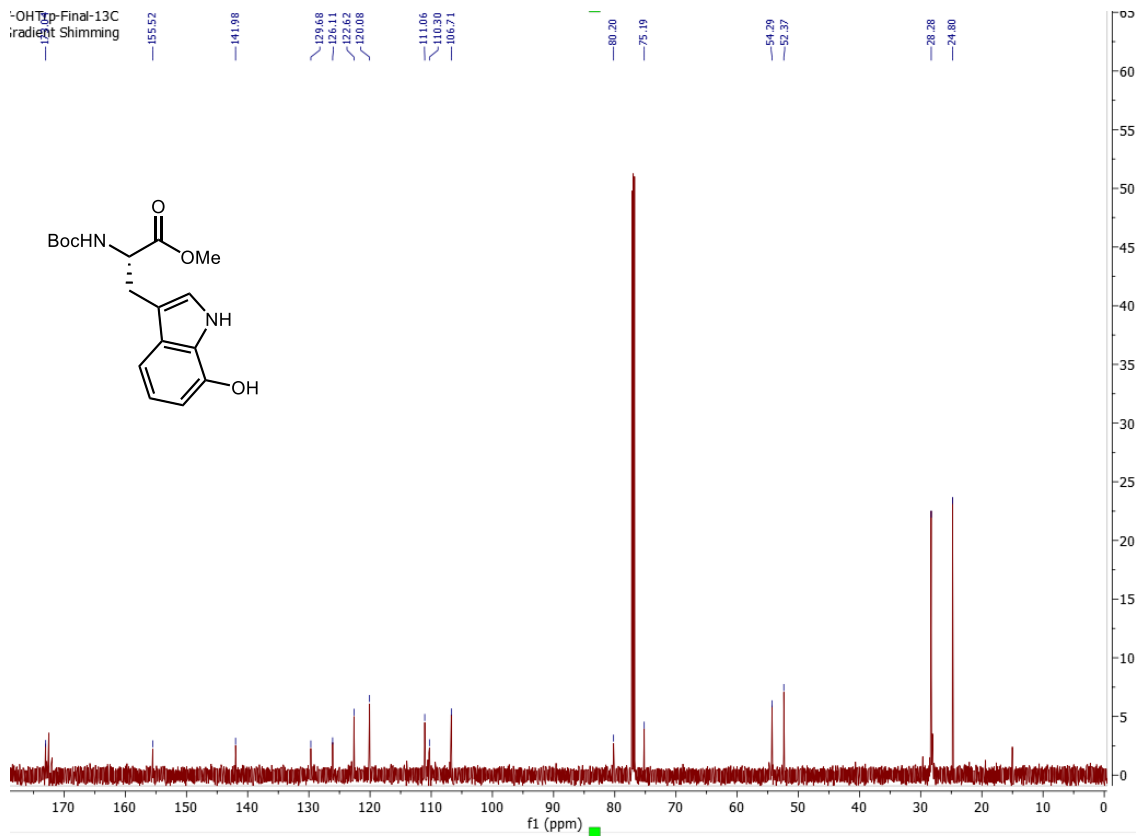
4.5b: ^1H NMR (600 MHz, CDCl_3)



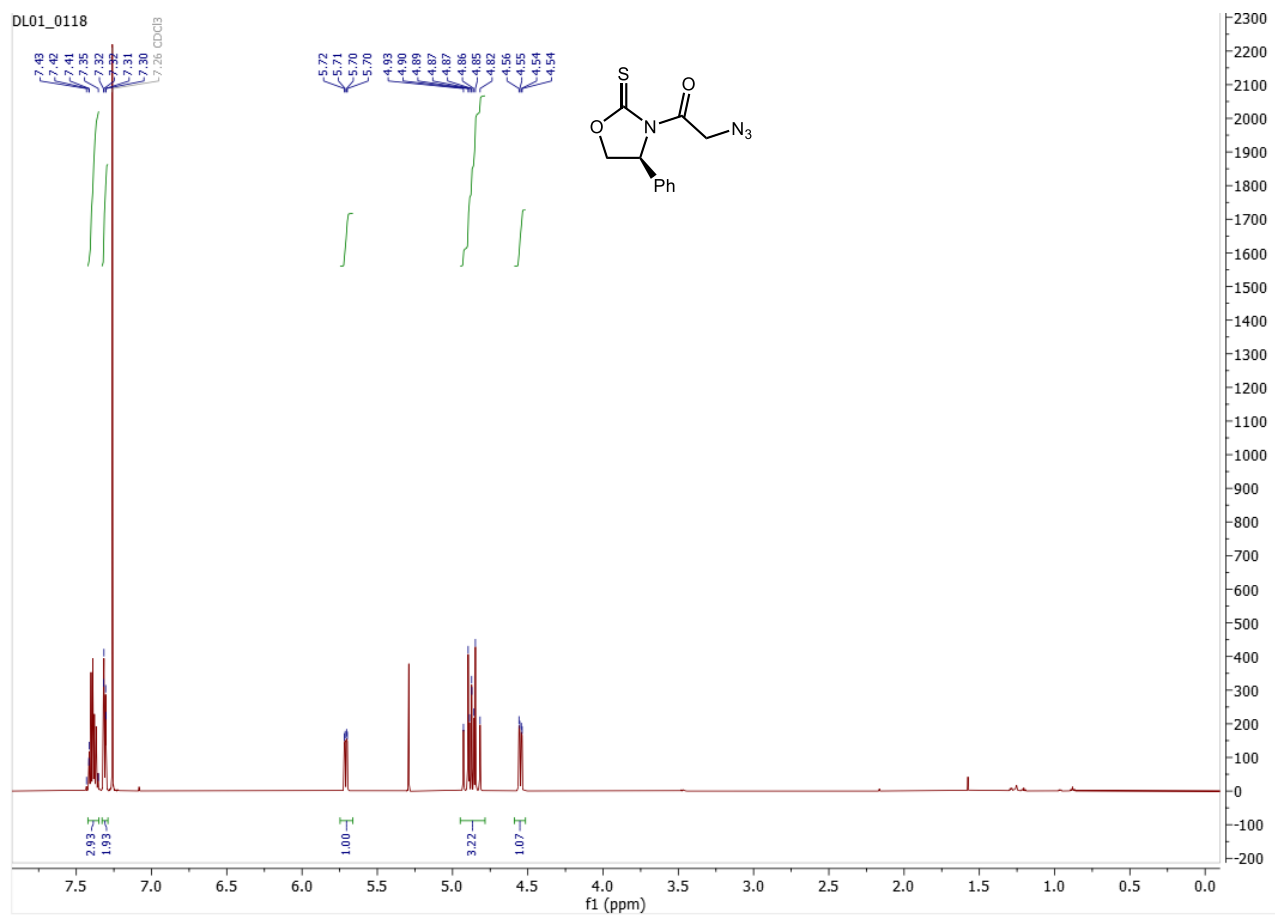
4.12: ^1H NMR (600MHz, CDCl_3)



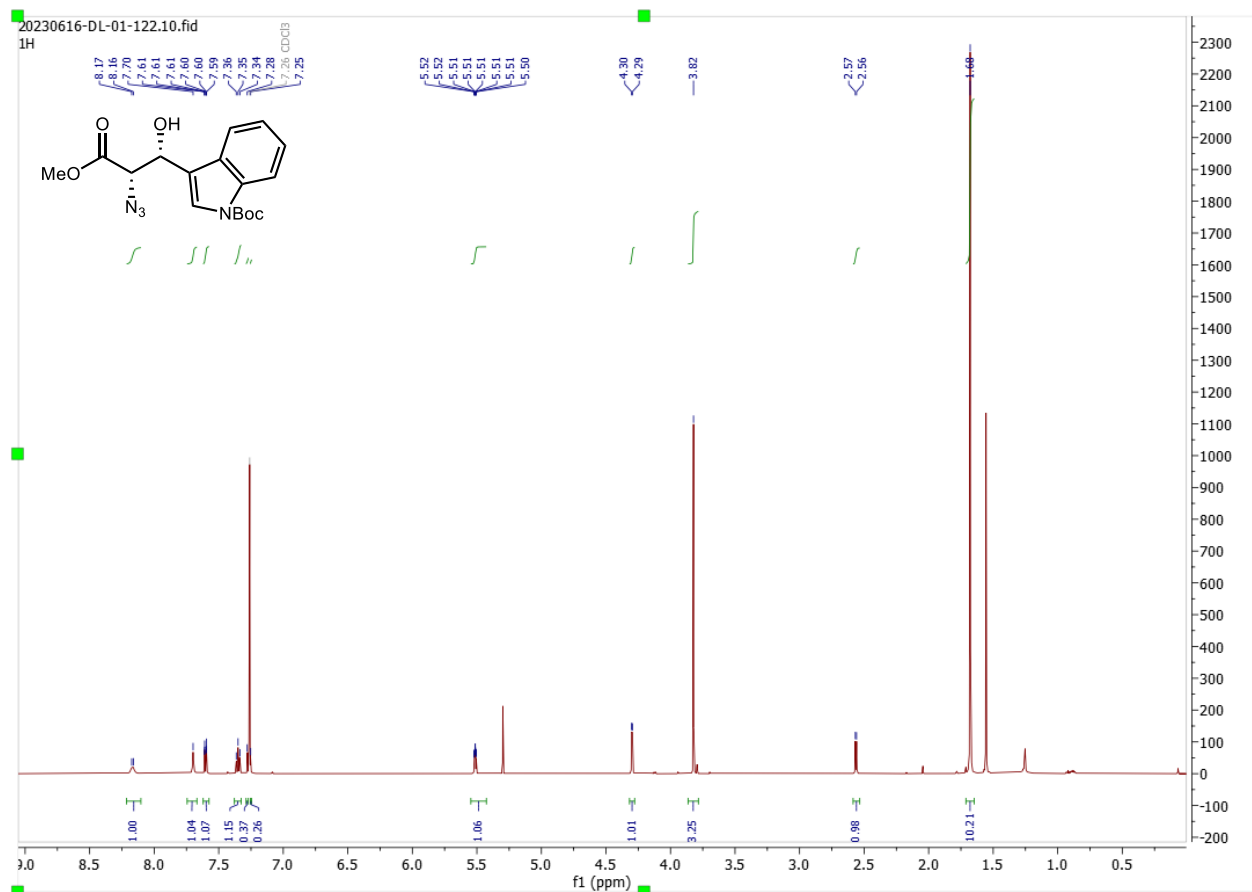
4.12: ^{13}C NMR (151MHz, CDCl_3)



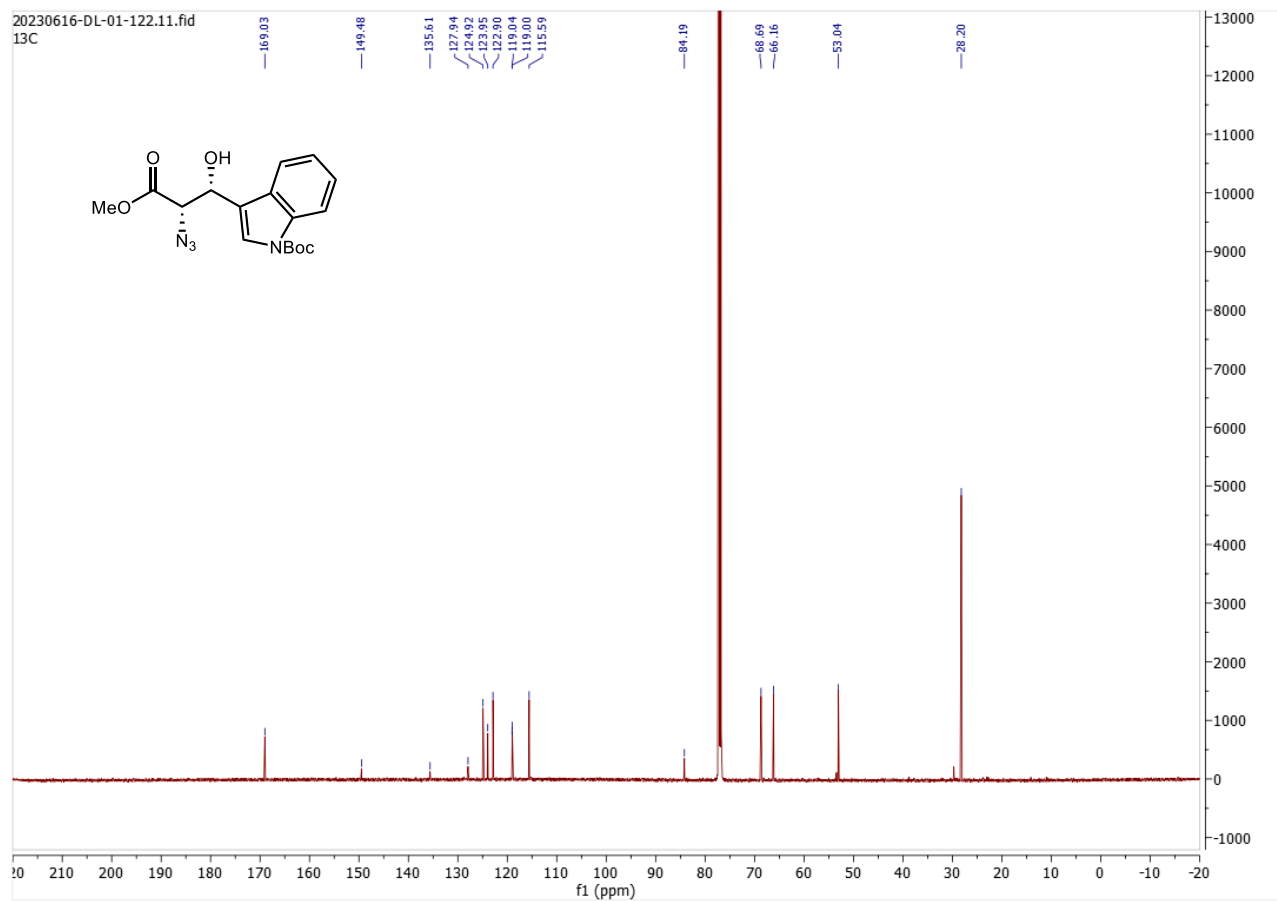
4.24: ^1H NMR (600 MHz, CDCl_3)



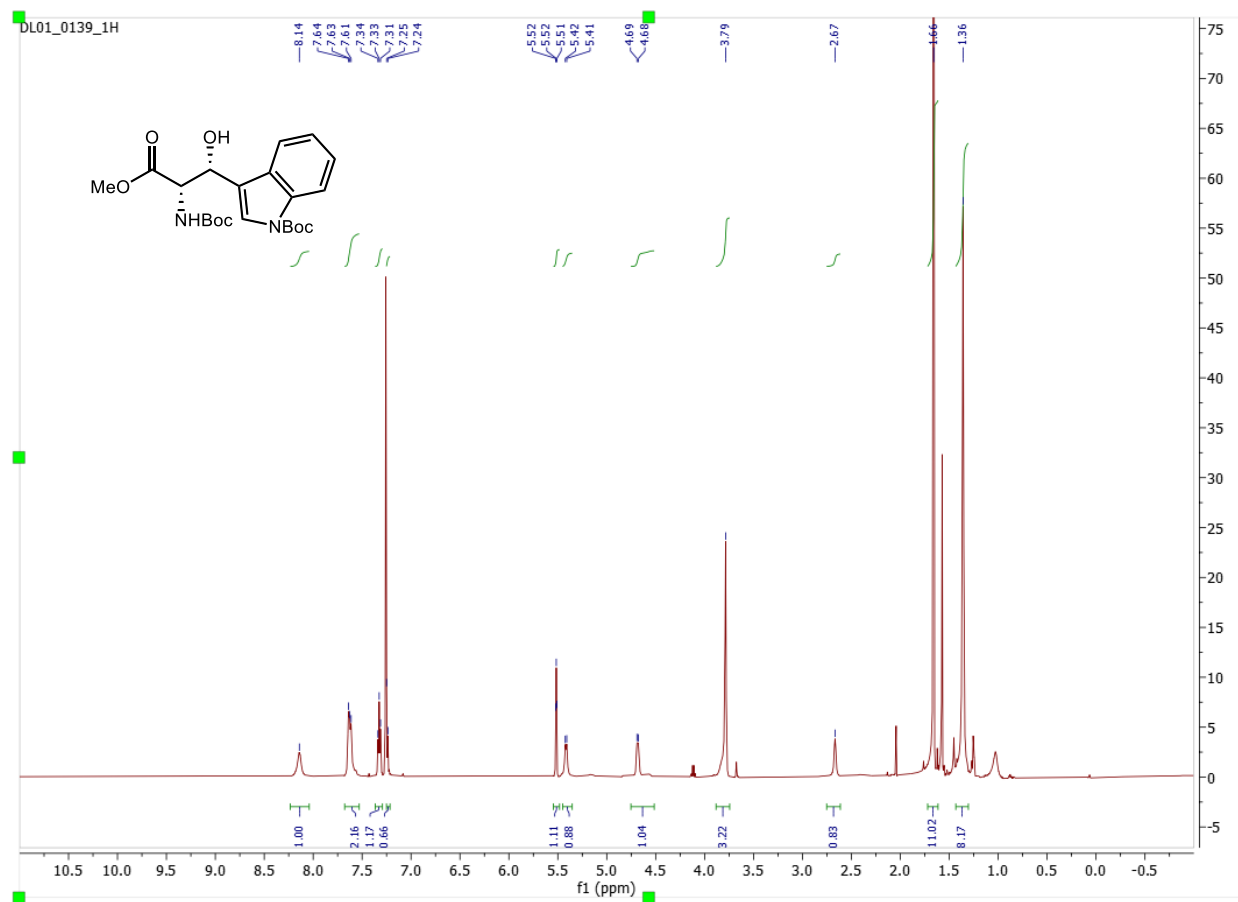
4.25: ^1H NMR (600 MHz, CDCl_3)



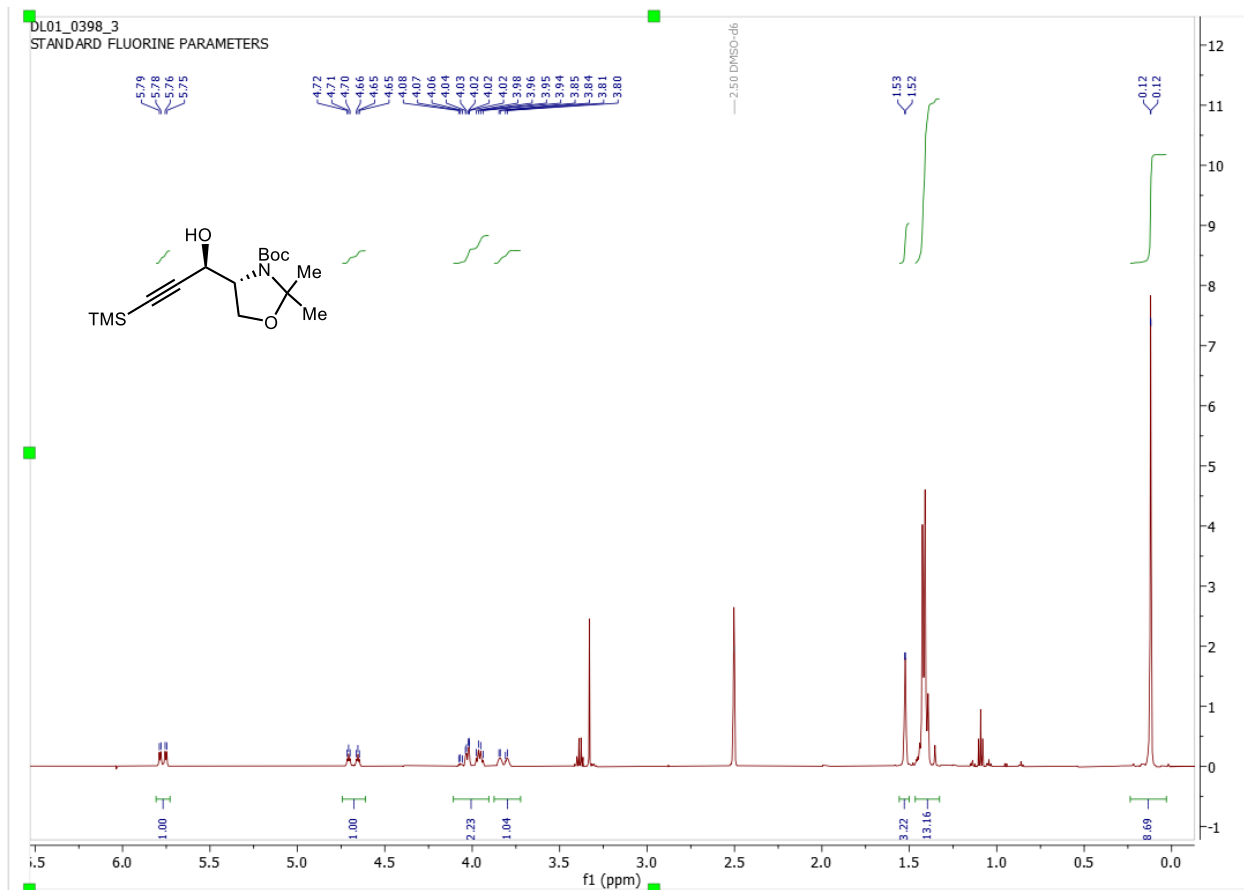
4.25: ^{13}C NMR (151 MHz, CDCl_3)



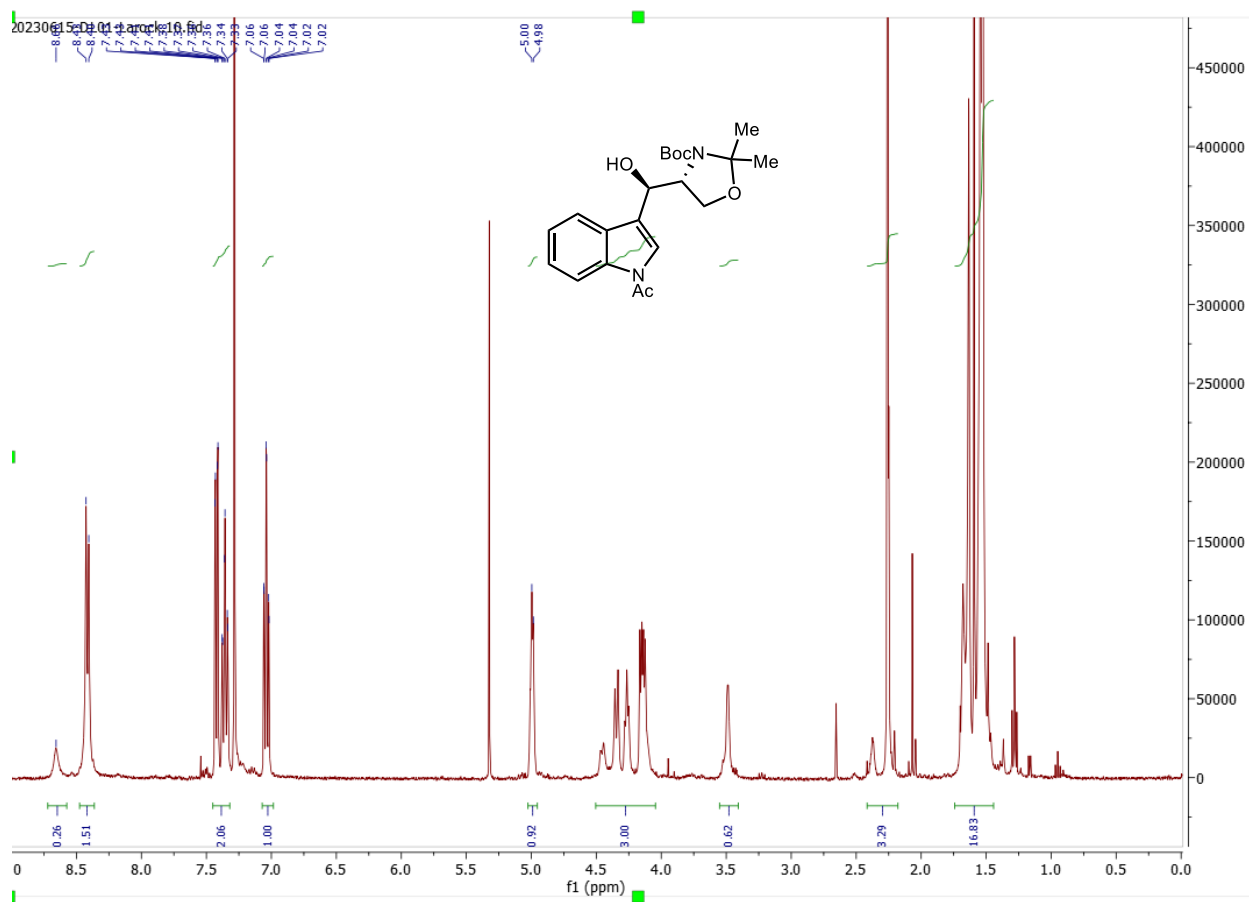
4.26: ^1H NMR (600 MHz, CDCl_3)



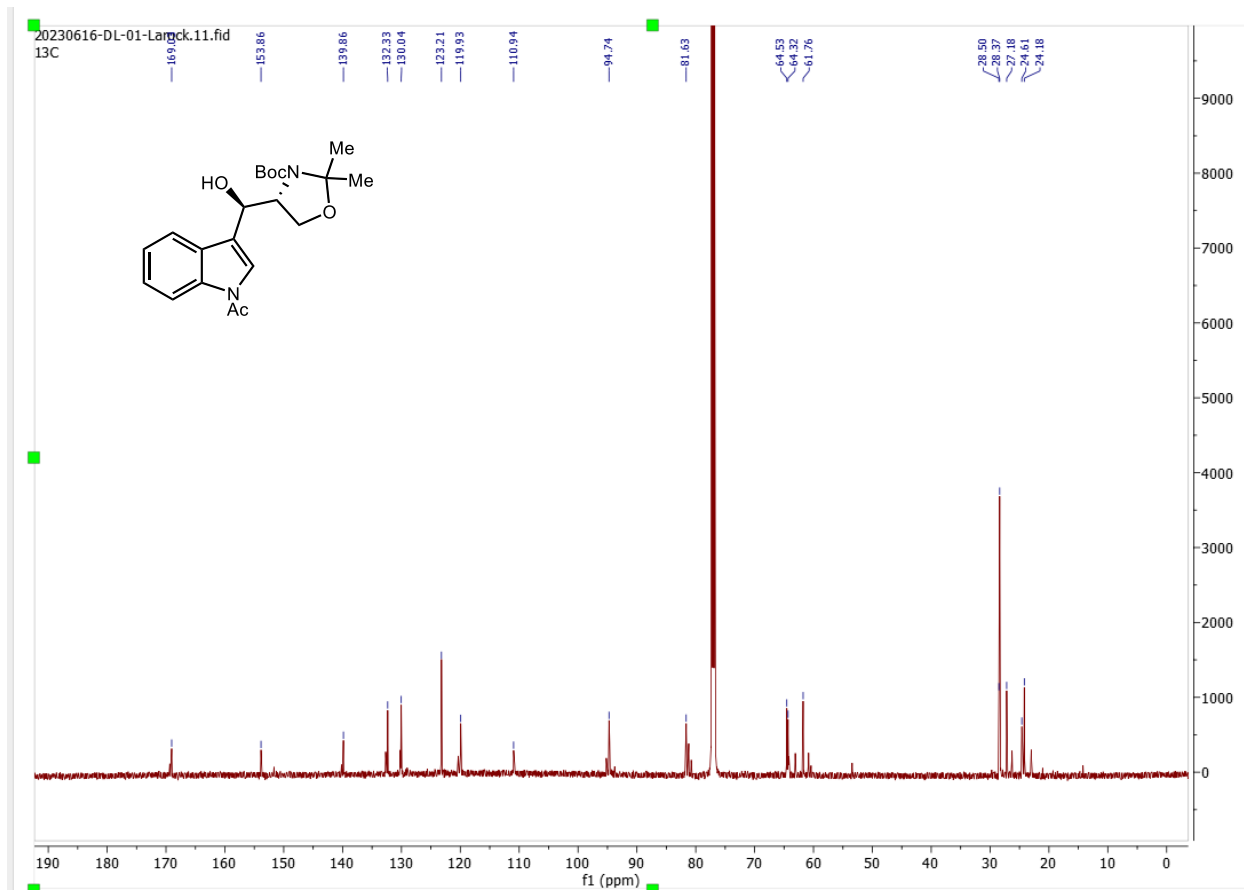
4.27: DMSO-*d*₆ (¹H NMR, 600 MHz)



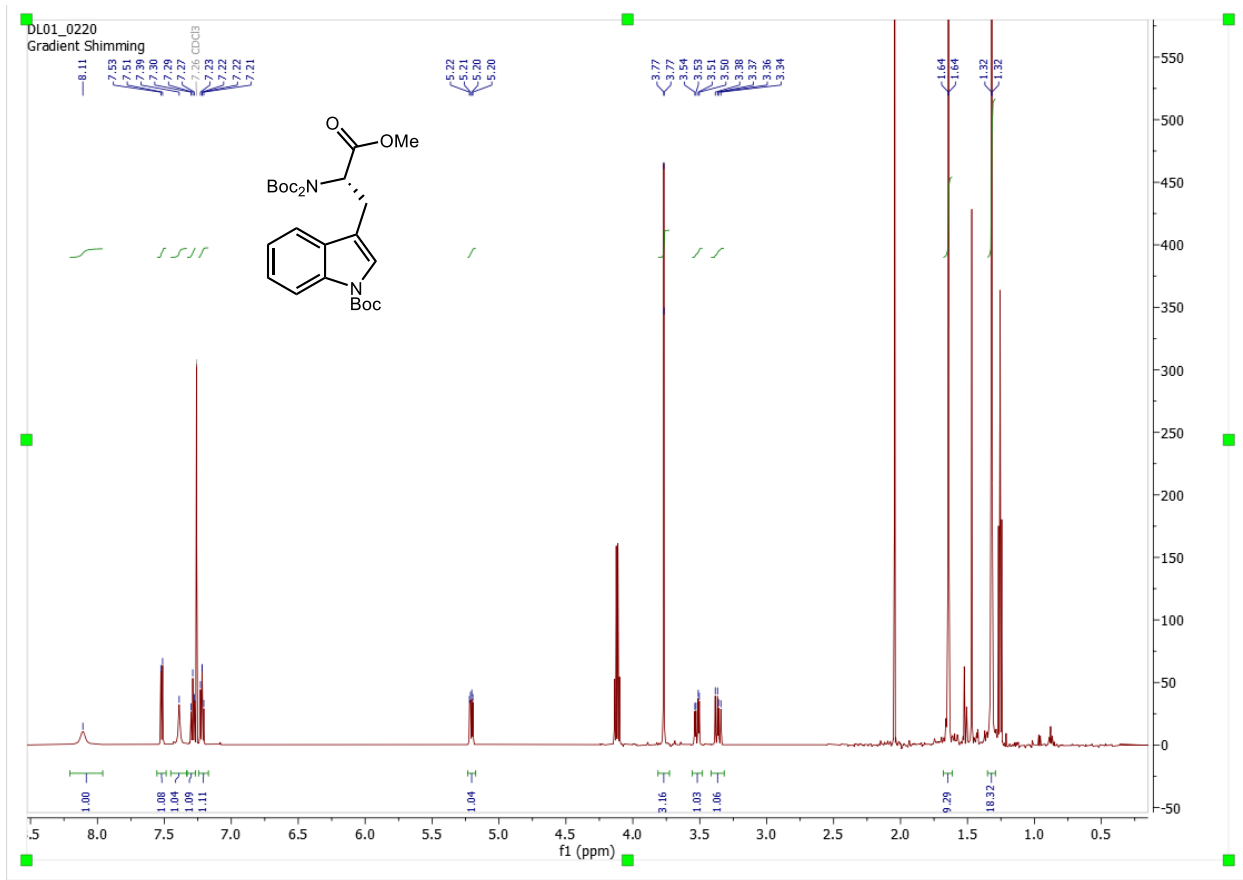
4.29: ^1H NMR (CDCl_3 , 600 MHz)



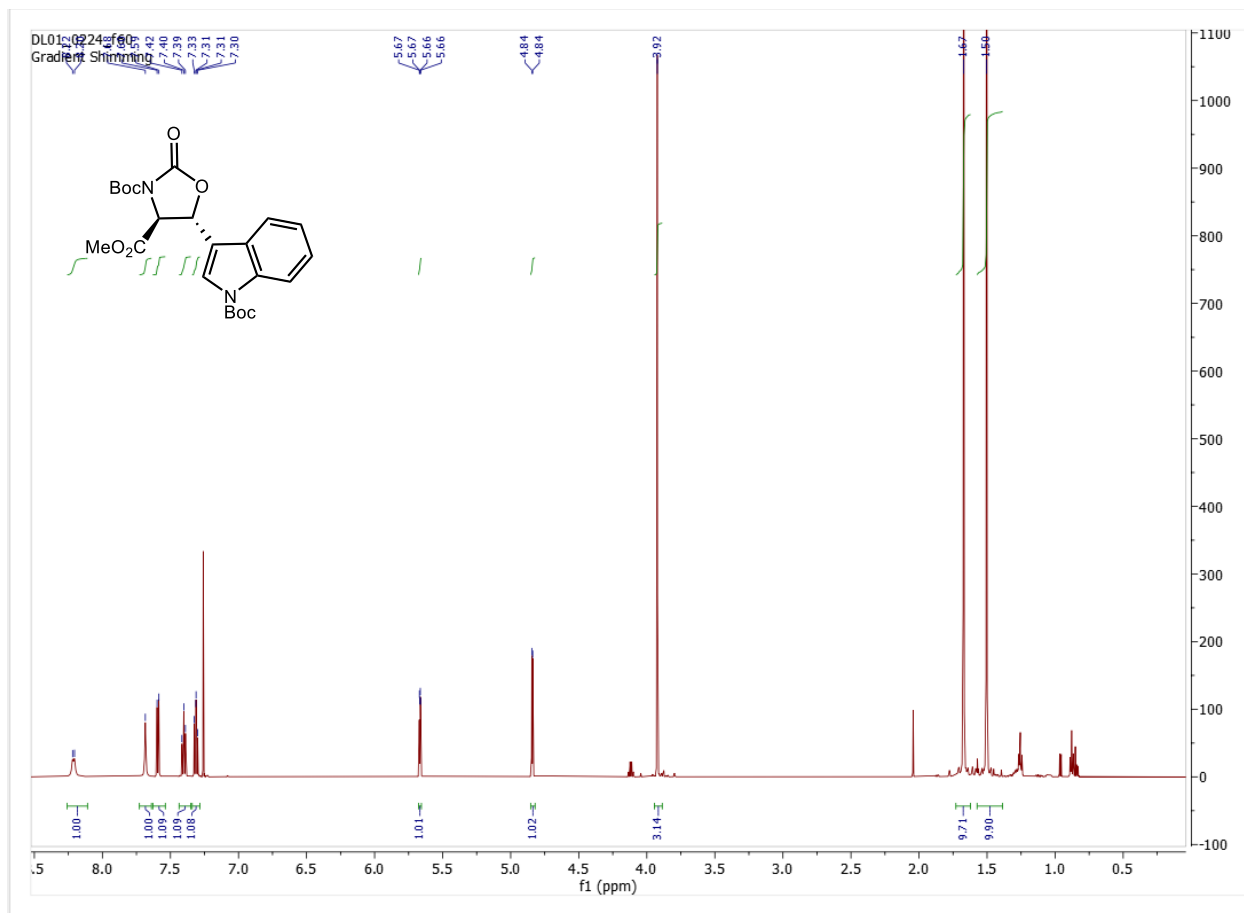
4.29: ^1H NMR (CDCl_3 , 151 MHz)



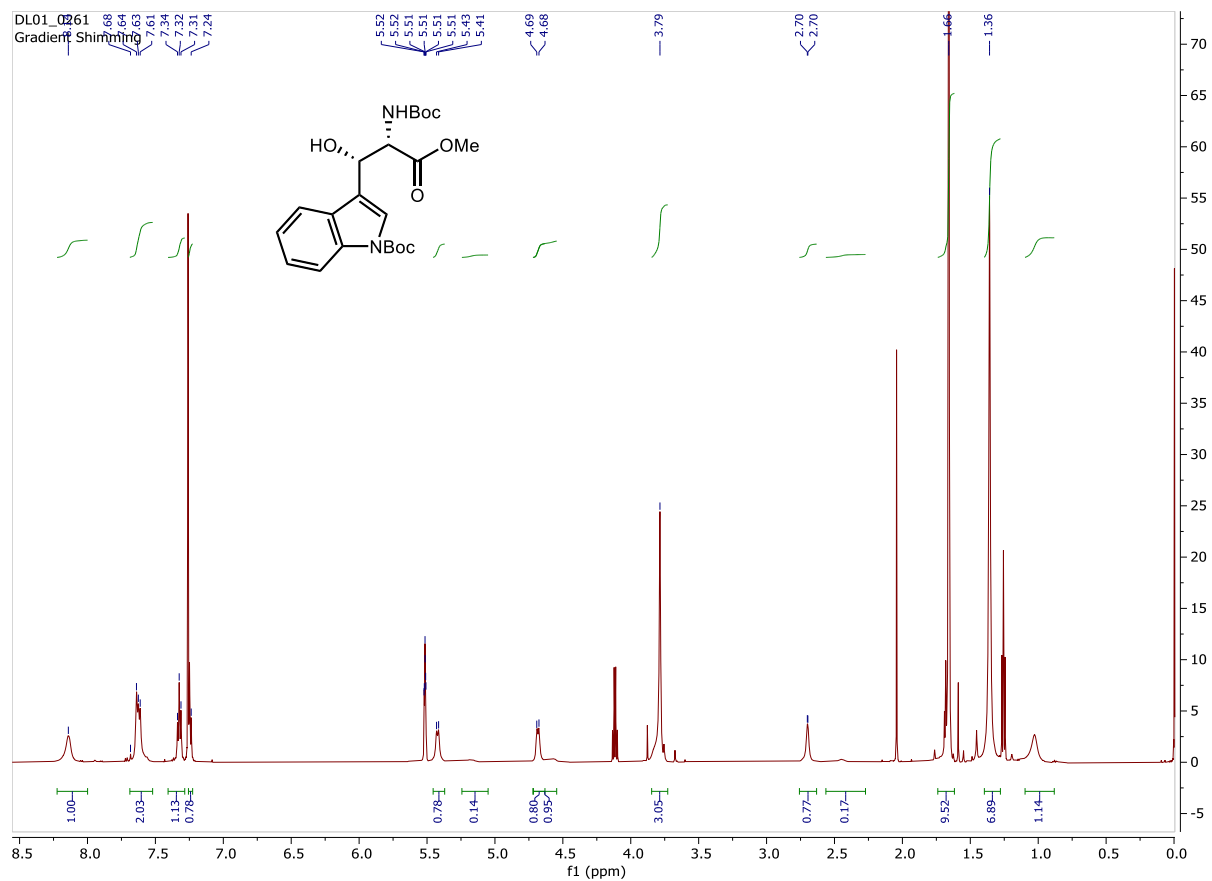
4.30: ^1H NMR (CDCl_3 , 600 MHz)



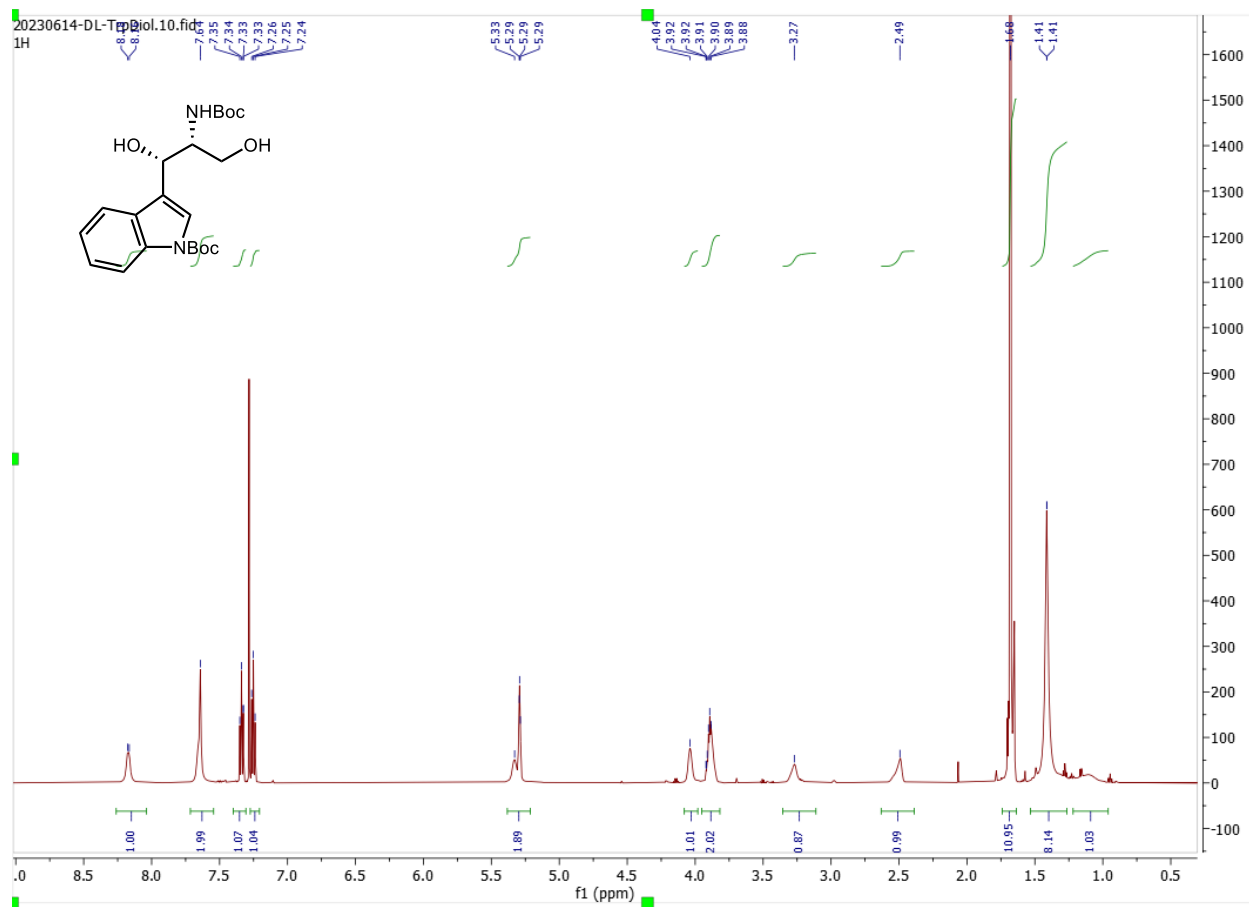
4.31: ^1H NMR (CDCl_3 , 600 MHz)



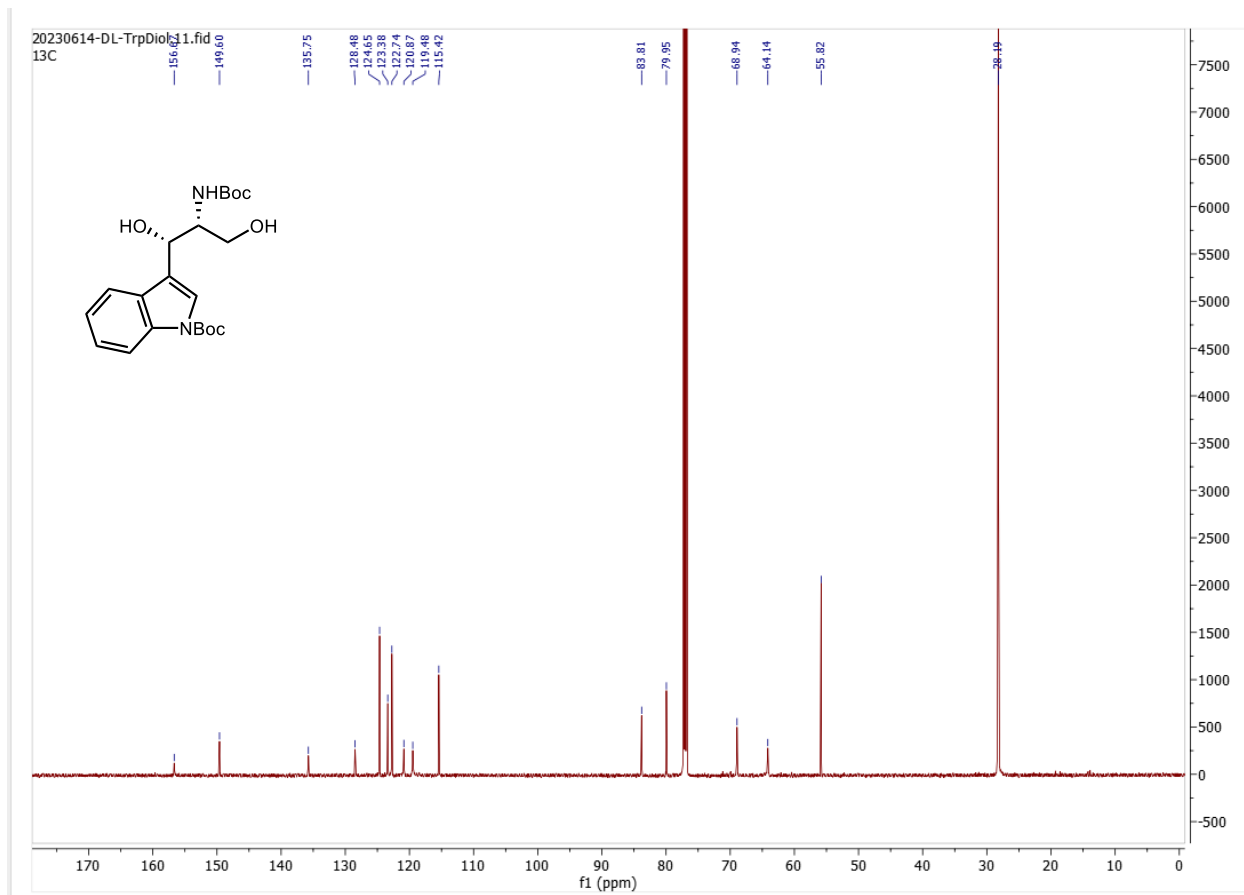
4.32: ^1H NMR (CDCl_3 , 600 MHz)



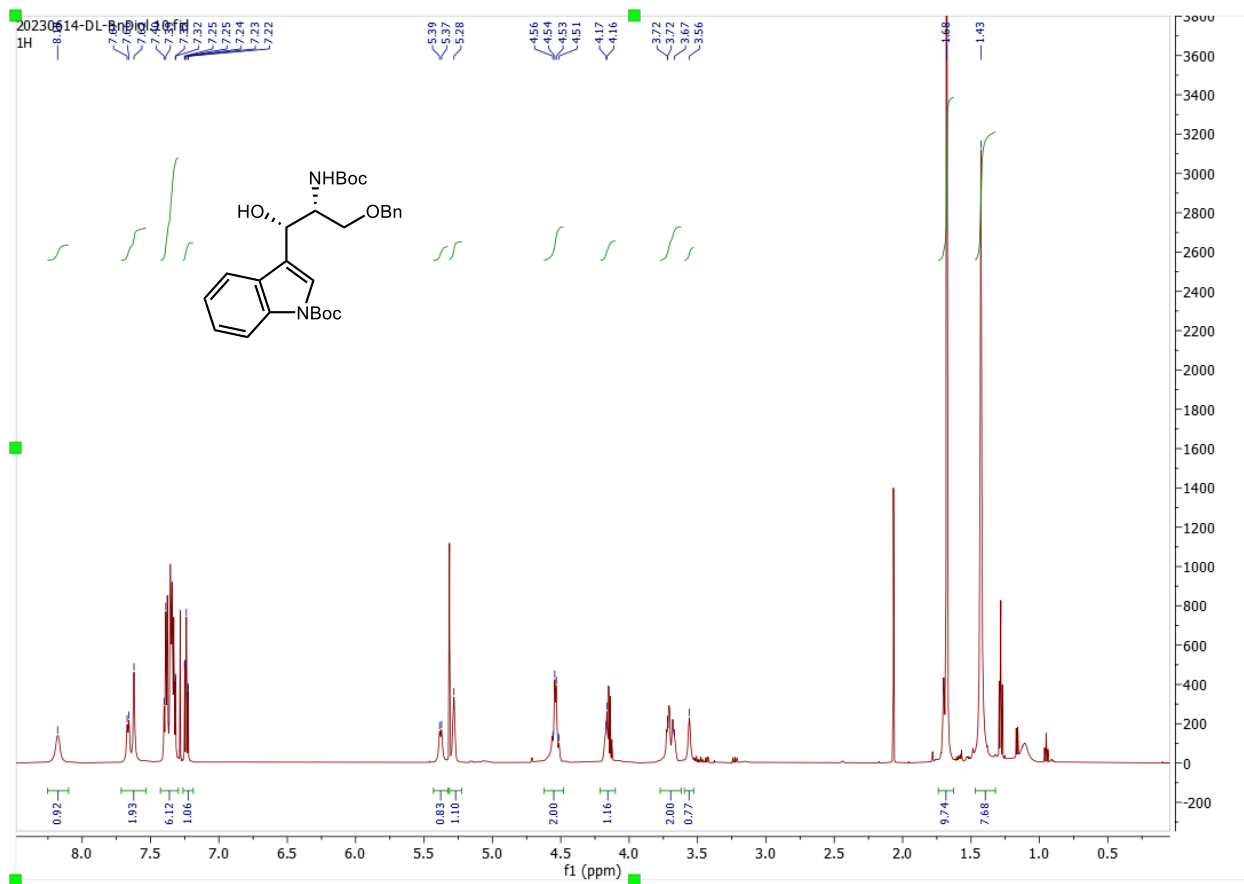
4.41: ¹H NMR (CDCl₃, 600 MHz)



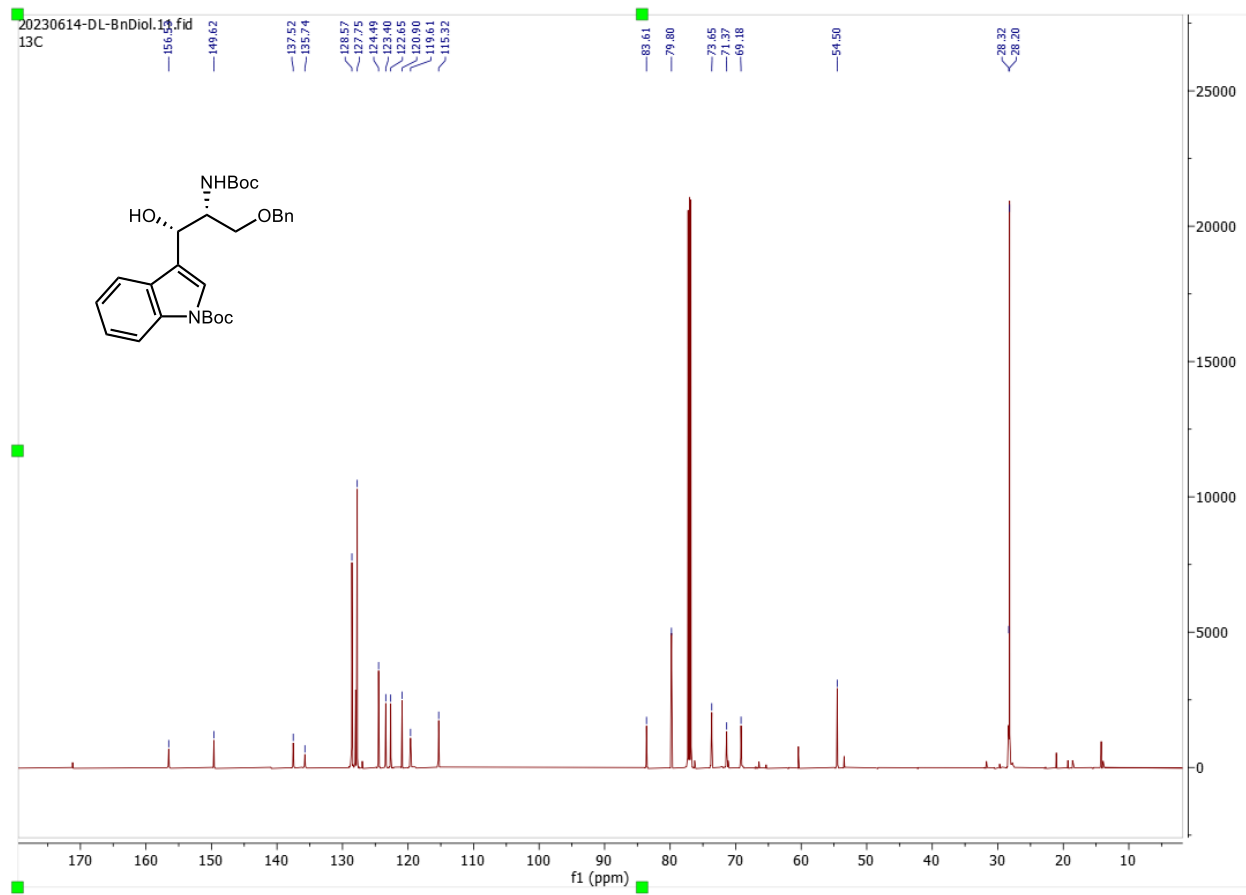
4.41: ^{13}C NMR (CDCl_3 , 151MHz)



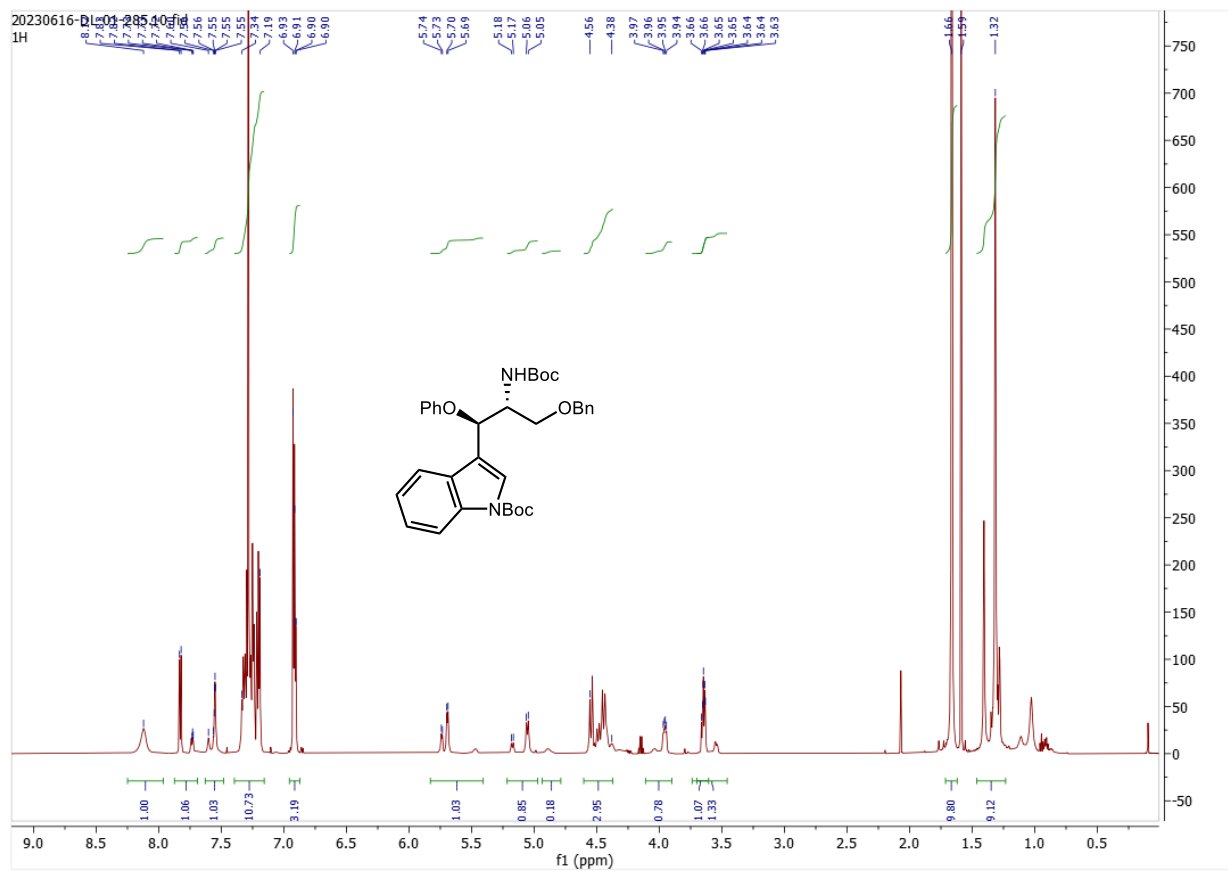
4.42: ^1H NMR (CDCl_3 , 600 MHz)



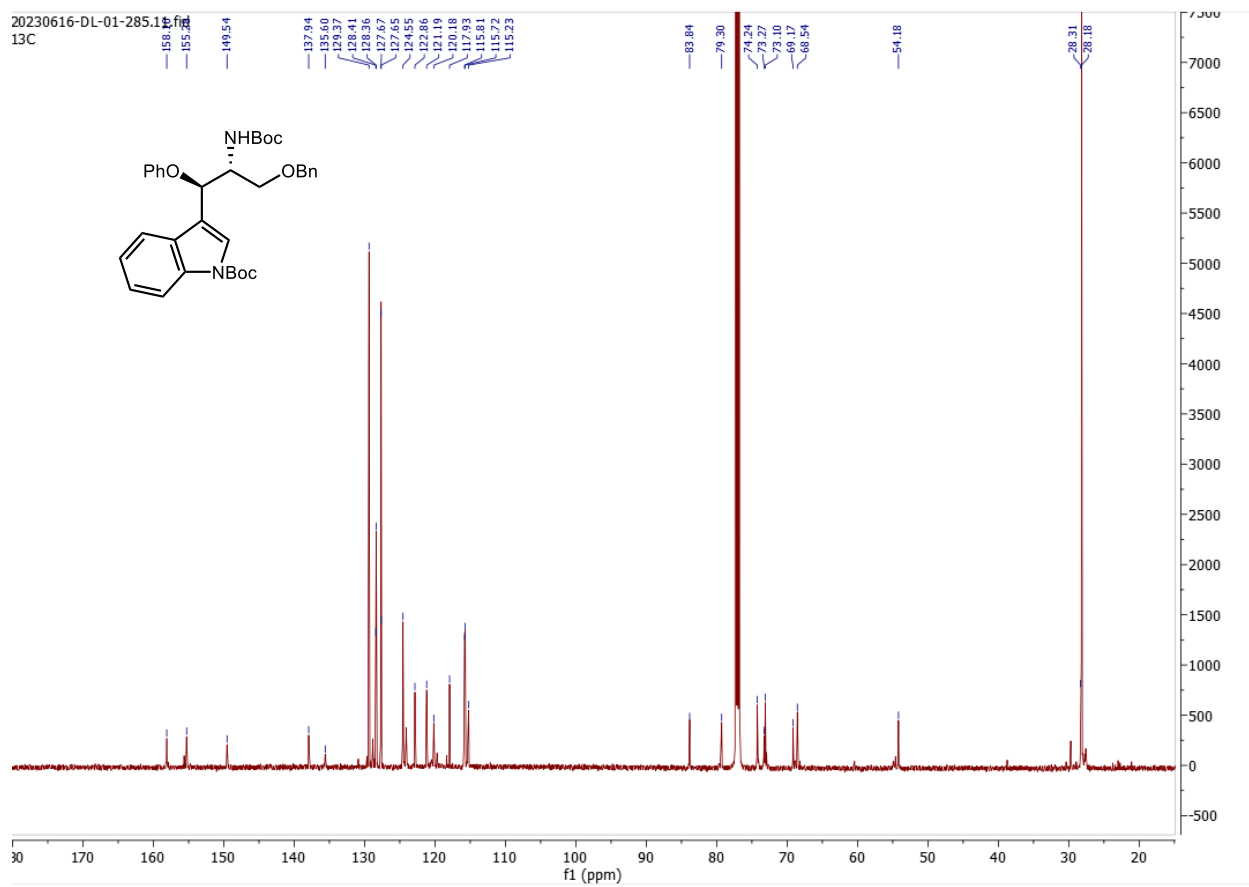
4.42: ^{13}C NMR (CDCl_3 , 151 MHz)



4.43: ^1H NMR (600 MHz, CDCl_3)



4.43: ^{13}C NMR (151MHz, CDCl_3)



4.7 References

- (120) Loach, R. P.; Fenton, O. S.; Amaike, K.; Siegel, D. S.; Ozkal, E.; Movassaghi, M. C7-Derivatization of C3-Alkylindoles Including Tryptophans and Tryptamines. *J. Org. Chem.* **2014**, *79* (22), 11254–11263. <https://doi.org/10.1021/jo502062z>.
- (121) Bartoccini, F.; Fanini, F.; Retini, M.; Piersanti, G. General Synthesis of Unnatural 4-, 5-, 6-, and 7-Bromo-d-Tryptophans by Means of a Regioselective Indole Alkylation. *Tetrahedron Lett.* **2020**, *61* (22), 151923. <https://doi.org/10.1016/J.TETLET.2020.151923>.
- (122) Mentzel, U. V.; Tanner, D.; Tønder, J. E. Comparative Study of the Kumada, Negishi, Stille, and Suzuki - Miyaura Reactions in the Synthesis of the Indole Alkaloids Hippadine and Pratosine. *J. Org. Chem.* **2006**, *71* (15), 5807–5810. https://doi.org/10.1021/JO060729B/SUPPL_FILE/JO060729BSI20060510_101238.PDF.
- (123) Eastabrook, A. S.; Wang, C.; Davison, E. K.; Sperry, J. A Procedure for Transforming Indoles into Indolequinones. *J. Org. Chem.* **2015**, *80* (2), 1006–1017. https://doi.org/10.1021/JO502509S/SUPPL_FILE/JO502509S_SI_001.PDF.
- (124) Hinman, R. L.; Bauman, C. P.; Nagasaka, T.; Ohki, S.; Büchi, G.; Deshong, P. R.; Katsumura, S.; Sugimura, Y.; Ohnuma, T.; Kimura, Y.; Ban, Y.; Palla, G. Extending Pummerer Reaction Chemistry. Application to the Oxidative Cyclization of Tryptophan Derivatives Scheme 1. Mechanistic Speculation Governing the Oxidative Cyclization of Tryptophan Derivatives. *Chem. Pharm. Bull.* **1964**, *29*, 59. <https://doi.org/10.1021/ol048974>.

- (125) Patel, J.; Clavé, G.; Renard, P. Y.; Franck, X. Straightforward Access to Protected Syn α -Amino- β -Hydroxy Acid Derivatives. *Angew. Chem. Int. Ed.* **2008**, *47* (22), 4224–4227. <https://doi.org/10.1002/ANIE.200800860>.
- (126) Passiniemi, M.; Koskinen, A. M. P. Garner's Aldehyde as a Versatile Intermediate in the Synthesis of Enantiopure Natural Products. *Beilstein J. Org. Chem.* **2013**, *9*, 2641. <https://doi.org/10.3762/BJOC.9.300>.
- (127) Zhang, X.; Van Der Donk, W. A. On the Substrate Specificity of Dehydration by Lactacin 481 Synthetase. *J. Am. Chem. Soc.* **2007**, *129* (8), 2212–2213. <https://doi.org/10.1021/ja067672v>.
- (128) Wensbo, D.; Eriksson, A.; Jeschke, T.; Annby, U.; Gronowitz, S.; Cohen, L. A. Palladium-Catalysed Synthesis of Heterocondensed Pyrroles. *Tetrahedron Lett.* **1993**, *34* (17), 2823–2826. [https://doi.org/10.1016/S0040-4039\(00\)73572-6](https://doi.org/10.1016/S0040-4039(00)73572-6).
- (129) Crich, D.; Banerjee, A. Expedient Synthesis of Threo- β -Hydroxy- α -Amino Acid Derivatives: Phenylalanine, Tyrosine, Histidine, and Tryptophan. *J. Org. Chem.* **2006**, *71* (18), 7106–7109. https://doi.org/10.1021/JO061159I/SUPPL_FILE/JO061159ISI20060630_023154.PDF.
- (130) El Khatib, M.; Molander, G. A. Copper(II)-Mediated O-Arylation of Protected Serines and Threonines. *Org. Lett.* **2014**, *16* (18), 4944–4947. https://doi.org/10.1021/OL5024689/SUPPL_FILE/OL5024689_SI_001.PDF.
- (131) Chen, Z.; Jiang, Y.; Zhang, L.; Guo, Y.; Ma, D. Oxalic Diamides and Tert-Butoxide: Two Types of Ligands Enabling Practical Access to Alkyl Aryl Ethers via Cu-Catalyzed

Coupling Reaction. *J. Am. Chem. Soc.* **2019**, *141* (8), 3541–3549.
<https://doi.org/10.1021/jacs.8b12142>.

(132) Zhang, L.; Israel, E. M.; Yan, J.; Ritter, T. Copper-Mediated Etherification via Aryl Radicals Generated from Triplet States. *Nature Synthesis* **2022**, *1* (5), 376–381.
<https://doi.org/10.1038/s44160-022-00061-0>.

(133) Yang, L.; Lu, H. H.; Lai, C. H.; Li, G.; Zhang, W.; Cao, R.; Liu, F.; Wang, C.; Xiao, J.; Xue, D. Light-Promoted Nickel Catalysis: Etherification of Aryl Electrophiles with Alcohols Catalyzed by a NiII-Aryl Complex. *Angew. Chem. Int. Ed.* **2020**, *59* (31), 12714–12719. <https://doi.org/10.1002/ANIE.202003359>.

(134) Shintou, T.; Mukaiyama, T. Efficient Methods for the Preparation of Alkyl-Aryl and Symmetrical or Unsymmetrical Dialkyl Ethers between Alcohols and Phenols or Two Alcohols by Oxidation-Reduction Condensation. *J. Am. Chem. Soc.* **2004**, *126* (23), 7359–7367.
https://doi.org/10.1021/JA0487877/SUPPL_FILE/JA0487877SI20040404_034620.PDF.

(135) He, S.; Dobbelaar, P. H.; Guo, L.; Ye, Z.; Liu, J.; Jian, T.; Truong, Q.; Shah, S. K.; Du, W.; Qi, H.; Bakshi, R. K.; Hong, Q.; Dellureficio, J. D.; Sherer, E.; Pasternak, A.; Feng, Z.; Reibarkh, M.; Lin, M.; Samuel, K.; Reddy, V. B.; Mitelman, S.; Tong, S. X.; Chicchi, G. G.; Tsao, K. L.; Trusca, D.; Wu, M.; Shao, Q.; Trujillo, M. E.; Fernandez, G.; Nelson, D.; Bunting, P.; Kerr, J.; Fitzgerald, P.; Morissette, P.; Volksdorf, S.; Eiermann, G. J.; Li, C.; Zhang, B. B.; Howard, A. D.; Zhou, Y. P.; Nargund, R. P.; Hagmann, W. K. SAR Exploration at the C-3 Position of Tetrahydro- β -Carboline Sstr3 Antagonists. *Bioorg. Med. Chem. Lett.* **2016**, *26* (6), 1529–1535. <https://doi.org/10.1016/J.BMCL.2016.02.022>.

- (136) Govek, S. P.; Overman, L. E. Total Synthesis of (+)-Asperazine. *Tetrahedron* **2007**, *63* (35), 8499–8513. <https://doi.org/10.1016/J.TET.2007.05.127>.
- (137) Chaumont, P.; Baudoux, J.; Maddaluno, J.; Rouden, J.; Harrison-Marchand, A. Access to Anti or Syn 2-Amino-1,3-Diol Scaffolds from a Common Decarboxylative Aldol Adduct. *J. Org. Chem.* **2018**, *83* (15), 8081–8091. https://doi.org/10.1021/ACS.JOC.8B00901/SUPPL_FILE/JO8B00901_SI_002.CIF.
- (138) Kinderman, S. S.; Wekking, M. M. T.; Van Maarseveen, J. H.; Schoemaker, H. E.; Hiemstra, H.; Rutjes, F. P. J. T. Catalytic N-Sulfonyliminium Ion-Mediated Cyclizations to α -Vinyl-Substituted Isoquinolines and β -Carbolines and Applications in Metathesis. *J. Org. Chem.* **2005**, *70* (14), 5519–5527. https://doi.org/10.1021/JO050503T/SUPPL_FILE/JO050503TSI20050503_115459.PDF.
- (139) Denoël, T.; Zervosen, A.; Gerards, T.; Lemaire, C.; Joris, B.; Blanot, D.; Luxen, A. Stereoselective Synthesis of Lanthionine Derivatives in Aqueous Solution and Their Incorporation into the Peptidoglycan of *Escherichia Coli*. *Bioorg. Med. Chem.* **2014**, *22* (17), 4621–4628. <https://doi.org/10.1016/J.BMC.2014.07.023>.
- (140) Grimster, N. P.; Gauntlett, C.; Godfrey, C. R. A.; Gaunt, M. J. Palladium-Catalyzed Intermolecular Alkenylation of Indoles by Solvent-Controlled Regioselective C–H Functionalization. *Angew. Chem. Int. Ed.* **2005**, *44* (20), 3125–3129. <https://doi.org/10.1002/ANIE.200500468>.
- (141) Saunthwal, R. K.; Patel, M.; Kumar, S.; Danodia, A. K.; Verma, A. K. Pd(II)-Catalyzed C–H Activation of Styrylindoles: Short, Efficient, and Regioselective Synthesis

of Functionalized Carbazoles. *Chem. Eur. J.* **2015**, *21* (51), 18601–18605. <https://doi.org/10.1002/CHEM.201503657>.

(142) Oikawa, M.; Ikoma, M.; Sasaki, M. Synthetic Studies on Dragmacidin D: Synthesis and Assembly of Three Fragments Towards an Advanced Intermediate. *Eur. J. Org. Chem.* **2011**, *2011* (24), 4654–4666. <https://doi.org/10.1002/EJOC.201100242>.

(143) Nocquet, P. A.; Corbu, A.; Meerpoel, L.; Stansfield, I.; Berthelot, D.; Angibaud, P.; Cossy, J. Diastereoselective Synthesis of Trans-2,3-Diaryl(Heteroaryl)-3,6-Dihydropyrans by an Allylboration/Ring-Closing-Metathesis Sequence. *Eur. J. Org. Chem.* **2017**, *2017* (23), 3343–3354. <https://doi.org/10.1002/EJOC.201700448>.

(144) Harada, S.; Sakai, T.; Takasu, K.; Yamada, K. I.; Yamamoto, Y.; Tomioka, K. Critical Profiles of Chiral Diether-Mediated Asymmetric Conjugate Aminolithiation of Enoate with Lithium Amide as a Key to the Total Synthesis of (–)-Kopsinine. *Tetrahedron* **2013**, *69* (15), 3264–3273. <https://doi.org/10.1016/J.TET.2013.02.035>.

(145) Moore, M. J.; Qu, S.; Tan, C.; Cai, Y.; Mogi, Y.; Jamin Keith, D.; Boger, D. L. Next-Generation Total Synthesis of Vancomycin. *J. Am. Chem. Soc.* **2020**, *142* (37), 16039–16050. https://doi.org/10.1021/JACS.0C07433/SUPPL_FILE/JA0C07433_SI_001.PDF.

(146) Shao, H.; Goodman, M. An Enantiomeric Synthesis of Allo-Threonines and β -Hydroxyvalines. *J. Org. Chem.* **1996**, *61* (8), 2582–2583. <https://doi.org/10.1021/JO960141C/ASSET/IMAGES/LARGE/JO960141CN00001.JPEG>